

**STUDIES ON CATALYSIS BY TRANSITION METAL  
PROMOTED SULPHATED ZIRCONIA**

*Thesis submitted to the  
Cochin University of Science & Technology  
in partial fulfilment of the requirements for the degree of*

*Doctor of Philosophy*

**In**

***Chemistry***

**In the Faculty of Science**



**By**

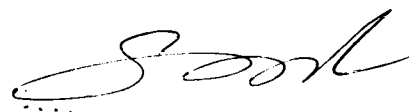
***Suja Haridas***

**DEPARTMENT OF APPLIED CHEMISTRY  
COCHIN UNIVERSITY OF SCIENCE AND TECHNOLOGY  
KOCHI-22**

**JANUARY - 2002**

## CERTIFICATE

This is to certify that the thesis is an authentic record of research carried out by Ms.Suja Haridas under my supervision, in partial fulfilment of the requirements for the Degree of Doctor of Philosophy, Cochin University of Science and Technology, and that no part thereof has been submitted before for award of any other degree.



Dr. S.Sugunan,

(Supervising Guide)

Department of Applied Chemistry,

Cochin University of Science and Technology,

Kochi-22.

Kochi-22


30-01-2002

## DECLARATION

I hereby declare that the work presented in this thesis entitled “Studies on catalysis by transition metal promoted sulphated zirconia” is an authentic work carried out by me independently under the supervision of Dr.S.Sugunan, Professor in Physical Chemistry, Department of Applied Chemistry, Cochin University of Science and Technology, and has not been included in any other thesis submitted previously for award of any other degree.

Kochi-22

30-01-2002



Suja Haridas

## ACKNOWLEDGEMENT

*It gives me a great pleasure to record my heart-felt gratitude to Dr.S.Sugunan for his constant support, encouragement and guidance throughout the period of my work. I am greatly obliged to him for the words of comfort, which evoked a new spirit in me during times of dejection.*

*My gratefulness is also due to Dr.K.K.Mohammed Yusuff, former Head, Department of Applied Chemistry, for the opportunity to carry out my work in this department and for the timely help and support extended. I owe a lot to Dr.S.Prathapan for his concern and guidance rendered during my M.Sc as well as research period. The valuable suggestions offered in proposing the reaction mechanisms are also remembered with gratitude. My thanks are also due to Dr.K.Sreekumar for his timely suggestions and help. I am grateful to Dr.P.Indrasenan, Head, Department of Chemistry, Kerala University, for providing the thermal analysis data. I am also thankful for the support rendered by the teaching and non-teaching staff, Department of Applied Chemistry.*

*I am greatly indebted to my lab-mates for their timely help. But for the lively and radiant atmosphere created by them the life in the lab would have been a monotonous experience. I hereby extend my earnest thanks to my friends Renu chechi, Rehna, Deepa, Nisha, Sreeja, Smitha, Fincy, Sunaja, Bejoy, Sanjay, Manju, Anas, Suja, Vineetha, Preetha and Jean for their support and co-operation on various occasions. My deepest sense of gratitude to Dr.C.G.Ramankutty for his valuable time spent in the critical reading of the thesis and for constant encouragement. The time devoted by Smitha in the patient reading of the thesis needs special mention in this context. Special thanks goes to Dr.K.O.Xavier, Dr.T.M.Jyothi and Dr.K.Sreekumar for their valuable suggestions and help during various stages of my work. I would also like to express my thanks to Siby.C.P for supplying thermogravimetric and IR data.*

*The whole-hearted technical assistance provided by Mr.Gopi Menon, Mr.Murali and Mr.Joshi, Department of USIC, is acknowledged with gratitude. Without their sincere co-operation, lab work would have been a tedious process. In this context, I also express my gratefulness to Mr.Suresh, Service Engineer, Chemito for his help during technical difficulties.*

*I remember with gratitude the warmth of friendship and help extended by Subrahmanyam and Venkata Subba Rao. My heart-felt thanks to little Daly for her sincere, loving and caring assistance and creative suggestions during different stages of my research work and thesis writing. Her constant company was a great relief in the midst of routine labwork. Words cannot express my appreciation to my parents and sister for their affectionate backing during my research time. Above all, I submit my heart-felt gratefulness before the supreme power of God Almighty for lifting up my sagging enthusiasm and guiding me through the critical stages in my life. The financial support offered by CSIR-NewDelhi is also acknowledged with gratitude.*

Suja Haridas



## PREFACE

The developments in catalysis during the last few decades have been mandated mainly by the considerations related to the abatement and prevention of pollution, conservation of raw materials and production of more efficient drugs. The amount of sulphate ion ultimately present in a sulphated zirconia catalyst can be controlled by impregnating the solid with desired quantity of sulphuric acid in water, evaporating the solvent and calcining the residue. The controlled impregnation technique allows the variation of the sulphate content without changing the calcination temperature. Moreover, this method also avoids the generation of waste sulphuric acid after the impregnation step. The sulphate content obtained by the controlled impregnation technique was higher than that obtained by the percolation method, when same amount of  $H_2SO_4$  was employed for sulphation. In spite of their high initial activity for different acid catalysed reactions at relatively low temperatures, sulphated zirconia suffers from the major draw back of rapid deactivation. Modification with various transition metal ions has been reported to alter the properties of the system depending on the nature of the ion incorporated. Even though several reports are available regarding the impact of different metal promoters on stability and catalytic activity, a consolidated and systematic investigation on the topic is lacking. Controversial reports exist regarding the influence of any particular ion on the physico-chemical and catalytic properties. The final property of the catalyst seems to be a function of the preparation procedure or particular reaction conditions. Thus, a true comparison of the promoting effect of the transition metal species requires a methodical study employing relatively similar preparation and reaction conditions. The present work is oriented to obtain a comparative evaluation of the physico-chemical properties and catalytic activity of sulphated zirconia systems incorporated with different transition metal species. Some reactions of industrial importance such as Friedel-Crafts reactions, phenol hydroxylation and nitration of toluene have been selected for the present venture. An initial attempt has also been directed towards the optimisation of sulphate content and the calcination temperature, since these are the prime factors influencing the nature of the catalyst.

# CONTENTS

## CHAPTER 1 INTRODUCTION

1.1	Catalysis- General Introduction	1
1.2	Solid acid catalysis	2
1.3	Solid superacids	3
1.4	Sulphated metal oxides	4
1.5	Zirconia as catalysts and catalyst supports	6
1.6	Mixed oxides of zirconia	8
1.7	Sulphated zirconia as catalysts	11
1.7.1	Preparation methods	11
1.7.2	Surface properties	14
1.7.3	Surface acidic properties	18
i	Nature of surface acidity	19
ii	Surface acidity determination	19
1.7.4	Catalytic activity	24
1.7.5	Structure of sulphated zirconia	27
1.8	Metal promoted sulphated zirconia	30
1.9	Main objectives of the present work	38
	References	40

## CHAPTER 2 EXPERIMENTAL

2.1	Introduction	48
2.2	Catalyst Preparation	48
2.2.1	Materials	48
2.2.2	Methods	49
i	Zirconium Hydroxide	49
ii	Optimisation of sulphate content	49
iii	Metal Promoted sulphated zirconia	50
iv	Iron promoted sulphated zirconia	50
2.3	Catalyst Characterisation	50
2.3.1	Materials	51
2.3.2	Methods	51
i	Surface area and pore volume measurements	51
ii	X-Ray diffraction	52
iii	Infra Red Spectroscopy	53
iv	Laser Raman Spectroscopy	53
v	Thermogravimetric analysis	54
vi	Energy Dispersive X-Ray analysis	54
vii	Scanning Electron Microscopy	55
viii	Surface acidity determination	55
	Ammonia TPD	56
	Perylene adsorption studies	56
	Thermodesorption studies	56
2.4	Reactivity studies	57

2.4.1	Materials	58
2.4.2	Methods	58
i	Liquid phase reactions	58
	Friedel-Crafts Benzoylation	58
	Friedel-Crafts Benzoylation	59
	Phenol Hydroxylation	59
	Nitration of toluene	59
ii	Gas Phase Reactions	60
	Methylation of aniline	60
	Cumene conversion reaction	60
	References	61

## CHAPTER 3 PHYSICO-CHEMICAL CHARACTERISATION

SECTION 1	OPTIMISATION STUDIES	62
3.1	Optimisation of calcination temperature	62
3.1.1	Surface area and sulphate content	63
3.1.2	XRD Patterns	64
3.1.3	Acidic Properties	64
i	Ammonia TPD	64
ii	Perylene adsorption studies	65
iii	Thermodesorption studies	66
3.2	Optimisation of sulphate loading	68
3.2.1	Surface area and pore volume	68
3.2.2	XRD analysis	69
3.2.3	Thermal Studies	71
3.2.4	Elemental analysis	72
3.2.5	Acidity measurement	73
i	Ammonia TPD	73
ii	Perylene adsorption studies	74
SECTION 2	PHYSICO-CHEMICAL CHARACTERISATION	76
3.3	Metal incorporated sulphated zirconia systems	76
3.3.1	Surface area and pore volume	76
3.3.2	XRD Analysis	77
3.3.3	Scanning Electron Microscopy	79
3.3.4	Thermal Studies	79
3.3.5	Infra Red Spectra	80
3.3.6	Laser Raman Spectra	81
3.3.7	Elemental analysis	82
3.3.8	Acidity measurement	82
i	Ammonia TPD	82
ii	Thermodesorption studies	83
iii	Perylene adsorption studies	86
3.4	Iron incorporated sulphated zirconia systems	88
3.4.1	Surface area and pore volume	88
3.4.2	XRD Analysis	89
3.4.3	Elemental analysis	89
3.4.4	Infra Red Spectra	90

3.4.5	Laser Raman Spectra	90
3.4.6	Thermal Studies	90
3.4.7	Acidity measurement	91
i	Ammonia TPD	91
ii	Thermodesorption studies	92
iii	Perylene adsorption studies	93
SECTION 3	TEST REACTION FOR ACIDITY	95
3.5	Cumene conversion reaction	95
3.5.1	Introduction	95
3.5.2	Cumene conversion over sulphated zirconia systems	97
	Conclusions	101
	References	102

## CHAPTER 4 FRIEDEL-CRAFTS REACTIONS

SECTION 1	FRIEDEL-CRAFTS BENZOYLATION AND BENZYLATION	105
4.1	Introduction	105
4.1.1	Sulphated metal oxides for Friedel-Crafts Reactions	107
4.1.2	Proposed Mechanism for Friedel-Crafts Reactions	108
4.2	Benzoylation of Arenes	109
4.2.1	Influence of catalyst composition	109
i	Influence of sulphate content	109
ii	Influence of metal incorporation	111
iii	Influence of iron content	114
4.2.2	Influence of substrate	115
4.2.3	Influence of reaction temperature	116
4.2.4	Influence of reaction time	118
4.2.5	Influence of molar ratio	118
4.2.6	Influence of calcination temperature	119
4.2.7	Reusability of the catalyst systems	121
4.2.8	Metal leaching	121
4.2.9	Influence of moisture	122
4.2.10	Mechanism of the reaction	123
4.3	Benzylation of aromatics	124
4.3.1	Benylation with benzyl chloride	124
4.3.1.1	Influence of catalyst composition	125
i	Influence of metal incorporation	125
ii	Influence of iron content	127
4.3.1.2	Influence of substrate	129
4.3.1.3	Influence of reaction temperature	130
4.3.1.4	Influence of reaction time	132
4.3.1.5	Influence of molar ratio	133
4.3.1.6	Influence of calcination temperature	134
4.3.1.7	Reusability of the catalyst systems	135
4.3.1.8	Metal leaching	136
4.3.1.9	Influence of moisture	137
4.3.1.10	Mechanism of the reaction	137
4.3.2	Benylation of toluene with benzyl alcohol	140
4.3.2.1	Influence of catalyst composition	140

i	Influence of metal incorporation	140
ii	Influence of iron content	142
4.3.2.2	Influence of reaction temperature	143
4.3.2.3	Influence of reaction time	144
4.3.2.4	Influence of molar ratio	145
4.3.2.5	Influence of calcination temperature	145
4.3.2.6	Metal leaching and reusability	146
4.3.2.7	Influence of moisture	146
4.3.2.8	Mechanism of the reaction	147
4.3.3	Comparison of benzylating agents	149

SECTION 2	ANILINE ALKYLATION	150
4.4	Vapour phase methylation of aniline	150
4.4.1	Introduction	150
4.4.2	Methylation of aniline over sulphated zirconia systems	152
4.4.2.1	Influence of catalyst composition	152
i	Influence of metal incorporation	153
ii	Influence of iron content	154
4.4.2.2	Influence of reaction temperature	155
4.4.2.3	Influence of molar ratio	156
4.4.2.4	Influence of feed rate	157
4.4.2.5	Influence of time on stream – deactivation studies	158
4.4.2.6	Mechanism of the reaction	160
	Conclusions	162
	References	163

## CHAPTER 5 PHENOL HYDROXYLATION

5.1	Introduction	166
5.2	Phenol oxidation over sulphated zirconia systems	169
5.2.1	Influence of catalyst composition	170
i	Influence of metal incorporation	170
ii	Influence of iron content	172
5.2.2	Influence of reaction temperature	174
5.2.3	Influence of reaction time	175
5.2.4	Influence of H <sub>2</sub> O <sub>2</sub> to phenol ratio	176
5.2.5	Influence of solvent	176
5.2.6	Mechanism of the reaction	177
	Conclusions	179
	References	181

## CHAPTER 6 NITRATION

6.1	Introduction	183
6.2	Nitration of toluene over sulphated zirconia systems	186
6.2.1	Influence of catalyst composition	186
i	Influence of metal incorporation	186
ii	Influence of iron content	188
6.2.2	Influence of reaction temperature	189

6.2.3	Influence of HNO <sub>3</sub> concentration	190
6.2.4	Influence of volume ratio	191
6.2.5	Influence of calcination temperature	191
6.2.6	Metal leaching and reusability	192
6.2.7	Mechanism of the reaction	194
	Conclusions	195
	References	196

## CHAPTER 7      SUMMARY AND CONCLUSION

7.1	Summary	198
7.2	Conclusions	200

### 1.1 CATALYSIS- GENERAL INTRODUCTION

A catalyst in simple terminology can be defined as a substance that transforms the chemical reactants into products through an uninterrupted and repeated cycle of elementary steps in which the catalyst participates while being regenerated in its original form at the end of each cycle during its life time. It alters the kinetics of a chemical reaction without affecting the thermodynamics [1].

Incidentally, the terms organic chemistry and catalysis were both coined by the Swedish chemist Berzelius in 1807 and 1835 respectively. Subsequently, catalysis and organic synthesis evolved along different paths. The branch of catalysis developed initially as a sub-discipline of physical chemistry. With the advent of petrochemical industry in 1920's, catalysis was widely applied in oil refining and to a large extent in bulk chemicals manufacture. Most of the early applications of catalysis in industry were confined to the manufacture of heavy chemicals, the major emphasis being on the petroleum and petrochemical industries. Fine chemical manufacture remained the domain of synthetic organic chemist who adhered to the stoichiometric reagents developed in the 19<sup>th</sup> century. In spite of the general advantages of being highly active and readily available, the classical stoichiometric technologies such as reductions with metal hydrides and dissolving metals, oxidations with permanganate and hexavalent chromium compounds, halogenations, nitrations, Grignard reactions and a wide variety of reactions employing stoichiometric amounts of mineral (HF, HCl, H<sub>2</sub>SO<sub>4</sub>, etc.) or Lewis (AlCl<sub>3</sub>, BF<sub>3</sub>, etc.) acids, produce large amounts of inorganic salts as waste, which, till recently was not considered to be a serious problem. With growing ecological concern, chemical producers have been subjected to increasing pressure to minimise the generation of waste chemicals. Consequently, traditional concepts of process efficiency, which had an exclusive focus on chemical yield, are being replaced by one which assign economic

value to waste elimination. The key role of catalysis in waste minimisation is evident. An additional benefit of catalytic conversions is that they often provide short-cut routes as alternatives to classical multistep syntheses. Catalysts, besides reducing the cost of production, also improve the product quality. Catalysis plays a key role in the stereo selective and stereo specific synthesis and the synthesis of chiral compounds, particularly in pharmaceutical and fine chemical industries.

Catalysis forms a link between the three main branches of chemistry namely inorganic, physical and organic chemistry. Most of the catalysts, being of inorganic nature, are prepared employing the basic principles of inorganic chemistry whereas their complete characterisation requires the application of techniques that form part of physical chemistry. The application of catalysis, being mainly in organic reactions and syntheses, requires a fundamental knowledge of the nature of reactions and their mechanisms. The large-scale practice of catalysis also incorporates principles of chemical engineering.

The present day chemists are faced with the challenge of developing catalysts, which are highly active, selective and stable and that can be easily recycled. The stress is on a technology that will reduce the dispersion of harmful chemicals in the environment and impart regenerability and durability to the catalysts in such a way as to increase the industrial competitiveness.

## 1.2 SOLID ACID CATALYSIS

Solid acids are sought as replacements for harmful, corrosive acids like  $\text{H}_2\text{SO}_4$ , HF,  $\text{AlCl}_3$ , etc. Large volumes of acids used as catalysts and waste of such acids formed by the decomposition/neutralisation is the strong driving force for developing environmentally benign processes based on solid acids. Substitution of liquid acid and bases by solid catalysts in organic reactions is the prime requisite for a better preservation of the environment. More and more complicated organic reactions have been investigated in presence of solid catalysts, the ultimate aim being the overall improvement of activity and selectivity. Poor selectivity results in wastage of materials, separation problems, waste disposal and concerned environmental issues. Another important aspect of catalysis is the suppression of unwanted side reactions.



In short, the major objectives guiding the development of solid catalysts include

- Increase of desired product selectivity
- Maximisation of product yield
- Replacement of stoichiometric reagents with non-stoichiometric and environmentally friendly catalysts
- Easy separation of final products from the reaction mixture and efficient catalyst recovery
- Reduction of waste disposal
- Enhancement of reusability and recycling options

In recent years, a large variety of organic transformations have been reported using catalysts like zeolites and other microporous materials, clays, oxides and mixed oxides. Almost all acid catalysed reactions, many of which require very corrosive acids in homogeneous conditions have been achieved using solid acid catalysts [2]. Metal oxides, mixed oxides and supported oxides form a highly versatile class of catalysts due to their easily manipulated properties and/or a wide range of preparation variables. Titanium and vanadium based microporous materials have been accepted as being efficient for oxidation reactions [3]. Cationic and anionic clays constitute another class of solid acids finding wide applications as ceramics, building materials, paper coatings, fillers, pharmaceuticals, etc. [4].

### 1.3 SOLID SUPERACIDS

As industry is turning increasingly towards the use of solid acid catalysts instead of liquid ones, solid superacids are being extensively studied [5]. The name "superacid" was first suggested by Hall and Conant for strongly acidic non-aqueous solutions [6]. Superacids can be defined as an acidic media. which exhibit an acidic strength higher than that of 100% sulphuric acid.

Three main types of solid superacids have been recognised [7]. These include (i) mounted acids obtained by the fixation of a liquid acid such as  $\text{SbF}_5$ ,  $\text{NbF}_5$ ,  $\text{SbF}_5\text{-FSO}_3\text{H}$ ,  $\text{BF}_3$ ,  $\text{TaF}_5$ , etc. on supports of high surface area such as  $\text{SiO}_2$ ,  $\text{SiO}_2\text{-Al}_2\text{O}_3$ , graphite, ion exchanged resin, etc. (ii) combined acid obtained by the combination of metal halides

with metal salts such as  $\text{AlCl}_3\text{-CuCl}_2$ ,  $\text{AlCl}_3\text{-CuSO}_4$ , etc. and (iii) sulphate promoted metal oxides. Superacids by metal oxides have also been reported [8-12]. These are synthesised in the same manner as that of sulphated superacids by supporting  $\text{ZrO}_2$ ,  $\text{SnO}_2$ ,  $\text{TiO}_2$  and  $\text{Fe}_2\text{O}_3$  with  $\text{WO}_3$  and  $\text{ZrO}_2$  with  $\text{MoO}_3$  and  $\text{B}_2\text{O}_3$ .

#### 1.4 SULPHATED METAL OXIDES

The first report of sulphated metal oxides as superacids appeared in 1962, when Holm and Bailey imposed superacidic nature in sulphated zirconia containing platinum [13]. The interest in these systems was revived after Arata and co-workers reported the exceptionally strong acidic nature of sulphated zirconia systems capable of catalysing the isomerisation of butane to *n*-butane even at room temperature [14,15]. Oxides of certain other transition metals like titanium, iron, hafnium, etc. also have been reported to exhibit superacidity upon proper treatment [8]. The superacidity is considered to be generated by the strong interaction between the oxide and sulphate ion. The nature and relative concentrations of surface acidic sites (both Lewis and Brønsted) turn out to depend primarily on the type and concentration of surface sulphate ions. The nature of the sulphur species seems important rather than the sulphate content in itself [16]. Considerable controversies exist regarding the superacidity of sulphated metal oxide systems. Several groups [17-19] claim that sulphated zirconia is not a superacid and is only comparable to that of 100% sulphuric acid.

A remarkable increase in surface acidity and catalytic activity of  $\text{Fe}_2\text{O}_3$  treated with sulphate ions followed by a thermal treatment was reported [20]. The system was found to be highly active for the well-known acid catalysed reactions [21] like dehydration of 2-propanol and ethanol. Iron oxide treated at high temperatures was also exceedingly active for the polycondensation of benzyl chloride [22] and the polymerisation of vinyl alkyl ethers [23] and isobutyl vinyl ether [24], which are generally promoted by Lewis acid catalysts like  $\text{TiCl}_4$  and  $\text{BF}_3\text{-etherate}$  [25].

The generation of superacidity was examined by introducing various sulphur compounds like ammonium sulphate,  $\text{SO}_3$ ,  $\text{SO}_2$  or  $\text{H}_2\text{S}$  onto  $\text{ZrO}_2$ ,  $\text{TiO}_2$ ,  $\text{Fe}_2\text{O}_3$ ,  $\text{Al}_2\text{O}_3$ ,  $\text{SnO}_2$ ,  $\text{SiO}_2$ , etc. Acid catalysed isomerisation of cyclopropane was employed as a test reaction [26]. High catalytic activity was observed for ammonium sulphate and  $\text{SO}_3$

modified  $\text{Fe}_2\text{O}_3$  while unpromoted and  $\text{SO}_2$  and  $\text{H}_2\text{S}$  modified  $\text{Fe}_2\text{O}_3$  were completely inactive. Oxidative treatment of  $\text{SO}_2/\text{Fe}_2\text{O}_3$  and  $\text{H}_2\text{S}/\text{Fe}_2\text{O}_3$  at  $450^\circ\text{C}$  resulted in pronounced catalytic activity whereas the reduction of ammonium sulphate and  $\text{SO}_3$  modified  $\text{Fe}_2\text{O}_3$  in  $\text{H}_2$  atmosphere resulted in a complete loss of activity. This suggests the importance of the oxidation state of sulphur in the generation of acidic properties. A +6 oxidation state of sulphur was critical for the development of superacidic properties. The catalytic activities of different sulphate promoted metal oxides for the isomerisation of cyclopropane at  $100^\circ\text{C}$  indicate that the electronegativity and co-ordination number of a metal cation in a metal oxide affect the acid strength.  $\text{ZrO}_2$ ,  $\text{TiO}_2$  and  $\text{Fe}_2\text{O}_3$  are classified as oxides having highly electronegative cations while  $\text{Al}_2\text{O}_3$  and  $\text{SnO}_2$  involve intermediate electronegative cations and the cations of all these oxides are 6- or 7- coordinated. Though  $\text{Si}^{4+}$  has high electronegativity, its co-ordination number is 4. Thus,  $\text{Si}^{4+}$  has difficulty in forming stable active sites, even when ammonium sulphate is admitted as promoter or to provide co-ordinatively unsaturated sites.

Acidity/basicity, electron donor properties and catalytic activity of sulphate modified stannic oxide [27] and sulphated samaria [28] for the esterification of acetic acid using *n*-butanol have been investigated by Sugunan *et al.* The surface electron donor properties of sulphate modified stannic oxide have been determined from the adsorption of electron acceptors of various electron affinities [7,7,8,8-tetracyanoquinodimethane (TCNQ, EA=2.84), 2,3,5,6-tetrachloro-*p*-benzoquinone (Chloranil, EA=2.4), 1,4-dinitrobenzene (PDNB, EA=1.77) and 1,3-dinitrobenzene (MDNB, EA=1.26)] on the oxide surface. When electron acceptors were adsorbed on the surface of oxides, corresponding anion radicals were formed on the surface. The surface develops remarkable colouration characteristic of each EA adsorbed and the oxide surface [29]. The colouration indicates the formation of new adsorbed species on the surface. A strong electron acceptor (TCNQ) can accept electrons from both strong and weak donor sites whereas a weak electron acceptor like MDNB can accept electrons from strong donor sites only. The difference in the limiting amount of TCNQ and MDNB adsorbed on the oxide surface would be an estimate of the number of weak and medium donor sites. Catalytic activities of the sulphated stannic oxide for the reduction of cyclohexanone in 2-propanol and oxidation of cyclohexanol with benzophenone have also been studied [27].

A comparative study of the anisole methylation activity of lanthanum promoted  $\text{SnO}_2$  catalyst and its sulphated analogue has also been carried out [30].

Following the reports of superacidity in  $\text{TiO}_2$  and  $\text{ZrO}_2$  the third member of the Titanium Group, Hf, was also tested for its superacidity [31]. The catalyst was obtained by exposing  $\text{Hf}(\text{OH})_4$  prepared by the hydrolysis of  $\text{HfCl}_4$  to 2N  $\text{H}_2\text{SO}_4$  and then calcining in air at 600-800°C. It was found to be active for the isomerisation of butane to isobutane and was found to be more stable and effective as a solid catalyst.

Non-metal sulphated materials like  $\text{SO}_4^{2-}/\text{SiO}_2$  system also show a similar enhancement in catalytic activity. In fact, higher activity of sulphated  $\text{SiO}_2\text{-Al}_2\text{O}_3$  for ethanol decomposition has been reported in comparison with unsulphated system [32]. Surface acidity of sulphated  $\text{TiO}_2\text{-SiO}_2$  sol-gels was also reported [33]. Sulphated silica is a highly active superacid catalyst, which quickly deactivates. Deactivation of  $\text{SO}_4^{2-}/\text{SiO}_2/\text{Pt}$  is less pronounced and still better is the deactivation resistance of  $\text{SO}_4^{2-}/\text{Pt}/\text{SiO}_2\text{-ZrO}_2$ . At the first glance it can be seen that Pt stabilises the  $\text{SO}_4^{2-}/\text{SiO}_2$  system and this role is also played by zirconia in the sulphated mixed oxide leading to a lower deactivation of the catalyst [34]. Sulphated metal oxides like  $\text{ZrO}_2$ ,  $\text{Fe}_2\text{O}_3$ ,  $\text{SnO}_2$ ,  $\text{TiO}_2$ , etc. have been shown to be the most promising superacidic catalysts for the low temperature processes of isomerisation, alkylation and cracking of paraffins [35,36]. The activity enhancement of metal oxides by sulphate addition was not observed for  $\text{MgO}$ ,  $\text{CaO}$ ,  $\text{CuO}$ ,  $\text{NiO}$ ,  $\text{ZnO}$ ,  $\text{CdO}$ ,  $\text{La}_2\text{O}_3$ ,  $\text{MnO}_2$ ,  $\text{ThO}_2$ ,  $\text{Bi}_2\text{O}_4$ ,  $\text{CrO}_3$ , etc.

## 1.5 ZIRCONIA AS CATALYSTS AND CATALYST SUPPORTS

Many solids that possess acid sites on the surface are used either as catalysts or catalyst carriers. The sites of the carrier influence the catalytic properties of a catalyst by interaction with the active components (support effect) or by providing acidic sites, which may make the catalyst bifunctional. Zirconia is currently attracting considerable scientific interest due to its potential use as a catalyst support or promoter for a variety of catalyst systems. In recent years zirconium dioxide has become very important in the field of high technology ceramics with improved mechanical properties (particularly in wear parts, *i.e.* engine applications) [37]. The acid-base polyfunctional nature, which determines the characteristic catalytic behaviour, has been studied by the adsorption of probe molecules

such as CO, CO<sub>2</sub>, pyridine and H<sub>2</sub> [38-40]. In view of the importance of the knowledge of the surface properties of ZrO<sub>2</sub>, a systematic investigation of the surface properties has been attempted to elucidate the role played by the preparation route, thermal history of the material and the presence of contaminant and/or dopant upon surface reactivity. Bolis *et al.* carried out a spectroscopic and calorimetric investigation on the development and suppression of surface acidity of monoclinic zirconia [41]. Zirconia is modified by the addition of other oxides (Y<sub>2</sub>O<sub>3</sub>, MgO, CaO), which stabilises the crystallographic phase and the microstructure required for a good performance as ceramic material [37].

The surface properties of zirconia have been extensively studied [42-44]. The catalytic activity of hydrous zirconium oxide calcined at different temperatures has been reported [45]. The existence of co-ordinatively unsaturated cations is responsible for Lewis acidity. Adsorption of water molecules results in the reversible transformation of Lewis acid sites into Brønsted acid sites. Brønsted acid sites and Lewis acid sites are the probable forms of acidity at lower and higher temperatures respectively [46].

Oppenauer oxidation of secondary alcohols proceeded efficiently over hydrous zirconium oxide [47]. However there was a difficulty with primary alcohols. This is due to the fact that the ability of a primary alcohol to provide a hydrogen donor is less than that of secondary alcohol [48]. Oppenauer oxidation of primary alcohols over hydrous zirconium (IV) oxide has been successfully carried out using *p*-benzoquinone or benzophenone as hydrogen acceptor [49].

Convenient preparation of acetals over hydrous zirconium oxide has been reported [50]. Acetalisation of carbonyl compounds occurred easily over hydrous zirconium oxide. The major advantages are (i) the oxide is not soluble in any solvent and the catalyst can be easily removed by filtration (ii) the oxide is highly stable in air and can be used for repeated reactions (iii) the oxide is not sensitive to air or water and the reaction does not require water free conditions (iv) reaction can proceed without the azeotropic removal of water and (v) the oxide does not have strong acidic sites and therefore acetalisation can apply for compounds which are unstable in acids. Because of the low acidity of zirconium oxide, dehydration to methyl vinyl ketone was suppressed and the acetalisation of the  $\alpha,\beta$ -unsaturated ketone proceeded mainly at room temperature.

Liquid phase reduction of aldehydes and ketones with 2-propanol was carried out over hydrous zirconium oxide [48]. The reaction is analogous to the well-known MPV reduction in which aldehydes and ketones are reduced with isopropanol in the presence of aluminum isopropoxide. MPV reduction needs a strong acid treatment to neutralise the alkoxide salt and isolation of products involve tedious procedures. These disadvantages are overcome in the use of heterogeneous catalysts. Vapour phase reduction of aldehydes and ketones with 2-propanol over hydrous zirconium oxide has been reported by Shibagaki *et al.* [51]. It was shown that the conjugated or sterically hindered ketones, which resisted the reduction in liquid phase, could be reduced in vapour phase, but dehydration competed at high reaction temperatures.

## 1.6 MIXED OXIDES OF ZIRCONIA

Mixed oxides behave differently from single oxide components. The generation of new and strong acid sites on mixing oxides has been ascribed to a charge imbalance localised on  $M_1$ -O- $M_2$  bonds formed in the mixed oxide where  $M_1$  is the host metal ion and  $M_2$  the doped metal ion [52]. Both Brønsted and Lewis sites contribute to the acidity of the oxides. At high activation temperatures Lewis sites are formed by the removal of water molecules from two hydroxyl groups [46]. The charge imbalance may originate even on single oxide due to surface imperfections in small crystallites. At much higher activation temperatures the lattice distortions also contribute to an increase in acid sites. The surface acidity/basicity studies reveal the presence of groups of sites having different energies. It has been suggested that the acid and base sites are metal ion and the  $O^{2-}$  on the surface and the site energy distribution is attributed to the presence of metal ions and  $O^{2-}$  in different co-ordinations, the lower co-ordinated ion sites being responsible for strong acid/base sites [53].

Studies on mixed oxides of zirconia with other oxides have been reported. The surface acidity and basicity of zirconium and its mixed oxide with samarium was estimated by Hammett indicator technique [54]. Acid base characteristics of binary oxides of Zr with Ce [55,56] and La [55,57] were examined by Sugunan *et al.* Incorporation of  $CeO_2$  into  $ZrO_2$  increases the acidity, which is evidenced by low  $H_{0\max}$  values. However, the incorporation of lanthanum increases the basicity upto 500°C and then it decreases at

higher activation temperatures. In the case of zirconia-ceria, moderately strong acid sites appear with increase in activation temperature. This may be due to the conversion of weak acid sites into stronger Lewis sites caused by the elimination of water molecules [52]. Binary oxides of zirconia and lanthanum and their ternary oxides with alumina of various compositions have been prepared by co-precipitation method from their nitrate solutions and were evaluated for acidity [57]. Acid base properties of mixed oxides of  $ZrO_2$  with  $SiO_2$  [58],  $SnO_2$  [59],  $TiO_2$  [60] and  $Y_2O_3$  [61] have also been reported.

Shimokawabe *et al.* [62] carried out characterisation of copper-zirconia catalysts prepared by impregnation method using tetramminecopper (II) nitrate solution. The copperammine complex held on the surface of zirconia support existed in three different states *i.e.*, (i) isolated Cu(II) ions (ii) clustered Cu(II) ions and (iii) tetrammine copper(II) nitrate. These precursors were transformed into bulky copper(II) oxide through highly dispersed copper(II) oxide depending on calcination temperature. *n*-Butane isomerisation over tungsten oxide supported on zirconia was investigated by Yori *et al.* [63].

Calafat *et al.* [64] reported the influence of preparation conditions on the surface area and phase changes of  $MoO_3/ZrO_2$  catalysts. Addition of Mo preserves the metastable phase of  $ZrO_2$ . The surface area of the systems increases and reaches a maximum value at a certain Mo content depending on the calcination temperature. At high  $MoO_3$  content, XRD patterns reveal the formation of  $Zr(MoO_4)_2$ . The effects of tungsten precursor and preparation conditions on the properties of platinum free or platinum containing  $WO_x$  promoted zirconia have been studied [9]. In spite of the different precursors employed, the same  $WO_x$  species was found in the catalyst. The most important differences are related to the migration of the precursor oxoanions into the narrowest pores of zirconium hydroxide, thus leading to different pore size distributions and size and amount of  $WO_3$  particles after calcination. Both amorphous and crystalline  $WO_3$  were detected on the surface.

Boyce *et al.* [10] investigated the crystallisation behaviour of tungstate supported on zirconia and its relationship to acidic properties. Zirconia-silica-tungstate aerogels were prepared by sol-gel technique followed by supercritical drying. Addition of silica stabilises zirconia-tungstate against sintering by heat treatment. On poorly mixed

zirconia-silica, tungstate remains dispersed on the mixed oxide surface, which consists largely of silica patches. Thus tungstate dispersion does not behave as it would on bulk silica but it is stabilised on the silica patches by the underlying zirconia. A reduction in the catalytic activity, compared to zirconia-tungstate, demonstrates that dispersed tungstate on silica patches does not stabilise the strong acid sites capable of *n*-butane isomerisation. Improving the mixing by sol-gel technique of prehydrolysis reduces the segregation of silica on zirconia surface.

Spectroscopic studies on tetragonal ZrO<sub>2</sub> supported MoO<sub>3</sub> and NiO systems were conducted by Liu *et al.* [11]. For tetragonal ZrO<sub>2</sub> supported MoO<sub>3</sub> system, LRS and UV-vis DRS results indicate the formation of monomolybdate and polymolybdate species in samples with low and high Mo loadings respectively. In ZrO<sub>2</sub> supported NiO-MoO<sub>3</sub> binary oxide systems, the loading order of the oxides is critical for the species formed on the surface. No trace of NiMoO<sub>4</sub> phase could be detected after inversion of the loading sequence. The interaction of MoO<sub>3</sub> with tetragonal ZrO<sub>2</sub> is stronger than with NiO and the interaction of MoO<sub>3</sub> with NiO is stronger than that of NiO with tetragonal ZrO<sub>2</sub>. The dispersion of MoO<sub>3</sub> on the NiO modified ZrO<sub>2</sub> depends on the calcination temperature, whereas it has no effect on the dispersion of NiO on the MoO<sub>3</sub> modified ZrO<sub>2</sub>, at least in the range 673-823 K.

The surface properties of zirconia and its mixed oxide with samaria have been correlated with the catalytic activity of these systems towards the liquid phase reduction of cyclohexanone in 2-propanol [54]. The lack of linear correlation between activity and basicity implies that the basic sites with  $H_0 \geq 4.8$  may be the catalytically active sites. The lowering of catalytic activity at higher activation temperatures has been accounted as due to the changes in crystallinity of ZrO<sub>2</sub> for which a phase transition from amorphous to monoclinic phase at higher temperatures has been confirmed by thermal analyses [65]. Liquid phase reduction of cyclohexanone in 2-propanol over ZrO<sub>2</sub>-Y<sub>2</sub>O<sub>3</sub> [61] and mixed oxides of Zr, La and Al [57] have also been reported. The acid-base and surface electron properties and the catalytic activity of cerium-zirconium mixed oxides at various compositions towards the liquid phase esterification of acetic acid with *n*-butanol were also tested [56].



## 1.7 SULPHATED ZIRCONIA AS CATALYSTS

The use of sulphated zirconia has attracted increasing interest in the literature because of the superacidic properties induced in these materials by the presence of  $\text{SO}_4^{2-}$  ions and these properties have been exploited in a variety of reactions. High surface area coupled with high acidity makes it a potential catalyst for many reactions generally catalysed by strong acids. Surface properties and catalytic activities of sulphated zirconia strongly depend on their preparation conditions [16,66,67]. Many preparative parameters have been observed to affect the nature and strength of the active sites on sulphate doped  $\text{ZrO}_2$  and quite important among these include the  $\text{ZrO}_2$  preparation procedure,  $\text{ZrO}_2$  pre-firing temperature, sulphate doping procedure, sulphate loading and temperature of catalyst calcination (activation) before reaction. The major interest on sulphated zirconia systems stems from its unusual ability to catalyse several reactions including paraffin isomerisation, paraffin cracking, isoparaffin alkylation and acylation of aromatics at relatively low temperatures [68]. The high initial activity may be attributed to its unusual acidity. Despite numerous studies, there is no universally accepted theory regarding the nature of the catalytically active sites. Some authors claim that strong Lewis centers [69] are responsible for high activity while others believe that the unusual activity is associated with Brønsted acid sites [70].

### 1.7.1 PREPARATION METHODS

Solid oxide catalysts or their carriers are frequently prepared by the precipitation from aqueous solution of suitable salts followed by their thermal treatment. Depending on the conditions of precipitation, the resulting products exhibit substantial differences not only in magnitudes of the specific surface area and pore size distribution but also in the surface properties. The differences in surface properties can be partially explained by the diversity in procedures of preparation, which influences the degree of hydration.

The conventional method of preparation of sulphated zirconia involves the first step preparation of zirconium hydroxide followed by a second step of sulphating the hydroxide. Arata and co-workers prepared zirconium hydroxide by the hydrolysis of  $\text{ZrOCl}_2$  or  $\text{ZrO}(\text{NO}_3)_2$  with aqueous ammonia and the hydroxide was sulphated using ammonium sulphate or sulphuric acid solution [14,15,71]. Calcination of the sulphated

oxide at high temperatures generates strong acidity [71-73]. Several other zirconium salts such as  $ZrCl_2$ ,  $Zr(NO_3)_4$ ,  $Zr(OC_3H_7)_4$  were also used as the zirconium source [35,73-77]. The salt utilised for the preparation of the hydroxide also has a significant impact on the crystal phase of zirconia obtained after drying and calcination [73]. Urea may be used for hydrolysis instead of aqueous ammonia [78]. The addition rate of the base, final pH etc. was also found to influence the crystalline structure and the surface properties of the catalyst [16,75,79,80].

The standard preparation method involves the filtration of dilute sulphuric acid through a bed of metal hydroxide [14,15,31,71,81-83]. This classical method was subsequently replaced by the immersion of the dried hydroxide [84-86] or oxide [69] in  $H_2SO_4$  solution, stirring the mixture to allow the adequate adsorption of  $SO_4^{2-}$ . The solid was separated by filtration or decantation and subjected to drying without prior washing. Ammonium sulphate also can be used for impregnation. Use of ammonium sulphate instead of acid leads to low sulphate concentration, surface area and poor activity [69,81,87,88]. Other sources of sulphur like  $SO_2$ ,  $H_2S$ ,  $CS_2$ ,  $SO_2Cl_2$ , etc. also can be used [39,76,80]. Less frequently, precipitation of the metal hydroxide from a sulphate salt and partial elimination of sulphate by washing are employed [89,90]. Hino and Arata also reported a dry kneading method in which the dried hydroxide is kneaded thoroughly with ammonium sulphate using mortar and pestle and then calcined [91].

The preparation of  $Zr(OH)_4$  has also been achieved by sol-gel technique [92]. Ward and Ko [93] reported a single step preparation of sulphated zirconia by sol gel method. Doping from the gas phase ( $SO_2+O_2$ ) was also reported [39]. Sulphated zirconia having a BET surface area of  $90\text{ m}^2/\text{g}$  and temperature resistant mesoporous texture was prepared by the thermolysis of zirconium sulphate at 1000 K [94,95]. Surface properties of this sample investigated by IR studies of surface sulphates, CO adsorption at 77K and room temperature adsorption of pyridine showed close similarity to those of sulphated zirconia prepared by impregnation technique. Mesoporous materials prepared in this way maintain high surface area even after calcination at high temperature [96]. This leads to a consolidated mesopore system, which was also observed for sulphate-doped  $\gamma$ -alumina [97]. Sulphate species remaining after thermolysis of the zirconium sulphate precursor

was found to be mainly at the oxide surface and showed enhanced Lewis and Brønsted acidity as compared with pure partially hydroxylated zirconia.

A common feature of the immersion technique in preparation procedure is that the solid adsorbs an undetermined and mostly unreported amount of sulphate from the excess it is exposed to and this results in lack of reproducibility in samples prepared in different batches. Sulphur content strongly influences the properties of the catalysts. The sulphur content depends strongly on the calcination temperature. Hence, some control of sulphate loading can be achieved by changing the calcination temperature [66,98]. A change in the acid concentration was suggested as an alternate method for changing the ultimate sulphate concentration [66]. But working under approximately the same conditions, there was no agreement in the loading levels reported from various laboratories. The major problem is that the procedure is inherently difficult to be described in sufficiently precise terms to be reproduced even by different workers in the same laboratory. The time needed for a solution to pass through the solid and the amount of liquid retained depends on the type of the filter or paper and its porosity, quantity of the solid and the size and distribution of the particles. In the case of adsorption in a beaker followed by decanting, the amount of liquid left in the vessel after decanting from a solid normally differs for different operations [99].

The relatively large excess of sulphuric acid used in the techniques constitute another difficulty because the acid decanted or filtered does not have the same concentration as the original acid and may also dissolve some cations present in the catalyst and so cannot be reused as such for the preparation of the next batch of the catalyst. The disposal or purification of this acid waste creates environmental problems. Taking into consideration all these factors, an efficient method seems to be the use of calculated amount of the acid in the impregnation step followed by evaporation of the solvent and calcination. A sulphate content higher than that obtained by the percolation method using the same amount of  $H_2SO_4$  is obtained by the controlled impregnation technique. This method seems to be employed in certain studies concerning the effect of sulphur content on the surface properties of the catalysts [76,77,100,101]. The controlled impregnation technique allows variation of the sulphur content without a change in the

calcination temperature [102]. Moreover, this method also avoids the generation of waste sulphuric acid after the impregnation step.

### 1.7.2 SURFACE PROPERTIES

In comparison to pure zirconia, sulphated zirconia showed a higher surface area after calcination at high temperature in air. Arata *et al.* [71,103] observed finer particles in sulphated zirconia than in pure zirconia. The larger surface area of sulphated zirconia can be attributed to the retardation of crystallisation and the resistance to sintering at high temperatures [16,35,78,80,104]. Two processes were identified as being responsible for the changes in pore structure and surface area: (i) crystallite growth and an accompanying phase transformation and (ii) intercrystalline sintering (neck formation and growth). Both these phenomena occur *via.* a mechanism of surface diffusion. The intercrystalline sintering becomes more pronounced at higher calcination temperatures [105]. The delay in the transition from amorphous to crystalline material is also supported by the thermal analysis results. The exothermic peak in the DTA curve at around 410°C, which can be attributed to the crystallisation of pure zirconia, is shifted to higher temperatures after sulphation indicating the retardation of crystallisation [106]. The higher the sulphate content, the higher the exotherm temperature [78,67,93,107]. Yamaguchi *et al.* [78] proposed that the exothermic peak is due to a phase transition from a metastable to a stable one, while Scurrall [35] proposed it as being due to the inhibiting effect of  $\text{SO}_4^{2-}$  for the crystallisation of  $\text{ZrO}_2$ . The existence of a glow exotherm was also observed in the DSC analysis of pure zirconia [105]. The existence of such an exotherm is not confined to zirconia alone, it being a well-documented feature of many metal oxide and hydrous oxide systems [105]. A satisfactory explanation of its origin is still lacking. Its occurrence in hydrous zirconia systems is commonly associated with the transition of an initially X-ray amorphous phase into a crystalline modification of zirconia.

Zirconia may exist in two crystal phases after calcination below 800°C - a metastable tetragonal phase and a thermodynamically favoured monoclinic phase. The XRD analysis reveals the co-existence of the tetragonal and monoclinic phases in pure zirconia after calcination above 550°C. At temperatures higher than 650°C, only monoclinic phase was observed. In contrast, for the sulphated samples only tetragonal

phase existed in the range 550-700°C. Monoclinic phase started to form after a calcination temperature of 800°C [108]. Thus sulphation stabilises the catalytically active tetragonal phase. The transformation from the metastable tetragonal phase to the monoclinic phase is related to the deterioration of the superacidity of the sample.

The formation and stability of the metastable tetragonal phase can be rationalised in several ways. On the basis of thermodynamic considerations, Garvie and co-workers [109-111] and Pyun *et al.* [112] attributed the stabilisation to surface and strain energy effects; these effects allowed the calculation of a critical crystallite size below which the tetragonal phase was more stable than the monoclinic modification. At low calcination temperatures the monoclinic crystallites are smaller than the metastable tetragonal crystallites but the situation is reversed at high calcination temperatures [105]. With increase in calcination temperature the tetragonal zirconia sinters to form increasingly larger crystallites: when a critical size is reached, the transformation from tetragonal phase to monoclinic phase occurs. Garvie and Goss calculated that tetragonal crystallites greater than approximately 100Å cannot exist at room temperature [109-111]. It was also observed that the monoclinic crystallites grow more rapidly than the tetragonal ones as the calcination temperature is increased [105].

In the tetragonal bulk phase, each zirconium atom is co-ordinated to eight different oxygens. Four Z-O bonds are significantly shorter than the other four. The four short Zr-O bonds constitute one distorted tetrahedron and the four long Zr-O bonds constitute another distorted tetrahedron [113]. In the absence of adsorbates, Zr atoms at the (001) surface of tetragonal zirconium oxide are co-ordinated to only six oxygen atoms. Each Zr atom can therefore interact with the surface adsorbates through two vacant co-ordination sites [114]. The facts that crystallisation can be retarded for sulphated zirconia and that tetragonal phase is stabilised when sulphur species is present indicate that the acid site structure is sensitive to the separation between the metal and oxygen atoms at the oxide surface. The multiple interactions may not be possible for monoclinic ZrO<sub>2</sub> because the Zr-O-Zr spacing is too large [115].

Norman *et al.* [104] proposed that the presence of the bridging sulphate in sulphated zirconia has three effects. The first is the improved thermal stability of sulphate

over hydroxyl bridges. According to Aiken *et al.* [116] the thermal stability of sulphate to zirconium linkages is much higher than that of the hydroxyl bridges across two Zr atoms. The presence of sulphate species, which are not removed until the temperature exceeds 700°C, delays the formation of some oxo bonds, retards sintering and thus stabilises the surface area. The second effect is that the replacement of  $\text{SO}_4^{2-}$  for  $\text{OH}^-$  increases the Zr-Zr separation from the range 3.3–3.7 Å for hydroxyl bridges to the range of 3.5–4.3 Å for the sulphate bridges. The formation of nuclei and the crystallisation of zirconia under these circumstances are therefore delayed. The third effect is related to the impeded diffusional processes due to the rigidity imparted to the structure by bridging sulphate ions.

High-resolution transmission electron microscopy has been used for the characterisation of the morphology and surface structure at an atomic level of sulphated and sulphate free zirconia [117]. The presence of sulphate groups stabilises the tetragonal phase of zirconia and also induces the formation of well-faceted small zirconia crystallites. The presence of sulphate groups also induces the preferential formation of relatively long flat (110) plane of tetragonal zirconia. The geometry of (110) plane is such that it can accommodate the sulphate groups in a two or three fold co-ordination *i.e.* bidentate or tridentate structure.

Farcasiu and Li [102] established a correlation between the surface properties of sulphated zirconia systems and the amount of sulphate retained after calcination. According to them, an optimum catalyst should contain the maximum amount of sulphate near the surface, but not necessarily on the surface and should crystallise in the tetragonal form. The crystal structure of sulphated zirconia is also affected by the sulphur content. The XRD data reveal that the sulphated zirconia with low or medium sulphur content crystallises only in the tetragonal form, whereas at higher sulphate content a minor fraction of monoclinic phase also appear. According to XPS data, at high sulphate loadings, part of the sulphate is present in the bulk phase, rather than on the surface. The decrease in surface area and the change in crystallinity with increase in sulphur uptake appear to be related to the sulphate migration into the bulk.

The primary products of thermal decomposition of sulphated zirconia are  $\text{SO}_2$  and  $\text{O}_2$  [115], which also agree with the mass spectrometric analysis results [107]. The facts that the absorbance band losses caused by heating sulphated zirconia correlate with the spectral changes observed when sulphated zirconia is made by adsorption of  $\text{SO}_2$  in excess  $\text{O}_2$  and that  $\text{SO}_2$  and  $\text{O}_2$  are the main products of thermal decomposition of sulphated zirconia suggest that the decomposition process may be the reverse of formation reaction when  $\text{SO}_2$  and  $\text{O}_2$  are employed for sulphation. TG-MS relative mass spectral ion intensities indicated that the amount of  $\text{SO}_2$  formed during the thermal decomposition exceeded the amount of  $\text{O}_2$  by more than a factor of 2. A 2:1 ratio of  $\text{SO}_2:\text{O}_2$  suggests the stoichiometric loss of  $\text{SO}_3$  on thermal decomposition of sulphated zirconia. The slight excess in the ratio may be due to the fact that not all oxygen atoms formed by thermal decomposition of sulphated zirconia yield  $\text{O}_2$ . Some oxygen atoms may have reacted with the surface impurities to form small amounts of oxygenated organics [115].

The deactivation of sulphated zirconia catalysts in the isomerisation of *n*-butane has been studied using a combined TGA/FT-IR technique [118]. Following deactivation in the *n*-butane isomerisation reaction, two  $\text{SO}_2$  desorption maxima, centered at  $600^\circ\text{C}$  and  $800^\circ\text{C}$  were observed under  $\text{N}_2$  flow. Coincident with the low temperature desorption maximum of  $\text{SO}_2$ , a  $\text{CO}_2$  desorption maximum was also observed. The area under the high temperature  $\text{SO}_2$  peak is rather insensitive to the time on stream whereas that corresponding to the low temperature  $\text{SO}_2$  peak at  $600^\circ\text{C}$  appears to increase with the deactivation time. Under  $\text{O}_2$  flow, the  $\text{CO}_2$  desorption peak got shifted to lower temperature ( $500^\circ\text{C}$ ) and only a single peak corresponding to  $\text{SO}_2$  evolution was observed. The loss of low temperature sulphur results in the irreversible deactivation of the catalyst in the isomerisation reaction. Under an oxygen flow, the coke could be selectively burned off without removing the low temperature sulphur, which results in complete restoration of catalytic activity. Regeneration in  $\text{N}_2$  at  $550^\circ\text{C}$  results in an irreversible loss of catalytic activity while regeneration in  $\text{O}_2$  at  $450^\circ\text{C}$  essentially restores the activity to that of fresh catalyst. In  $\text{N}_2$  flow, the carbon atoms deposited at the surface sites react with the oxygen atoms of the surface sulphate groups to form  $\text{CO}_2$ . The evolution of  $\text{CO}_2$  destabilises the surface sulphate groups due to a change in the co-

ordination of surface sulphur atoms, which results in the immediate evolution of  $\text{SO}_2$ . This also accounts for the evolution of  $\text{CO}_2$  and  $\text{SO}_2$  at approximately the same temperature. In oxygen flow the oxygen from the gas phase reacts directly with the surface carbon atoms to form  $\text{CO}_2$ .

### 1.7.3 SURFACE ACIDIC PROPERTIES

The acid-base properties of metal oxide carriers can significantly affect the final selectivity of heterogeneous catalysts [21]. In acid catalysis, the activity, selectivity and stability of acid solids are determined to a large extent by their surface acidity, *i.e.* the number, nature, strength and density of acid sites. The acidity required for catalysing the transformation of reactants into valuable products or into byproducts is quite different. Certain reactions demand strong acid sites, while some others are catalysed by weak acid sites [119]. The rate of certain bimolecular reactions depends on the space between acid sites probably because their catalysis requires several acid sites [120,121]. For skeletal transformations of hydrocarbons, the rate depends essentially on the Brønsted acidity of the catalysts [119,122]. Good correlation has been obtained between the concentration of Brønsted sites and the rate of cumene dealkylation [123,124] xylene isomerisation [125], disproportionation of toluene [126] and ethyl benzene [127,128], *n*-hexane cracking [129], etc. Lewis sites in the vicinity of protonic sites increases the Brønsted acid strength and consequently their activity [130]. The dependence of the catalytic properties on the acid properties of solid catalysts is often more complex for the reactions of functional compounds. The acid sites (Lewis and/or Brønsted) and base sites, which co-exist in adjacent positions on the surface of acid catalysts, participate together in most of these reactions (acid-base bifunctional catalysis) [21]. The rate and selectivity of reactions that do not occur by acid catalysis can also be affected by acidity. This is evident from the oxidation of hydrocarbons on transition metal oxides. Acid-base properties of these oxides either influence the adsorption and the desorption rates of the reactants and products or initiate side reactions [131]. The acidity of solids plays a significant role when these are used as supports. Interaction of the support with the active component can influence their catalytic properties. Thus, characterisation of the acidity of catalysts is an important step in the prediction of their catalytic utility [132].



### *i) Nature of surface acidity*

The nature and relative concentrations of surface acidic sites (both Lewis and Brønsted) at the surface of sulphate doped zirconia catalysts depend primarily on the type of the sulphates present at the surface. The type of sulphate is found to depend on several preparative parameters and the most important among them are the overall surface sulphate concentration, hydration-dehydration degree and the activation temperature [77]. Some authors claim that strong Lewis centres [69,76,88] are responsible for high activity while others believe that the unusual activity is associated with Brønsted acid sites [70,133]. For any given surface sulphate loading below the monolayer coverage, the particle morphology of the starting  $ZrO_2$  system turns out to be of primary importance in determining the type and amount of sulphates and consequently the type and amount of the surface acidity that is induced by the surface sulphates. In particular, the crystallographically defective terminations yield the thermally most stable sulphate groups. With increasing surface sulphation, more and more surface  $Zr^{4+}$  cations located on the regular patches of low index crystal planes, which in the case of hydrated  $ZrO_2$  are covered by surface -OH groups, become shielded by the sulphate groups. The latter are thermally more stable than the surface -OH groups of pure  $ZrO_2$ . Most sulphate groups which form on the exposed patches of regular crystalline planes can induce protonic acidity, especially if they are in the form of complex polynuclear sulphates favoured at high loadings [77].

### *ii) Surface acidity determination*

Benesi method (*n*-butyl amine titration) has been widely employed as a conventional method for determining the acid strength distribution of solid acid surfaces [134,135]. This involves the titration of the solid acid suspended in a non-aqueous medium like benzene with *n*-butyl amine. When suspended in non-aqueous medium in presence of the indicator, the solid develops a colour depending on the  $pK_a$  value of the indicator as well as that of the solid acid. If the colour developed is that of the acid form of the indicator, then  $H_0$  of the acid is less than or equal to the  $pK_a$  of the conjugate acid of the indicator. The lower the  $pK_a$  of the indicator, the higher the acid strength of the solid. It is assumed that the adsorption equilibrium of both amine and indicator molecules

with acid sites is attained on the solid surface. This assumption has been questioned on the basis of the heterogeneity and anisotropy of solid surfaces. The establishment of adsorption equilibrium needs the adsorption-readsorption cycles of basic molecules once adsorbed on the surface. According to Take *et al.*, it is very difficult for either *n*-butyl amine or indicators, particularly the former, to reach adsorption equilibrium with acid sites under the usual conditions in the *n*-butylamine titration method [136]. This was also confirmed by Deeba and Hall [137] and Adeeva *et al.* [19] by independent works. Disregard of this difficulty might lead to an over estimation of the acid strength. Some serious limitations are also associated with the experimental procedure - the uncertainty in observing the colour changes of indicators by naked eyes, possible interaction between solvents and catalysts, etc. This method is also not suitable for coloured materials and may have some problems when the pore sizes of solids are too small for the large molecules of the indicators and if there exists any interactions between indicators and any sites (basic or redox sites) other than acidic sites.

Another method most frequently used is based on the chemisorption of basic compounds [21,122,131]. Adsorption of bases followed by calorimetry or thermodesorption of stable bases followed by gravimetry or volumetry gives the total number of acid sites (Lewis and Brønsted) and their distribution according to their strength but do not differentiate between Lewis and protonic acid sites. The temperature programmed desorption (TPD) of an adsorbed base like pyridine [138-140], NH<sub>3</sub> [67,106,140-143], benzene [106,140,144], etc. can be used for characterising the acid strength distribution and amount. The method, however, suffers from the major drawback associated with the strong interaction between the adsorbate molecules and the surface sulphate species leading to oxidative decomposition of the adsorbed species during heating.

When sulphated Fe<sub>2</sub>O<sub>3</sub> was heated, decomposition of the sulphate species resulted in the evolution of gaseous SO<sub>2</sub>. In addition to desorbed pyridine, SO<sub>3</sub>, N<sub>2</sub>, CO<sub>2</sub> and H<sub>2</sub>O were also detected. Thus, the preadsorption of pyridine lowers the temperature of sulphate decomposition. The TPD spectrum of NH<sub>3</sub> preadsorbed on sulphated Fe<sub>2</sub>O<sub>3</sub> was also complicated although to a lesser extent compared to that of preadsorbed pyridine. The

formation of  $N_2$  was observed at the same temperature as that for  $SO_2$  formation indicating that a portion of ammonia decomposes as a result of sulphate decomposition [145]. Interaction of the adsorbate and sulphate group reduces the thermal stability of sulphate groups [146-148]. Thus the interaction of the sulphate groups with adsorbate molecules should be taken into consideration when using ammonia or pyridine as probe molecules.

IR spectroscopy of a solid on which pyridine or ammonia is adsorbed can be employed to distinguish between Lewis and Brönsted sites. The nature of acid sites contributes to hinder the pyridine chemisorption. While no specific configuration is required for the formation of the pyridinium ion on Brönsted sites, co-ordinated pyridine interacts with its electron pair on Lewis centers in a configuration perpendicular to the surface sites implying larger diffusion restrictions in the case of microporous solids. There are IR bands characteristic of pyridine adsorbed on Brönsted acid sites ( $1545\text{ cm}^{-1}$ ) and pyridine adsorbed on Lewis site ( $1440\text{-}1465\text{ cm}^{-1}$ ). The existence of both Brönsted and Lewis acid sites on sulphated zirconia is confirmed by the DRIR spectra of adsorbed pyridine [149]. Kustov *et al.* [18] determined the Brönsted acidity of sulphated zirconia by adsorption of a weak base like benzene. The band shift of OH groups to lower frequency due to hydrogen bonding with the benzene molecules was taken as a measure of Brönsted acid strength. The larger the shift, the stronger is the acid strength.

Babou *et al.* [150] by IR spectroscopic study using  $H_2O$  and  $CO$  molecules to probe the acid strength suggested that sulphated zirconia with a sulphur content of 2 wt% equivalent to complete coverage of its surface, can be visualised as a  $H_2SO_4$  compound grafted onto the surface of zirconia in a way, which makes it very sensitive to water in a reversible way. Its acidity is similar to that of sulphuric acid but it is not really superacidic. They suggested that the sulphation of  $Zr(OH)_4$  proceeds *via* the following steps. (i)  $H_2SO_4$  dissociates in the aqueous solution (ii)  $Zr(OH)_4$  surface is ionised by trapping protons (iii) the ionised surface traps  $SO_4^{2-}$  anions (iv) upon outgassing, the dehydration proceeds depending on the outgassing temperature. Under severe dehydration conditions,  $(SO_3)_{ads}$  species are formed. These species exhibit strong Lewis acidity

capable of ionising benzene molecules into  $C_6H_6^+$  radical cations. At intermediate dehydration degrees  $H_3O^+$  and  $HSO_4^-$  species induce Brönsted acidity.

The acidic properties of pure and sulphated zirconia determined by FTIR spectroscopy of adsorbed CO and  $NH_3$  as probe molecules detected only Lewis acidity in pure zirconia [151]. The sulphation of tetragonal and monoclinic zirconia creates new bridging OH groups. Two types of Brönsted acidic centers and two types of Lewis acidic centers with enhanced acid strength were identified. The sulphation of tetragonal and monoclinic zirconia causes the same enhancement in Lewis acid strength. The coordination of the basic probe molecules on to the Lewis acid sites induces a decrease in the intrinsic Brönsted acidity of the bridging OH groups. The observed shift of the OH band induced by the adsorption of CO molecules and the related virtual Brönsted acidity of the OH groups are lower than the intrinsic acidity of the material. A comparison of the shifts of the OH bands by adsorption of CO under saturation conditions for sulphated zirconia with those of other strong Brönsted acidic materials like HZSM-5 [152,153] or H-mordenite [153] suggests that the sulphated zirconia is a weaker Brönsted acid than the acidic zeolites. Similar results were also obtained by the  $^1H$ -MAS-NMR spectroscopy with acetonitrile as probe molecule [19].

Pyridine (Py) and dimethylpyridine (DMP), which specifically adsorb on Lewis and Brönsted sites, have been used as probe molecules to investigate the surface acidic properties. Pyridine is adsorbed on the Lewis acid sites by donation of lone pair of nitrogen to the acid site (sigma donation to a co-ordinatively unsaturated cation) whereas pyridinium ions are adsorbed on Brönsted acid sites. DMP is specifically adsorbed on Brönsted sites due to steric effect and due to its higher basic strength it will detect even the weakest acid centers [154,155]. IR spectroscopic investigation after pyridine adsorption reveals quasi-identical concentration of Lewis and Brönsted sites at low calcination temperatures (below  $600^\circ C$ ). For higher calcination temperatures, Lewis acidity increased at the expense of Brönsted acidity [156].

Hall and co-workers [17,157] developed a UV-visible spectroscopic method for the measurement of acidity of solid catalysts. They pointed out that, due to red shifts of bands of unprotonated indicators, the visual observation of a yellow colour on adsorption

can be misleading, and the spectroscopic determination of peak maxima is essential for correct determination of the acid strength using Hammett indicators. Electron paramagnetic resonance (EPR) is able to detect paramagnetic carbocations formed by the charge transfer between surface sites and organic molecules. This has been used to characterise strong ionising sites on solid acid catalysts using probe molecules difficult to ionise, such as benzene. Coster *et al.* [158] used aniline as a probe molecule and obtained signals for the corresponding radical cation. Yamaguchi *et al.* reported that the adsorption of perylene on sulphated zirconia gave the typical EPR signal corresponding to a radical cation whereas no signal was observed for the nonsulphated  $\text{ZrO}_2$  indicating that the oxidising property of  $\text{ZrO}_2$  is generated by the introduction of the sulphate ion [78].

Acid strength of sulphated zirconia catalysts can also be measured by NMR technique [159]. The  $^{31}\text{P}$  solid magic angle spinning (MAS) NMR spectroscopy of adsorbed trimethyl phosphine (TMP) is an effective method for probing the acidity of heterogeneous catalysts [158,160-163]. The method has the advantage over infrared spectroscopy of adsorbed pyridine in that the amount of TMP bound in a particular state can be readily quantified [162]. Moreover, the chemical shifts of TMP co-ordinated to different types of Lewis acid sites are distinctly different. Very strong Lewis acid sites in sulphated  $\text{ZrO}_2$  and sulphated  $\text{HfO}_2$  were revealed by the downfield shift of  $^{31}\text{P}$  NMR lines. Riemer *et al.* [164] reported a  $^1\text{H}$  MAS NMR study of Brønsted acid strength on sulphated  $\text{ZrO}_2$ . The significant  $^1\text{H}$  downfield chemical shifts of sulphated zirconia samples in comparison with pure  $\text{ZrO}_2$  were correlated with the acid strength of surface -OH groups induced by sulphation.

Raman spectroscopy is potentially one of the most powerful techniques for characterising catalysts. However, conventional Raman spectroscopy using visible laser excitation often suffers from two limitations in catalysis studies - inherently low Raman scattering signals and strong fluorescence, which often obscures the weak Raman signal. Asher *et al.* have demonstrated that fluorescence does not interfere with the Raman spectrum for a number of systems when an ultraviolet laser was used as the excitation source [165-167]. Ultraviolet Raman spectra can not only diminish the fluorescence interference, but also greatly increase the Raman signal, especially when the laser

frequency falls in an absorbance region of the system [168]. UV-Raman spectral studies of sulphated zirconia before and after testing for butane isomerisation, together with those of regenerated catalyst clearly showed a surface phase change associated with deactivation [169].

The spectrum of regenerated sulphated zirconia seems to be intermediate between that of fresh and deactivated samples. The sulphate group on the fresh sample co-ordinates to the zirconia surface in a multiple bonding configuration [76,95,164] which stabilises the surface tetragonal phase. For a deactivated sample, either the chemical identity or the co-ordination geometry of the sulphate groups must be altered. Accordingly the bonding between the sulphate group and surface of zirconia is softened and as a result the surface phase transforms from tetragonal to monoclinic. An oxidation treatment regenerates the surface sulphate groups, restores the original bonding configuration with the zirconia surface and the surface phase is reconstructed back to the tetragonal structure. UV-Raman spectroscopic studies by Zalewski *et al.* [170] revealed the existence of tetragonal phase in catalytically active samples, whereas those with monoclinic phase showed little activity. Examination of fresh, spent and regenerated catalyst did not reveal any evidence for a phase transformation, indicating that catalyst deactivation was most likely caused by the accumulation of hydrocarbon fragments on the surface.

#### 1.7.4 CATALYTIC ACTIVITY

The best method for characterisation of industrial catalysts is through model reactions [119,131]. The operating conditions being similar to those of industrial processes, they provide a more correct evaluation of the catalytic utility. Acid catalysed reactions such as skeletal isomerisation of *n*-butane to iso-butane at low temperature [15,103] are widely used as a test reaction for superacidity since it is not catalysed by 100% H<sub>2</sub>SO<sub>4</sub> or others under these conditions.

Isomerisation of light paraffins, leading to the formation of branched isomers is an important process in petroleum refining industry and is known to be catalysed by very strong acid sites. Sulphated zirconia was reported to catalyse the isomerisation of light alkanes at mild temperatures [8,16,19,71,79,88,156,171,172]. The extraordinary activity

of these catalysts is caused by a good stabilisation of the surface intermediates in presence of the surface sulphate species. As for the role played by the hydration/dehydration stage reached by the catalyst before the reaction, contradictory data are available in the literature. Tanabe *et al.* [72] reported that when exposed to the air at ambient temperature, solid superacids lose their superacidic activity by absorbing moisture. Parera [79] reported that the partial rehydration of superacid catalysts with air saturated with water vapour with consequent regeneration of some OH groups and the possible transformation of some Lewis acid sites into Brönsted sites does not affect the catalytic activity in the isomerisation reaction of *n*-butane. Morterra *et al.* has also reviewed the effect of hydration on the acid catalysed isomerisation of light paraffins on sulphated zirconia system [172]. Catalytic activity of the system was found to be maximum when the surface sulphates are in highly covalent configuration, and the Lewis acidity is maximum and Brönsted acidity, a minimum. Small amounts of protonic sites remain at all dehydration stages up to the temperatures at which the surface sulphates start being thermally decomposed [172,173]. The existence of both Brönsted and Lewis acid sites on sulphated catalysts has also been confirmed by IR spectra of adsorbed pyridine [150].

Sulphated zirconia has proved to be an efficient catalyst in reactions like alkylation of isobutane with 2-butene [174] and acylation of toluene [175]. The significantly higher activity of the sulphated zirconia systems for carbocationic reaction is due to the presence of sulphate ions covalently bonded to the metal oxide lattice [15,78,87,88]. The catalytic activity of these materials also depends on the sulphur content. Acylation of toluene with acetic and benzoic acids catalysed by solid superacid was reported by Hino *et al.* [175]. Acid sites stronger than  $H_0 = -15$  are needed for the formation of the acyl cation from a carboxylic acid.

Batamack *et al.* [176] reported the electrophilic chlorination of methane over superacidic sulphated zirconia at temperatures below 225°C with selectivity greater than 80% to methyl chloride. The electrophilic chlorination is considered to proceed by the insertion of a zirconium co-ordinated electrophilic chlorine species and/or electron deficient metal into the methane C-H bond followed by chlorinolytic cleavage to give

methyl chloride. Addition of metal ions to sulphated zirconia improves the methyl chloride selectivity but lowers the conversion.

Sulphated zirconia has been found to catalyse a number of isomerisation reactions of industrial importance like isomerisation of 1,2-epoxides, citronellal and unsaturated hydrocarbons. Yadav and Satoskar [177] conducted a detailed investigation of the rearrangement of 1,2-epoxyoctane with a variety of solid acid catalysts. Among the different products obtained, formation of allylic alcohols and 1-octanal demand commercial importance. Low epoxide conversion was obtained with sulphated zirconia even though the formation of aldol product was suppressed to a large extent. However, high selectivity to allylic alcohols was observed. A comparative evaluation of sulphated zirconia and H-mordenite catalysts for the hydroisomerisation-cracking of *n*-octane was also investigated [178]. Farcasiu *et al.* studied the activity of sulphated zirconia systems for the isomerisation of methylcyclopentane to cyclohexane and the best results were obtained for sulphur content around 3% [153,179]. Absence of shape selectivity and microporosity of sulphated zirconia was reflected in the isomerisation of *d*-citronellal to isopulegol [180]. *n*-Alkane isomerisation reactions are also reported to proceed efficiently over sulphated zirconia systems under mild conditions [7]. Unmodified sulphated zirconia systems showed low selectivity and rapid deactivation due to coking of the catalytic sites.

Sulphated zirconia systems are also proved to be a convenient catalyst for condensation reactions. Kumbhar and Yadav investigated the use of sulphated zirconia for the condensation of hydroquinone with aniline and substituted anilines [181]. The condensation of aniline and hydroquinone lead to the formation of *N,N'*-di-*o*-toluyl-*p*-phenylenediamine and *N,N'*-diphenylenediamine. Cyclocondensation of aniline with acetone results in the formation of 2,2,4-trimethyl-1,2-dihydroquinoline, an important antioxidant, especially used with insulating polymers in cable industry [182].

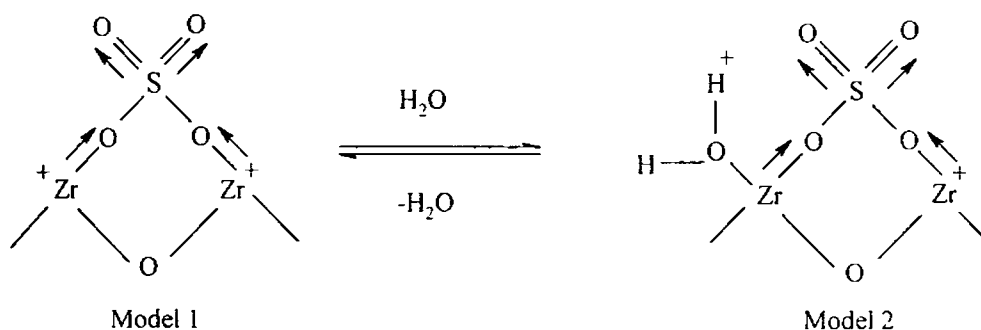
Sulphated zirconia has also been applied for the etherification and dehydration reactions. The etherification of *tert*-butyl alcohol and methanol to form methyl *tert*-butylether (MTBE), the fastest growing gasoline oxygenate, is a combination of several series and parallel reactions leading to a number of products [183]. Quiroga *et al.* carried out the synthesis of MTBE from methanol and isobutylene in a gas-solid heterogeneous



system over sulphated zirconia system [184]. The etherification of  $\beta$ -naphthol with methanol to give  $\beta$ -naphthyl methyl ether, a precursor of acylated ether used in the manufacture of the drug, naproxene, was studied by Yadav and Krishnan [185]. Dehydration of 2-octanol resulted in high selectivity to 1-octene [186]. Methanol has also been dehydrated to dimethyl ether using sulphated zirconia catalysts [187]. Sulphated zirconia has also been tested for a number of esterification reactions of phenethyl alcohol and cyclohexanol with acetic acid, [188] and that of phthalic anhydride with alkanols like 2-ethyl hexanol, isoamyl alcohol and *n*-butanol [189].

### 1.7.5 STRUCTURE OF SULPHATED ZIRCONIA

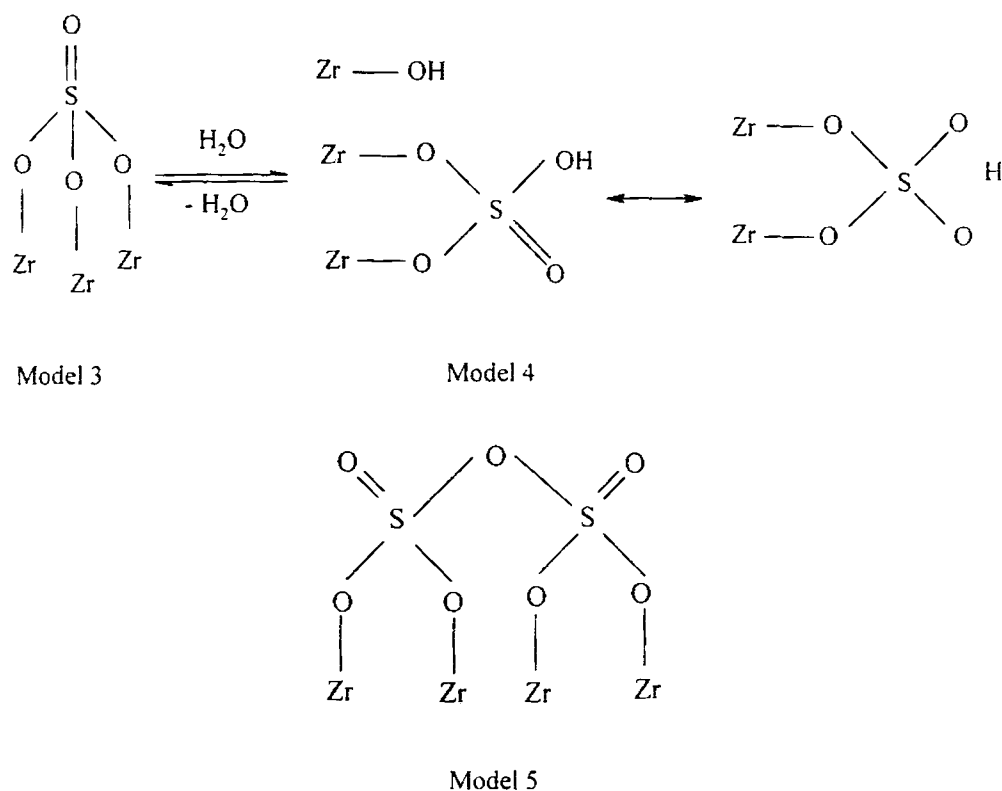
Different structures have been postulated for sulphate-doped zirconia systems from time to time depending on various experimental observations. Arata and co-workers proposed a bidentate sulphate structure in which sulphate bridges across two Zr atoms [71,103]. The IR data of adsorbed pyridine show the existence of both Brönsted and Lewis acid sites with easy conversion of Lewis to Brönsted acid sites by adsorption of water molecules. Arata pointed out that the S=O double bond nature in the sulphate complex is much stronger than that of simple metal sulphate. Thus the Lewis acid strength of  $Zr^{4+}$  sites becomes remarkably greater by the inductive effect of S=O in the complex. The Lewis acid sites predominate in the absence of water and after high temperature calcination. In presence of water, Lewis sites are converted into Brönsted acid sites *via* proton transfer (Scheme 1). These structures however suffer from the drawback of not being able to explain the adverse effect of water on the acidity and activity of the catalyst.



**Scheme 1**

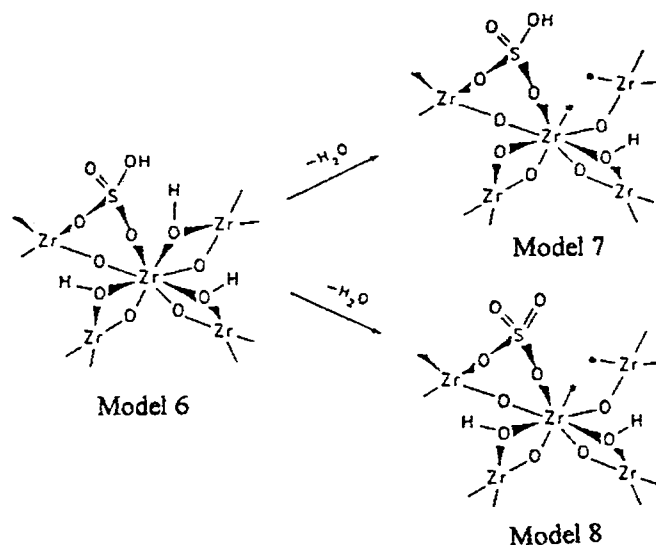
Lavalley *et al.* [76,100,191] found that for dehydrated sulphated zirconia with low sulphate loading, the structure is as in model 3, which in presence of moisture transforms into a bridged bidentate form (model 4). The increase in Brönsted acidity on hydration is attributed to the formation of bisulphate group, S-OH. On sulphated zirconia with high loadings, a polysulphate structure was proposed (model 5).

According to the IR studies of adsorbed pyridine by Morterra *et al.* [77,192], the activation at high temperatures bring about the elimination of all but small fraction of the Brönsted sites. Brönsted sites are fully recovered on exposure to water vapour at ambient temperature. Experimental studies [18,150,163,164,187,193,194] as well as theoretical calculations [195] suggest the existence of bisulphate on sulphated zirconia. However, specific IR bands ascribable to the bisulphate OH groups may be difficult to be detected due to their hydrogen bonding with the surface.



Scheme 2

Clearfield *et al.* [194] ruled out the possibility of chelation of a surface Zr atom by sulphate (which would leave it co-ordinatively saturated) and proposed a dual Brønsted–Lewis model 6. The uncalcined catalyst contains protons as bisulphate and as hydroxyl groups bridging two Zr ions. Loss of water during calcination results in the formation of two species 7 and 8 (Scheme 3). In 7 the bisulphate groups remain intact and results in a Lewis acid site adjacent to Brønsted site, which contributes to the strong acidity. The importance of the models put forward by Clearfield *et al.* is that these can qualitatively explain both the beneficial and adverse effects of water on the catalytic activity of sulphated zirconia catalysts for the Brønsted acid catalysed reactions.



Scheme 3

Based on these models, Lunsford *et al.* [163] rationalised the effect of water on the activity of sulphated zirconia for the alkylation of isobutene with 2-butene. The calcined sulphated zirconia once aged in air was inactive for the alkylation of isobutene with 2-butene. But the activation of the aged samples at 100°C resulted in an active catalyst. Thermal treatment at higher temperatures resulted in a loss of activity, which parallels a decrease in the Brønsted acid sites and an increase in the Lewis acid sites, as a result of dehydroxylation. Referring to the models proposed by Clearfield *et al.* [194], Lunsford *et al.* [163] pointed out that strong Brønsted acidity requires the interaction of the bisulphate groups with the adjacent Lewis acid sites. The aged sulphated zirconia catalyst had almost no Lewis acid sites, presumably because of the molecularly adsorbed water. Activation at

100°C removed adsorbed water, leading to an active catalyst with an adequate ratio of the Brönsted to Lewis acid sites. According to these authors, the decrease in catalytic activity upon treatment of the catalyst at progressively higher temperatures indicates that the Lewis acid sites are not directly responsible for the catalytic reaction. Fraenkel [196] suggested that an effective superacidic sulphated zirconia system should contain critical amount of moisture, which may create polysulphate S-OH surface groups as the active catalytic species.

By introducing H<sub>2</sub>O or CO into a reaction feed of *n*-butane isomerisation, Morterra *et al.* [172,197] observed a poisoning of the catalytic activity, thus suggesting that the presence of Lewis acid sites is vital for the catalytic activity (CO is known to chemisorb around ambient temperature on d<sup>0</sup> oxidic systems through a  $\sigma$ -coordination to the co-ordinatively unsaturated surface cations, acting as strong Lewis acid sites.). These arguments contradict those of several other researchers who claimed the Brönsted sites to be vital for the *n*-butane isomerisation. This can be rationalised on the basis of the Clearfield model. H<sub>2</sub>O or CO adsorbs on the co-ordinatively unsaturated Lewis acid sites and decreases their ability to withdraw electrons. This, in turn, decreases the Brönsted acid strength. The experimental results of Nascimento *et al.* [66] provide direct evidence supporting the dual-site model. They observed that the maximum catalyst activity for *n*-butane isomerisation corresponds to the presence of both the Brönsted and Lewis acid sites with a ratio of Brönsted to Lewis IR band intensities close to 1.

## 1.8 METAL PROMOTED SULPHATED ZIRCONIA

In spite of their high activity, the sulphated zirconia systems suffer from the major drawback of rapid deactivation. Several reasons have been proposed for this rapid deactivation such as change in sulphur oxidation state [198], sulphur leaching or decomposition during the reaction [199], coke deposition at high temperatures [16], phase changes from tetragonal to monoclinic [169], etc. Deactivation limits the industrial use of this catalyst. Constant efforts are on the way to improve the stability and reusability of the systems. Incorporation of transition metal oxides has been reported to enhance the stability of the surface sulphate species and the thermal stability. However, the nature of such an enhancement is far from clear. The processes involved when a support is

impregnated with a solution of a metal salt are generally very complex. Metal distribution depends on the diffusion into the pore and the adsorption of the salt. Pore blocking can occur when big molecules of adsorbate diffuse into the small pores of the adsorbent and this will affect the distribution of the metal over the solid surface. Incorporation of the second or third component may affect the superacidity and the catalytic activity of the superacids either positively or negatively depending on the nature of the metal components.

Sulphated zirconia catalysts containing noble metals, most often platinum has been the widely studied [7,71,78,85,200]. The noble metal crystallites were considered to greatly enhance the catalytic activity and stability. The state and role of platinum in these materials are still a matter of debate [86,171,201,202]. Common feature in the preparation procedures is the impregnation of aqueous  $\text{H}_2\text{SO}_4$  or  $(\text{NH}_4)_2\text{SO}_4$  on previously precipitated  $\text{Zr}(\text{OH})_4$  followed by drying and subsequent impregnation of  $\text{H}_2\text{PtCl}_6$  solution. Final operation is the calcination step. This relatively complex set of operations can lead to the formation of samples with different characteristics, which may be the origin of the different interpretations proposed for the nature of Pt and its role in catalytic performance. Wen *et al.* [85] found that the presence of small amounts of moisture in the reaction system enhances the catalytic activity of platinum doped solid superacid  $\text{Pt}/\text{SO}_4^{2-}/\text{ZrO}_2$  in the hydroisomerisation and hydrocracking of *n*-heptane, probably due to the transformation of Lewis sites into Brönsted sites. Wen *et al.* [85] suggested a bifunctional role of Pt whereas Ebitani *et al.* [203-206] considered that Pt induces a promoting effect of hydrogen by dissociation of the latter, which is followed by spill over and generation of strong Brönsted acid sites. Ebitani *et al.* also suggested that the unique properties of  $\text{Pt}/\text{SO}_4^{2-}/\text{ZrO}_2$  arise from the fact that a large fraction of Pt remained as PtO and PtS and the metallic fraction was low [204]. Sayari and Dicko [207] reported that metallic Pt was present after activation of this catalyst at 600°C in air, a result confirmed by XAFS measurements on a catalyst, which had been heated at 725°C [208].

It has been pointed out that addition of Pt, Rh and Ni to sulphated zirconia superacid catalysts improves the performance in skeletal isomerisation of alkanes, the  $\text{Pt}/\text{SO}_4^{2-}/\text{ZrO}_2$  system being the one with highest activity [203] as well as the one with

lowest deactivation when used in reactions that are carried out in presence of hydrogen [209]. The effect of hydrogen on *n*-butane isomerisation over Pt/SO<sub>4</sub><sup>2-</sup>/ZrO<sub>2</sub> and Pt/SiO<sub>2</sub>+SO<sub>4</sub><sup>2-</sup>/ZrO<sub>2</sub> (physical mixture) was reviewed by Tomishige *et al.* [210]. The inhibition effect was attributed to the hydride formed by the hydrogen spill over phenomenon. The possibility of regeneration of Pt promoted sulphated zirconia systems was also investigated [211]. Complete restoration of activity could be achieved by an oxidation method.

Preparation of superacid of iron-supported zirconia for the reaction of butane to isobutane was carried out by Hino [212]. Iron supported zirconia with the iron concentration equivalent to 7 wt% platinum showed remarkable activity for the reaction of butane to isobutane, the conversions being dependent on calcination temperature and period. The species move into the inner part or interact gradually stronger with the support during calcination. Highly active sites are created by the interaction of iron with the support ZrO<sub>2</sub>, while chemical reactions such as oxidation and/or reduction take place with the sulphur oxides originated from the decomposition of the sulphate matter during calcination [207].

Miao *et al.* undertook a study on the sulphate promoted mixed oxide superacids [213]. Among the sulphated binary oxides, the addition of Cr increases the catalytic activity most evidently. The addition of V, Ti, Al, Fe, Ni, or Co enhances the catalytic activity only slightly while the addition of Mo, W, Mn or Sn diminishes the catalytic activity. Comparing the data of sulphated ternary oxides, it is clear that the combination of Mn or V and Cr cannot further improve the catalytic activity of the Cr-Zr binary oxide system, but the addition of a third metal component to the Fe-Zr, binary oxide system may increase the catalytic activity remarkably. The characteristic peaks of the metal oxides except ZrO<sub>2</sub> were not observed in the XRD patterns of the sulphated binary and ternary oxides implying that the metal oxides are present in the form of oxide solid solution or highly dispersed on the surface of ZrO<sub>2</sub>. Besides, the addition of metal component results in an increase in the crystallisation temperature of ZrO<sub>2</sub> at least by 50°C. Samples exhibiting higher stability of the tetragonal phase have higher superacidity and better catalytic activity. Factors such as the formation of the oxide solid solution and

enhancement of the quantity and bonding of the sulphate groups on the oxide surface retards the phase transformation of  $ZrO_2$  and at the same time causes an increase in the superacidity and catalytic activity [213].

Unpromoted sulphated zirconia (SZ) and sulphated zirconia promoted with iron and manganese ions (FMSZ) have been tested as catalysts for *n*-butane isomerisation [19]. FMSZ is a superior catalyst, its activity at 60°C being equal to that of SZ at 180°C. FTIR analysis of adsorbed CO and acetonitrile revealed the presence of both Brønsted and Lewis sites in both the catalysts. Acetonitrile is strongly adsorbed on FMSZ and the subsequent desorption is destructive with the evolution of  $CO_2$ ,  $SO_2$  and  $O_2$ . The temperature programmed oxidation reveals that no carbon containing products are left on the surface. FTIR studies using CO probe reveals equal acidity for the Lewis sites in SZ and FMSZ. Changes in proton NMR and FTIR parameters caused by adsorption of acetonitrile showed that the acid strengths of the Brønsted sites of SZ and FMSZ are similar to that of the lower OH frequency protons in zeolite HY but weaker than the protons in HZSM-5. This indicates that the remarkable activity of SZ and FMSZ is not caused by exceptionally strong acid sites but by the stabilisation of the transition state complex at the surface.

*n*-Butane isomerisation has also been investigated over different transition metal promoted sulphated zirconia catalysts. Fe alone was an efficient promoter than Mn and Cr and mixtures like Fe-Mn, Fe-Cr and Fe-V [214]. Doping sulphated zirconia with Fe and Mn gives catalysts active for skeletal isomerisation of butane even at room temperature [69,144,215-218]. Apparently the impressive catalytic behaviour of metal modified sulphated zirconia cannot be rationalised in terms of superacidity. Kinetic measurements indicated that the doped catalysts were about three times more active than sulphated  $ZrO_2$  [215,216]. Cheung *et al.* [218] demonstrated that the isomerisation of *n*-butane is accompanied by the disproportionation and other less well understood, acid catalysed reactions and the catalyst undergoes rapid deactivation associated with the deposition of carbonaceous material. Tran *et al.* [156] also identified the deactivation of strong acid sites by carbonaceous deposits. The metal promoted sulphated zirconia catalysed the formation of propane, isobutane, *n*-pentane and isopentane (with traces of methane,

ethane and hexanes) at temperatures of 40-225°C. The selectivity of formation of isobutane was over 85% for conversions less than 60%. The performance of the catalyst recorded as a function of time on stream indicates an induction period followed by a period of deactivation. The break-in was suggested as being an indication of the changes in the properties of the catalyst, such as the oxidation state of the sulphur or promoter components. The observation of the reaction products suggests the involvement of a C-8 intermediate, which is also supported by Bearez *et al.* [121,219,220].

*n*-Butane conversion over Fe and Mn promoted sulphated zirconia was carried out by Garcia *et al.* [221] for exploring the role of Mn in the catalytic activity of iron doped sulphated zirconia. A promoting effect of Fe and a positive influence of Mn in FMSZ catalysts for the isomerisation of butane were established by these studies. Mn alone did not improve the catalytic activity SZ. Low concentrations of Mn disperse iron on the surface. Temperature programmed reduction studies indicate that more sulphate species are resistant to reduction when promoters are present over sulphated zirconia. Increasing the Mn amount results in a decrease in the fraction of reducible sulphate. Addition of Ni to SZ is reported to cause a rise in the activity enhancement comparable to that caused by the addition of Fe and Mn [222]. Sulphated oxides of Cr-Zr, Fe-Cr-Zr, Fe-V-Zr, etc. were found to be two or three times more active than sulphated Fe-Mn-Zr for *n*-butane isomerisation [213,223].

It was also reported that acidity of these materials could be evaluated by temperature programmed desorption (TPD) of benzene [216,224]. A significantly higher temperature of desorption was observed for Fe/Mn/SO<sub>4</sub><sup>2-</sup>/ZrO<sub>2</sub> than for nondoped SO<sub>4</sub><sup>2-</sup>/ZrO<sub>2</sub>. This was interpreted as demonstrating the greater acid strength of the former [216]. The use of benzene to measure superacid strength has been demonstrated in solution [225]. Only very strong superacids were amenable to measurement with this indicator. To understand better the interaction of benzene with the catalyst, a comparative study of the TPD of benzene and pyridine was conducted. If the desorption temperature is determined by the strength of acid-base interaction, pyridine, a stronger base than benzene by 24-25 orders of magnitude, should desorb at a temperature much higher than that of the latter. In



fact the two bases gave desorption peaks at almost equal temperatures. Thus, it appears questionable whether the TPD experiments measured acid-base interactions [226].

Reaction of benzene and pyridine on metal promoted sulphated zirconia catalysts upon heating between 100-800°C in an inert atmosphere was studied on a TG-MS instrument [227]. Benzene was converted into CO<sub>2</sub> and coke whereas most of the pyridine reacted in the same way but a minor amount was desorbed unchanged. The main reaction occurring upon heating (in an inert atmosphere) benzene and pyridine adsorbed on sulphated zirconia or Mn/Fe-promoted sulphated zirconia is oxidation to CO<sub>2</sub> and coking. SO<sub>2</sub> and O<sub>2</sub> were also evolved indicating that the sulphate is the oxidising species. The data show that TPD of very weak base (benzene) or even stronger organic bases (pyridine) does not measure the acidity of sulphated zirconia or composite materials based on it. As a general rule, one should establish that no reaction other than hydrogen transfer occurs between the probe base and the surface before trying to use TPD for comparison of the acid strength of catalysts.

Scheithauer *et al.* [228] investigated the structures of iron promoted sulphated zirconia (FSZ), manganese promoted sulphated zirconia (MSZ) and iron and manganese promoted sulphated zirconia (FMSZ) by UV-vis diffuse reflectance, ESR, Laser Raman, XPS spectroscopies and transmission electron microscopy with energy dispersive X-Ray micro analysis. Laser Raman Spectral analysis reveals that the bulk structure of tetragonal zirconia and the surface sulphate structure of SZ remained virtually unchanged when the promoters were added. According to UV-vis spectra, iron was presented in aggregated structures and not as atomically isolated species. Raman spectra identify these structures as Fe<sub>2</sub>O<sub>3</sub> and the electron micrographs confirm the presence of particulate structures on the surfaces of FSZ and FMSZ but not on SZ and MSZ. XPS provides confirming evidence of Fe<sup>3+</sup> consistent with the presence of Fe<sub>2</sub>O<sub>3</sub>, and the ESR spectra show the presence of Fe<sup>3+</sup> ions in a broad distribution of co-ordination environments.

Tungsten oxide modified sulphated zirconia was found to be an active catalyst for hexane conversion than unmodified sulphated zirconia [229]. Both WO<sub>3</sub> and SO<sub>4</sub><sup>2-</sup> ions prevent the agglomeration of ZrO<sub>2</sub> particles and therefore stabilise the tetragonal phase and enhance the surface area of the catalysts. The dispersed WO<sub>3</sub> species stabilises the

sulphate ions coadsorbed on zirconia and the increased sulphate concentration accounts for the activity enhancement. Monolayer dispersed  $\text{WO}_3$  stabilises the surface sulphate and surface area whereas the presence of crystalline  $\text{WO}_3$  has a negative effect.

The promoting effect of Al on various types of sulphated metal oxide catalysts has been investigated [230]. Incorporation of appropriate amount of  $\text{Al}_2\text{O}_3$  to sulphated titania, zirconia and iron oxide before sulphation was found to increase the acidity, activity and stability of the catalysts for the isomerisation of *n*-butane and *n*-pentane significantly. The addition of  $\text{Al}_2\text{O}_3$  stabilises the surface sulphate complex on the oxides and increases the number of catalytically active acid sites on the catalysts. The high catalytic activity and slow deactivation was attributed to the increase in the number of intermediate strong acid sites providing long-term activity.

Sohn and Jang [231], who investigated the activity of sulphate modified and unmodified  $\text{ZrO}_2\text{-SiO}_2$  towards 2-propanol dehydration and cumene dealkylation reactions; observed an enlargement of catalytic activity with the sulphated samples. Salmones *et al.* [232] determined the catalytic performance of  $\text{Pt/SO}_4^{2-}/\text{ZrO}_2\text{-SiO}_2$  in the hydroisomerisation of *n*-pentane and the catalytic activity was found to be dependent on the zirconia content. Catalytic properties of  $\text{ZrO}_2\text{-SiO}_2$  for cyclohexene conversion (skeletal isomerisation and hydrogen transfer) have also been studied [233]. XRD, TG-DTA, surface area measurement, FTIR and acidity determination by pyridine and dimethyl pyridine chemisorption were used to characterise the samples. The effect of the sulphation on the surface structure and catalytic activity/selectivity was also studied. The characterisation and catalytic activity studies of sulphated  $\text{ZrO}_2\text{-TiO}_2$  mixed oxides was attempted by Lonyi *et al.* [234]. Addition of titania as a second oxide to zirconia hinders its aggregation. It modifies the extensive properties but not the intensive, acidic properties of the sulphated catalysts. The surface area of the sulphated mixed oxide was controlled by the titania rather than by the sulphate.

High temperature calcination, which is necessary for the formation of active sites, results in the loss of sulphur and concomitant transformation of tetragonal zirconia to monoclinic form. One strategy to enhance the formation of tetragonal zirconia and to obtain higher retention of sulphate is to find an appropriate support. Huang *et al.* [235]

reported the use of zirconium sulphate as a precursor for the preparation of silica and alumina supported sulphated zirconia. The catalysts were characterised by XRD, FT-Raman and XRF and tested for hexane conversion. Decomposition of zirconium sulphate forms zirconium oxide and releases  $\text{SO}_3$ . At the same time some sulphate ions are retained on the surface. The interaction of the retained sulphate ions with zirconium oxide forms the active sites. Supporting enhances the decomposition of zirconium sulphate, the formation of tetragonal zirconia, the retention of sulphate ions and hence the activity for hexane conversion.

Sulphated zirconia supported on alumina and silica was investigated by Lei *et al.* [236]. Zirconyl nitrate was used as precursor for the preparation. In the case of SZ/ $\text{Al}_2\text{O}_3$  series, the tetragonal phase was stabilised after supporting; the acid strength and the amount of strong acid sites also increased. However, for SZ/ $\text{SiO}_2$  series, although the tetragonal phase of zirconia was stabilised, the lower number of strong acid sites probably limited the increase in catalytic activity for butane isomerisation. Grau *et al.* [237] observed that the crystallisation temperature shifts to a higher value after supporting  $\text{ZrO}_2$  on  $\gamma$ -alumina and  $\text{SiO}_2$  carriers. However, the shift of the former is much larger than that of the latter, which implies a stronger interaction between  $\text{ZrO}_2$  and  $\gamma$ -alumina. The interaction between zirconia and carriers limits the agglomeration of zirconia particles and thereby suppresses the tetragonal to monoclinic transformation. The catalytic activity of SZ improved when it was combined with high surface area materials like  $\text{SiO}_2$  or  $\text{Al}_2\text{O}_3$  [167]. Increased activity was obtained only when the additives and SZ was mixed as hydroxides before calcination indicating that some mixed oxide formation occurs. Alumina is weakly acidic and displays strong interaction with SZ, while silica is nonacidic and only weakly interacts with SZ.

The effect of the preparation method and the nature of the sulphated mixed oxide catalysts on the acid strength distribution were examined by Vijayanand *et al.* [238]. The supports were prepared by ammonia hydrolysis and precipitation from homogeneous solutions. The amorphous nature of the sulphated samples at  $620^\circ\text{C}$  may be due to the retardation of crystallisation due to the presence of amorphous alumina or silica. Microcalorimetric measurements of ammonia adsorption indicates that the sulphation of

metal oxides caused the enhancement of acid sites with  $\Delta H > 130$  kJ/mol. The microcalorimetric data suggests that the mixed oxides are strong acids but not superacids.

## 1.9 MAIN OBJECTIVES OF THE PRESENT WORK

The major objectives of the present work includes

- ❖ Preparation of sulphated zirconia systems by controlled impregnation technique.
- ❖ To optimise the calcination temperature taking sulphated and iron incorporated sulphated zirconia systems as reference.
- ❖ To investigate the influence of sulphate loading on the physico-chemical properties of sulphated zirconia and to verify the trends in the case of iron promoted sulphated zirconia. The sulphate content was varied by changing the amount of sulphuric acid used in the impregnation step.
- ❖ To prepare metal promoted sulphated zirconia samples by incorporating different transition metal ions. The samples are denoted as XSZ, where X = V, Cr, Mn, Fe, Co, Ni, Cu, Zn, Mo or W. The metal loading in the samples was kept to 2%.
- ❖ To prepare iron incorporated sulphated zirconia with different percentage of metal loadings. The metal loading in the samples was varied from 2 to 10%.
- ❖ Physico-chemical characterisation of the prepared samples using BET surface area pore volume measurements, XRD, EDX, TG and IR spectroscopy. Selected samples were also analysed by Laser Raman Spectroscopy and Scanning Electron Microscopy.
- ❖ A thorough investigation of the surface acidic properties of the prepared catalytic systems. Total acidity as well as acid site distribution obtained by ammonia TPD method was also supported by the thermodesorption studies using pyridine as probe. Adsorption studies using perylene as electron acceptor provided information regarding the Lewis sites in presence of Brønsted acid sites. The TG analysis of the samples after adsorption of sterically hindered 2,6-dimethylpyridine served to obtain a comparative evaluation of the Brønsted acidity of different systems.

- ❖ To compare the surface acidic properties using cumene cracking as test reaction.
- ❖ To assess the catalytic activity of the systems towards industrially important Friedal Crafts benzylation and benzylation of aromatics and to examine the impact of the various reaction parameters like aromatic substrate to benzylation/ benzylation agent molar ratio, reaction temperature, reaction time etc on the activity and selectivity. Benzyl chloride and benzyl alcohol has been employed as benzylation agents. The metal leaching and deactivation of the systems during the reaction has also to be studied.
- ❖ To test the applicability of the catalytic systems for the vapour phase methylation of aniline at different reaction temperatures, molar ratios and feed rates. The deactivation studies also needs special attention.
- ❖ The redox properties of afore mentioned catalytic systems has been rarely exploited. Thus, it becomes our major concern to test the applicability of the systems for phenol oxidation reaction. The conversion of phenol, a major water pollutant to industrially important diphenols (catechol and hydroquinone) forms a convenient route to their efficient disposal. The impact of the reaction parameters like  $H_2O_2$  to phenol volume ratio, reaction temperature and the solvent effect has to be explored.
- ❖ To evaluate the activity of the systems for the nitration of toluene under different experimental conditions. Nitrotoluenes and dinitrotoluenes find application as intermediates in the manufacture of dyes, explosives, perfumes, fertilizers and pharmaceutical compounds.

## REFERENCES

1. M.Boudart, "Perspectives of catalysis", J.M.Thomas, K.I.Zamaraev (Eds.) Blackwell, Oxford (1992) p.183.
2. W.F.H.Foelderich, H.V.Bekkum, *Stud. Surf. Sci. Catal.*, 58 (1991) 631.
3. P.Kumar, R.Kumar, B.Pandey, *Synlett* (1995) 289.
4. A.Vaccari, *Appl. Clay Sci.*, 14 (1999) 161.
5. G.A.Olah, G.K.Surya Prakash, J.Sommer, "Superacids", Wiley, NewYork (1985) p.54.
6. N.F.Hall and J.B.Conant, *J. Am. Chem. Soc.*, 49 (1927) 3047, 3062.
7. T. Yamaguchi, *Appl. Catal.*, 61 (1990) 1.
8. K.Arata, *Appl. Catal. A: Gen.*, 146 (1996) 3.
9. S.R.Vaudagna, R.A.Comelli, N.S.Figoli, *Appl. Catal. A: Gen.*, 164 (1997) 265.
10. R.A.Boyse, E.I.Ko, *J. Catal.*, 179 (1998) 100.
11. Z.Liu, Y.Chen, *J.Catal.*, 177 (1998) 314.
12. J.Santiesteban, J.C.Vartuli, S.Han, R.D.Bastian, C.D.Chang, *J.Catal.*, 168 (1997) 431.
13. V.C.F. Holm, G.C. Bailey, *U.S. Patent*, 3032599 (1962).
14. M. Hino, S. Kobayashi, K. Arata, *J. Am. Chem. Soc.*, 101 (1979) 6439.
15. M.Hino, K.Arata, *J. Chem. Soc. Chem. Commun.*, (1980) 851.
16. F.R.Chen, G.Coudurier, J.F.Joly, J.C.Vedrine, *J.Catal.*, 143 (1993) 616.
17. B.S. Umansky, J.Engelhardt, W.K.Hall, *J. Catal.*, 127 (1991) 128.
18. L.M.Kustov, V.B.Kazansky, F.Figuera, D.Tichit, *J. Catal.*, 150 (1994) 143.
19. V.Adeeva, J.W.de Haan, J.Janchen, G.D.Lei, V.Schunemann, L.J.M.van de ven, W.M.H.Sachtler, R.A.van Santen, *J.Catal.*, 151 (1995) 364.
20. M.Hino, K.Arata, *Chem. Lett.*, (1979) 477.
21. K.Tanabe, "Solid acids and bases and their catalytic properties", Academic Press, NewYork (1970) 103-158.
22. K.Arata, A.Fukui, I.Toyoshima, *J. Chem. Soc. Chem. Commun.*, (1978) 121.
23. M.Hino, K.Arata, *J. Poly. Sci. Poly. Lett.*, 16 (1978) 529.
24. M.Hino, K.Arata, *Chem. Lett.*, (1979) 477.
25. S.Nakano, K.Iwasaki, H.Fukutani, *J. Poly. Sci.: A*, 1 (1963) 3277.
26. T.Yamaguchi, T.Gin, K.Tanabe, *J. Phys. Chem.*, 90 (1986) 3148.
27. S.Sugunan, C.R.Kumaree Seena, *Ind. J. Chem.*, 37A (1998) 669.
28. S.Sugunan, C.R.Kumaree Seena, *Ind. J. Chem.*, 37A (1998) 438.
29. M.Che, N.Naccache, B.Imelic, *J. Catal.*, 24 (1970) 328.
30. T.M.Jyothi, S.Sugunan, B.S.Rao, *Catal. Lett.*, 70 (2000) 187.
31. K.Arata, M.Hino, *React. Kinet. Catal. Lett.*, 25 (1-2) (1984) 143.

32. H.Matsubishi, M.Hino, K.Arata, *Catal. Lett.*, 8 (1991) 269.
33. J.Navarrete, T.Lopez, R.Gomez, F.Figueras, *Langmuir*, 12 (1996) 4385.
34. J.Salmones, R.Licon, J.Navarrete, P.Salas, *Catal. Lett.*, 36 (1996) 135.
35. M.S.Scurrrell, *Appl. Catal.*, 34 (1987) 109.
36. J.C.Yori, J.C.Luy, J.M.Parera, *Catal. Today*, 5 (1989) 493.
37. R.Stevens, "Zirconia and Zirconia Ceramics", 2<sup>nd</sup> Ed., Magnesium elektron Ltd., Manchester (1986).
38. Y.Nakano, T.Iizuka, H.Hattori, K.Tanabe, *J. Catal.*, 57 (1979)1.
39. M.Bensitel, O.Saur, J.C.Lavalley, G.Mabilon, *Mater. Chem. Phys.*, 17 (1987) 249.
40. M.Bensitel, V.Moravek, J.Lamotte, O.Saur, J.C.Lavalley, *Spectrochim. Acta*, 43A (1987) 1487.
41. V.Bolis, C.Morterra, M.Volante, L.Orio, B.Fubini, *Langmuir*, 6 (1990) 695.
42. T.Yamaguchi, Y.Nakano, T.Iizuka, K.Tanabe, *Chem. Lett.* (1988) 281.
43. K.Nishiwaki, N.Kakuta, N.Ueno, H.Nakabayashi, *J.Catal.*, 118 (1989) 498.
44. H.Nakabayashi, N.Kakuta, A.Ueno, *Bull. Chem. Soc. Jpn.*, 64 (1991) 2428.
45. M.Shibagaki, K.Takahashi, H.Kuno, H.Matsushita, *Bull. Chem. Soc. Jpn.*, 63 (1990) 258.
46. K. Tanabe, "Solid Acid and Bases", Academic Press, NewYork (1990) 136.
47. H.Kuno, K.Takahashi, M.Shibagaki, H.Matsushita, *Bull. Chem. Soc. Jpn.*, 63 (1990) 1943.
48. M. Shibagaki, K.Takahashi, H.Matsushita, *Bull. Chem. Soc. Jpn.*, 61 (1988) 3283.
49. H.Kuno, M.Shibagaki, K.Takahashi, H.Matsushita, *Bull. Chem.Soc.Jpn.*, 64 (1) (1991) 312.
50. M.Shibagaki, K.Takahashi, H.Kuno, H.Matsushita, *Bull. Chem. Soc. Jpn.*, 63 (4) (1990) 1258.
51. M.Shibagaki, K.Takahashi, H.Kuno, H.Kawakami, H.Matsushita, *Chem. Lett.*, (1988) 1633.
52. K.R.P.Sabu, K.V.C.Rao, C.G.R.Nair, *Bull. Chem. Soc. Jpn.*, 64 (1991) 1920.
53. V.R.Choudhary, V.H.Rane, *J.Catal.*, 130 (1991) 411.
54. S.Sugunan, Sunitha Kurur, Anto Paul, *Ind. J. Chem.*, 33A, (1994) 1096.
55. S.Sugunan, G.V.Chemparathy, Anto Paul, *Ind. J. Engg. Mater. Sci.*, 3 (1996) 45.
56. S. Sugunan, Binsy Varghese, *Ind. J. Chem.*, 37A (1998) 806.
57. S.Sugunan, Anto Paul, *Ind. J. Chem.*, 36A (1997) 300.
58. H. Dzisko, *Proc. Inter. Cong. Catal.*, Amsterdam (1964) 19.
59. G.W.Weng, H.Hattori, K.Tanabe, *Bull. Chem. Soc. Jpn.*, 56 (1983) 2407.
60. K.Shibata, T.Kiyoura, J.Kitagawa, T.Sumiyoshi, K.Tanabe, *Bull. Chem. Soc. Jpn.*, 46 (1973) 2985.
61. S.Sugunan, Anto Paul, *Ind. J. Chem.*, 36A (1997) 1068.
62. M.Shimokawabe, H.Asakawa, N. Takezawa, *Appl. Catal.*, 59 (1990) 45.
63. J.C.Yori, C.R.Vera, J.M.Parera, *Appl. Catal. A: Gen.*, 163 (1997) 165.
64. A.Calafat, L.Avilan, J.Aldana, *Appl. Catal. A:Gen.*, 201 (2000) 215.

65. K.Esumi, K.Meguro, *Bull. Chem. Soc. Jpn.*, 55 (1982) 315.
66. P.Nascimento, C.Akratopoulou, M.Oszagyan, G.Coudurier, C.Travers, J.F.Joly, J.C.Vedrine, *Stud. Surf. Sci. Catal.*, 75B (1993) 1185.
67. A. Corma, V.Fornes, M.I.Juan Rajadell, J.M.Lopez Nieto, *Appl. Catal. A: Gen.*, 116 (1994) 151.
68. Ganapathy.D. Yadav, Jayesh.J.Nair, *Microporous and mesoporous materials*, 33 (1999) 1.
69. E.J.Hollstein, J.T.Weij, C.Y.Hsu, *US Patent*, 4 918 041 (1990).
70. G. Yalaris, R.B.Larson, J.M.Kobe, M.R.Gonzales, K.B.Fogash, J.A.Dumesic, *J. Catal.*, 158 (1996) 336.
71. A.Arata, *Adv. Catal.*, 37 (1990) 165.
72. K.Tanabe, H.Hattori, T.Yamaguchi, *Crit. Rev. Surf. Chem.*, 1 (1990) 1.
73. B.H.Davis, R.A.Keogh, R.Srinivasan, *Catal. Today*, 20 (1994) 219.
74. M.S.Surrell, M.Cooks, *Stud. Surf. Sci. Catal.*, 36 (1988) 433.
75. R.Srinivasan, D.Taulbee, B.H.Davis, *Catal. Lett.*, 9 (1991) 1.
76. M.Bensitel, O.Saur, J.C.Lavalley, B.A.Morrow, *Mater. Chem. Phys.*, 19 (1988) 147.
77. C.Morterra, G.Cerrato, C.Emanuel, V.Bolis, *J. Catal.*, 142 (1993) 349.
78. T.Yamaguchi, K.Tanabe, Y.C.Kung, *Mater. Chem. Phys.*, 16 (1986) 67.
79. J.M.Parera, *Catal. Today*, 15 (1992) 481.
80. J.R.Sohn, H.W.Kim, *J. Mol. Catal.*, 52 (1989)361.
81. M.Hino, K.Arata, *Chem. Lett.*, (1979) 477.
82. M.Hino, K.Arata, *J. Chem. Soc. Chem. Commun.*, (1979) 1148.
83. V.Adeeva, G.D.lee, W.M.H. Sachtler, *Appl. Catal. A: Gen.*, 118 (1994) L 10.
84. M.Nitta, H.Sakoh, K.Aomura, *Appl. Catal.*, 10 (1984) 215.
85. M.Y.Wen, I.Wender, J.Tierney, *Energy Fuels*, 4 (1990) 372.
86. F.Garin, D.Andriamasinoro, A.Abdul Samad, J.Sommer, *J. Catal.*, 131 (1991) 199.
87. T.Yamaguchi, T.Gin, K.Tanabe, *J. Phys. Chem.*, 90 (1986) 3148.
88. T.Jin, T.Yamaguchi, K.Tanabe, *J. Phys. Chem.*, 90 (1986) 4794.
89. K.Tanabe, A.Kayo, T.Yamaguchi, *J. Chem. Soc. Chem. Commun.* (1981) 602.
90. W.Przystajko, R.Fiedorow, I.G.Dalla Lana, *Appl. Catal.*, 15 (1985) 265.
91. M.Hino, K.Arata, *Catal. Lett.*, 30 (1995) 25.
92. D.A.Ward, E.I.Ko, *Ind. Eng. Chem. Res.*, 34 (1995) 421.
93. D.A.Ward, E.I. Ko, *J. Catal.*, 150 (1994) 18.
94. E.E.Platero, M.P.Mentruit, C.O.Arean, A.Zecchina, *J. Catal.*, 162 (1996) 268.
95. E.E.Platero, M.P.Mentruit, *Catal. Lett.*, 30 (1995) 31.
96. E.E.Platero, M.P.Mentruit, *Mater. Lett.*, 14 (1992) 318.
97. C.O.Arean, E.E.Platero, *Adsorption Sci. Technol.*, 1 (1984) 159.



98. I.Wender, *Stud. Surf. Sci. Catal.*, 75 (1993) 1194.
99. D.Farcasiu, J.Q.Li, *Appl. Catal. A: Gen.*, 128 (1995) 97.
100. O.Saur, M.Bensitel, A.B.M. Saad, J.C.Lavalley, C.P.Tripp, B.A.Morrow, *J. Catal.*, 99 (1986) 104.
101. G.Morterra, L.Orio, V.Bolis, P.Ugliengo, *Mater. Chem. Phys.*, 29 (1991) 457.
102. D.Farcasiu, J.Q.Li, S.Cameron, *Appl. Catal. A: Gen.*, 154 (1997) 173.
103. K.Arata, M.Hino, *Mater. Chem. Phys.*, 26 (1990) 213.
104. C.J.Norman, P.A.Goulding, I.Mc Alpine, *Catal. Today*, 20 (1994) 313.
105. P.D.L.Mercera, J.G.Van Ommen, E.B.M.Doesburg, A.J.Burggraaf, J.R.H.Ross, *Appl. Catal.*, 57 (1990) 127.
106. X.Song, A.Sayari, *Appl. Catal. A: Gen.*, 110 (1994) 121.
107. S.Chokaram, R.Srinivasan, D.R.Milburn, B.H.Davis, *J. Colloid Interface Sci.*, 165 (1994) 160.
108. A.Dicko, M.Sc Thesis, Universite Laval (1994).
109. R.C.Garvie, *J. Phys. Chem.*, 69 (1965) 1238.
110. R.C. Garvie, M.F.Goss, *J. Mater. Sci.*, 21 (1986) 1253.
111. R.C.Garvie, *J. Phys. Chem.*, 82 (1978) 218.
112. S-I.Pyun, H-J. Jung, G-D.Kim, P. Vincenzini (Ed) "High Tech Ceramics", Elsevier, Amsterdam (1987) p. 271.
113. Teufer.G., *Acta. Crystallogr.*, 15 (1962) 1187.
114. F.Babou, B.Bigot, P.Sautet, *J. Phys. Chem.*, 97 (1993) 11501.
115. R.L. White, E.C.Sikabwe, M.A. Coelho, D.E.Resasco, *J. Catal.*, 157 (1995) 755.
116. B.Aiken, W.P.Hsu, E.Matijevic, *J. Mater. Sci.*, 25 (1990) 1886.
117. M.Benaissa, J.G.Santiesteban, G.Diaz, C.D.Chang, M.J-Yacaman, *J. Catal.*, 161 (1996) 694.
118. B.Li, R.D.Gonzalez, *Appl. Catal. A: Gen.*, 165 (1997) 291-300.
119. M.Guisnet, "Catalysis by Acids and Bases", B.Imelik et al. (Eds), *Stud. Surf. Sci.Catal.*, 20, Elsevier, Amsterdam, 1985, 283-297.
120. H.S.Bierenbaum, R.D.Partridge, A.H.Weiss, *Adv. Chem. Ser.*, 121 (1973) 605.
121. M.Guisnet, F.Avendano, C.Bearez, F.Chevalier, *J. Chem. Soc. Chem. Commun.* (1985) 336.
122. H.A.Benesi, B.H.C. Winquist, *Adv. Catal.*, 27 (1978) 97.
123. J.Turkevich, Y.Ono, *Adv. Catal.*, 20 (1969) 135-152.
124. P.A.Jacobs, H.E.Leeman, J.B.Uytterhoeven, *J. Catal.*, 33 (1974) 17.
125. J.W.Ward, R.C.Hansford, *J. Catal.*, 13 (1969) 154.
126. T. Aonuma, M.Sato, T.Shiba, *Shokubai*, 5 (1963) 274.
127. H.G.Karge, J.Ladbeck, Z.Sarbak, K.Hatada, *Zeolites*, 2 (1982) 94.
128. H.G.Karge, K.Hatada, Y. Zhang, R.Fiedorow, *Zeolites*, 3 (1983) 13.

129. J.W.Ward, *J. Catal.*, 10 (1968) 34.
130. C.Mirodatos, D.Barthomeuf, *J. Chem. Soc. Chem. Commun.* (1981) 39.
131. J. Kijenski, A.Baiker, *Catal. Today*, 5 (1989) 1.
132. M.R.Guisnet, *Acc. Chem. Res.*, 23 (11) (1990) 393.
133. P.Nascimento, C.Akratopolou, M.Oszagyan, G.Coudurier, C.Travers, J.F.Joly, J.C.Vedrine. "New Frontiers in Catalysis", L.Guczi, F.Solymosi, P.Tetenyi (Eds.), *Proceeding of the 10<sup>th</sup> international Congress on Catalysis, Stud. Surf. Sci. Catal.*, Vol. 75, Elsevier, Amsterdam (1993) p. 1185.
134. H.A.Benesi, *J. Phys. Chem.*, 61 (1957) 970.
135. H.A.Benesi, *J. Am. Chem. Soc.*, 78 (1956) 5490.
136. J.Take, Y.Nomizo, Y.Yoneda, *Bull. Chem. Soc. Jpn.*, 46 (1973) 3568.
137. M.Deeba, W.K.Hall, *J. Catal.*, 60 (1979) 417.
138. K.Ebitani, J.Konishi, A.Horie, H.Hattori, K.Tanabe, "Acid-base Catalysis", K.Tanabe, H.Hattori, T.Yamaguchi, T.Tanaka (Eds), Tokyo (1989) p. 491.
139. H.Matsushashi, H.Motoi, K.Arata, *Catal. Lett.*, 26 (1994) 325.
140. F.Arene, R.Dario, A.Parmaliana, *Appl. Catal. A: Gen.*, 170 (1998) 127.
141. T.Okuhara, T.Nishimura, H.Watanabe, M.Misono, *J. Mol. Catal.*, 74 (1992) 247.
142. A.Corma, M.I.Juan-Rajadell, J.M.Lopez-Nieto, C.Martinez, *Appl. Catal., A: Gen.*, 111 (1994) 175.
143. A.Corma, A.Martinez, C.Martinez, *J. Catal.*, 149 (1994) 52.
144. C.H. Lin, C.Y.Hsu, *J. Chem. Soc. Chem. Commun.*, 20 (1992) 1479.
145. X.Song, A. Sayari, *Catal. Rev. Sci. Eng.*, 38 (3) (1996) 329-412.
146. J.S.Lee, D.S.Park, *J. Catal.*, 120 (1989) 46.
147. J.S.Lee, M.H.Yeom, D.S.Park, *J. Catal.*, 126 (1990) 361.
148. D.S.Park, J.S.Lee, *React. Kinet. Catal. Lett.*, 40 (1989) 101.
149. Hino.M, Arata.K, Yabe.K. *Shokubai*, 22 (1980) 232.
150. F.Babou, G.Coudurier, J.C.Vedrine. *J. Catal.*, 152 (1995) 341.
151. D. Spielbauer, G.A.H. Mekhemer, M.I. Zaki, H.Knozinger, *Catal. Lett.*, 40 (1996) 71.
152. I. Mirsojew, S.Ernst, J. Weitkamp, H.Knozinger, *Catal. Lett.*, 24 (1994) 235.
153. E.Garrone, R.Chippetta, G.Spotto, P. Ugliengo, A.Zecchina, F.Fajula, "Proc. 9<sup>th</sup> Int. Zeolite Conf.", Vol II, Montreal, R.von Ballmoos, J.B.Higgins, M.M.J.Tyreacy (Eds.), Butterworth-Heinemann, London (1992).
154. A.Corma, C.Rodellas, V.Fornes, *J. Catal.*, 88 (1994) 374.
155. H.A.Benesi, *J. Catal.*, 28 (1973) 76.
156. M.-Trung Tran, N.S. Gnep, G.Szabo, M.Guisnet, *Appl. Catal. A:Gen.*, 171 (1998) 207.

157. B.S.Umansky, W.K.Hall, *J. Catal.*, 124 (1990) 97.
158. D.J.Coster, A.Bendada, F.R.Chen, J.J.Fripiat, *J. Catal.*, 140 (1993) 497.
159. V.Semmer, P.Batamack, C.Doremieux-Morin, R.Vincent, J.Fraissard, *J. Catal.*, 161 (1996) 186.
160. W.P.Rothwell, W.X. Shen, J.H.Lunsford, *J. Am. Chem. Soc.*, 106 (1984) 2452.
161. J.H.Lunsford, W.P.Rothwell, W.X. Shen, *J. Am. Chem. Soc.*, 107 (1985) 1540.
162. J.H.Lunsford, P.N.Tutunjian, P.Chu, E.B.Yah, D.J.Zalewski, *J. Phys. Chem.*, 93 (1989) 2590.
163. J.H.Lunsford, H.Sang, S.M.Campbell, C.H.Liang, R.G.Anthony, *Catal. Lett.*, 27 (1994) 305.
164. T.Riemer, D.Spielbauer, M.Hunger, G.A.H. Mekhemer, H. Knozinger, *J. Chem. Soc. Chem. Commun.* (1994) 1181.
165. C.R.Johnson, S.A.Asher, *Anal. Chem.*, 56 (1984) 2261.
166. S.A.Asher, *Anal. Chem.*, 65 (1993) 201 A.
167. R.W.Bornett, S.A.Asher, *J. Appl. Phys.*, 77 (1995) 5916.
168. S.A. Asher, *Anal. Chem.*, 65 (1993) 57 A.
169. C.Li, P.C.Stair, *Catal. Lett.*, 36 (1996) 119.
170. D.J. Zalewski, S. Alerasool, P.K. Doolin, *Catal. Today*, 53 (1999) 419.
171. E.Iglesia, S.L.Soled, G.M.Kramer, *J. Catal.*, 144 (1993) 238.
172. C.Morterra, G.Cerrato, F.Pinna, M.Signoretto, G. Strukul, *J. Catal.*, 149 (1994) 181.
173. C.Morterra, V.Bolis, G.Cerrato, *Catal. Today*, 17 (1993) 505.
174. G.Canxiong, Y.Sheng, C.Jianhua, Q.Zaihu, *Appl. Catal. A: Gen.*, 107 (1994) 229.
175. M.Hino, K.Arata, *J. Chem. Soc. Chem. Commun.*, 3 (1985) 112.
176. P. Batamack, I.Bucsi, A.Molnar, G.A.Olah, *Catal. Lett.*, 25 (1994) 11.
177. G.D.Yadav, D.V.Satoskar, *J. Am. Oil Chem. Soc.*, 74 (4) (1997) 397.
178. J.M.Grau, J.M.Parera, *Appl. Catal.A: Gen.*, 162 (1-2) (1997) 17.
179. D.Farcasiu, J.Q.Li, *Appl. Catal. A: Gen.*, 175 (1998) 1.
180. G.D.Yadav, J.J.Jadhav, Paper presented at the *Indian Chemical Engineering Congress, CHEMCON-94*, Indian Institute of Technology, Kharagpur, Dec. 16-19 (1994).
181. P.S.Kumbhar, G.D.Yadav, *Chem. Eng. Sci.*, 44 (11) (1989) 2535.
182. G.D.Yadav, A.B.Dixit, Paper presented at the *46<sup>th</sup> Indian Chemical Engineering Congress, CHEMCON-93*, Indian Institute of Chemical Engineers Mumbai, Dec. 15-18 (1993).
183. G.D.Yadav, N.Kirthivasan, *J. Chem. Soc. Chem. Commun.* (1995) 203.
184. M.E.Quiroga, N.S.Figoli, U.A.Sedran, *Chem. Eng. J.*, (Lausanne) 67 (3) (1997) 199.
185. G.D.Yadav, M.S.Krishnan, *Ind. Eng. Chem. Res.*, 27 (1998) 3358.
186. R.Srinivasan, B.H.Davis, *Prepr. Pap. Am. Chem. Soc. Div. Pet. Chem.*, 36 (4) (1991) 635.
187. M.Waqif, J.Bachelier, O.Saur, J.C.Lavalley, *J. Mol. Catal.*, 72 (1992) 127.
188. G.D.Yadav, P.H.Mehta, *Ind. Eng. Chem. Res.*, 33 (9) (1994) 2198.

189. T.S.Thorat, V.M.Yadav, G.D.Yadav, *Appl. Catal. A: Gen.*, 90 (2) (1992) 73.
190. R.J.Gillespie, E.A.Robinson, *Can. J. Chem.*, 41 (1963) 2074.
191. B.A.Morrow, R.A.Mc Farlane, M.Lion, J.C.Lavalley, *J. Catal.*, 107 (1987) 232.
192. C.Morterra, G.Cerrato, F.Pinna, M.Signoretto, *J. Phys. Chem.*, 98 (1994) 12373.
193. F.Babou, B.Bigot, G.Coudurier, P.Sautet, J.C.Vedrine, *Stud. Surf. Sci. Catal.*, 90 (1994) 519.
194. A.Clearfield, G.P.D.Serrette, A.H.Khasi-Syed, *Catal. Today*, 20 (1994) 295.
195. F.Babou, B.Bigot, P.Sautet, *J. Phys. Chem.*, 97 (1993) 11501.
196. D.Fraenkel, *Absr. Book. 14<sup>th</sup> North Am. Meeting Catal. Soc.*, Snowbird, Utah, June (1995) p. T-48.
197. F.Pinna, M. Signoretto, G.Strukul, G.Cerrato, C.Morterra, *Catal. Lett.*, 26 (1994) 339.
198. J.C.Yori, J.C.Luy, J.M.Parera, *Appl. Catal.*, 46 (1989) 103.
199. R.A.Comelli, C.R.Vera, J.M.Parera, *J. Catal.*, 151 (1995) 96.
200. T.Hosoi, T.Shimadzu, S.Itoh, S.Baba, H.Takaoka, T.Imai, N.Yokoyama, *Prepr. Am. Chem. Soc. Div. Petrol. Chem.*, 33 (1988) 562.
201. M.Signoretto, F.Pinna, G. Strukul, *Catal. Lett.*, 36 (1996) 129.
202. K.Ebitani, T.Tanaka, H.Hattori, *Appl. Catal. A: Gen.*, 102 (1993) 79.
203. K.Ebitani, J.Konishi, H.Hattori, *J. Catal.*, 130 (1991) 257.
204. K.Ebitani, T.Tsuji, H.Hattori, H.Kita, *J. Catal.*, 135 (1992) 609.
205. K.Ebitani, H.Konno, T.Tanaka, H.Hattori, *J. Catal.*, 135 (1992) 60.
206. K.Ebitani, H.Konno, T.Tanaka, H.Hattori, *J. Catal.*, 143 (1993) 322.
207. A. Sayari, A.Dicko, *J. Catal.*, 145 (1994) 561.
208. J.Zhao, G.P.Huffman, B.H.Davis, *Catal. Lett.*, 29 (1994) 385.
209. H.Hattori "New aspects of spillover effects in catalysis" Elsevier, Amsterdam (1993) p. 69.
210. K. Tomishige, A.Okabe, K.Fujimoto, *Appl. Catal. A: Gen.*, 194-195 (2000) 383.
211. R.A.Keogh, R.Srinivasan, D.E.Sparks, S.Khorfan, B.H.Davis, *Fuel*, 78 (1999) 721.
212. M.Hino, *Catal. Lett.*, 34 (1996) 125.
213. C. Miao, W.Hua, J.Chen, Z.Gao, *Catal. Lett.*, 37 (1996) 187.
214. J.A.Moreno, G.Poncelet, *Appl. Catal. A: Gen.*, 210 (2001) 151.
215. E.J.Hollstein, J.T.Wei, C.Y.Hsu, *US Patent*, 4 956 519 (1990).
216. C.Y.Hsu, V.K.Patel, D.H.Vahlsing, J.T.Wei, H.Y.Myers, *US Patent*, 5 019 671 (1991).
217. C.Y.Hsu, C.R.Heimburch, C.T.Armes, B.C.Gates, *J. Chem. Soc. Chem. Commun.*, (1994) 1645.
218. T-K.Cheung, J.L.D' Itri, B.C.Gates, *J. Catal.*, 151 (1995) 464.
219. C.Bearez, F.Chevalier, M.Guisnet, *React. Kinet. Catal. Lett.*, 22 (1983) 405.
220. C.Bearez, F.Avendano, F.Chevalier, M.Guisnet, *Bull. Soc. Chim. Fr.*, (1985) 346.
221. E.A.Garcia, E.H.Rueda, A.J.Rouco, *Appl. Catal. A: Gen.*, 210 (2001) 363.

222. M.A.Coelho, D.E. Resasco, E.C.Sikabwe, R.L.White, *Catal. Lett.*, 32 (1995) 253.
223. C.X.Miao, W.M.Hua, J.M.Chen, Z.Gao, *Sci. China B.*, 39 (1996) 406.
224. V.R. Choudhury, K.R.Srinivasan, A.P.Singh, *Zeolite*, 10 (1990) 16.
225. D.Farcasiu, S.L.Fisk, M.T.Melchior, K.D.Rose. *J. Org. Chem.*, 47 (1982) 453.
226. D. Farcasiu, *Symposium on Surface Science of Catalysis, Strong Solid Acids, Abstract COLL 211*, 206<sup>th</sup> ACS National Meeting Chicago, IL (1993).
227. R.Srinivasan, R.A.Koegh, A.Ghenciu, D.Farcasiu, B.H.Davis, *J. Catal.*, 158 (1996) 502.
228. M. Scheithauer, E. Bosch, U.A. Schubert, H. Knozinger, T.K. Cheung, F.C.Jentoft, B.C.Gates, B.Tesche, *J. Catal.*, 177 (1998) 137.
229. Y-Y.Huang, B-Y.Zhao, Y-C.Xie, *Appl. Catal.A: Gen.*, 171 (1998) 75.
230. W.Hua, Y.Xia, Y.Yue, Z.Gao, *J. Catal.*, 196 (2000) 104.
231. J.R.Sohn, H.J.Jang, *J. Mol. Catal.*, 64 (1991)349.
232. J.Salmones, R.Licon, J.Navarrete, P.Salas, *Catal. Lett.*, 36 (1996) 135.
233. J.A.Navio, G.Colon, M.Macias, J.M.Campelo, A.A.Romero, J.M.Marians, *J.Catal.*, 161 (1996) 605.
234. F.Lonyi, J.Valyon, J.Engelhardt, F.Mizukami, *J. Catal.*, 160 (1996) 279.
235. Y.-y.Huang, B.-y.Zhao, Y.-c.Xie, *Appl. Catal. A: Gen.*, 173 (1998) 27.
236. T. Lei, J.S.Xu, Y.Tang, W.M.Hua, Z.Gao, *Appl. Catal. A: Gen.*, 192 (2000) 181.
237. J.M.Grau, C.R.Vera, J.M.Parera, *Appl. Catal. A: Gen.*, 172 (1998) 311.
240. P.Vijayanand, N.Viswanadham, N.Ray, J.K.Gupta, T.S.R.Prasada Rao, "Recent Advances in Basic and Applied Aspects of Industrial Catalysis". T.S.R.Prasada Rao, G.Murali Dhar (Eds.) *Stud. Surf. Sci. Catal.*, Vol 113 (1998) p. 999.

## 2.1 INTRODUCTION

Catalysis is a surface phenomenon involving a complex interaction between the reactant molecules and the active sites on the catalyst. A proper understanding of the phenomenon of catalysis requires a thorough knowledge of the nature of the active sites and the type of interaction. The catalytic activity depends not only on the reaction parameters but also on the nature of the active sites concerned. Surface properties and catalytic activities of sulphated zirconia systems strongly depend on their preparation conditions. The type of precursor and precipitating agent, solution pH, sulphating agent employed, method of impregnation, calcination temperature etc. play a crucial role in deciding the final properties [1-2]. Even the minute variations in preparation or activation conditions profoundly influence the physico-chemical properties of the catalyst. Thus, the preparation method employed and proper characterisation forms the fundamental aspect in the field of catalysis. This chapter discusses the preparation methods and the characterisation techniques employed in the present work.

## 2.2 CATALYST PREPARATION

### 2.2.1 MATERIALS

Zirconyl Nitrate	CDH
Ammonia	Merck
Conc. H <sub>2</sub> SO <sub>4</sub>	Merck
Ammonium metavanadate	Merck
Chromium (III) nitrate	Merck
Manganese (II) nitrate	Merck
Ferric nitrate	Merck
Cobalt (II) nitrate	Merck
Nickel (II) nitrate	Merck

Copper (II) nitrate	Merck
Zinc (II) nitrate	Merck
Ammonium heptamolybdate	Merck
Tungstic acid	Merck

### 2.2.2 METHODS

#### *i) Zirconium hydroxide:*

Zirconium hydroxide was chosen as precursor for the preparation of sulphated samples since it is generally agreed that the sulphation of crystallised zirconium oxide does not produce strong acidity [2-5].

Hydrous zirconium oxide was prepared by the hydrolysis of zirconyl nitrate with 1:1 ammonia. Zirconyl nitrate was dissolved in minimum amount of doubly distilled water. To a boiling solution of zirconyl nitrate in water, aqueous ammonia was added dropwise with constant stirring till complete precipitation was achieved. The pH of the final solution was in the range 10-11. The solution was boiled for about 15 minutes and allowed to stand overnight. The mother liquor was then decanted and the precipitate was washed several times with distilled water till it was completely free of nitrate ions confirmed by the brown ring test. The precipitate was filtered and dried overnight at 120°C. The hydroxide obtained was sieved to get particles of 75-100 microns mesh size.

#### *ii) Optimisation of sulphate content*

For the optimisation study, sulphated zirconia samples were prepared by controlled impregnation technique [6]. The sulphate content was varied by changing the quantity of sulphuric acid used in the impregnation step. Sulphated zirconia samples were obtained by impregnating hydrous zirconium oxide with the requisite amount of 1N H<sub>2</sub>SO<sub>4</sub> solution. 2.5, 5.0, 7.5 and 10 ml of 1N H<sub>2</sub>SO<sub>4</sub> (per gram of zirconium hydroxide) were used as modifier solutions and the samples were denoted as SZ(2.5), SZ(5), SZ(7.5) and SZ(10) respectively. These were dried overnight at 120°C and calcined at 700°C for 3 hours.

The trends were re-examined in the case of iron promoted sulphated zirconia systems, which was prepared by the single step impregnation using the requisite amount

of 1N H<sub>2</sub>SO<sub>4</sub> and ferric nitrate solution. The samples were designated as FeSZ(2.5), FeSZ(5), FeSZ(7.5) and FeSZ(10) based on the amount of H<sub>2</sub>SO<sub>4</sub> solution used per gram of hydrous zirconium oxide. The iron loading in these samples was kept to 2%. The samples were calcined at 700°C after drying overnight at 120°C.

*iii) Metal promoted sulphated zirconia*

Metal incorporated sulphated zirconia samples were prepared from zirconium hydroxide by a single step impregnation using metal salt solution and 1N H<sub>2</sub>SO<sub>4</sub> solution (10 ml/g. of hydrous zirconium oxide). Cr, Mn, Fe, Co, Ni, Cu and Zn incorporated samples were prepared from the corresponding nitrates. Vanadia and molybdenum were added as ammonium metavanadate and ammoniumheptamolybdate respectively while tungsten was incorporated using tungstic acid solution. The metal content in all the samples was kept to 2%. The samples were denoted as XSZ where X stands for the metal incorporated (V, Cr, Mn, Fe, Co, Ni, Cu, Zn, W or Mo). The samples after overnight drying at 120°C were calcined for 3 hours at 700°C.

*iv) Iron promoted sulphated zirconia*

Iron promoted sulphated zirconia systems were prepared from zirconium hydroxide by a single step impregnation using 1N H<sub>2</sub>SO<sub>4</sub> solution (10 ml/g of hydrous zirconium oxide) and ferric nitrate solution. The metal loading was varied from 2 to 10% (as indicated in the parentheses during sample notation) by changing the amount of ferric nitrate used in the impregnation step. The samples after overnight drying at 120°C were calcined at 700°C for 3 hours.

## 2.3 CATALYST CHARACTERISATION

The recent technological advances have resulted in the development of several modern characterisation techniques, a proper utilisation of which provides a greater insight into the molecular aspects of the catalysts and the nature of the active sites involved. The prepared catalyst systems were characterised by BET surface area and pore volume measurements, X-Ray Diffraction, Infra Red Spectroscopy, Energy Dispersive X-Ray analysis and Thermal Analysis (TG-DTA). Selected samples were subjected to surface analysis by Laser Raman Spectroscopy and Scanning Electron Microscopy.



Surface acidic properties were investigated by means of ammonia TPD. Thermodesorption studies using pyridine as probe supported the TPD data. The electron acceptor adsorption studies using perylene provided a measure of the Lewis acidity of the samples in presence of Brönsted acid sites. TG analysis of the samples after 2,6-dimethylpyridine adsorption served to obtain a quantitative idea of the Brönsted acid sites. Prior to each characterisation, the samples were activated at 700°C for half an hour.

### 2.3.1 MATERIALS

Liquid nitrogen	Manorama Oxygen Pvt. Ltd.
Potassium bromide	Merck
Perylene	Merck
Pyridine	Merck
2,6-dimethylpyridine	Merck

### 2.3.2 METHODS

#### *i) Surface area and pore volume measurements*

BET method forms the widely accepted procedure for the determination of surface area of catalysts [7]. The general form of BET equation can be written as

$$P / [V(P_0 - P)] = [1 / (V_m C)] + [(C - 1) / V_m C](P/P_0)$$

where C is a constant for a given system at a given temperature and is related to the heat of adsorption

V - volume adsorbed at equilibrium pressure, P

V<sub>m</sub> - volume of the adsorbate required for monolayer coverage.

P<sub>0</sub> - saturated vapour pressure of the adsorbate

A plot of P/[V(P<sub>0</sub>-P)] against P/P<sub>0</sub> is a straight line with slope (C-1)/V<sub>m</sub>C and intercept 1/V<sub>m</sub>C. From the slope and intercept, V<sub>m</sub> can be calculated and the surface area of the sample can be calculated using the relation,

$$A = V_m N_0 A_m / 22414$$

Where N<sub>0</sub> is the Avagadro number and A<sub>m</sub> the molecular cross sectional area of the adsorbate (0.162 nm<sup>2</sup> for N<sub>2</sub>).

Specific surface area is the surface area per unit weight of the sample. In BET method, adsorption of N<sub>2</sub> is carried out at liquid nitrogen temperature. The advantage with

nitrogen as adsorbate lies in that the value of C on almost all surfaces is sufficiently small to prevent the localised adsorption and at the same time large enough to prevent the adsorption layer from behaving as a two dimensional gas [8]. The linearity of the plot is normally confined to relative pressures in the range 0.1-0.3.

Simultaneous determination of surface area and total pore volume of the samples was achieved in a Micromeritics Gemini Surface area analyser by low temperature N<sub>2</sub> adsorption method. Prior to the measurement, the samples were activated in a nitrogen atmosphere at 200°C for half an hour.

### *ii) X-Ray Diffraction*

Powder XRD analysis constitutes a versatile technique for the qualitative determination of the solid phase of crystalline samples. It provides evidence of the purity of the substance and the presence of foreign materials in the crystal lattice. It also enables the determination of the crystallite size of the samples. Each crystalline substance is characterised by a unique XRD pattern depending on the crystalline phase. The XRD analysis gains special importance in the case of modified metal oxides since they record the phase changes due to the modifications and thus reveals the nature of the structure attained.

The principle of XRD is based on the diffraction of monochromatic X-rays by the different planes in the crystal lattice. The diffraction obeys the Braggs equation,  $n\lambda = 2d \sin\theta$ , where n is an integer called the order of reflection,  $\lambda$  is the wave length of the monochromatic X-ray used,  $\theta$  is the angle between the crystal plane and the X-ray and d is the interplanar distance. Planes are identified by a set of Miller indices (hkl). A rough estimate of crystallite size can be obtained from the line broadening using the Scherrers equation [9],  $t = \lambda / B \cos\theta$ , where B is the Full Width –Half Maximum of the strongest peak, t – crystal diameter,  $\theta$  – Bragg angle.

XRD patterns were recorded in a Rigaku D-max C X-ray diffractometer using Ni filtered Cu-K<sub>α</sub> radiation ( $\lambda = 1.5406 \text{ \AA}$ ). The crystalline phases was identified by comparison with the standard JCPDS (Joint Committee on Powder Diffraction Standards) data file.

### *iii) Infra Red Spectroscopy*

Infrared spectroscopy serves to identify the various functional groups of the catalyst as well as the identification of the adsorbed species and reaction intermediates on the catalyst surface. Major difficulties arise due to absorption of the IR radiations by the solid itself and the shift in the IR frequency as a consequence of interaction of the adsorbed species with the adsorbent surface. IR spectroscopy also enables the determination of the surface acidity of the solid acid catalysts using suitable probe molecules like ammonia or pyridine. Distinction between Brønsted and Lewis acid sites on the catalyst surface is also feasible by this technique. Fourier Transform Infra Red (FTIR) spectra have the advantages of improved spectral quality, higher sensitivity and suitability for use in the low frequency region when compared with conventional IR technique.

FTIR spectra of the samples were recorded in a Shimadzu spectrophotometer (DR 8001) using KBr pellet method. This served to confirm the presence of sulphate ions in the samples. Specific peaks due to the sulphate groups could be located in the IR spectrum of modified zirconia samples.

### *iv) Laser Raman Spectroscopy*

Raman spectroscopy is based on the inelastic scattering of photons, which lose energy by exciting sample vibration mode. Raman spectroscopy is adaptable for *in situ* studies, which makes it an ideal tool for studying catalytic systems. Catalyst supports such as silica and alumina are weak Raman scatterers so that the spectrum of adsorbed species can be recorded. A major disadvantage of the Raman spectroscopy is that many important catalyst samples display a fluorescence, which obscures the desired bands. Raman scattering occurs both at the surface and from the bulk of a sample. However, the outermost portion of the sample dominates the recorded Raman spectrum since the bulk signal is attenuated with depth [10]. Laser Raman Spectroscopy allows the identification of the surface crystalline phase. Laser Raman spectroscopic analysis of the samples was carried out in a Dilor-Jobin spectrophotometer.

### ***v) Thermogravimetric Analysis***

Thermal analysis has a significant role in catalyst characterisation since it reveals the thermal stability and phase transformation of the catalyst systems. Most commonly used thermal methods include Thermogravimetry (TG) and Differential Thermal Analysis (DTA). TG-DTA analysis can also play a role in the elucidation of structure and composition of the samples.

In TG, weight of a sample is continuously recorded as a function of time or temperature while the substance is subjected to a controlled linear heating. The thermogravimetric curve yields information regarding the history of the sample during heating. Any decomposition of the sample is indicated by a dip in the curve. These dips correspond to the weight loss due to decomposition and hence provide an idea about the species lost during the heating step. Thus, thermogravimetric analysis throws light on the thermal stability of the samples.

Differential thermal analysis records the temperature difference between the sample and an inert reference as a function of time or temperature while they are being subjected to a controlled heating. This method provides information regarding the physical phenomena like crystalline changes, fusion, sublimation, vapourisation etc. occurring during the heating process which are not generally accompanied by weight changes and hence become undetectable by thermogravimetric analysis. The enthalpic effects are also associated with chemical phenomena like decomposition or dissociation, oxidation, reduction and other combinations. Thus DTA analysis provides a complete picture regarding the physical and chemical processes happening during the thermal treatment of the sample.

TG and DTA analyses of the samples were achieved in a Shimadzu Thermogravimetric Analyser (TGA-50) in nitrogen atmosphere at a heating rate of 20°C/min. Alumina was employed as the reference material for DTA analysis.

### ***vi) Energy Dispersive X-Ray Analysis***

Energy Dispersive X-Ray (EDX) analysis is a relatively new technique for the qualitative and quantitative elemental analysis of solid samples. In this method,

characteristic X-Rays are separated on the basis of photon energies rather than on their wavelengths. The Si(Li) detector cooled by liquid N<sub>2</sub> receives undispersed characteristic X-Rays from the specimen. The amplified detector output is then digested and the pulses accumulated in channels, each channel representing a small range of energy. For quantitative analysis, data are transferred to a computer for the calculation of elemental concentrations. For qualitative analysis, the data may be displayed in a number of ways, as a series of peaks (intensity vs. energy) on a cathode ray oscilloscope. The simultaneous measurement and display of the energy spectrum result in rapid qualitative and quantitative elemental analysis. EDX spectra of the samples were recorded in a Stereoscan 440 apparatus.

#### *vii) Scanning Electron Microscopy*

Scanning electron microscopy allows the imaging of the topography of a solid surface. The electrons on account of their strong interaction with matter and appreciable scattering by small crystallites form a better probe for the surface analysis of solid samples. They can also be conveniently deflected and focused by electronic or magnetic fields so that magnified real space images can be formed [11]. The technique provides a rough idea of the particle size of the sample and the extent of dispersion or cluster formation in the case of supported metal oxides. The disadvantage with this technique is that the scan results may not represent the entire sample. This can be compensated by recording the images at different sample locations. The Scanning Electron Micrographs of the samples were recorded in a Stereoscan 440: Cambridge, U.K Scanning electron microscope.

#### *viii) Surface Acidity Determination*

Characterisation of the acidity of catalysts is an important step in the prediction of their catalytic utility. In acid catalysis, the activity, selectivity and stability of solid acids are determined to a large extent by their surface acidity - the number, nature, strength and density of acid sites. The acidity required for catalysing the transformation of reactants into valuable products or into by-products is quite different. In the present study, the surface acidity determination was carried out by three independent methods - ammonia

TPD studies, electron acceptor adsorption studies using perylene and thermodesorption studies of pyridine and 2,6-dimethylpyridine.

### **Ammonia TPD**

Temperature programmed desorption [12] of ammonia serves as a dependable technique for the quantitative determination of the acid strength distribution. For TPD studies, pelletised catalyst was activated at 700°C inside the reactor under nitrogen flow for half an hour. After cooling to room temperature, ammonia was injected in absence of the carrier gas flow and the system was allowed to attain equilibrium. The excess and physisorbed ammonia was flushed out by a current of nitrogen. The temperature was then raised in a stepwise manner at a linear heating rate of about 20°C/min. The ammonia desorbed from 100°C to 600°C at intervals of 100°C was trapped in dilute sulphuric acid solution and estimated volumetrically by back titration with NaOH.

### **Perylene Adsorption Studies**

Adsorption studies using perylene as electron donor gives information regarding the Lewis acidity in presence of Brønsted acidity [13, 14]. Perylene adsorption was carried out by stirring a weighed amount of the catalyst with different concentrations of perylene in benzene solvent. Perylene after electron donation gets adsorbed on the catalyst surface as radical cation. The amount of perylene adsorbed was determined by measuring the absorbance of the solution in a UV-VIS spectrophotometer (Shimadzu UV-160 A) before and after adsorption. The limiting amount of perylene adsorbed was obtained from Langmuir plots.

### **Thermodesorption Studies**

The thermodesorption studies were carried out using pyridine and 2,6-dimethylpyridine as probe molecules. The applicability of pyridine as probe to superacids and binary oxide catalysts has been demonstrated [15]. Pyridine being adsorbed both at the Lewis and Brønsted sites, its thermodesorption studies do not allow the differentiation between the two but it provides a rough estimate of the total acidity. Thus pyridine adsorption merely serves to support the TPD data.

The chemisorption of sterically hindered substituted pyridines as proton specific probes for the selective characterisation of the Brönsted acid sites is well reported [16-18]. The thermodesorption study of 2,6-dimethylpyridine was carried out with an intention of obtaining a comparative evaluation of the Brönsted acidity in the samples. Due to the steric hindrance of the methyl groups 2,6-DMP gets selectively adsorbed at the Brönsted acid sites and thus the percentage weight loss during thermal treatment corresponds to the Brönsted acidity of the sample.

The activated samples were kept in a desiccator containing pyridine/2,6-dimethylpyridine under vacuum for 48 hours to allow equilibrium adsorption and then subjected to thermal analysis in N<sub>2</sub> atmosphere at a heating rate of 20°C/ min. The amount of pyridine/2,6-dimethylpyridine desorbed provides a measure of the acidic sites involved.

## 2.4 REACTIVITY STUDIES

The ultimate aim of catalysis being the overall improvement of activity and selectivity, a good catalyst should be one, which provides a convenient route for the synthesis of industrially important fine chemicals. Suppression of unwanted side reactions is an important aspect of catalysis. Poor selectivity results in wastage of materials, separation problems, waste disposal and the concerned environmental issues. The catalytic activity of the prepared catalyst systems was tested for some well-known industrially important reactions. The reactions can be carried out in liquid phase or vapour phase. Liquid phase reactions suffer from the limitation that the maximum temperature that can be attained is the refluxing temperature. This restriction is efficiently overcome in the vapour phase conditions.

The reactivity studies carried out in the present work can be grouped into liquid phase and vapour phase reactions. Friedel-Crafts benzoylation and benzylation of aromatics, nitration of toluene and phenol oxidation reactions were carried out in liquid phase whereas methylation of aniline was conducted in vapour phase. Cumene conversion reaction carried out in vapour phase served as a test reaction for acidity.

**2.4.1 MATERIALS**

Benzene	Merck
Toluene	Merck
<i>o</i> -Xylene	Merck
Benzoyl chloride	Merck
Benzyl chloride	Merck
Benzyl alcohol	Merck
Phenol	Merck
H <sub>2</sub> O <sub>2</sub> (30%)	Qualigens
Nitric acid (Conc.)	Merck
Aniline	Merck
Methanol	Merck
Cumene	Merck

**2.4.2 METHODS*****i) Liquid Phase Reactions*****Friedel-Crafts Benzoylation**

The liquid phase benzoylation of benzene, toluene and xylene using benzoyl chloride was carried out in a 50 ml double-necked flask fitted with a spiral condenser. The temperature was maintained using an oil bath. In a typical run, the aromatic substrate (benzene, toluene or xylene as the case may be) and benzoyl chloride in the specific molar ratio was added to 0.1 g of the catalyst in the R.B flask and the reaction mixture was magnetically stirred. The product analysis was done using a Chemito 8610 Gas Chromatograph equipped with a flame ionisation detector and SE-30 column. The aromatic substrate being taken in excess, the yields were calculated based on the amount of acylating agent. The selectivity for a product is expressed as the amount of the particular product divided by the total amount of products and multiplied by 100.

The influence of the reaction temperature and duration of run on the reactivity and selectivity were also subjected to investigation. The catalyst activity was also screened for different molar ratios of toluene and benzoyl chloride using a representative system. The present work also attempts a closer look into the metal leaching and deactivation of the



systems under the reaction conditions to obtain a better understanding of the nature and course of the reaction.

### **Friedel-Crafts Benzylation**

For the benzylation reaction, the aromatic substrate and the benzylating agent in the required molar ratio was taken in a 50 ml R.B flask containing 0.1 g of the catalyst. The mixture was magnetically stirred at the desired temperature maintained using an oil bath. Benzyl chloride and benzyl alcohol were used as benzylating agents. The influence of the reaction parameters like substrate to benzylating agent molar ratio, reaction temperature etc. were investigated in detail. The reusability of the catalyst and the metal leaching were also tested for understanding of the molecular aspects of the reaction. The product analysis was done using a Chemito 8610 Gas Chromatograph equipped with a flame ionisation detector and SE-30 column.

### **Phenol Hydroxylation**

The catalytic oxidation of phenol was conducted at atmospheric pressure in a 100 ml R.B flask equipped with a condenser and a magnetic stirrer. The reactants (phenol, 30% H<sub>2</sub>O<sub>2</sub> and solvent) in the required ratio were stirred with 0.1 g of the catalyst. The products were identified by comparison with authentic samples in a Chemito 8610 Gas Chromatograph using SE-30 column. The conversions and product selectivity were scanned for different H<sub>2</sub>O<sub>2</sub>/phenol ratios and reaction temperatures. The solvent effect was also subjected to investigation.

### **Nitration of Toluene**

Nitration of toluene was carried out in a 50 ml R.B flask fitted with a spiral condenser. The reactants (toluene and aqueous nitric acid) in desired volume ratio along with 0.1 g of the catalyst was magnetically stirred for a required period at a desired temperature. The nitric acid concentration was varied from 20-70%. The samples were analysed using SE-30 column in a Chemito 8610 Gas Chromatograph using a flame ionisation detector. Prior to injection in GC, the unreacted nitric acid was neutralised using aqueous Na<sub>2</sub>CO<sub>3</sub> to a pH 6-7. Reaction was repeated for different reaction

temperatures, HNO<sub>3</sub> to toluene volume ratio and HNO<sub>3</sub> %. Solvent aided nitration was carried out with CCl<sub>4</sub> as the solvent.

### ***ii) Gas Phase Reactions***

The vapour phase reactions were conducted in a fixed bed reactor inserted into a furnace. The catalyst in powdered form (0.3g) was placed on a glass wool bed packed between inert silica beads. The thermocouple positioned near the catalyst bed monitored the reaction temperature. The temperature was regulated using a temperature controller. The reactants in the required molar ratio were fed into the reactor with the help of a syringe pump at a controlled flow rate. The condensed reaction mixture was collected downstream from the reactor in a receiver connected through a cold water circulating condenser. The products were collected at regular time intervals and analysed gas chromatographically.

### **Methylation of Aniline**

Aniline and methanol were mixed in the required molar ratio and fed into the reactor bed maintained at the desired temperature. The product analysis was conducted using SE-30 column in a Chemito 8610 Gas Chromatograph. The influence of feed rate, reaction temperature and methanol to aniline molar ratio were also investigated. Deactivation studies were also conducted for the different catalyst systems.

### **Cumene Conversion Reaction**

Cumene conversion reaction was conducted as a test reaction for acidity. Cumene was fed into the reactor at a flow rate of 6 ml/hr. The reactor bed was maintained at 350°C. The product analysis was achieved gas chromatographically by comparison with authentic samples.

## REFERENCES

1. A.Corma, V.Fornes, J.M.Lopez-Nieto, M.I.Juan-Rajadell. *Appl. Catal. A*, 116 (1994) 151.
2. F.R.Chen, G.Coudurier, J.F.Joly, J.C.Vedrine. *J. Catal.*, 143 (1993) 616.
3. A.Arata, *Adv. Catal.*, 37 (1990) 165.
4. K.Arata, M.Hino, *Mater. Chem. Phys.*, 26 (1990) 213.
5. R.A.Comelli, C.R.Vera, J.M.Parera, *J. Catal.*, 151 (1995) 96.
6. D.Farcasiu, J.Q.Li, S.Cameron, *Appl. Catal. A: Gen.*, 154 (1997) 173.
7. S.Brunauer, P.H.Emmett, E.Teller, *J. Am. Chem. Soc.*, 60 (1938) 309.
8. S.Lowell, J.E.Shields, "Powder Surface Area and Porosity" 3<sup>rd</sup> edition, Chapman and Hall (1991) p. 38.
9. H.Lipson, H.Steeple. "Interpretation of X-Ray Powder Diffraction Patterns", Macmillan. London (1970) p. 261.
10. C.Li, P.C. Stair. *Catal. Lett.*, 36 (1996) 119.
11. A.Howie, "Characterisation of Catalysts", J.M.Thomas, R.M.Lambert (Eds.), John Wiley. NewYork (1980) p. 89.
12. F.Arene, R.Dario, A.Parmaliana, *Appl. Catal. A: Gen.*, 170 (1998) 127.
13. J. Kijenski, A.Baiker, *Catal. Today*, 5 (1989) 1.
14. B.D.Flockart, J.A.N.Scott, R.C.Pink., *Trans. Faraday Soc.*, 62 (1966) 730.
15. H. Matsushashi, H.Motoi, K.Arata, *Catal. Lett.*, 26 (1994) 325.
16. A. Corma, C.Rodellas, V.Fornes. *J. Catal.*, 88 (1984) 374.
17. H.A.Benesi, *J. Catal.*, 28 (1973) 176.
18. A. Satsuma, Y.Kamiya, Y.Westi, T.Hattori, *Appl. Catal. A: Gen.*, 194-195 (2000) 253.

# PHYSICO-CHEMICAL CHARACTERISATION

---

This chapter is divided into three sections. The first section deals with the optimisation studies of calcination temperature and the sulphate loading. The second part is concerned with the detailed physico-chemical characterisation of the different metal incorporated sulphated zirconia catalysts. The third section describes cumene conversion reaction as the test reaction for acidity.

## SECTION 1 - OPTIMISATION STUDIES

### 3.1 OPTIMISATION OF CALCINATION TEMPERATURE

Calcination involves the medium to high temperature treatment of the catalyst with an aim to eliminate the extraneous materials such as binders, lubricants as well as the volatile and unstable cations and anions that may have been previously introduced but are not desired in the final catalyst. Calcination is generally carried out in an oxidising atmosphere and the selection of calcination temperature is of critical importance in catalysis. In the case of mixed metal oxides, substantially elevated temperature may be required to cause mixing by diffusion of individual species to form a desired compound or crystal phase.

In the case of sulphated metal oxides, calcination introduces strongly bonded sulphate moieties on the surface and immediately underneath [1-3] thereby imparting a combination of acidity and one electron oxidising ability to the catalyst [4,5]. The calcination temperature significantly affects the physico-chemical properties and the catalytic performance of sulphated zirconia systems [6]. Sulphur content of the sulphated zirconia systems strongly depend on the calcination temperature. Increase in calcination temperature usually results in the gradual removal of sulphur from the catalyst surface. Calcination at an appropriate temperature is also essential for the formation of the sulphate species with a proper configuration that generates strong acidity [7,8,9]. The

crystalline phase formation also depends on the calcination temperature. During high temperature calcination, sulphur evolution results in lowering of surface area and pore volume and the stabilisation of the tetragonal phase is diminished.

Calcination temperatures from 500 to 700°C were tried in the present study for optimisation. SZ(10) and FeSZ(10) were selected as representative systems for the purpose. Calcination at 500°C gave a catalyst that was hygroscopic perhaps due to its high sulphate content. This nature was completely eliminated by high temperature calcination.

### 3.1.1 SURFACE AREA AND SULPHATE CONTENT

The results of the physico-chemical characterisation at different calcination temperatures are given in Table 3.1.

Table 3.1 Influence of calcination temperature on the physical properties

Calcination temperature (°C)	Catalyst	Surface area (m <sup>2</sup> /g)	Sulphate content (wt %)	% sulphate retained
500	SZ	125.47	28.90	81.30
	FeSZ	159.50	32.15	90.46
550	SZ	99.17	27.42	77.15
	FeSZ	123.41	32.08	90.26
600	SZ	78.63	25.59	72.00
	FeSZ	99.48	31.24	87.90
650	SZ	66.19	20.48	57.60
	FeSZ	84.75	30.97	87.14
700	SZ	44.81	18.14	51.04
	FeSZ	61.09	30.10	84.70

An increase in calcination temperature resulted in lowering of the surface area and sulphate content. The removal of excess sulphate by high temperature calcination also lends stability to the systems. At 700°C, only strongly bonded sulphates are retained. The retained sulphate contributes to the high activity of the systems. A rather steep decrease in sulphate content was observed in the case of simple sulphated systems during high

temperature calcination. Incorporation of iron improved the sulphate retaining ability. The sulphate content of the iron promoted samples was considerably higher, when compared with simple sulphated systems, especially at elevated temperatures. Iron doping brings about a considerable reduction in the extent of sulphate loss at high temperatures. An increase in the calcination temperature from 500°C to 700°C caused only a minor decrease in the percentage sulphate retained (90.46% to 84.70%).

### 3.1.2 XRD PATTERNS

The XRD patterns of pure and sulphated samples at different calcination temperatures are illustrated in Fig. 3.1. High temperature calcination seems essential for the formation of the catalytically active tetragonal phase. Pure ZrO<sub>2</sub> was crystalline even at 500°C with only the tetragonal phase. The sulphated samples were all amorphous at this temperature. Above 500°C, traces of monoclinic phase were also detected in the XRD pattern of pure zirconia, the intensity of which increased with the increase in calcination temperature. At 700°C, both SZ(10) and FeSZ(10) were crystalline with a predominant tetragonal phase and traces of monoclinic phase. The appearance of monoclinic phase may be attributed to the high sulphate loading in the samples [1]. The low peak intensity in the iron-incorporated sample reveals the lowering of crystallinity after iron incorporation. The intensity of the monoclinic peak was considerably lower in the iron promoted sample when compared to the simple sulphated sample. This indicates the stabilisation of the tetragonal phase by the incorporation of iron moieties.

### 3.1.3 ACIDIC PROPERTIES

#### i) Ammonia TPD

The temperature programmed desorption (TPD) of adsorbed bases like pyridine, NH<sub>3</sub>, benzene etc. can be used for characterising the acid strength distribution and amount [10]. The surface acidic properties at different calcination temperatures were estimated by ammonia TPD and the distribution profiles are presented in Table 3.2. In the case of pure zirconia, no significant change could be noticed in the total acidity values with increase in calcination temperature. However, an enhancement in the amount of strong acid sites was quite evident at high calcination temperatures. In the case of SZ(10) and FeSZ(10) systems, a gradual increase was observed in the total acidity values with an

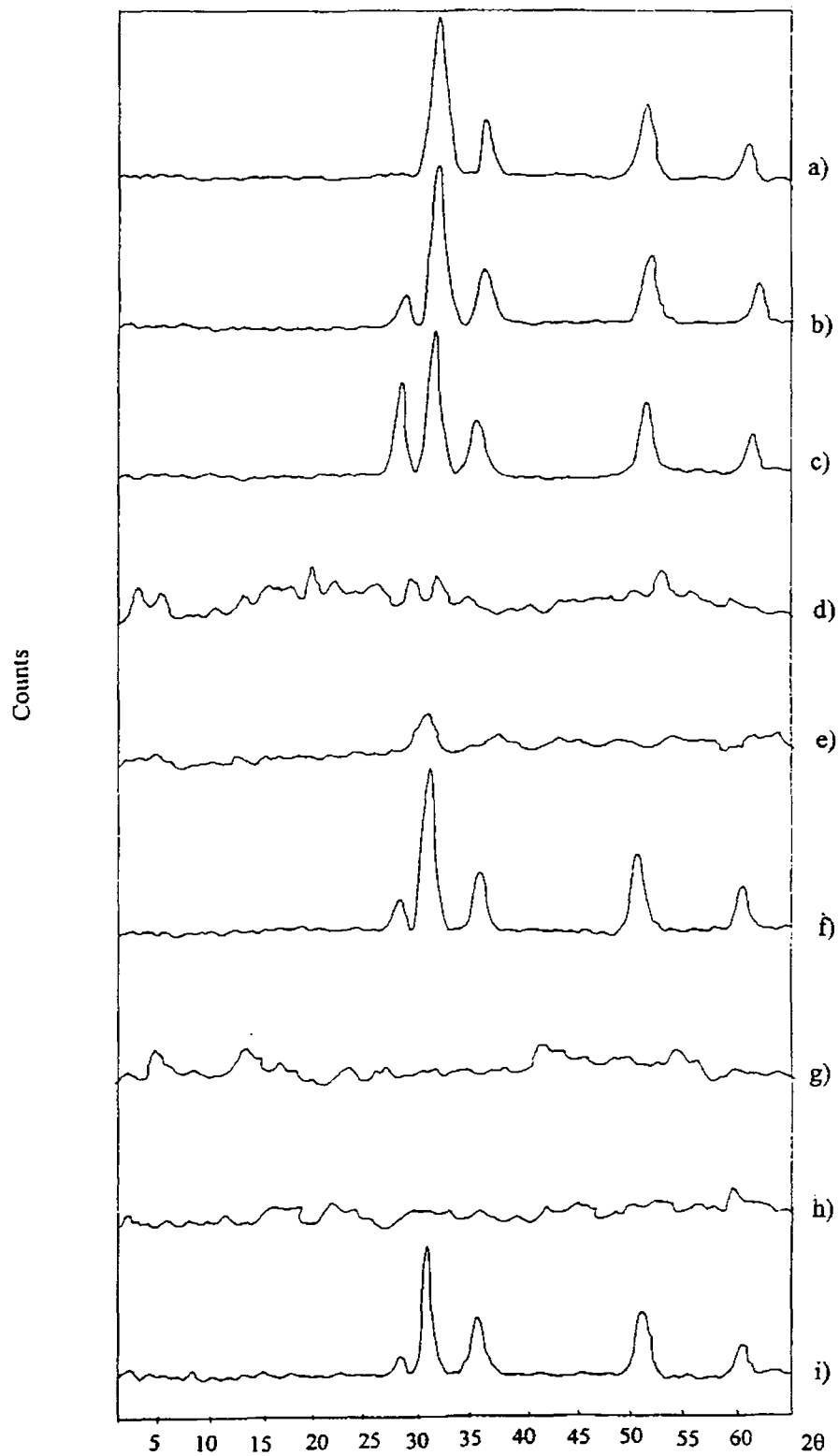


Fig. 3.1 Influence of calcination temperature on the XRD patterns of pure and modified zirconia

- |                             |                             |                             |
|-----------------------------|-----------------------------|-----------------------------|
| a) ZrO <sub>2</sub> (500°C) | b) ZrO <sub>2</sub> (600°C) | c) ZrO <sub>2</sub> (700°C) |
| d) SZ-10 (500°C)            | e) SZ-10 (600°C)            | f) SZ-10 (700°C)            |
| g) FeSZ-10 (500°C)          | h) FeSZ-10 (600°C)          | i) FeSZ-10 (700°C)          |

increase in the calcination temperature. The increase may be due to the structural rearrangement on thermal treatment as well as the formation of the catalytically active crystalline phase. The distribution patterns in all the cases showed a shift favouring the formation of strong acid sites. This supports the view that high temperature calcination is necessary for the generation of strong acidity in sulphated metal oxides [7-9].

Table 3.2 Acid strength distribution at different calcination temperatures

Calcination Temperature (°C)	Catalyst	Amount of ammonia desorbed (mmol/g)			
		Weak	Medium	Strong	Total
500	ZrO <sub>2</sub>	0.1184	0.0831	0.1135	0.315
	SZ(10)	0.3856	0.2573	0.2041	0.847
	FeSZ(10)	0.4073	0.2854	0.2393	0.932
550	ZrO <sub>2</sub>	0.0925	0.0932	0.1153	0.301
	SZ(10)	0.3512	0.2681	0.2767	0.896
	FeSZ(10)	0.3795	0.2918	0.3137	0.985
600	ZrO <sub>2</sub>	0.0764	0.0957	0.1359	0.308
	SZ(10)	0.3254	0.2891	0.3425	0.957
	FeSZ(10)	0.3158	0.3097	0.4335	1.059
650	ZrO <sub>2</sub>	0.0812	0.0810	0.1498	0.312
	SZ(10)	0.2867	0.3152	0.4101	1.012
	FeSZ(10)	0.2894	0.3418	0.5078	1.139
700	ZrO <sub>2</sub>	0.0880	0.0501	0.1690	0.307
	SZ(10)	0.2256	0.3008	0.5186	1.045
	FeSZ(10)	0.2601	0.3796	0.5952	1.235

### ii) Perylene Adsorption Studies

Useful information regarding Lewis acidity in presence of Brønsted acidity can be obtained by adsorption techniques using perylene as electron donor [11]. This technique has previously [12] been employed for the characterisation of metal oxide catalysts. Perylene adsorption technique is based on the ability of the catalyst surface site to accept a single electron from an electron donor like perylene to form charge transfer complexes.



The perylene adsorption was done at room temperature from a solution in benzene. Adsorption of perylene on the catalyst surface as radical cations result in the transformation of white or pale yellow colour of the catalysts to light green. The limiting amount of perylene adsorbed was obtained from the Langmuir plots. The results of the perylene adsorption studies on the systems at different calcination temperatures are presented in Fig. 3.2. A well-defined enhancement in the Lewis acidity was obtained at high calcination temperature. This may be due to the gradual removal of adsorbed water during high temperature calcination [13,14]. Such an increase in the Lewis acidity at the expense of Brönsted acidity during high temperature calcination has been previously reported [13].

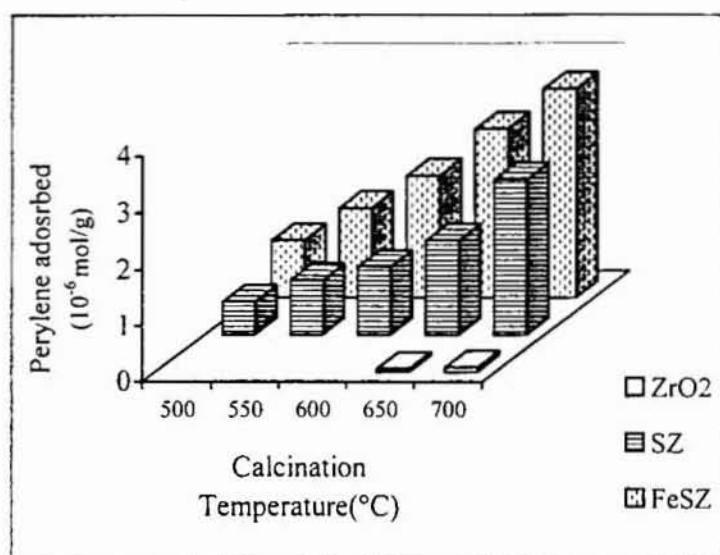


Fig. 3.2 Variation in Lewis acidity with calcination temperature

### iii) Thermodesorption Studies

The reversible transformation of Lewis acid sites into Brönsted acidic sites was confirmed by thermodesorption studies using 2,6-dimethylpyridine. The possibility of the chemisorption of sterically hindered dimethyl and tert-butyl pyridines as proton specific probes for the selective characterisation of the Brönsted acid sites has been suggested [15,16]. The formation of weak bonds between 2,6-DMP and Lewis acid sites has been observed in alumina, boron phosphates and zeolites [15,17]. The IR bands corresponding to Lewis acid site associated dimethyl pyridine disappeared with an increase in desorption

temperature [15]. Dewing *et al.* [18] have also suggested the presence of “special” Lewis sites in  $\gamma$ -alumina for which sterically hindered pyridines do not show any hindrance. The importance of the purging temperature for selective adsorption of DMP on Brönsted acid sites has been previously reported [19]. 2,6-DMP is believed to be held co-ordinatively on the Lewis acid sites at lower temperature due to the rather weak effect of the steric hindrance due to the methyl groups in the neighbourhood of the basic sites of pyridine. Satsuma *et al.* [19] also reported a complete elimination of the co-ordinatively adsorbed 2,6-DMP on Lewis acid sites after purging at an appropriate temperature (above 573K). Thus, we presume that the amount of 2,6-DMP desorbed at temperatures above 300°C originates exclusively due to desorption from Brönsted acid sites. The relative percentage weight loss upon thermal treatment may be taken as a measure of the Brönsted acidity of the systems and the results are presented in Table 3.3.

Table 3.3 Thermodesorption studies at different calcination temperatures

Calcination Temperature (°C)	2,6-DMP desorption (Relative percentage weight loss)			
	Total	Weak (300-400°C)	Medium (400-500°C)	Strong (500-700°C)
500	3.906	1.097	1.591	1.218
600	3.167	0.764	0.966	1.437
700	2.895	0.314	0.886	1.695

As expected, an increase in the calcination temperature resulted in a lowering of the total Brönsted acidity. However, there was a pronounced enhancement in the amount of medium and strong Brönsted acid sites at the expense of weak sites. This may be accounted for on the basis of the increase in the Lewis acidity at high calcination temperatures. Lunsford *et al.* [20] pointed out that strong Brönsted acidity requires the interaction of the bisulphate groups with the adjacent Lewis acid sites. Presence of Lewis sites adjacent to Brönsted acid sites results in enhancement of the Brönsted acidity due to the electron withdrawing inductive effect.

Based on the results of physical characterisation and acidity evaluation studies, 700°C was chosen as the optimum calcination temperature for further studies.

### 3.2 OPTIMISATION OF SULPHATE LOADING

The sulphate content is found to affect the physico-chemical properties of the catalyst tremendously [1,2]. The relative amounts of Lewis and Brønsted sites depend mainly on the concentration of the surface sulphate species and their nature [21,22]. Thus, an optimisation study of sulphate loading becomes quite relevant.

#### 3.2.1 SURFACE AREA AND PORE VOLUME

The variation in the surface area and pore volume with sulphate loading for sulphated zirconia and iron promoted sulphated zirconia is presented in Table 3.4. Consistent with the earlier reports, the sulphated samples showed a higher surface area as compared to pure zirconia. Sulphation reduces the extent of surface area loss during high temperature calcination. This can be explained on the basis of higher resistance to sintering as well as the delayed transformation from amorphous to crystalline state acquired by doping with sulphate ions [7,9,23-26]. Sulphate doping suppresses particle growth and also facilitates the dispersion of the zirconia particles resulting in a higher surface area.

Table 3.4 Influence of sulphate loading on the physical properties

Catalyst	Surface area (m <sup>2</sup> /g)	Pore volume (cm <sup>3</sup> /g)	Sulphate content (wt %)	% Sulphate retained
ZrO <sub>2</sub>	34.68	0.0654	-	-
SZ-2.5	80.23	0.0868	2.85	20.8
SZ-5.0	78.04	0.0808	5.91	24.3
SZ-7.5	69.51	0.0789	10.11	32.9
SZ-10	54.81	0.0686	18.54	47.6
FeSZ-2.5	83.12	0.0981	5.27	42.6
FeSZ-5.0	78.81	0.0958	11.51	47.0
FeSZ-7.5	66.47	0.0868	22.81	74.3
FeSZ-10	61.09	0.0821	30.10	84.7

An increase in sulphate loading resulted in a decrease in the surface area value. The decrease was only marginal in the case of low sulphate loaded samples, whereas for high loaded samples the decrease was quite noticeable. Thus it can be assumed that for

low sulphate loadings the stabilising effect of the sulphate ions gets the upper hand. At high sulphate loadings plugging of the pores may result in a reduction in the surface area [27]. The decrease in surface area can also be correlated with sulphur migration into the bulk phase or an alteration of crystalline structure [1]. Even though the sulphur migration into the bulk predicts a decrease in the surface area, the lower degree of crystallinity, as evident from the XRD patterns discussed below, tends to increase the value. The observed surface area may be due to a fine balance between the two.

The iron promoted samples showed a higher surface area as compared to the unpromoted samples. The dispersed  $\text{Fe}_2\text{O}_3$  particles along with the  $\text{SO}_4^{2-}$  species prevent the agglomeration of zirconia particles leading to an enhanced surface area. In the case of iron promoted samples also, an increase in sulphate content resulted in a decrease in surface area value, which may be attributed to the migration of sulphate species into the bulk. However, the surface area loss is considerably less for the iron promoted samples when compared to their simple sulphated analogues. Thus it can be assumed that the incorporation of iron resists the surface area loss during high temperature calcination.

The pore volume of the samples also showed a decreasing trend with increased sulphate loading which again supports the pore blockage at higher sulphate concentrations. The pore volumes of the iron-incorporated samples were higher when compared to those of their simple sulphated analogues.

### 3.2.2 XRD ANALYSIS

The gradual transformation of tetragonal into thermodynamically stable monoclinic phase with an increase in the calcination temperature has been reported earlier [9,23]. At temperatures higher than  $650^\circ\text{C}$ , only monoclinic phase was observed [28]. However, in our case, a predominance of the tetragonal phase was observed even after calcination at  $700^\circ\text{C}$ . The formation and stabilisation of a metastable tetragonal phase can be rationalised in several ways. It can be assumed that due to the existence of an activation energy for the transformation arising from kinetic factors, not all of the potentially tetragonal crystallites convert into the monoclinic phase under the conditions employed. On the basis of thermodynamic considerations, Garvie and co-workers [29-31] and Pyun *et al.* [32] attributed the stabilisation to surface and strain energy effects; these

effects allowed the calculation of a critical crystallite size below which the tetragonal phase was more stable than the monoclinic modification.

The intensity of the monoclinic bands was considerably lowered in the sulphated samples. Sulphate doping thus imparts special stabilisation to the catalytically active tetragonal phase at high calcination temperatures [7,25,26,33-35]. In the thermodynamic standard state of macroscopic crystals, monoclinic zirconia is stable while cubic and tetragonal forms are metastable. However, for small particles, tetragonal  $ZrO_2$  has a lower Gibbs free energy than monoclinic  $ZrO_2$ . Agglomeration of zirconia particles beyond a critical crystallite size result in  $ZrO_2(t)$  transformation into  $ZrO_2(m)$  [29,30]. Prevention of agglomeration *via*. sulphation accounts for the stabilisation of the tetragonal phase.

The crystal structure of sulphated zirconia is greatly affected by the sulphur content (Fig. 3.3 and 3.4). Lowering of peak intensities in the XRD patterns supports a gradual decrease in the degree of crystallinity with an increase in the sulphate concentration. An increased sulphate content delays the particle growth and hinders the crystallisation process. The development of crystallinity could be observed in low loaded samples even after calcination at 600°C. The peak intensity increased with increase in the calcination temperature indicating an increase in the crystallinity. The low loaded samples showed almost complete crystallisation at 700°C, with the peak intensity remaining almost the same with an increase in the calcination time. Samples with high sulphate loadings were amorphous at 600°C. The XRD patterns indicate the incomplete crystallisation in the case of high loaded samples even at 700°C. Traces of monoclinic phase could also be detected in the XRD pattern at high sulphate loading. It can be concluded that sulphated zirconia with low or medium sulphur content crystallises only in the tetragonal form, whereas at higher sulphate content a minor fraction of monoclinic phase also appears [1].

Incorporation of iron had no significant effect on the XRD patterns except for a slight lowering in the degree of crystallinity. The intensity of the peak corresponding to the monoclinic phase was also lowered in the iron-incorporated samples indicating the stabilisation of the tetragonal phase. The absence of characteristic peaks corresponding to  $Fe_2O_3$  implies that the metal oxide is present in the form of solid solution or it is highly

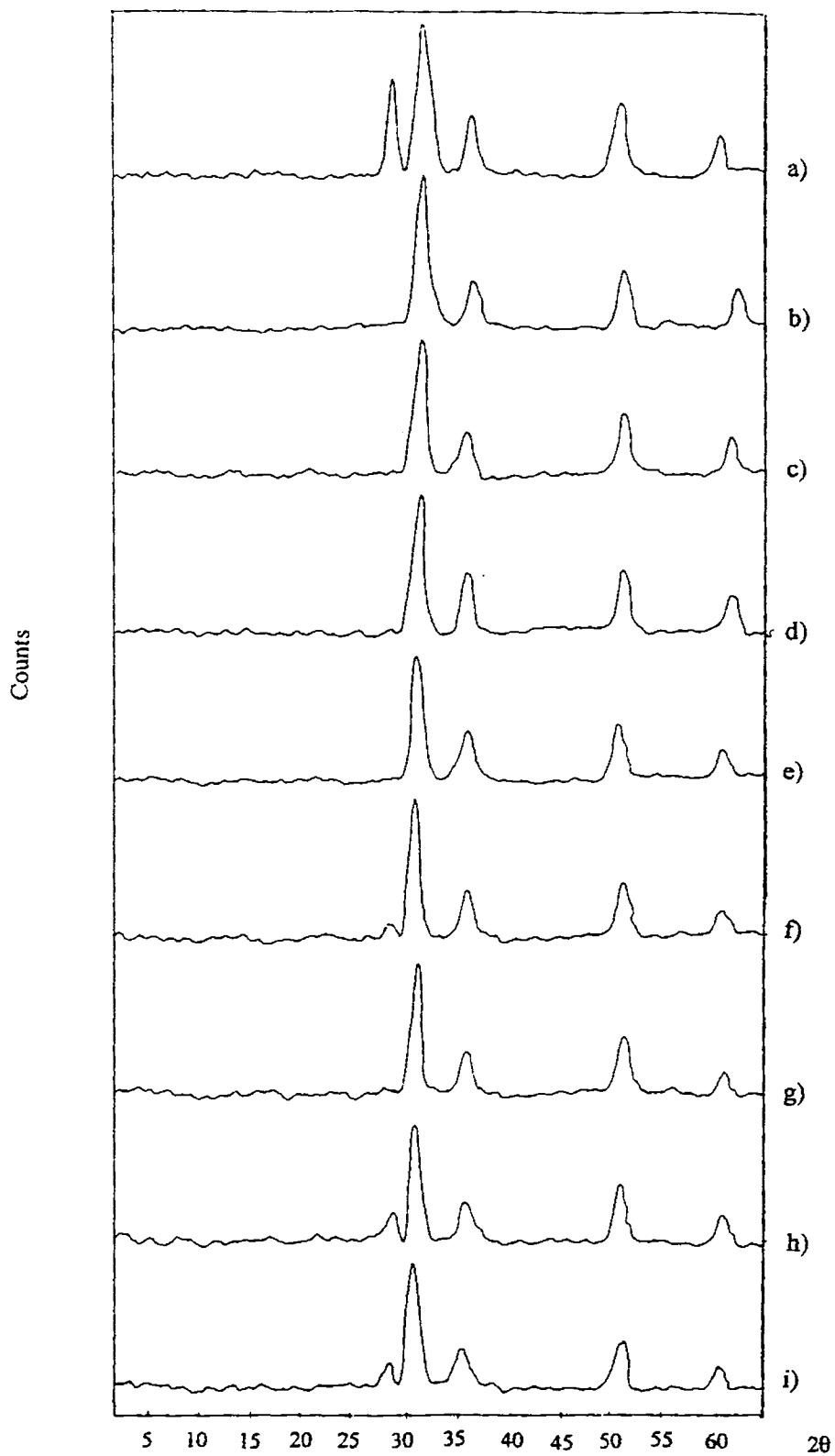


Fig. 3.3 Influence of sulphate content on the XRD patterns

- |                     |             |             |
|---------------------|-------------|-------------|
| a) ZrO <sub>2</sub> | b) SZ-2.5   | c) FeSZ-2.5 |
| d) SZ-5.0           | e) FeSZ-5.0 | f) SZ-7.5   |
| g) FeSZ-7.5         | h) SZ-10    | i) FeSZ-10  |

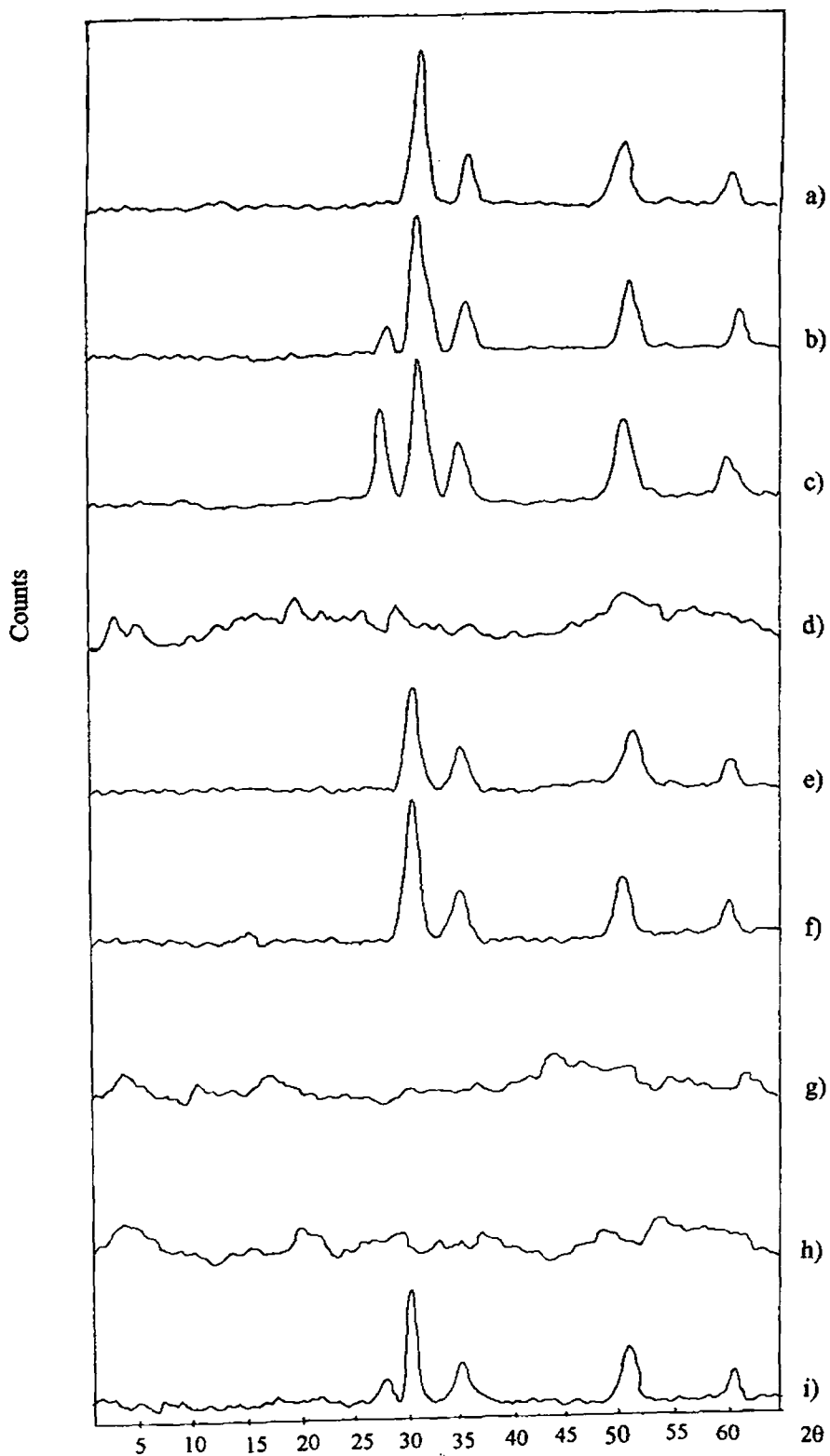


Fig. 3.4 Influence of sulphate content on the development of crystallinity at different calcination temperatures

- |                             |                             |                             |
|-----------------------------|-----------------------------|-----------------------------|
| a) ZrO <sub>2</sub> (500°C) | b) ZrO <sub>2</sub> (600°C) | c) ZrO <sub>2</sub> (700°C) |
| d) FeSZ-2.5 (500°C)         | e) FeSZ-2.5 (600°C)         | f) FeSZ-2.5 (700°C)         |
| g) FeSZ-10 (500°C)          | h) FeSZ-10 (600°C)          | i) FeSZ-10 (700°C)          |

dispersed on the  $ZrO_2$  surface. The dispersion of  $Fe_2O_3$  particles causes the stabilisation of the tetragonal phase and also imparts higher surface area.

### 3.2.3 THERMAL STUDIES

TG pattern of hydrous zirconia is typical of that found with a gel; dehydration occurring continuously over the entire temperature range studied (Fig. 3.5). The sulphated samples showed an initial weight loss at around  $100^\circ C$ , which can be due to the removal of surface adsorbed water of hydration. The onset of sulphate decomposition was observed around  $650^\circ C$  for simple sulphated systems. An increase in sulphate loading shifts this decomposition to higher temperature. In the case of SZ-10, the decomposition was found to set in around  $690^\circ C$ .

The iron promoted samples exhibited a higher thermal stability. The commencement of decomposition in these cases occurred only above  $700^\circ C$ . Thus, it can be inferred that, besides delaying the crystallisation process, the addition of iron also serves to stabilise the surface sulphate species. As for simple sulphated systems, the decomposition temperature showed an upshift with an increase in sulphate content. In the case of FeSZ-10, the initiation of decomposition occurred around  $750^\circ C$ .

The DTA analysis of  $ZrO_2$  shows an exothermic peak with peak maxima around  $410^\circ C$ . The existence of such an exotherm has been observed for several metal oxide and hydrous oxide systems. This exothermic peak can be proposed as being due to a phase transition from an amorphous into a crystalline form of zirconia. Srinivasan *et al.* [36] observed that the exothermic peak appeared at the same temperature for samples, that after calcination, lead to pure monoclinic or tetragonal zirconia.

The delay in the transition from amorphous to crystalline material by sulphate doping is supported by the thermal analysis results. The exothermic peak in the DTA curve at around  $410^\circ C$ , which can be attributed to the crystallisation of pure zirconia, is shifted to higher temperatures after sulphation indicating the retardation of crystallisation. Scurrill [23] proposed it as being due to the inhibiting effect of sulphate for the crystallisation of  $ZrO_2$ . The sulphate content was also found to have some influence on the temperature of this exothermic transition. Consistent with the earlier reports



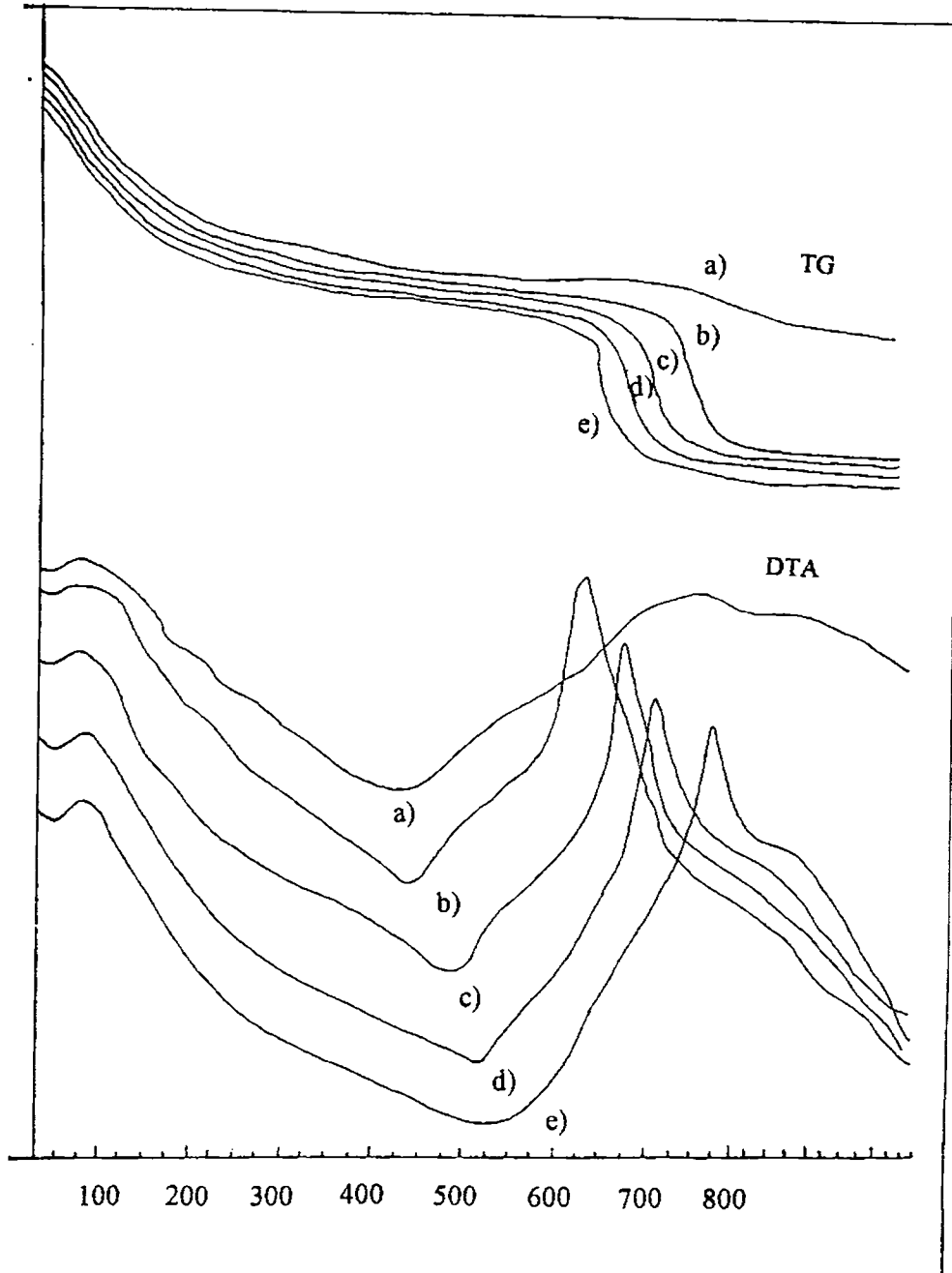


Fig. 3.5 Influence of sulphate loading on thermal stability

- |              |             |           |
|--------------|-------------|-----------|
| a) $ZrO_2$   | b) SZ(2.5)  | c) SZ(10) |
| d) FeSZ(2.5) | e) FeSZ(10) |           |

[24,26,33,37], an increase in the sulphate loading shifted the peak maxima towards the high temperature region. In low loaded samples the peak maximum was obtained at around 430°C whereas for high loaded system the maxima was observed at 472°C. The broadness of the peak suggests that the crystallisation may be occurring over a temperature range. This explains why the high loaded samples seemed amorphous in the XRD pattern even at 600°C while the exothermic maximum was obtained at 472°C. The exothermic peak may be considered to represent the initiation of the crystallisation process.

The further stabilisation of the tetragonal phase by incorporation of iron is also established by the DTA studies. The exothermic peak maxima in the case of iron promoted samples were at considerably higher temperatures (500-550°C) when compared to their simple sulphated analogues.

#### 3.2.4 ELEMENTAL ANALYSIS

The sulphate content as obtained from EDX analysis is given in Table 3.4. The sulphate content increases with an increase in the amount of acid used as modifier solution per gram of hydrous zirconium oxide. The sulphate concentration was found to be very low when compared to the values estimated based on the amount of acid used for impregnation. This may be due to the sulphate removal induced by high temperature calcination. The low sulphate loaded systems showed a poor retention as compared to the high loaded systems. This along with the surface area results lends support to the proposed migration of sulphate into the bulk at high loadings [1]. The retained sulphate on the surface and immediately underneath imparts high acidity and one electron oxidising ability to the systems. It may be assumed that, at high sulphate loadings part of the sulphate is present in the bulk phase, rather than on the surface.

The incorporation of iron was found to improve the sulphate retaining ability of the systems. The iron promoted samples showed a higher sulphate content when compared to the unpromoted samples. The presence of iron stabilises the surface sulphate species. This is also in agreement with the thermal analysis results, which predicts a higher stability and decomposition temperature after incorporation of iron. Simple sulphated systems for which sulphate removal sets in around 650°C had a low sulphate

content as compared to the metal promoted ones. In the case of unpromoted systems the sulphate retaining ability varied from 20 to 47% whereas for iron incorporated samples the corresponding values were in the range 42 to 84 %.

### 3.2.5 ACIDITY MEASUREMENT

#### i) Ammonia TPD

The results of TPD studies on different sulphate loaded systems are given in Fig. 3.6. The acid distribution profiles show the presence of weak (100-200°C), medium (300-400°C), and strong (500-600°C) acid sites.

Considerable enhancement of both strong and weak acid sites was observed after sulphation. A gradual increase in the total acidity was observed with an increase in sulphate loading. However, a considerable difference could be noticed in the distribution pattern. Low sulphate loaded samples exhibited quasi-identical values of weak and strong acid sites whereas there seems to be a considerable enhancement of strong acid sites for high sulphate loaded samples. Thus, it may be inferred that even though the nature of sulphate species is important than the sulphate content, an abundance of surface sulphate species corresponds to an increase in the surface acidity and surface active sites.

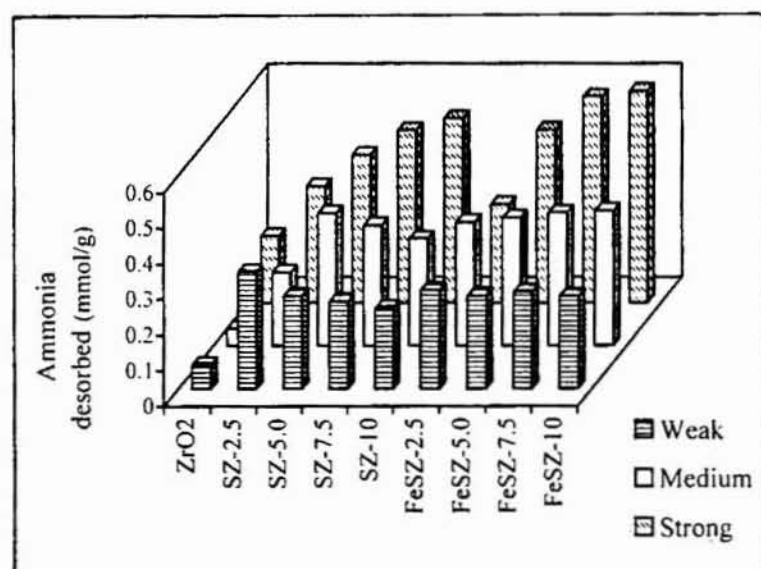


Fig. 3.6 Acid site distribution as obtained from ammonia TPD studies

In the case of strong acid sites it can be either Lewis sites or Brønsted sites adjacent to Lewis acid sites as proposed by Clearfield *et al.* [38]. The enhancement of Lewis acidity can be attributed to the increase of the electron accepting properties of the three co-ordinated zirconium cations *via* the inductive effect of the sulphate anions, which withdraw electron density through the bridging oxygen atom [8,37]. The removal of sulphate from the surface sites induced by high temperature calcination can also result in the generation of strong co-ordinatively unsaturated Zr(IV) Lewis acid sites [39].

According to the dual Brønsted-Lewis site model proposed by Clearfield [38] uncalcined catalyst contains protons as bisulphate and as hydroxyl groups bridging two zirconium ions. During calcination, either the bisulphate anion can react with an adjacent hydroxyl group resulting in a Lewis acid site or two adjacent hydroxyl groups can react keeping bisulphate ion intact thereby generating Brønsted acidity. The combination of these Brønsted sites with the adjacent Lewis sites can also generate strong acidity.

The iron promoted samples was found to have a higher acidity as compared to the simple sulphated samples. This increase may be partially attributed to the higher sulphate content of the iron promoted samples. The structural changes accompanied by incorporation of iron moieties may also be contributing to the acidity enhancement. As in the case of simple sulphated systems, at low sulphate loadings weak and strong acid sites were obtained in almost equal proportions while considerable enhancement of the strong acid sites was observed at high sulphate loading.

#### *ii) Perylene Adsorption Studies*

Electron acceptor adsorption studies gave information regarding the presence of Lewis acid sites in presence of Brønsted acid sites. The adsorption of perylene from a solution in benzene was done at room temperature. After adsorption, the pale yellow or white colour of the catalyst samples was changed into green, while the perylene solution lost its fluorescent green colour and turned pale yellow or almost colourless. The special one electron oxidising ability of these catalyst systems may be considered to be generated by the interaction of sulphate groups with the metal oxide. Perylene after electron donation gets adsorbed on the Lewis sites as radical cation. As the concentration of perylene in the solution increases, amount adsorbed also increases up to a certain limiting

value after which it remains constant. The limiting amount adsorbed is a measure of the Lewis acidity or the electron accepting capacity. The oxidising (single electron accepting) property of sulphated zirconia systems has also been established by the ESR study after perylene adsorption by Yamaguchi *et al.* [24]. The results of adsorption studies given in Fig 3.7 clearly show a considerable enhancement of Lewis acidity on sulphation.

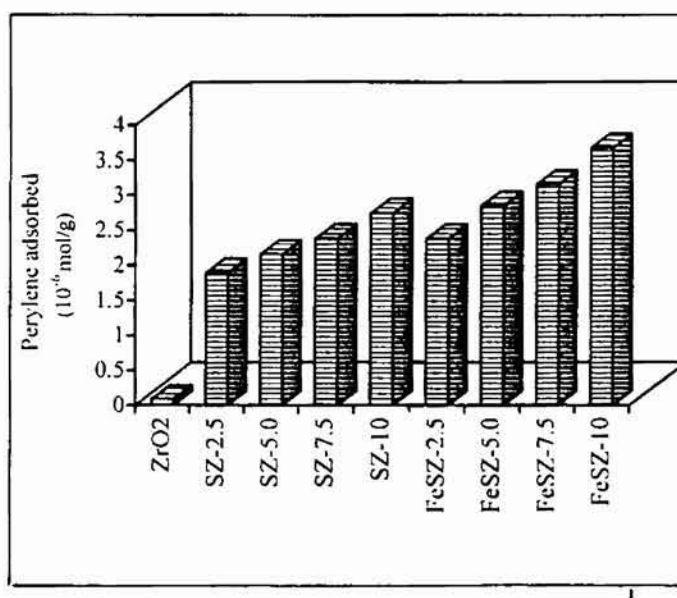


Fig. 3.7 Variation in Lewis acidity with sulphate loading

The Lewis acidity was found to increase with an increase in the sulphate loading. This is in contrast to the earlier reports, which predicted an increase in Brønsted acidity at high sulphate loading when sulphates mostly existed in the form of polynuclear pyrosulphates [10]. This can be explained on the basis of the IR results, which indicate the absence of the polynuclear species in our systems in spite of high sulphate loading. It is generally agreed that most sulphate groups which form on the exposed patches of regular crystalline planes can induce protonic acidity, especially if they are in the form of complex polynuclear sulphates favoured at high loadings [10]. The high calcination temperature employed may also be a reason for the high Lewis acidity of the samples.

The same trend was observed for the iron promoted samples also. The iron incorporated samples had a higher Lewis acidity when compared to their simple sulphated analogues.

Based on the different physico-chemical characterisation results, 10 ml/g of 1 N H<sub>2</sub>SO<sub>4</sub> solution was used as the modifier solution for the further preparation of the different metal incorporated sulphated zirconia systems.

## SECTION 2 - PHYSICO-CHEMICAL CHARACTERISATION

The physical characterisation of the prepared catalyst samples was conducted by BET surface area and pore volume measurements, XRD, TG-DTA, EDX and IR spectroscopic analysis. The Laser Raman spectra and Scanning Electron Micrographs of the representative samples were also recorded.

Ammonia TPD served as an efficient tool for the comparative evaluation of the total acidity as well as the acid site distribution of the various catalytic systems. Thermodesorption studies after adsorption of pyridine support the ammonia TPD studies. The electron acceptor adsorption studies with perylene provided an idea regarding the Lewis acidic sites in presence of Brønsted acid sites. 2,6-dimethylpyridine was used as probe molecule for the identification of the Brønsted acid sites.

### 3.3 METAL INCORPORATED SULPHATED ZIRCONIA SYSTEMS

This section includes a systematic analysis of the physico-chemical characteristics of sulphated zirconia systems incorporated with different transition metals, the metal content being kept a constant.

#### 3.3.1 SURFACE AREA AND PORE VOLUME

The results of surface area and pore volume measurements are given in Table 3.5. The surface areas of pure and sulphated zirconia are also given for comparison. The retention of surface area by the sulphated samples even after high temperature calcination can be explained on the basis of the higher resistance to sintering acquired by doping with sulphate ions [1]. Suppression of particle growth is evident from the enhanced surface area of modified zirconia in comparison with unmodified zirconia. Addition of transition metal species causes a further setback to the crystallisation and sintering process, which is evident from the higher surface area of the samples in comparison with the simple sulphated system. The metal oxide species along with the sulphate ions prevent the

agglomeration of zirconia particles resulting in a higher surface area. Only exception was vanadia incorporated sample for which there was a slight lowering of surface area. Among the different metal systems, there was no significant variation in the surface area value.

The pore volume of the different systems also remained in almost the same range. The low pore volume of vanadia-loaded system may be ascribed to the blocking of the pores by the crystalline vanadia species.

Table 3.5 Metal promoted sulphated zirconia systems -A comparative evaluation of physical properties

Catalyst	Surface area (m <sup>2</sup> /g)	Pore volume (cm <sup>3</sup> /g)	Crystallite size (Å°)	Sulphate content (wt %)	% Sulphate retained
ZrO <sub>2</sub>	32.68	0.0654	8.581	-	-
SZ	44.81	0.0786	3.987	18.54	47.6
VSZ	38.14	0.0621	2.764	25.19	56.87
CrSZ	62.90	0.0870	2.315	26.56	74.82
MnSZ	58.13	0.0818	2.421	28.57	80.47
FeSZ	61.09	0.0821	2.194	30.10	84.70
CoSZ	54.92	0.0882	2.483	28.29	79.69
NiSZ	67.56	0.0845	2.349	29.37	82.73
CuSZ	65.31	0.0801	2.539	26.37	74.28
ZnSZ	59.62	0.0836	2.409	27.18	76.56
MoSZ	64.09	0.0782	2.219	29.37	82.73
WSZ	64.47	0.0837	2.284	26.23	73.89

### 3.3.2 XRD ANALYSIS

The XRD patterns of pure and modified samples are given in Fig. 3.8. In the case of pure zirconia, a co-existence of tetragonal and monoclinic phases was observed at 700°C. The predominance of tetragonal phase may be attributed to the existence of activation energy for the transformation arising from kinetic factors [40]. Only a fraction of the potentially tetragonal crystallites convert into the stable monoclinic phase under the

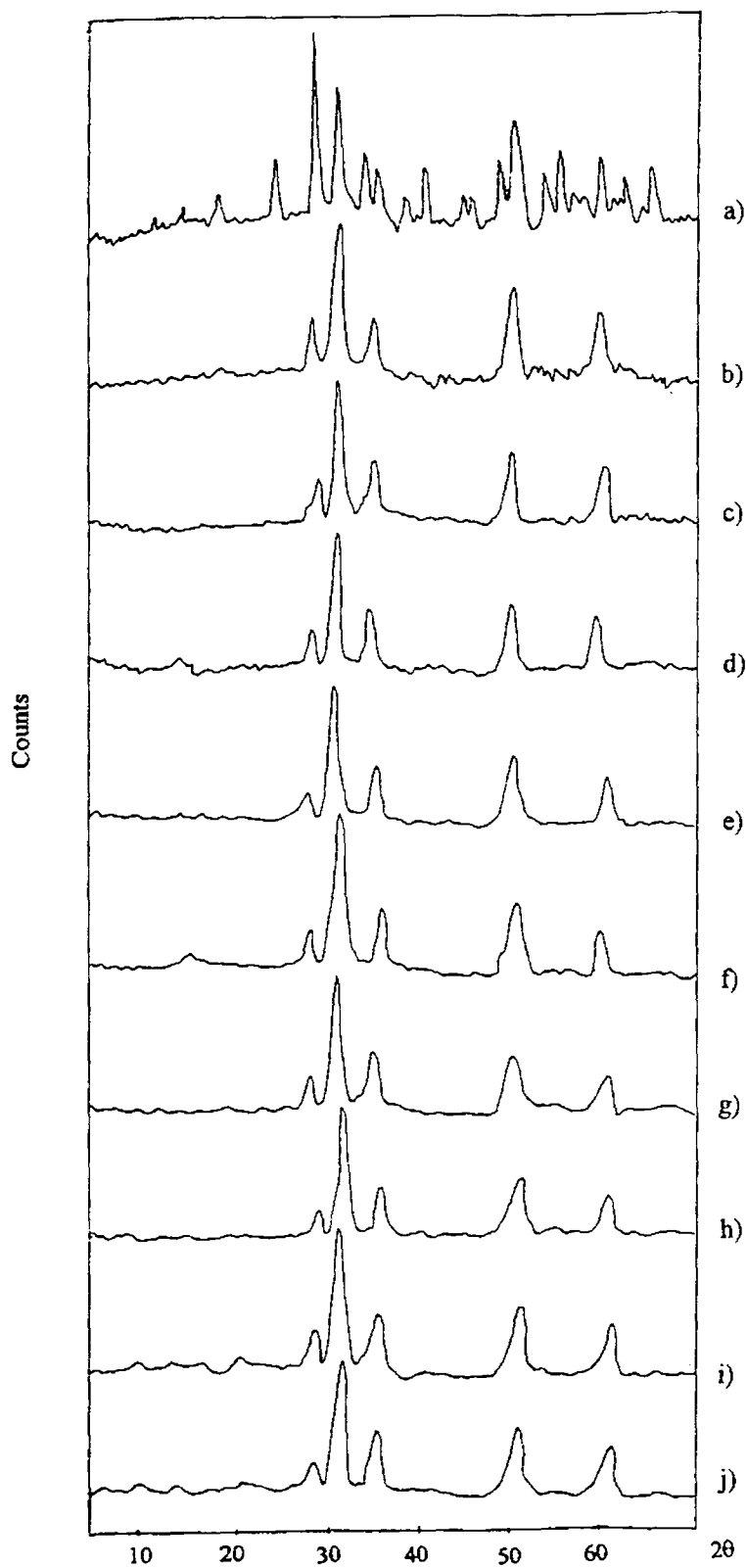


Fig. 3.8 XRD Patterns of metal promoted sulphated zirconia systems

- |         |         |         |         |
|---------|---------|---------|---------|
| a) VSZ  | b) CrSZ | c) MnSZ | d) FeSZ |
| e) CoSZ | f) NiSZ | g) CuSZ | h) ZnSZ |
| i) MoSZ | j) WSZ  |         |         |



calcination conditions employed. The sulphate doping imparts special stabilisation to the catalytically active tetragonal phase at high calcination temperatures by prevention of agglomeration of zirconia particles [34,35,41]. Like the sulphate promotion effect, incorporation of transition metal species also results in the stabilisation of tetragonal phase of zirconia by delaying the transformation of this metastable phase into the thermodynamically favoured monoclinic phase. The presence of these species on the surface prevents the zirconia from an undisturbed crystallisation.

In comparison with pure and simple sulphated zirconia, the metal incorporated systems showed enrichment of the tetragonal phase except for the vanadia promoted system, for which the monoclinic phase predominated. The existence of traces of monoclinic phase at high sulphate loadings has been reported by Farcasiu *et al.* [1]. The sulphate content higher than that required for monolayer coverage implies the migration of the sulphate moieties into the bulk [1]. The bulk sulphate species may be retained to a greater extent when compared to the surface species during high temperature calcination. It may be assumed that the dispersion of transition metal species restricts the sulphate groups more or less to the surface minimising their migration into the bulk, which facilitates their easy removal during high temperature calcination.

The absence of characteristic peaks corresponding to the metal oxide species in the metal promoted systems implies that the added metal species are present in the form of solid solution or it is highly dispersed on the ZrO<sub>2</sub> surface, which can be accounted on the basis of the low metal loading studied. In addition to the monoclinic phase, peaks corresponding to V<sub>2</sub>O<sub>5</sub> and also the orthovanadate species could be detected in the case of vanadia loaded system. The predominance of the monoclinic phase may be due to the high calcination temperature employed. This also explains the lower surface area and pore volume obtained for the vanadia promoted system in comparison with others. The crystallisation of vanadia itself may result in the pore blockage in zirconia. Calcination at lower temperatures gives the tetragonal phase without contamination of the monoclinic phase.

XRD data was also useful in calculating the approximate crystallite size of the systems using the Scherrers equation,  $t = \lambda / B \cos\theta$ , where B is the Full Width-Half

Maximum of the strongest peak,  $t$  - crystal diameter,  $\theta$  –Bragg angle. The crystallite size obtained for various samples are included in Table 3.5. In comparison with pure zirconia, the crystallite size was greatly reduced in the sulphated samples. The addition of metal promoters resulted in a slight lowering of the crystallite size, which may be a consequence of the fine dispersion of the sulphate and metal species on the surface. This also results in the higher surface area of the catalyst. The higher crystallite size of the vanadia-incorporated samples may be accounted for on the basis of the predominant monoclinic phase.

### 3.3.3 SCANNING ELECTRON MICROSCOPY

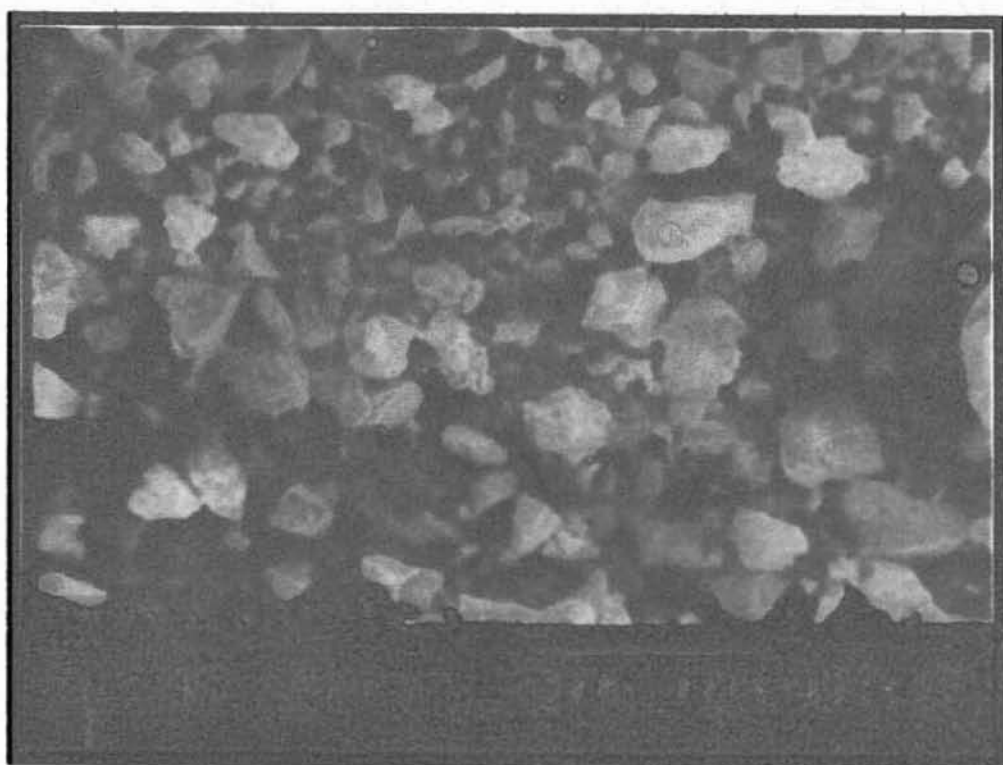
The scanning electron micrograms of representative samples are given in Fig. 3.9. In comparison with pure zirconia, the sulphated samples showed particles of lower crystallite size. The particle size of the iron promoted systems was still lower. This supports the retarding effect of metal and sulphate doping on the development of crystallinity.

### 3.3.4 THERMAL STUDIES

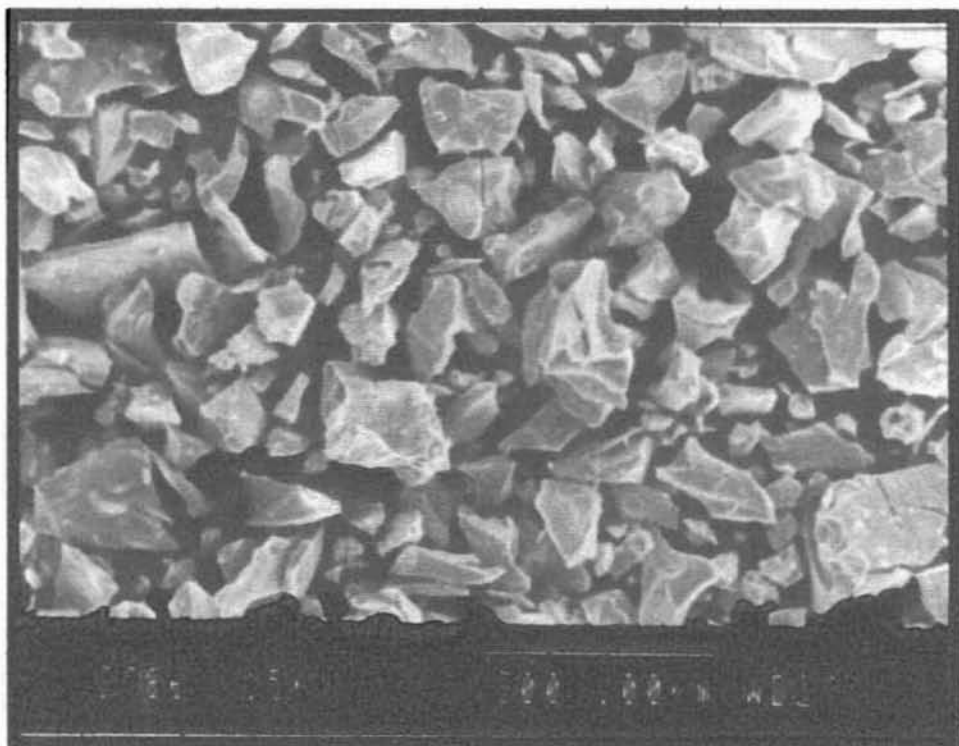
The thermal stability of the samples was examined by TG-DTA analysis. As discussed in the previous section, the TG pattern of pure zirconia indicated dehydration occurring continuously over the entire temperature range scanned. In the case of sulphated samples the initial weight loss corresponds to the removal of surface adsorbed water of hydration. The high temperature weight loss peak can be ascribed to the decomposition of the sulphate species. The onset of sulphate decomposition in the case of simple sulphated system was observed at around 690°C. The metal incorporated samples exhibited a higher thermal stability. The commencement of decomposition was observed at around 750°C for the metal promoted systems. The thermal analysis curves for Fe(2)SZ system is given as representative (Fig. 3.10). It is inferred that besides delaying the crystallisation process, the addition of the metal species also serves to stabilise the surface sulphate species. In the case of vanadia-loaded sample, decomposition occurred at around 725°C. This indicates the lower thermal stability of the vanadia promoted system. This also reflects in the predominance of the monoclinic phase in the XRD pattern of the same.



(a)



(b)



(c)

Fig. 3.9 Scanning Electron Micrographs of pure and sulphated samples

a)  $ZrO_2$

b) SZ

c) FeSZ

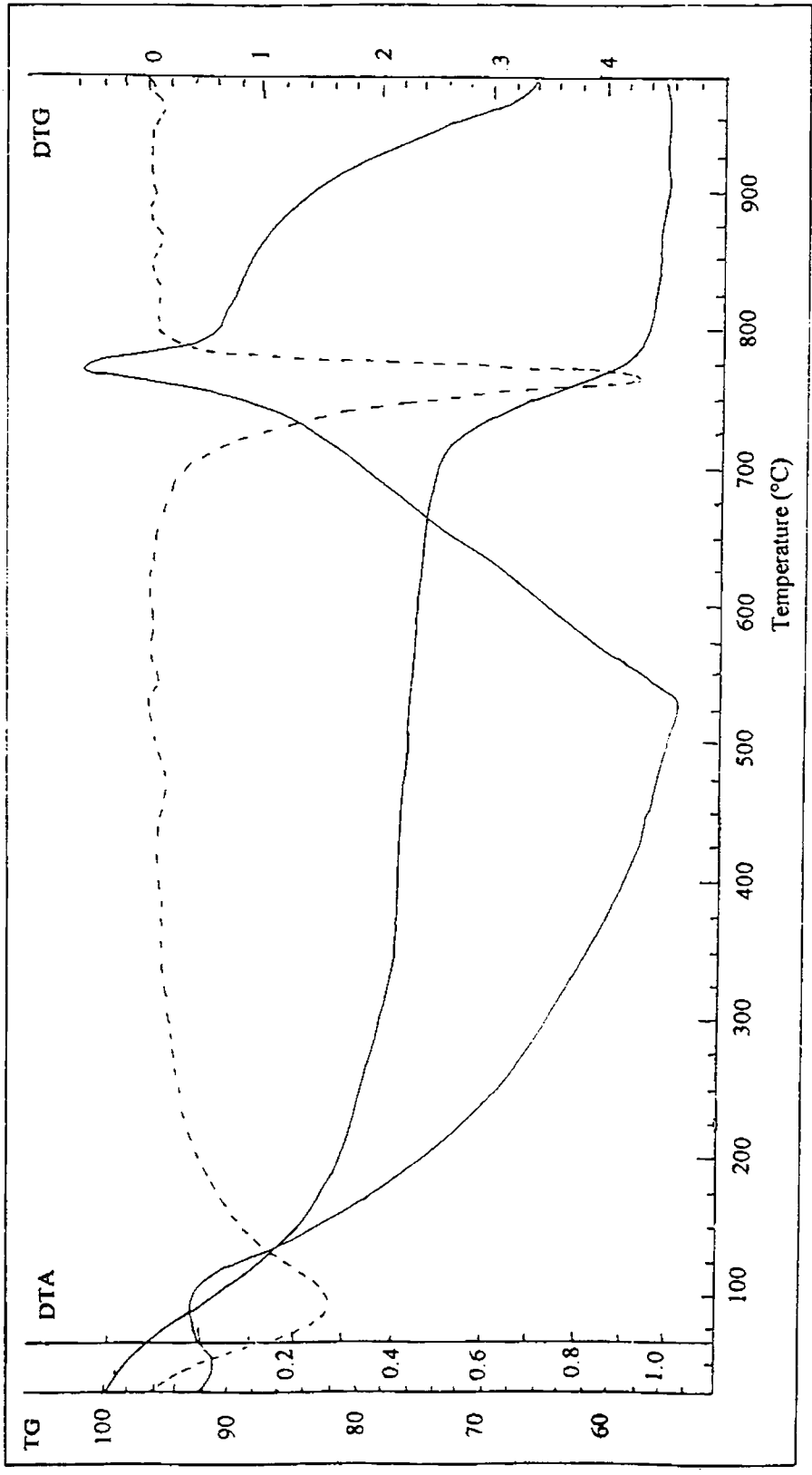


Fig. 3.10 Thermal analysis curves of FeSZ system

### 3.3.5 INFRA RED SPECTRA

In comparison with pure zirconia the spectrum of acid treated samples (Fig. 3.11) exhibits a broad peak with shoulders at around  $1200\text{ cm}^{-1}$ . The peaks at  $1029$ ,  $1076$  and  $1222\text{ cm}^{-1}$  are typical of the S-O mode of vibration of a chelating bidentate sulphate ion co-ordinated to a metal cation [42]. The band at  $1222\text{ cm}^{-1}$  results from the lowering of symmetry of the free sulphate group ( $T_d$  point group). When  $\text{SO}_4^{2-}$  is bound to the zirconia surface, the symmetry can be lowered to either  $C_{3v}$  or  $C_{2v}$  [43]. The band around  $1375\text{ cm}^{-1}$  arises from the highly covalent character of the S=O on a highly dehydrated oxide surface [35]. According to Morterra *et al.* [10,21] the peaks in this region correspond to isolated surface sulphates whereas generation of polynuclear sulphates at high sulphate loadings shifts the peak to around  $1400\text{ cm}^{-1}$ . The absence of peaks around  $1400\text{ cm}^{-1}$  suggests the absence of polynuclear species in the samples irrespective of the high sulphate loading.

The bands around  $1626\text{ cm}^{-1}$  and  $3400\text{ cm}^{-1}$  corresponds to the bending and stretching modes of the -OH groups of water molecules present in the sample. The existence of these bands even after calcination at  $700^\circ\text{C}$  points to the presence of Brönsted acidity in the samples even after high temperature calcination. The protonic site generation is believed to occur *via* the interaction of sulphate groups with water [10]. The presence of Brönsted sites in spite of the high calcination temperature employed is consistent with earlier reports [21,44]. For sulphated and metal promoted samples, the peak maximum was shifted to  $3429\text{ cm}^{-1}$ . This shift in the -OH peak to a lower stretching frequency suggests the enhancement in acid strength for the sulphated samples. The increase in Brönsted acidity during sulphation may be ascribed to the generation of S-OH groups [38] or to the acidity enhancement of the surface -OH groups [34]. However, specific IR bands characteristic of bisulphate -OH are difficult to detect due to the hydrogen bonding to the surface. So the specific categorisation of the -OH band as bisulphate group or as surface -OH becomes difficult.

Much difference could not be observed in the IR spectrum after incorporation of different metal species. In the case of vanadia incorporated system, peaks corresponding to  $\text{V}_2\text{O}_5$  were expected at around  $1000\text{ cm}^{-1}$ . But these could not be distinctly detected due

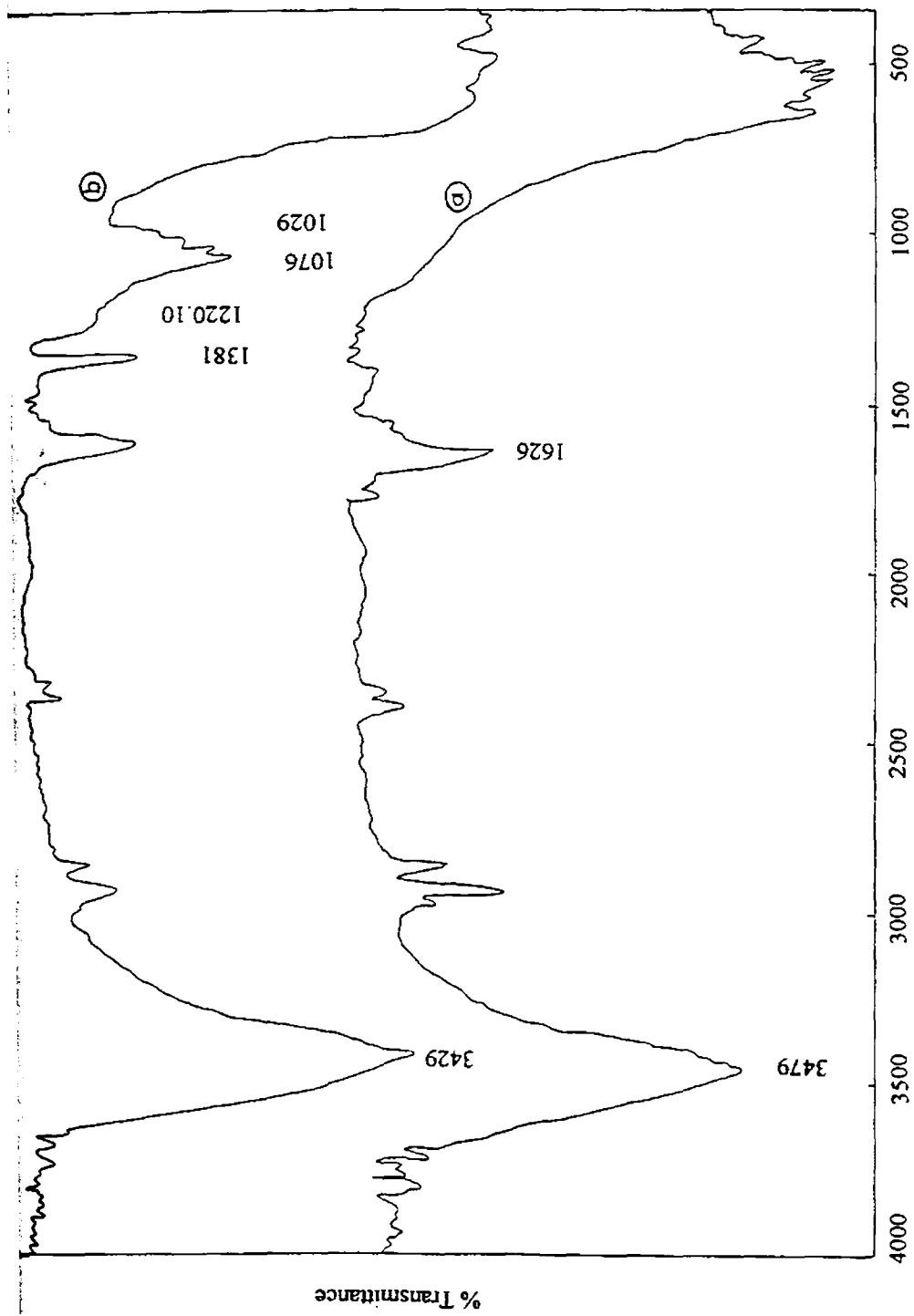


Fig. 3.11 FTIR spectra of pure and modified zirconia systems

a)  $ZrO_2$       b) FeSZ

to the overlapping of the peak corresponding to the sulphate species, which also appeared at around the same region.

### 3.3.6 LASER RAMAN SPECTRA

Laser Raman spectra of the representative samples (Fig. 3.12) complement the XRD and IR results. The peaks at 336, 370 and 472  $\text{cm}^{-1}$  clearly indicate the predominance of monoclinic phase of  $\text{ZrO}_2$  in pure sample. This, however, contradicts the XRD results according to which tetragonal phase dominates. This can be rationalised bearing in mind the fact that Laser Raman spectroscopy is a surface characterisation technique while XRD remains a tool for the bulk analysis. The surface seems to be predominated by the monoclinic phase while the bulk remains as tetragonal.

In the case of modified zirconia samples, a broadening of peaks was observed indicative of low crystallinity. The broadening of peaks also creates some uncertainty regarding the correct assignment of the peak positions to the respective crystalline phases. In sulphated samples, along with low intensity monoclinic bands, additional peaks appeared at 148, 270, 466, 624  $\text{cm}^{-1}$  representing the tetragonal phase of zirconia [40,45,46]. This establishes the stabilisation of the tetragonal phase by sulphate modification. Peaks due to S-O and S=O stretching modes of surface sulphate species show up near 1059 and 1319  $\text{cm}^{-1}$  respectively [45]. The high intensity of the S-O band points to the high sulphate content in the samples. The poor resolution of the peak at 1319  $\text{cm}^{-1}$  makes the complete characterisation of sulphate co-ordination impossible.

Laser Raman spectrum of the iron, tungsten and molybdenum incorporated samples were also recorded as representative of the different metal promoted systems. The lack of a significant change in the peak position after metal incorporation indicates that the sulphate structure remains unaltered by addition of promoters. The Raman spectra reveal the presence of iron dispersed as  $\text{Fe}_2\text{O}_3$ . The peaks at 300, 224 and 409  $\text{cm}^{-1}$  correspond to the literature data for  $\text{Fe}_2\text{O}_3$  [45]. The spectrum in the case of tungsten and molybdenum promoted samples were rather ambiguous due to broadening which may be a consequence of lower degree of crystallinity. However, peaks corresponding to  $\text{WO}_3$  [47-51] and  $\text{MoO}_3$  [52-54] species could be located in the spectrum. Additional peaks appeared at around 815 and 720  $\text{cm}^{-1}$  (stretching and bending modes of W-O bond) for



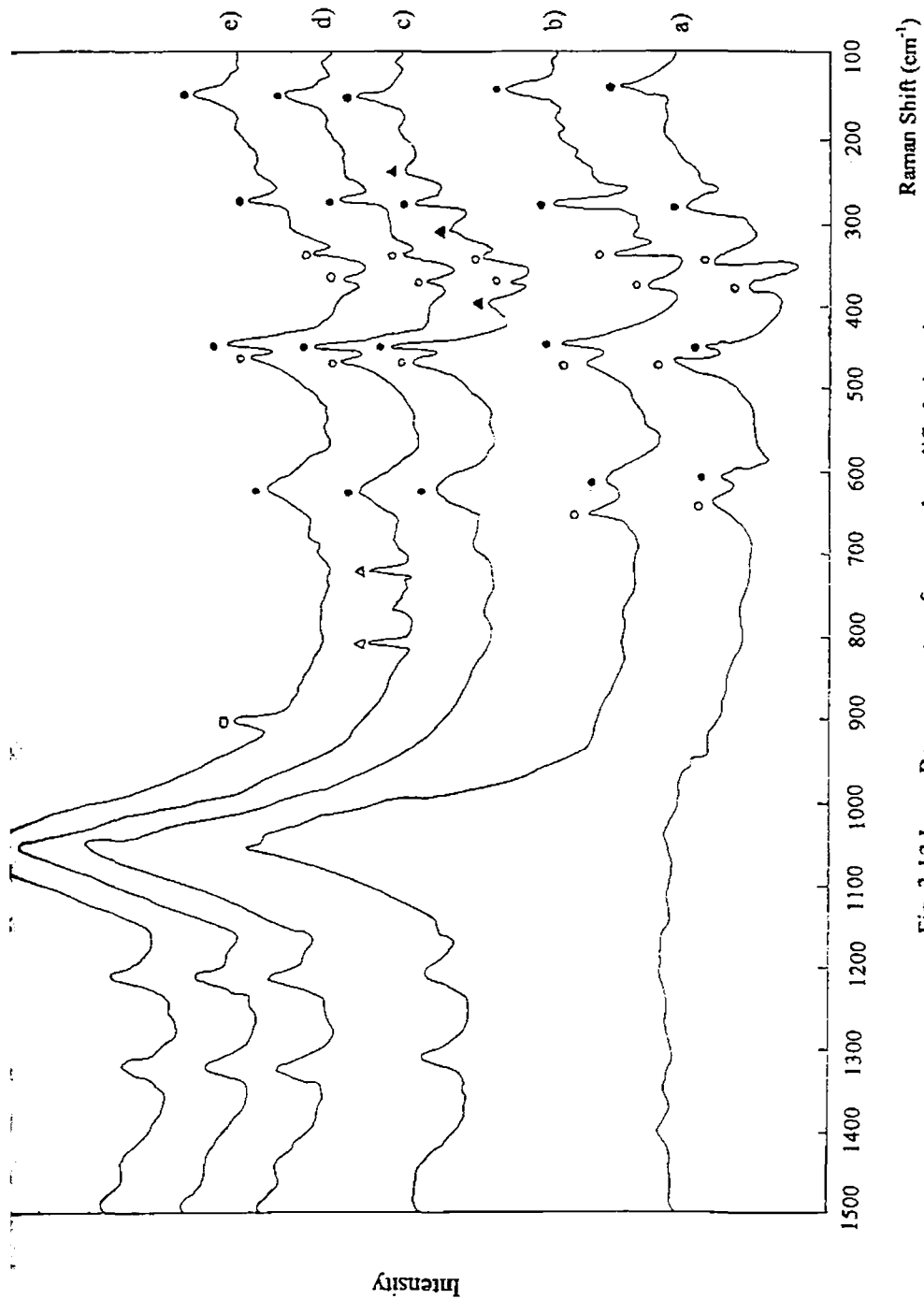


Fig. 3.12 Laser Raman spectra of pure and modified zirconia systems

a)  $ZrO_2$       b) SZ      c) FeSZ  
d) WSZ      e) MoSZ

W-promoted system while that for Mo-promoted system was observed at  $928\text{ cm}^{-1}$  (Mo=O vibration of monomolybdate species).

### 3.3.7 ELEMENTAL ANALYSIS

The sulphate contents of different samples as obtained from the EDX analysis is presented in Table 3.5. The sulphate content of the metal incorporated samples was higher when compared to the simple sulphated system. This points to the stabilisation of the surface sulphate species by the incorporated transition metal species. The sulphate content for the various systems remained in the range 25.19 to 30.10%. The iron-incorporated sample showed a maximum sulphate retention capacity while it was lowest for vanadia supported system.

### 3.3.8 ACIDITY MEASUREMENT

#### i) Ammonia TPD

The temperature programmed desorption (TPD) of ammonia enabled the characterisation of the acid strength distribution of the systems. The acid site distribution profiles (Table 3.6) show the presence of weak (desorption at  $100\text{-}200^\circ\text{C}$ ), medium ( $200\text{-}400^\circ\text{C}$ ) and strong ( $400\text{-}600^\circ\text{C}$ ) acid sites. The results for pure and sulphated zirconia samples are also given for the sake of comparison.

The total acidity of the sulphated zirconia system was considerably higher than that of pure  $\text{ZrO}_2$ . Considerable enhancement was observed in the amount of both strong and weak acid sites after incorporation of sulphate and metal species. The total acidity values obtained from ammonia TPD were comparable for the different metal incorporated systems. The difference from simple sulphated system was also marginal. In fact, no correlation could be obtained between the sulphate content of the various samples and their total acidity values. This clearly indicates that the sulphate content alone is not the deciding factor for the acidity and catalytic activity of the samples. However, a distinct difference was observed in the distribution patterns as is evident from the TPD profiles. The nature of the acid sites is greatly altered by the nature of the ions incorporated into the lattice. The distribution change may be a coupled effect of the crystalline and

structural changes. The change in the acid strength distribution for the different systems may be related to the interaction of the added metal cations with the zirconium oxide.

Table 3.6 Ammonia TPD studies on transition metal promoted sulphated zirconia catalysts- A comparative evaluation of acid strength distribution

Catalyst	Amount of ammonia desorbed (mmol/g)			
	Weak	Medium	Strong	Total
ZrO <sub>2</sub>	0.068	0.05	0.1890	0.3070
SZ	0.2256	0.3008	0.5185	1.0450
VSZ	0.6542	0.3428	0.1951	1.1921
CrSZ	0.4254	0.3724	0.3459	1.1438
MnSZ	0.3246	0.4095	0.4379	1.1721
FeSZ	0.2601	0.3796	0.5952	1.2349
CoSZ	0.4210	0.4211	0.3465	1.1886
NiSZ	0.4924	0.3624	0.3646	1.2194
CuSZ	0.3891	0.3409	0.4372	1.1672
ZnSZ	0.4943	0.2936	0.3444	1.1323
MoSZ	0.3630	0.3157	0.5178	1.1965
WSZ	0.4856	0.2338	0.5082	1.2276

### ii) Thermodesorption Studies

The TG pattern of the samples was recorded after adsorption of pyridine and 2,6-dimethylpyridine (DMP) to have a better understanding of the nature of surface acidity. Desorption was noted till the calcination temperature of 700°C since the distinct assignment of the weight decrease to pyridine/DMP desorption or sulphate decomposition or even dehydroxylation becomes impossible above this calcination temperature. The results are presented as percentage of pyridine/DMP desorbed in the specific temperature range.

Pyridine adsorption was carried out to support the TPD data. The applicability of pyridine as probe to superacids and binary oxide catalysts has been demonstrated [55]. The TG curves after pyridine adsorption showed a continuous weight loss in the region

from ambient temperature to 700°C. Pyridine, being adsorbed both at the Lewis and Brönsted sites, does not allow the differentiation between the two but it provides a rough estimate of the total acidity. The percentage desorption at different temperature ranges was also noted to have an idea regarding the acid site distribution (Table 3.7). The pyridine desorption study results were in good agreement with the ammonia TPD data. The total percentage weight loss which could be identified as a measure of the total acidity of the samples were almost the same for the different metal incorporated samples indicating that the total acidity remained in the same range irrespective of the metal species involved.

Table 3.7 Thermodesorption of pyridine- Relative distribution of acid sites

Catalyst	Pyridine desorption (Relative % weight loss)			
	Weak	Medium	Strong	Total
ZrO <sub>2</sub>	1.08	0.58	0.32	1.98
SZ	1.56	1.94	2.79	6.29
VSZ	3.84	2.49	1.28	7.61
CrSZ	3.85	2.15	1.35	7.15
MnSZ	1.54	1.90	3.75	7.19
FeSZ	1.48	3.41	4.12	9.01
CoSZ	3.10	2.92	1.81	7.83
NiSZ	3.93	2.48	1.63	8.04
CuSZ	2.65	1.30	3.32	7.27
ZnSZ	3.84	2.08	1.32	7.24
MoSZ	1.70	2.42	3.64	7.76
WSZ	2.29	2.03	4.25	8.57

The thermodesorption study of 2,6-dimethylpyridine was carried out with an intention of obtaining a comparative evaluation of the Brönsted acidity in the samples. The cumulative percentage weight loss for the different metal promoted sulphated zirconia systems are portrayed in Fig. 3.13.

from ambient temperature to 700°C. Pyridine, being adsorbed both at the Lewis and Brönsted sites, does not allow the differentiation between the two but it provides a rough estimate of the total acidity. The percentage desorption at different temperature ranges was also noted to have an idea regarding the acid site distribution (Table 3.7). The pyridine desorption study results were in good agreement with the ammonia TPD data. The total percentage weight loss which could be identified as a measure of the total acidity of the samples were almost the same for the different metal incorporated samples indicating that the total acidity remained in the same range irrespective of the metal species involved.

Table 3.7 Thermodesorption of pyridine- Relative distribution of acid sites

Catalyst	Pyridine desorption (Relative % weight loss)			
	Weak	Medium	Strong	Total
ZrO <sub>2</sub>	1.08	0.58	0.32	1.98
SZ	1.56	1.94	2.79	6.29
VSZ	3.84	2.49	1.28	7.61
CrSZ	3.85	2.15	1.35	7.15
MnSZ	1.54	1.90	3.75	7.19
FeSZ	1.48	3.41	4.12	9.01
CoSZ	3.10	2.92	1.81	7.83
NiSZ	3.93	2.48	1.63	8.04
CuSZ	2.65	1.30	3.32	7.27
ZnSZ	3.84	2.08	1.32	7.24
MoSZ	1.70	2.42	3.64	7.76
WSZ	2.29	2.03	4.25	8.57

The thermodesorption study of 2,6-dimethylpyridine was carried out with an intention of obtaining a comparative evaluation of the Brönsted acidity in the samples. The cumulative percentage weight loss for the different metal promoted sulphated zirconia systems are portrayed in Fig. 3.13.

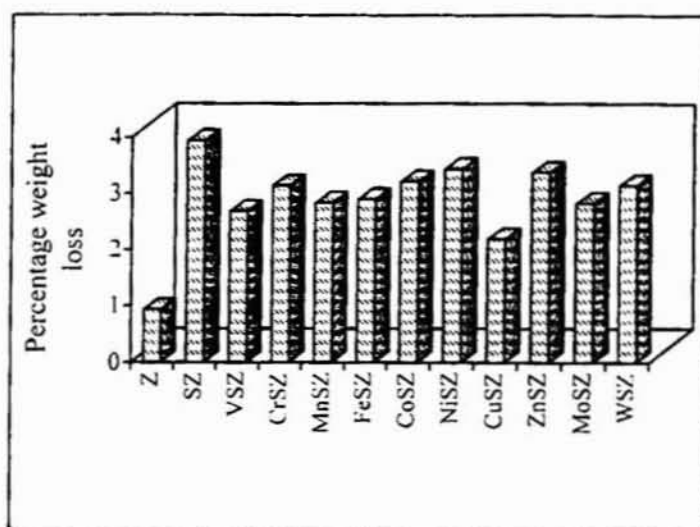


Fig. 3.13 DMP thermodesorption studies – Measure of Brönsted acidity

Table 3.8 Bronsted acid strength distribution from thermodesorption studies

Catalyst	2,6-dimethylpyridine desorption (Relative % weight loss)			
	Weak 300-400°C	Medium 400-500°C	Strong 500-700°C	Medium + Strong
ZrO <sub>2</sub>	0.395	0.356	0.186	0.542
SZ	1.895	0.983	1.062	2.045
VSZ	0.849	0.986	0.845	1.831
CrSZ	1.045	0.967	1.128	2.095
MnSZ	0.584	1.197	1.049	2.246
FeSZ	0.314	0.886	1.695	2.581
CoSZ	1.058	1.166	0.986	2.152
NiSZ	1.391	0.863	1.176	2.039
CuSZ	0.632	0.694	0.864	1.558
ZnSZ	1.569	1.168	0.633	1.801
MoSZ	1.326	1.097	0.397	1.494
WSZ	1.593	0.981	0.566	1.547

As in the case of pyridine and ammonia desorption studies, the acid strength distribution can be stated in the case of 2,6-DMP also. Upon thermal treatment, 2,6-DMP gets desorbed at different temperature ranges depending on the strength of the acidic sites on which they are adsorbed. Those molecules adsorbed at strong acid sites desorb only at high temperatures while those adsorbing on weak and medium acidic sites desorb at relatively low temperatures. Desorption below 300°C was omitted in the calculation since it contains contribution from the Brønsted as well as weak Lewis acid sites. So for a crude approximation, it may be assumed that the desorption in the range 300 to 400°C arises from the weak sites and those in the range 400 to 500°C corresponds to medium acid strength while the strong acid sites give desorption above 500°C. The distribution can be tabulated as in Table 3.8.

### iii) Perylene Adsorption Studies

After adsorption, the pale yellow, white or off-white colour of the catalyst samples turned green. The colour change was difficult to observe in the case of vanadium incorporated samples which itself was green in colour. The special one electron oxidising ability of the catalysts arises from the interaction of the sulphate groups with the metal ions. Perylene, after electron donation, gets adsorbed on the catalyst surface as radical cation. The limiting amount of perylene adsorbed which gives a measure of the Lewis acidity or the electron accepting capacity, was obtained from the Langmuir plots and is shown in Fig 3.14.

The Lewis acidity enhancement upon sulphate doping can be ascribed to the increase in the electron acceptor properties of the three co-ordinate zirconium cations *via* the inductive effect of the sulphate anions, which withdraw electron density from the zirconium cations through the bridging oxygen atom. Incorporation of metal ions influences the acid strength *via* electronic interactions. Introduction of the metal cation into the crystal lattice may result in the formation of some complex structures (Scheme 1) in some local areas on the surface.

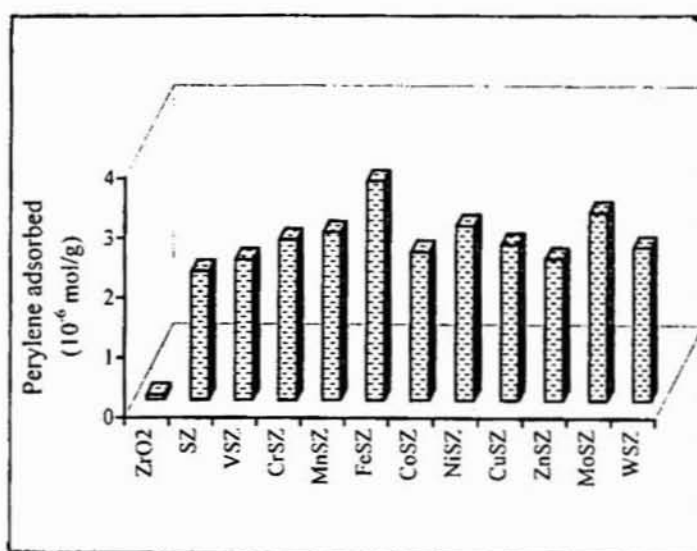
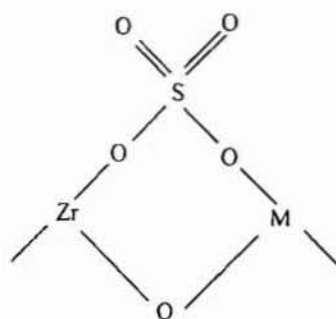


Fig. 3.14 Perylene adsorption studies- Measure of Lewis acidity



Scheme 1

According to the principle of electronegativity equalisation proposed by Sanderson [56], the electronegativity  $S_{int}$  of the complex structure and the partial charge  $\delta_{Zr}$  on  $Zr^{4+}$  can be written as

$$S_{int} = [S_M^x S_{Zr} S_S S_O^z]^{1/2+x+z}$$

$$\delta_{Zr} = (S_{int} - S_{Zr}) / 2.08 S_{Zr}^{1/2}$$

where  $S_M$ ,  $S_{Zr}$ ,  $S_S$  and  $S_O$  are the electronegativities of M, Zr, S and O and x, z are the numbers of M and O in the neighbourhood of  $Zr^{4+}$ . Introduction of transition metal ions having electronegativity higher than that of  $Zr^{4+}$  results in an overall increase in the electronegativity of the surface complex ( $S_{int}$ ). Consequently,  $\delta_{Zr}$  becomes more positive thereby resulting in enhanced Lewis acidity. The electronegativity of the incorporated ions being higher than that of Zr, an increase in Lewis acidity is expected in all the cases.



which is observed experimentally also. However, the Lewis acidity enhancement does not match with the electronegativity values indicating that some other factors may also be operating. The nature of interaction of the metal species with the zirconium oxide also may be important.

### 3.4 IRON INCORPORATED SULPHATED ZIRCONIA SYSTEMS

Considering the superiority of the physico-chemical properties of iron-doped systems in comparison with others, we found it quite reasonable to examine the influence of the iron content on the catalyst properties. The iron content was varied from 2 to 10% keeping other parameters constant and the characterisation results are presented in the following section.

#### 3.4.1 SURFACE AREA AND PORE VOLUME

The surface area values for pure and sulphated zirconia samples are presented in Table 3.9. The dispersion of the iron and sulphate moieties on the surface explains the higher surface area of the modified zirconia samples. The presence of iron improves the dispersion thereby facilitating the retardation of crystallisation. However, an increase in iron loading did not have any remarkable influence on the surface area. A slight lowering observed in the surface area values may be a result of the partial agglomeration of the iron particles at high metal loadings.

Table 3.9 Influence of iron content on the physical properties

Catalyst	Surface area (m <sup>2</sup> /g)	Pore volume (cm <sup>3</sup> /g)	Crystallite size (Å°)	Sulphate content (wt %)	% Sulphate retained
ZrO <sub>2</sub>	32.68	0.0654	8.581	-	-
SZ	44.81	0.0786	3.987	18.54	47.6
Fe(2)SZ	61.09	0.0821	2.194	30.10	84.70
Fe(4)SZ	60.43	0.0830	2.189	28.86	81.29
Fe(6)SZ	59.58	0.0846	2.284	27.13	76.42
Fe(8)SZ	57.29	0.0745	2.315	24.65	69.44
Fe(10)SZ	55.65	0.0882	2.483	23.05	64.93

### 3.4.2 XRD ANALYSIS

Consistent with the earlier reports [57], XRD data support the stabilisation of the catalytically active tetragonal phase and retardation of crystallisation after incorporation of sulphate and iron species. In comparison with pure  $ZrO_2$ , the XRD patterns of sulphated and iron incorporated zirconia samples showed an enrichment of the tetragonal phase (Fig. 3.15).

The bulk structure of SZ remains virtually unchanged by the incorporation of iron except for a lowering in crystallinity. The lowering of crystallinity becomes prominent with increased iron loading. The absence of the characteristic peaks of  $Fe_2O_3$ , implies the high dispersion of the iron particles on the zirconia surface. The fact that the surface area is only slightly lowered at high iron loadings also hints the presence of iron in dispersed form rather than in a crystalline state. Traces of monoclinic phase detected along with a predominant tetragonal phase in SZ and low loaded FeSZ samples may be attributed to the high sulphate loadings in these systems. The special stability of the tetragonal phase diminishes at high sulphate loadings [1]. At high iron loadings, monoclinic phase disappears completely indicating the stabilisation of the tetragonal phase aided by the dispersion of  $Fe_2O_3$  particles and the reduction of sulphate content as shown by EDX analysis.

The average crystallite size of the samples calculated using the Scherrers equation is given in Table 3.9. As stated earlier, the crystallite size was considerably reduced by the incorporation of sulphate and iron moieties. Addition of iron improves the dispersion of the particles thereby resulting in a higher surface area and lower crystallite size. However, higher iron content reduces the surface area and increases the crystallite size perhaps due to the agglomeration of iron moieties on the surface.

### 3.4.3 ELEMENTAL ANALYSIS

The sulphate content as obtained by EDX analysis is presented in Table 3.9. Incorporation of iron significantly improves the sulphate retaining ability. The sulphate content higher than that required for monolayer coverage implies the migration of the sulphate moieties into the bulk [1]. The bulk sulphate species may be retained to a greater extent when compared to the surface species during high temperature calcination. A slight

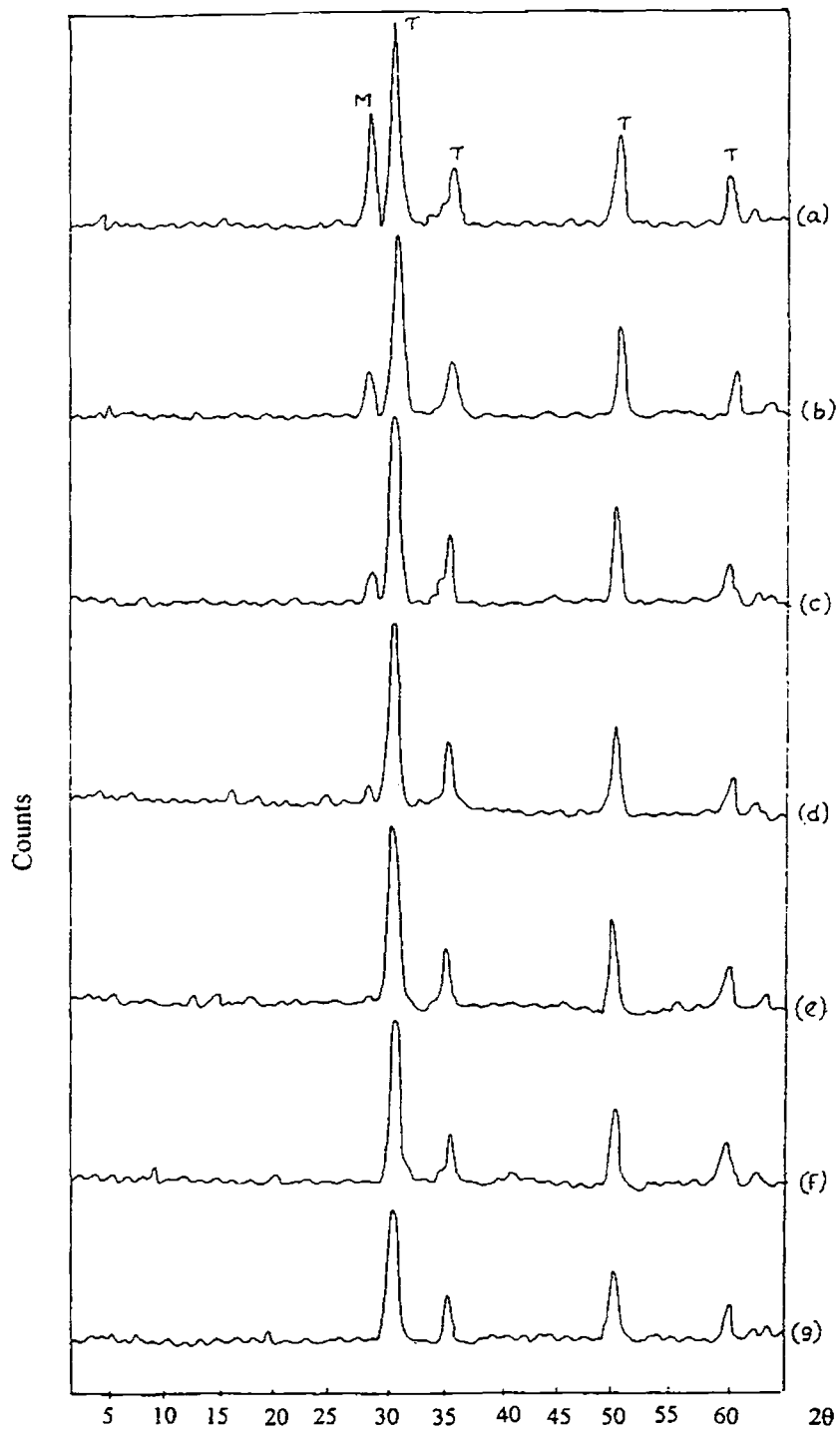


Fig. 3.15 XRD Patterns of iron promoted sulphated zirconia systems

- |            |            |             |            |
|------------|------------|-------------|------------|
| a) $ZrO_2$ | b) SZ      | c) Fe(2)SZ  | d) Fe(4)SZ |
| e) Fe(6)SZ | f) Fe(8)SZ | g) Fe(10)SZ |            |

lowering of the sulphate content was observed at high iron loadings. It may be assumed that the dispersion of iron particles restricts the sulphate species more or less to the surface minimising their migration into the bulk, which facilitates their easy removal during high temperature calcination.

#### 3.4.4 INFRA RED SPECTRA

The IR spectra of the Fe(2)SZ and Fe(10)SZ samples are traced in Fig. 3.16. The spectrum of pure zirconia is also given for comparison. As in the case of different metal promoted systems, no difference could be detected in the spectrum of samples when iron loading was increased. The broad peak around  $1059\text{ cm}^{-1}$  represents the S-O mode of vibration of a chelating bidentate sulphate ion co-ordinated to a metal cation [42,43]. The band around  $1375\text{ cm}^{-1}$  arises from the highly covalent character of the S=O of isolated sulphate species on a highly dehydrated oxide surface [35,41].

#### 3.4.5 LASER RAMAN SPECTRA

The Laser Raman spectra of Fe(2)SZ and Fe(10)SZ are portrayed in Fig. 3.17. The spectra of pure  $\text{ZrO}_2$  and simple sulphated sample are also given for comparison. As discussed in the previous section, in sulphated and iron incorporated samples with low metal loading (Fe(2)SZ), along with low intensity monoclinic bands, additional peaks appeared at 148, 270, 466,  $624\text{ cm}^{-1}$  representing the tetragonal phase of zirconia [40,45,46]. In samples with higher iron content, the monoclinic phase was completely absent. Peaks due to S-O and S=O stretching modes of surface sulphate species show up near  $1059$  and  $1319\text{ cm}^{-1}$  respectively [45]. In comparison with the spectrum of Fe(2)SZ the peaks at 300, 224 and  $409\text{ cm}^{-1}$  was more prominent for Fe(10)SZ signifying the higher iron content. The appearance of the  $\text{Fe}_2\text{O}_3$  peaks in the Laser Raman spectrum and its absence in the XRD pattern further confirms the presence of iron in highly dispersed form even at high iron loadings.

#### 3.4.6 THERMAL STUDIES

The TG analysis confirms the thermal stability of the systems. The higher thermal stability of the iron incorporated systems explains their high sulphate content. An increase in the iron loading did not have any significant effect on the sulphate decomposition

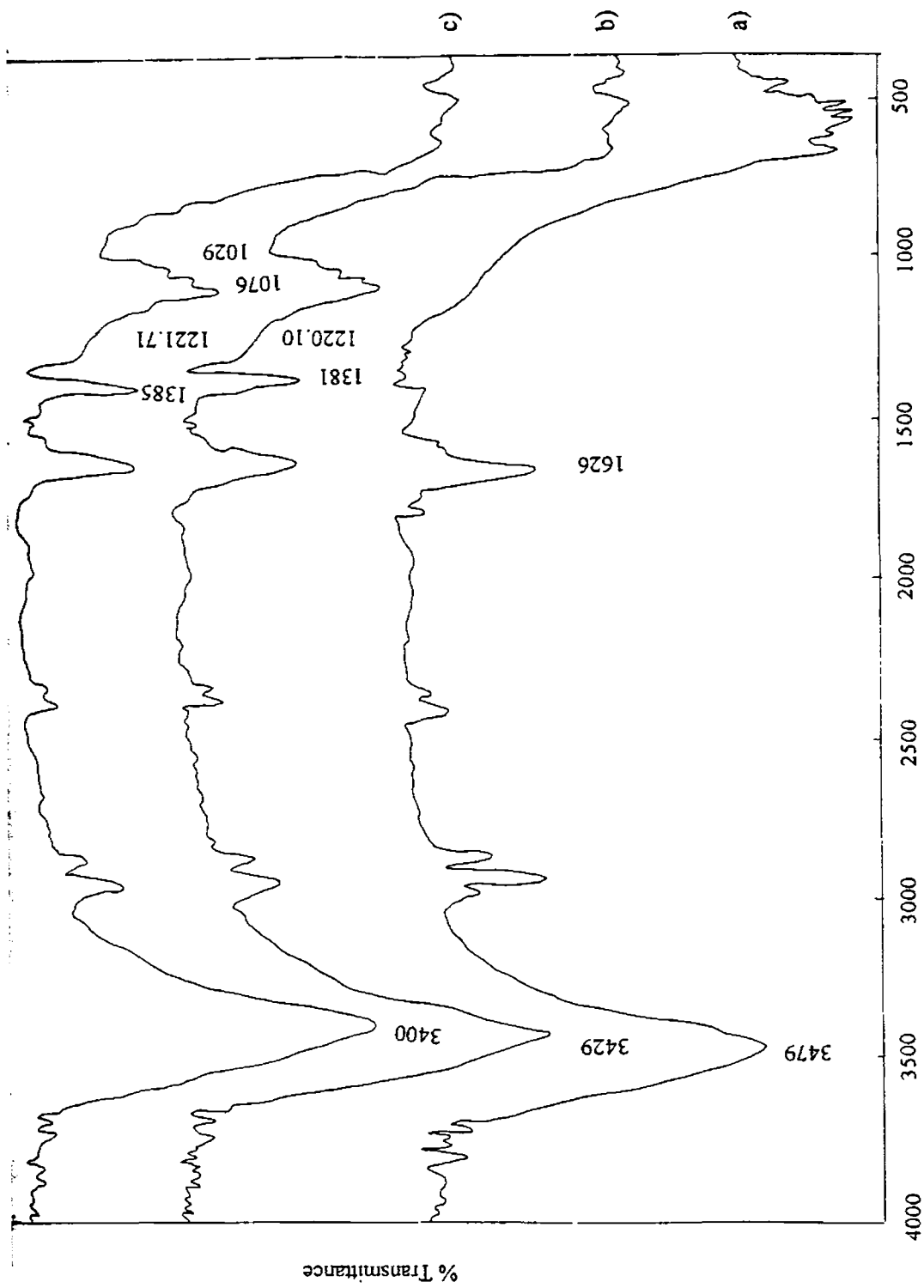


Fig. 3.16 FTIR Spectra of iron promoted sulphated zirconia systems

a)  $ZrO_2$       b) Fe(2)SZ      c) Fe(10)SZ

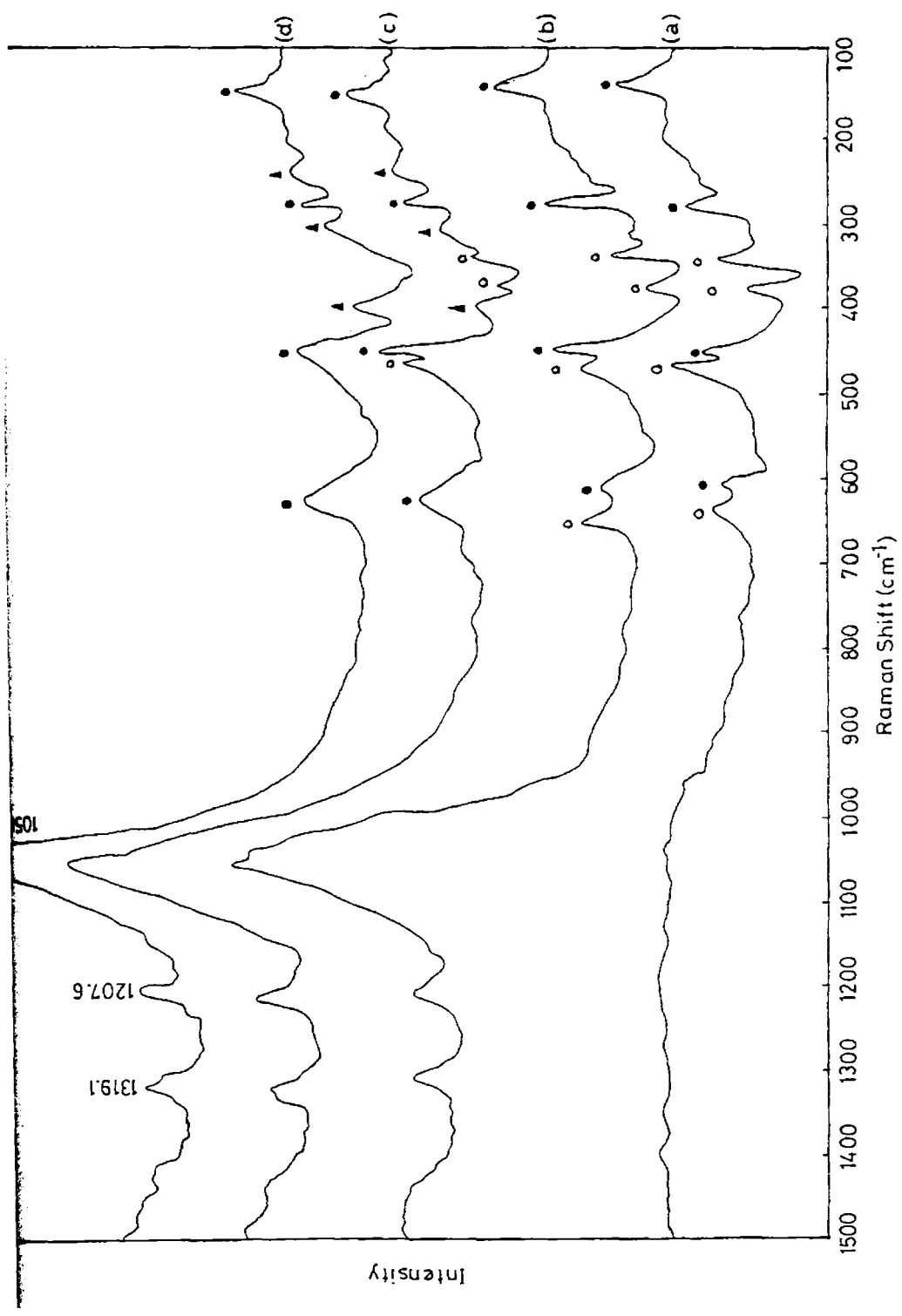


Fig. 3.17 Laser Raman Spectra of iron promoted sulphated zirconia systems

a) ZrO<sub>2</sub>      b) SZ      c) Fe(2)SZ      d) Fe(10)SZ

temperature. Sulphate decomposition was found to occur at around 750°C for all the samples.

### 3.4.7 ACIDITY MEASUREMENT

#### i) Ammonia TPD

The TPD of ammonia was used to characterise the acid site distribution and further more to obtain the quantitative amount of acid sites in the specified temperature range. The distribution pattern can be classified into weak (desorption at 100-200°C), medium (200-400°C) and strong (400-600°C) acid sites. A broadening of the distribution curve was observed for pure  $ZrO_2$  asymmetric on the high temperature side with a maximum at around 500°C. The acid site distribution profiles for the modified zirconia samples exhibit two distinct maxima at around 300° and 500°C (Fig. 3.18).

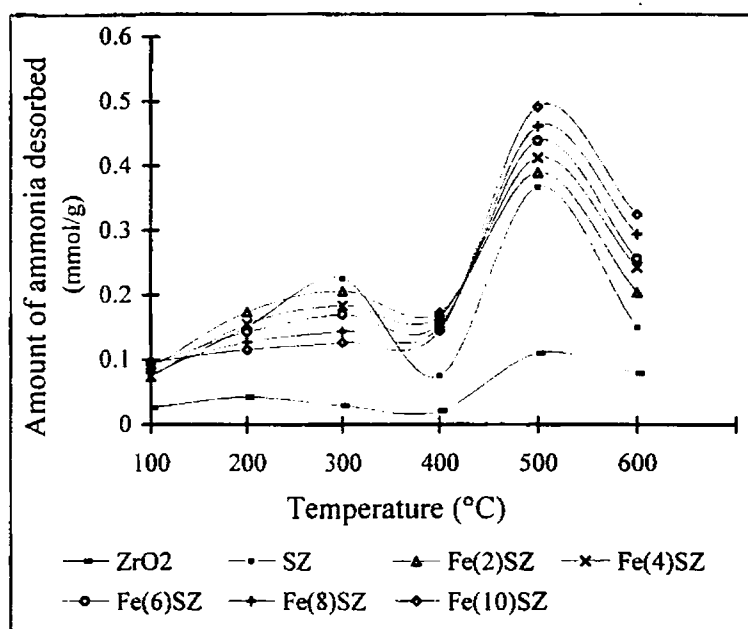


Fig. 3.18 Acid site distribution profiles from ammonia TPD

Considerable enhancement of both strong and weak acid sites was observed after incorporation of sulphate and iron moieties. Only a slight enhancement was observed in the total acidity values of SZ and FeSZ systems in spite of the fact that the iron incorporated samples had almost double the sulphate content when compared to simple sulphated system (Table 3.9). This clearly indicates that the sulphate content alone is not

the deciding factor for the acidity and catalytic activity of the samples. The incorporation of promoters results in a rearrangement in the acid strength distribution in a direction favouring the formation of strong acid sites. The distribution change may be a coupled effect of the crystalline and structural changes. The amount of ammonia desorbed and hence the total acidities for the different iron promoted samples were also comparable. However, a significant difference was observed in the distribution pattern. A well-defined enhancement of the strong acid sites at the expense of weak ones with an increase in the iron loading is quite evident from the TPD profiles.

### ii) Thermodesorption Studies

Pyridine adsorption studies (Fig. 3.19) lend support to the TPD results. The sharp weight loss observed in the high temperature region may be due to the oxidative decomposition of sulphate species by interaction with pyridine. The total percentage weight loss was almost constant for the iron incorporated samples except for Fe(10)SZ. The anomalous increase in the percentage weight loss observed for Fe(10)SZ may be a consequence of the lowering of the sulphate decomposition temperature at high iron loading. The interaction of sulphated iron oxide and pyridine has been reported earlier [58-60].

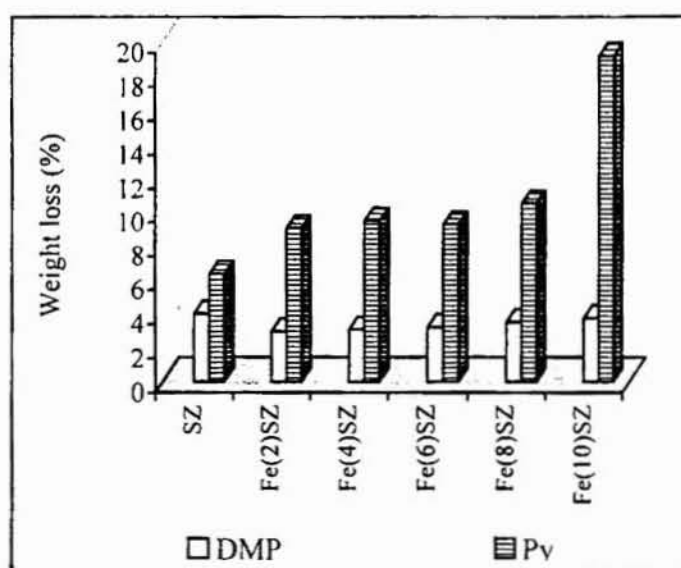


Fig.3.19 Thermodesorption studies using Pyridine and 2,6-DMP as probes



The thermodesorption studies using 2,6-dimethylpyridine (Fig. 3.19) provides a comparative evaluation of the Brönsted acidity in the samples and the acid strength distribution is tabulated (Table 3.10). The steric hindrance by the methyl groups, selective adsorption of 2,6- dimethylpyridine occurs at the Brönsted acid sites [15,16]. On the basis of the reported interaction of 2,6-dimethylpyridine with Lewis sites at low temperatures [15,18,19], we presume the amount of 2,6-DMP desorbed at temperatures above 300°C to be arising due to desorption from Brönsted acid sites. Taking a cumulative plot, the amount of 2,6-DMP desorbed showed a trivial increase with increase in the iron loading. This we take as an approximate measure of the Brönsted acidity. The low percentage values may be due to the trace amount of Brönsted acidity left after high temperature calcination or it may be a consequence of neglecting the desorption at lower temperature.

Table 3.10 Bronsted strength distribution from thermodesorption studies

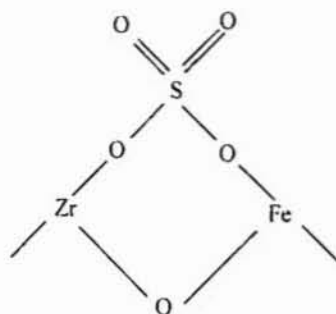
Catalyst	2,6-dimethylpyridine desorption (Relative % weight loss)			
	Weak 300-400°C	Medium 400-500°C	Strong 500-700°C	Medium + Strong
ZrO <sub>2</sub>	0.395	0.356	0.186	0.542
SZ	1.895	0.983	1.062	2.045
Fe(2)SZ	0.314	0.886	1.695	2.581
Fe(4)SZ	0.351	0.952	1.713	2.665
Fe(6)SZ	0.438	0.862	1.859	2.721
Fe(8)SZ	0.597	0.896	1.964	2.860
Fe(10)SZ	0.627	0.921	2.142	3.063

### iii) Perylene Adsorption Studies

A comparative evaluation of Lewis acidity obtained from perylene adsorption studies is sketched in Fig. 3.20. The Lewis acidity enhancement can be ascribed to the increase in the electron acceptor properties of the three co-ordinate zirconium cations *via* the inductive effect of the sulphate anions, which withdraw electron density from the zirconium cations through the bridging oxygen atom. Incorporation of iron enhances the

acid strength *via* electronic interactions. Introduction of the metal cation into the crystal lattice may result in the formation of some complex structures (**Scheme 2**) in some local areas on the surface.

As discussed in the previous section, the electronegativity of  $\text{Fe}^{3+}$  being larger than that of  $\text{Zr}^{4+}$ , the electronegativity of the surface complex,  $S_{\text{int}}$  is increased and  $\delta_{\text{Zr}}$  becomes more positive when Fe is introduced, thereby resulting in enhanced Lewis acidity. This also explains the increase in Lewis acidity at higher iron loadings. Incorporation of iron in higher concentrations leads to the development of more and more localised complex structures, thereby contributing to an overall increase in the Lewis acidity.



Scheme 2

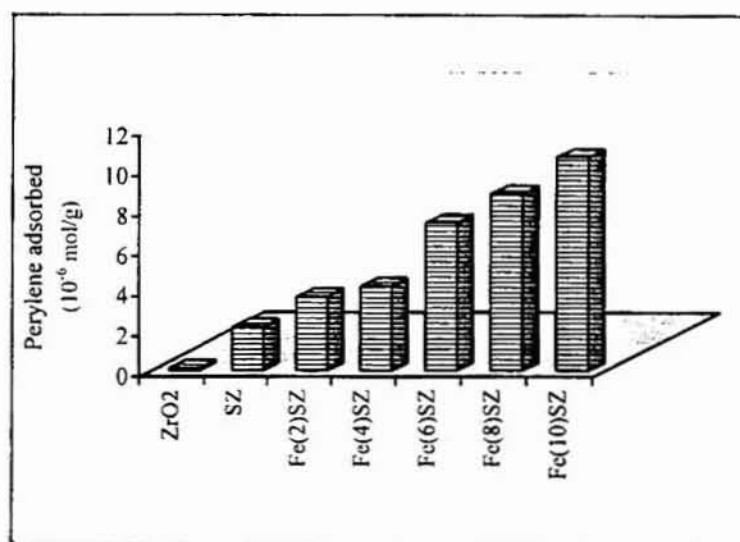


Fig. 3.20 Lewis acidity of iron promoted systems obtained from perylene adsorption studies

## SECTION 3 - TEST REACTION FOR ACIDITY

## 3.5 CUMENE CONVERSION REACTION

Cumene conversion reaction was chosen as a test reaction for acidity. The cumene conversion and relative product selectivity could be correlated with the surface acidic properties as established by the following discussions.

## 3.5.1 INTRODUCTION

The cumene conversion reaction can be schematically represented as shown in Fig. 3.21.

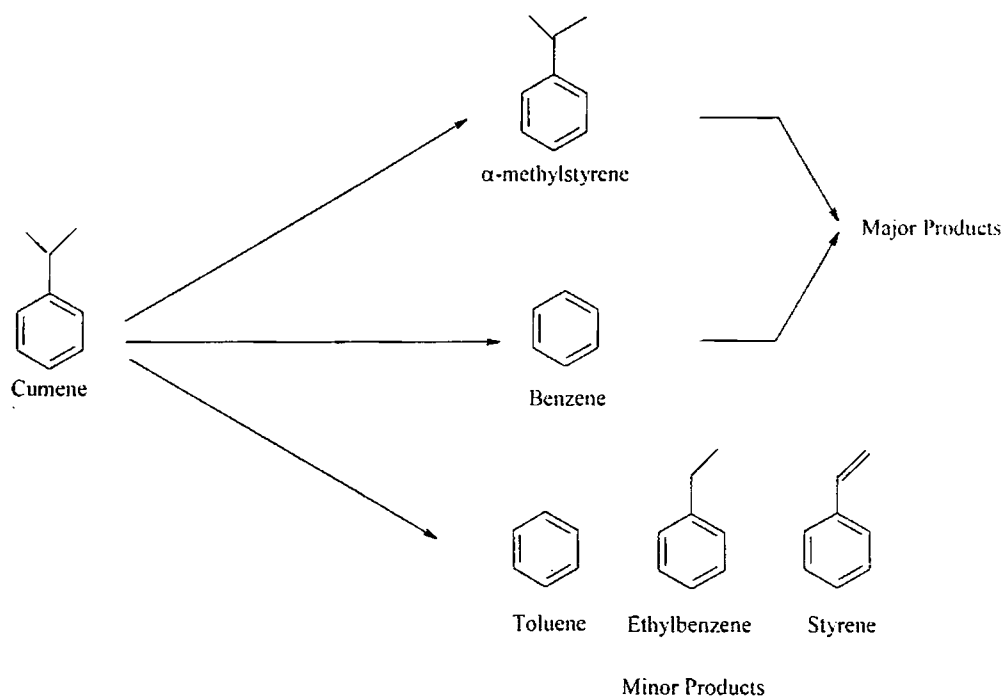
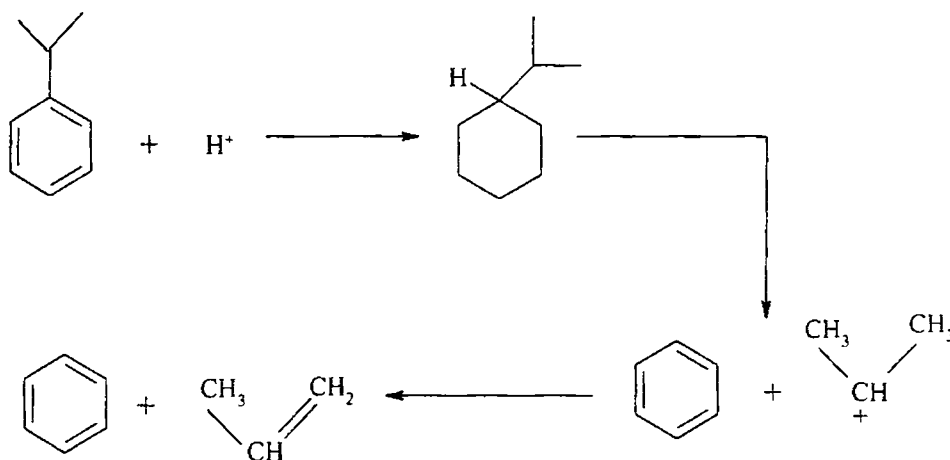


Fig. 3.21 Schematic representation of cumene conversion reaction

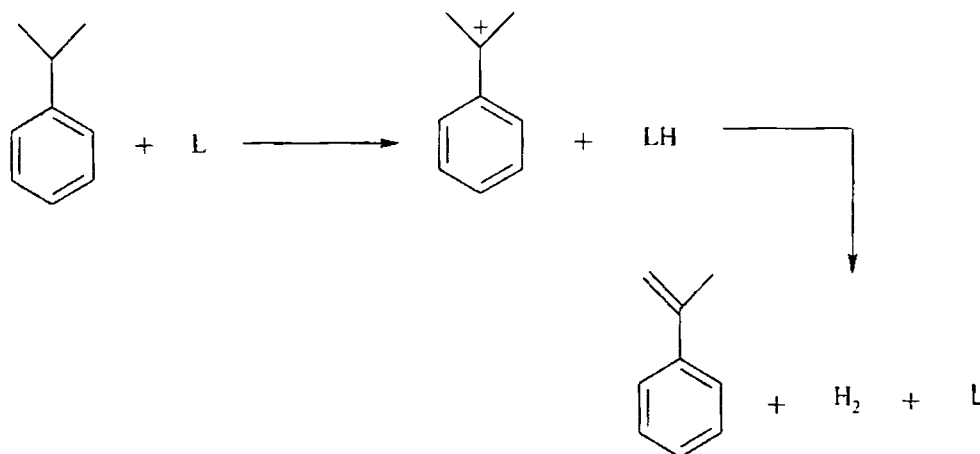
The major reactions occurring during cumene conversion may be grouped into dealkylation (cracking) and dehydrogenation. Another possibility is the cracking of the alkyl chain to give ethylbenzene. Ethylbenzene on dehydrogenation give styrene. Cracking of cumene to benzene (Scheme 3) is generally attributed to the action of Brönsted sites by a carbonium ion mechanism [61-64] while dehydrogenation of cumene yields  $\alpha$ -methylstyrene as the major product (Scheme 4), the formation of which has

been ascribed to the Lewis acid sites [61]. Mechanism of cumene conversion may be represented as in Fig. 3.22.

Boorman *et al.* prepared a series of catalysts containing fluoride, cobalt and molybdenum as additive to  $\gamma$ -alumina, both individually and in combination and the surface acidity of these systems was correlated with their reactivity for cumene conversion [65,66]. Sohn and Jang [67] correlated the activity for cumene dealkylation with both acidity and acid strength distribution of sulphated  $ZrO_2$ - $SiO_2$  catalysts



Scheme 3



Scheme 4

Fig. 3.22 Mechanism of cumene conversion reaction

### 3.5.2 CUMENE CONVERSION OVER SULPHATED ZIRCONIA SYSTEMS

Cumene conversion reaction was carried out at 350°C at a flow rate of 6 ml/hr. The time on stream of 2 hours was maintained for the reaction. The conversions and product selectivity for the different metal incorporated systems are shown in Table 8. Pure zirconia was totally inactive towards the reaction while the different metal promoted systems exhibited low conversions under the conditions studied (Table 3.11). The incorporation of transition metal species did not alter the conversion to any significant extent. However, a quick deactivation as reported with such systems was not observed after incorporation of promoters. A gradual deactivation could be noticed with an increase in the time on stream.

Table 3.11 Cumene cracking over metal promoted sulphated zirconia systems

Catalyst	Conversion (%)	Selectivity (%)	
		Cracking products	$\alpha$ -methyl styrene
ZrO <sub>2</sub>	-	-	-
SZ	5.85	50.46	49.54
VSZ	5.90	33.58	66.42
CrSZ	7.32	40.04	59.96
MnSZ	9.18	37.03	62.97
FeSZ	11.15	18.29	81.17
CoSZ	7.93	43.71	56.21
NiSZ	8.52	34.68	65.32
CuSZ	8.84	31.70	66.78
ZnSZ	6.37	45.32	54.66
MoSZ	10.04	5.78	94.22
WSZ	9.57	40.18	59.82

Cumene conversion is known to be catalysed by strong [68] or moderate [69] acid sites. In our case, the cumene conversion seemed to be dependent on the amount of strong acid sites (Fig. 3.23). Metal doped systems were found to be more active when compared to the simple sulphated system even though sulphated zirconia sample had sufficiently high amount of strong acid sites. As represented in the reaction scheme,  $\alpha$ -methylstyrene

and benzene were obtained as the major products. Ethylbenzene and styrene appeared in minor quantities. In some cases toluene was also detected in trace amounts. The selectivity towards dehydrogenated products may be ascribed to the Lewis acidity of the systems as indicated in Fig. 3.24. Similarly the generation of cracking products agreed well with the Brönsted acidity of the systems (Fig. 3.25).

Abnormally high selectivity to  $\alpha$ -methylstyrene (94.22%) was observed in the case of molybdenum incorporated sample and the cracking products were obtained only in trace amounts. These results do not agree with its Brönsted acidity value. This suggests that the Brönsted acid sites associated with  $\text{MoO}_3$  are not active in initiating the cracking reaction even though they accelerate the dehydrogenation reaction. This explains the high selectivity to  $\alpha$ -methylstyrene observed in this case. Such a suppression of cracking after molybdenum incorporation has been previously reported [65,66]. Another factor that contributes to the inhibition of cracking is the deposition of coke. Any dealkylation that occurs initially would generate propene, which through acid catalysed polymerisation results in coke formation [64]. Although, not so prominent as in the case of Mo, the relative selectivity for cracking products was lower for Cr, Mn, Fe and Ni promoted systems when compared to their Brönsted acidity values. This may be attributed partially to the poisoning of the active Brönsted sites by the deposition of coke. This also explains the slow deactivation of the systems observed after a time on stream value of 4 hours.

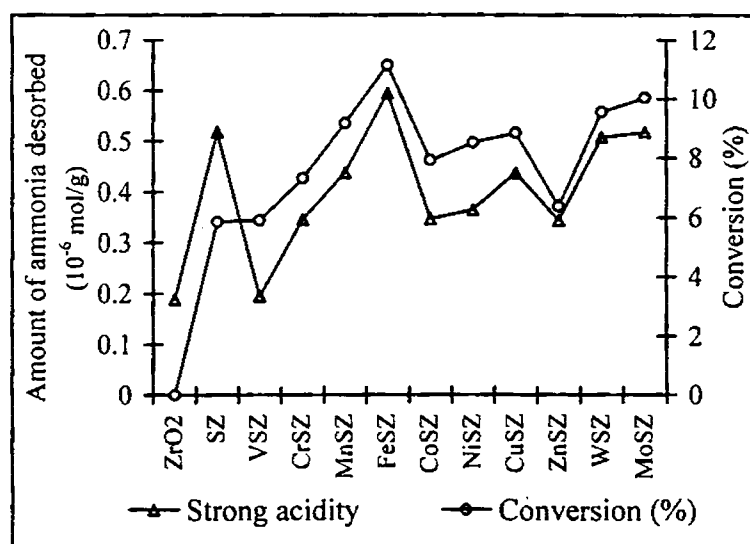


Fig. 3.23 Cumene conversion correlated with strong acidity of the systems

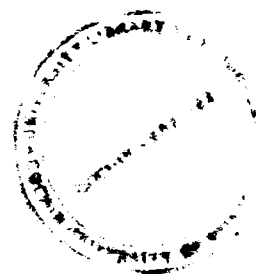
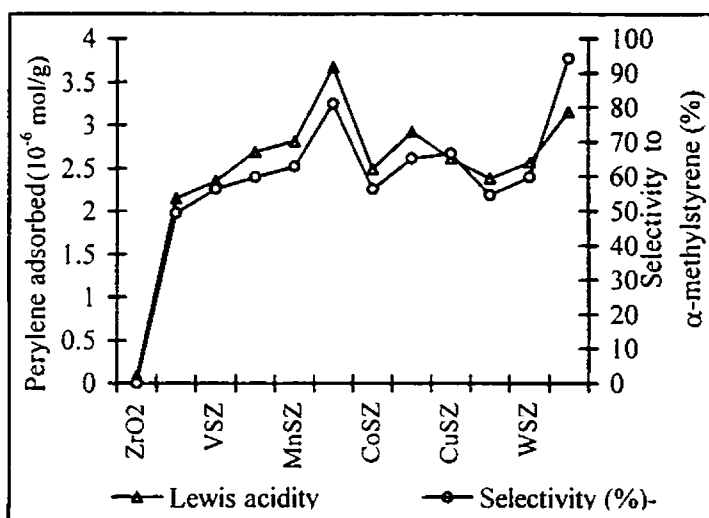


Fig. 3.24 Correlation of Dehydrogenation selectivity with Lewis acidity

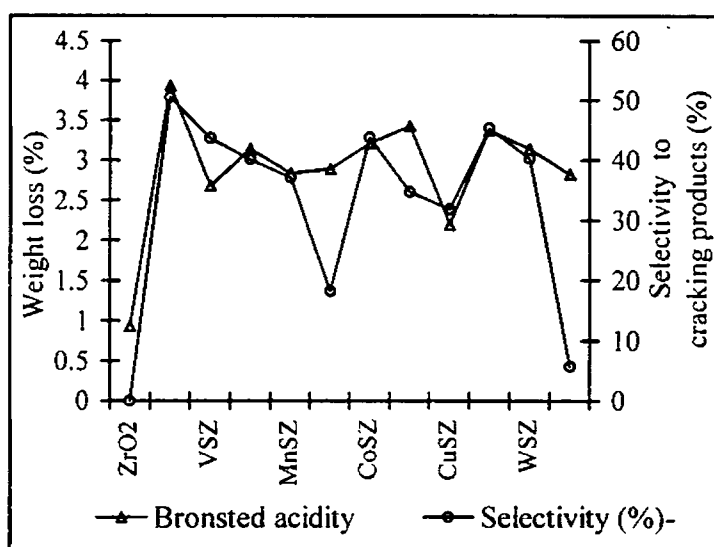


Fig. 3.25 Correlation of cracking selectivity with Brønsted acidity

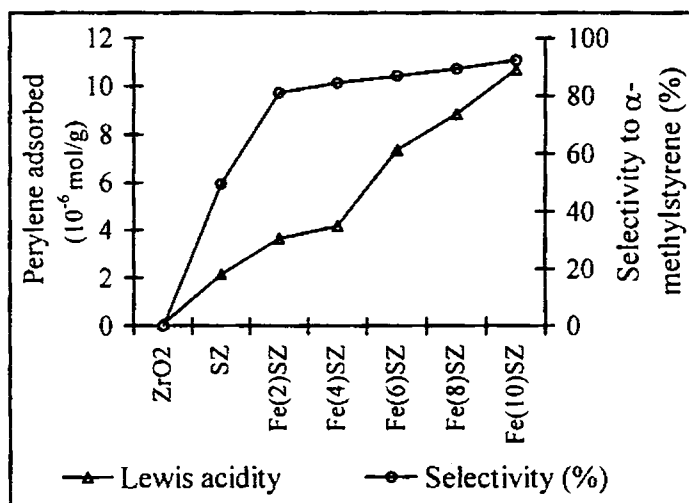
The results of cumene cracking over iron promoted sulphated zirconia systems are given in Table 3.12. In comparison with the simple sulphated systems, iron promoted samples showed higher conversion rates. Low loaded iron systems seemed to be more efficient in catalysing the reaction. An increase in the iron loading had a detrimental effect on the cumene conversion. Thus, a correlation between the cumene conversion and the amount of strong acid sites, as obtained in the case of different transition metal promoted samples could not be established. Also, high iron loaded systems were quickly

deactivated in comparison with low loaded systems. Quick deactivation may be accounted for on the basis of the strong acidity of the iron-doped systems, which may induce coke formation resulting in the blockage of active sites.

Table 3.12 Cumene Cracking over iron incorporated sulphated zirconia

Catalyst	Conversion (%)	Selectivity (%)	
		Cracking products	$\alpha$ -methyl styrene
ZrO <sub>2</sub>	-	-	-
SZ	5.85	50.46	49.54
Fe(2)SZ	11.15	18.29	81.17
Fe(4)SZ	10.58	15.42	84.58
Fe(6)SZ	9.53	12.93	87.07
Fe(8)SZ	8.92	10.54	89.46
Fe(10)SZ	8.54	7.59	92.41

The selectivity towards dehydrogenation showed a marginal increase with increase in iron loading while there was a gradual decline in the cracking activity. Thus, the selectivity pattern for dehydrogenation was almost in line with the increase in Lewis acidity of the systems (Fig. 3.26). The drop off in the selectivity towards cracking products, in spite of the slight enhancement of Brønsted acidity at high iron loadings may be explained on the basis of the poisoning by coke deposition.

Fig. 3.26 Correlation of  $\alpha$ -methylstyrene selectivity with Lewis acidity



## CONCLUSIONS

Sulphate incorporation significantly affects the physico-chemical properties of zirconia. The calcination temperature and the sulphate loading play a crucial role in deciding the catalyst properties. High calcination temperature is required for the generation of strong acidity in sulphated zirconia systems. Sulphation causes an increase in the surface area and surface acidic properties. Another important consequence is the special stabilisation of the tetragonal phase. High sulphate loading is accompanied by the lowering of surface area and the tetragonal phase stabilisation, which may be an after-effect of the sulphate migration into the bulk. Transition metal incorporation improves the physico-chemical properties of sulphated zirconia systems. Even though a specific enhancement of total acidity was rather ambiguous, a well-defined variation could be observed in the acid strength distribution pattern. The metal incorporation had a positive influence on the thermal stability also. Among the different metal promoted systems, iron doped samples exhibited high Lewis acidity and possessed the maximum amount of strong acid sites. An increase in iron loading resulted in an enhancement in surface acidity. Monoclinic phase was completely absent in high loaded iron systems indicating the stabilisation of the tetragonal phase. Cumene conversion reaction proved to be a satisfactory test reaction for surface acidity. The percentage conversion could be correlated with the total acidity of the systems, while the dehydrogenation and cracking product selectivity followed trends in the Lewis and Brönsted acidity of the samples respectively.

## REFERENCES

1. D.Farcasiu, J.Q.Li, S.Cameron, *Appl. Catal. A: Gen.*, 154 (1997) 173.
2. D.Farcasiu, J.Q.Li. *Appl. Catal. A: Gen.*, 175 (1998) 1.
3. C.R.Vera, J.M.Parera, *J. Catal.*, 165 (1997) 254.
4. A.Ghenciu, D.Farcasiu, J.Q.Li, *J. Catal.*, 158 (1996) 116.
5. A.Ghenciu, D.Farcasiu, *Catal. Lett.*, 44 (1997) 29.
6. M.-Trung Tran. N.S. Gnep, G.Szabo, M.Guisnet, *Appl. Catal. A:Gen.*, 171 (1998) 207.
7. F.R. Chen, G. Coudurier, J.F. Joly, J.C. Vedrine, *J. Catal.*, 143 (1993) 616.
8. T. Yamaguchi, *Appl. Catal.*, 61 (1990) 1.
9. A.Arata, *Adv. Catal.*, 37 (1990) 165.
10. F. Arena, R. Dario, A. Parmaliana, *Appl. Catal. A: Gen.*, 170 (1998) 127.
11. J. Kijenski, A.Baiker, *Catal. Today*, 5 (1989) 1.
12. B.D. Flockart, J.A.N.Scott, R.C.Pink, *Trans.Farad. Soc.*, 62 (1966) 730.
13. C.Morterra, G.Cerrato, C.Emanuel, V.Bolis, *J. Catal.*, 142 (1993) 349.
14. K.Arata, M.Hino. *Mater. Chem. Phys.*, 26 (1990) 213.
15. A. Corma, C.Rodellas. V.Fornes. *J. Catal.*, 88 (1984) 374.
16. H.A.Benesi, *J. Catal.*, 28 (1973) 176.
17. H.Knozinger, H.Krietenbrink, P. Ratnasamy. *J. Catal.*. 48 (1977) 436.
18. J.Dewing, G.T.Monks. B.Youll, *J. Catal.*. 44 (1976) 226.
19. A. Satsuma, Y.Kamiya, Y.Westi, T.Hattori. *Appl. Catal. A: Gen.*, 194-195 (2000) 253.
20. J.H.Lunsford, H.Sang, S.M.Campbell, C.H.Liang. R.G.Anthony, *Catal. Lett.*, 27 (1994) 305.
21. C.Morterra, V.Bolis. G.Cerrato, *Catal. Today*, 17 (1993) 505.
22. P.Nascimento, C.Akratopolou, M.Oszagyan. G.Coudurier, C.Travers, J.F.Joly, J.C.Vedrine,  
"Proceeding of the 10<sup>th</sup> international Congress on Catalysis", "New Frontiers in Catalysis",  
L.Guczi (Ed.) (1993) p. 2585.
23. M.S.Surrell, *Appl. Catal.*, 34 (1987) 109.
24. T.Yamaguchi, K.Tanabe, Y.C.Kung, *Mater. Chem. Phys.*. 16 (1986) 67.
25. J.R.Sohn, H.W.Kim. *J. Mol. Catal.*, 52 (1989) 361.
26. D.A.Ward, E.I. Ko. *J. Catal.*, 150 (1994) 18.
27. A.K.Dalai, R.Sethuraman, S.P.R.Katikeneni, R.O.Idem, *Ind. Eng. Chem. Res.*, 37 (1998) 3869.
28. A.Dicko, M.Sc Thesis. Universite Laval. 1994.
29. R.C.Garvie, *J. Phys. Chem.*, 69 (1965) 1238.
30. R.C. Garvie, M.F.Goss, *J. Mater. Sci.*, 21 (1986) 1253.
31. R.C.Garvie, *J. Phys. Chem.*, 82 (1978) 218.

32. S.-I.Pyun, H.-J. Jung, G.-D.Kim, P. Vincenzini (Ed), "High Tech Ceramics", Elsevier, Amsterdam (1987) p. 271.
33. S.Chokaram, R.Srinivasan, D.R.Milburn, B.H.Davis, *J. Colloid Interface Sci.*, 165 (1994) 160.
34. L.M.Kustov, V.B.Kazansky, F.Figueras, D.Tichit, *J. Catal.*, 150 (1994)143.
35. O.Saur, M.Bensitel, A.B.M.Saad, J.C.Lavalley, C.P.Tripp, B.A.Morrow, *J. Catal.*, 99 (1986) 104.
36. R.Srinivasan, D.Taulbee, B.H.Davis, *Catal. Lett.*, 9 (1991) 1.
37. A.Corma, V.Fornes, M.I.Juan Rajadell, J.M.Lopez Nieto, *Appl. Catal. A: Gen.*, 116 (1994) 151.
38. A.Clearfield, G.P.D.Serrete, A.H.Khazi-Syed, *Catal. Today*, 20 (1994) 295.
39. F.Lonyi, J.Valyon, J.Engelhardt, P.Mizukami, *J. Catal.*, 160 (1997)279.
40. P.D.L.Mercera, J.G.van Ommen, E.B.M.Doesburg, A.J.Burggraaf, J.R.H.Ross, *Appl. Catal. A: Gen.*, 57 (1990) 127.
41. C.Morterra, G.Cerrato, F.Pinna, M.Signoretto, *J. Catal.*, 157 (1995) 109.
42. G.D.Yadav, J.J.Nair, *Microporous and Mesoporous Materials*, 33 (1999) 1.
43. S.K.Samantaray, T.Mishra, K.M.Parida, *J. Mol. Catal. A: Chem.*, 156 (2000) 267.
44. C.Morterra, G.Cerrato, F.Pinna, M.Signoretto, *J. Phys. Chem.*, 98 (1994) 12373.
45. M. Scheithauer, E.Bosch, U.A. Schubert, H. Knozinger, T.K. Cheung, F.C.Jentoft, B.C.Gates, B.Tesche, *J. Catal.*, 177 (1998) 137.
46. J.A.Moreno, G.Poncelet, *Appl. Catal. A:Gen.*, 210 (2001) 151.
47. L.Salvati, E.Makovsky, J.Stencel, F.Brown, D.Hercules, *J. Phys. Chem.*, 85 (1981) 3700.
48. D.S.Kim, M.Ostromecki, I.E.Wachs, *Catal. Lett.*, 33 (1995) 209.
49. D.S.Kim, M.Ostromecki, I.E.Wachs, *J. Mol. Catal. A:Chem.*, 106 (1996) 93.
50. R.A.Boyse, E.I.Ko, *J. Catal.*, 179 (1998) 100.
51. S.R.Vaudagna, R.A.Comelli, N.S.Figoli, *Appl. Catal. A: Gen.*, 164 (1997) 265.
52. P.Dufresne, E.Payen, J.Grimblot, J.P.Bonnelle, *J. Phys. Chem.*, 85 (1981) 2344.
53. H.Hu, I.E.Wachs, *J. Phys. Chem.*, 99 (1995) 10897.
54. Z.Liu, Y.Chen, *J. Catal.*, 177 (1998) 314.
55. H. Matsushashi, H.Motoi, K.Arata, *Catal. Lett.*, 26 (1994) 325.
56. R.T.Sanderson, "Chemical Bonds and Bond Energy", Academic Press, NewYork (1976) p.75.
57. X.Song, A.Sayari, *Catal. Rev. - Sci. Eng.*, 38 (3) (1996) 329.
58. J.S.Lee, D.S.Park, *J. Catal.*, 120 (1989) 46.
59. J.S.Lee, M.H.Yeom, D.S.Park, *J. Catal.*, 126 (1990) 361.
60. D.S.Park, J.S.Lee, *React. Kinet. Catal. Lett.*, 40 (1989) 101.
61. A.Corma, B.W.Wojciechowski, *Catal. Rev. Sci. Eng.*, 24 (1982) 1.
62. J.W.Ward, *J. Catal.*, 9 (1967) 225.
63. W.Przystajko, R.Fieddorow, I.G.Dalla Lana, *Appl. Catal.*, 15 (1985) 265.

64. H.Pines, "*The chemistry of catalytic hydrocarbon conversions*", Academic Press, New York (1981) p.85.
65. P.M.Boorman, R.A.Kydd, Z.Sarbak, A.Somogyvari, *J. Catal.*, 96 (1985) 115.
66. P.M.Boorman, R.A.Kydd, Z.Sarbak, A.Somogyvari, *J. Catal.*, 100 (1986) 287.
67. J.R.Sohn, H.J.Jang, *J. Mol. Catal.*, 64 (1991) 349.
68. Y-y.Huang, B-y.Zhao, Y-c.Xie, *Appl. Catal. A: Gen.*, 171 (1998) 65.
69. S.J.Decanio, J.R.Sohn, P.O.Paul, J.H.Lunsford, *J. Catal.*, 101 (1986) 132.

# FRIEDEL-CRAFTS REACTIONS

---

The present chapter is divided into two sections. The first section covers the Friedel-Crafts benzylation and benzylation of aromatics over modified sulphated zirconia systems. The second section discusses the vapour phase methylation of aniline over the different systems. Each section is preceded by a general introduction.

### SECTION 1

## FRIEDEL-CRAFTS BENZOYLATION AND BENZYLATION

### 4.1 INTRODUCTION

Friedel-Crafts acylation constitutes the most important method for the preparation of aryl ketones while Friedel-Crafts alkylation enables the introduction of alkyl chains to the aromatic rings. A wide range of homogeneous catalysts like  $\text{FeCl}_3$ ,  $\text{AlCl}_3$  and  $\text{BF}_3$  and protonic acids like  $\text{HF}$  and  $\text{H}_2\text{SO}_4$  have been found to be well suited for the reaction [1,2]. These catalysts, however, suffer from the inherent drawback of extreme corrosivity, high susceptibility to water and difficulty in catalyst recovery. The stoichiometric amounts of the catalyst with respect to the benzoylating agent required for the reaction makes the work-up procedure tedious. The moisture sensitivity of these homogeneous catalysts demand moisture free solvents and reactants, anhydrous catalyst and dry atmosphere for its handling. The high Lewis acidity of these homogeneous catalysts also results in several undesirable side reactions leading to secondary reaction products.

The development of solid acid catalysts has been a breakthrough in this field. The environmental concerns and the drive towards a “clean technology” prompt the replacement of the liquid acids by eco-friendly solid acid catalysts. Strongly acidic reagents are generally required for the efficient catalysis of Friedel-Crafts reactions. A wide range of solid acid catalysts from clays [3-5] and zeolites [6-10] to heteropolyacids [11-13] has been widely tested for their applicability towards this reaction.

$\text{Ga}_2\text{O}_3$  and  $\text{In}_2\text{O}_3$  supported on mesoporous Si-MCM-41 or even on micro- or macroporous inert catalyst carriers were found to be efficient for the catalysis of benzoylation of benzene and acylation of aromatics even in presence of moisture [14]. Moisture was found to have a beneficial effect, especially for acylation reaction. Catalytic activity of mesoporous molecular sieves has also been tested for the alkylation of benzene [15,16], toluene and *m*-xylene [15]. Lanthanum trichloride supported on silica acted as an active catalyst for the alkylation and acylation [17,18].  $\text{LaCl}_3$  deposited on K-10 montmorillonite was recovered quantitatively on the support after use whereas for analogous scandium catalyst only 12% of the scandium salt was recovered.

Shape selectivity and high acidity comparable to that of liquid acids render zeolites a good option for the Friedel-Crafts reactions. The reaction was limited by the poisoning of the active sites by adsorption of the product and pore blockage due to coke-type products. H-ZSM 5 has been used in the acylation of less substituted aromatic molecules like benzene, phenol, toluene, etc. [19,20] while zeolites with large pores such as H- $\beta$  and HY have been used extensively in the acylation of arylethers like anisole and poly-substituted aromatics like xylene, mesitylene, etc. [19,21,22]. Botella *et al.* investigated the influence of reaction conditions and physico-chemical properties on the acylation of toluene with acetic anhydride over  $\beta$ -Zeolite [23]. Liquid phase benzoylation and benzoylation of *o*-xylene using various zeolite catalysts was carried out by Singh *et al.* [9,10]. Reaction time, xylene to benzyl/benzoyl chloride molar ratio, reaction temperature,  $\text{SiO}_2/\text{Al}_2\text{O}_3$  ratio, etc. was found to have a great influence on the percentage conversion and selectivity. Benzoylation of naphthalene over H- $\beta$  and H-Y zeolites using benzyl chloride as the benzoylating agent has also been investigated [24].

Acid treated [25], pillared [26-28] and transition metal containing clays [29-31] also find wide use as Friedel-Crafts catalysts. A comparative study on  $\text{H}_2\text{SO}_4$ ,  $\text{HNO}_3$  and  $\text{HClO}_4$  treated metakaolinite as Friedel-Crafts alkylation catalyst has been reported [32]. The effect of impregnating  $\text{ZnCl}_2$ ,  $\text{FeCl}_3$ ,  $\text{MnCl}_2$ ,  $\text{SnCl}_2$  and  $\text{AlCl}_3$  on the catalytic activity of natural kaolinite and its activated form for the Friedel-Crafts alkylation of benzene with benzyl chloride is examined [33]. The process leads to catalysts with improved activity, the maximum activity being associated with  $\text{FeCl}_3$ . Montmorillonite supported

zinc and nickel chlorides were proposed to be highly active and selective for Friedel-Crafts alkylation [29]. Lenarda *et al.* investigated the catalytic activity of montmorillonite pillared with aluminium or aluminium-gallium polyoxycations and their respective repillared derivatives for the liquid phase alkylation of benzene with ethylene to produce ethylbenzene [34].

#### 4.1.1 SULPHATED METAL OXIDES FOR FRIEDEL-CRAFTS REACTIONS

Reports of superacidity in the sulphated metal oxides prompted several researchers to investigate on its application to different industrially important reactions, of which Friedel-Crafts reactions needs special mention. Several reports are available in literature concerning the utility of these catalysts for Friedel-Crafts reactions [35,36]. Arata *et al.* reported the Friedel-Crafts acylation of toluene with benzoyl chloride and benzoic anhydride catalysed by solid superacids [37-39]. Arata and co-workers also successfully carried out the vapour phase acylation of toluene with acetic acid and benzoic acid [40]. Sulphated oxides of tin, zirconium, titanium, aluminium, hafnium and iron gave good conversions. Supported oxides like  $\text{WO}_3/\text{ZrO}_2$ ,  $\text{WO}_3/\text{TiO}_2$ ,  $\text{WO}_3/\text{SnO}_2$  and  $\text{MoO}_3/\text{ZrO}_2$  were also active whereas  $\text{WO}_3/\text{Fe}_2\text{O}_3$  and  $\text{B}_2\text{O}_3/\text{ZrO}_2$  were completely inactive [37]. James Clark investigated the use of sulphated zirconia as catalysts for the alkylation of benzene with long chain linear alkenes to form linear alkylbenzenes [41]. Quaschnig *et al.* [42] investigated the catalytic activity of zirconia modified by different sulphating agents like ammonium sulphate, ammonium sulphite,  $\text{SOCl}_2$  and  $\text{SF}_4$  for the benzoylation of anisole and obtained satisfactory results.

Samantaray [43] studied the physico-chemical properties and catalytic activity of sulphated titania for the gas phase alkylation of benzene and substituted benzenes using isopropanol as alkylating agent. Catalytic activity was found to be dependent on the sulphate ion concentration in the catalyst and also benzene to alcohol molar ratio. Promoting effect of Al on sulphated oxide catalysts was subjected to investigation [44]. Introducing small amounts of alumina into sulphated zirconia, titania and iron oxide enhances the activity for the benzoylation of toluene with benzoyl chloride considerably. The enhanced long-term activity of Al-promoted catalysts is associated with an increase

in acid sites of intermediate strength, which is caused by the formation of Al-O-Zr and Al-O-Ti bonds in the mixed oxides.

Inversion of relative reactivities and selectivities of benzyl chloride and benzyl alcohol in Friedel-Crafts alkylation with toluene using different solid acid catalysts was also investigated [45,46]. When reacted separately, benzyl chloride is more reactive than benzyl alcohol. It is proposed that when present together; benzyl alcohol is preferentially and strongly adsorbed on the catalytic sites and prevents any adsorption of benzyl chloride thereby preventing it from reacting with toluene. Only when some sites are vacant due to complete depletion of alcohol by reaction, benzyl chloride molecules get a chance to adsorb and react.

#### 4.1.2 PROPOSED MECHANISMS FOR FRIEDEL-CRAFTS REACTIONS

Friedel-Crafts reaction is supposed to occur by a carbocationic mechanism [2]. Several possible mechanisms have been suggested for Friedel-Crafts reaction based on solid acid catalysts. Brönsted and Lewis acid sites have been proposed to play a role in deciding the catalytic activity [32]. Benzoyl/benzyl chloride can be activated at the Lewis or Brönsted sites. The probable mechanism of acylation or alkylation was assumed to proceed *via* the polarisation of benzoyl/benzyl chloride at the acidic sites followed by the attack of the electrophilic species on the aromatic ring [9,10]. Quaschnig *et al.* proposed the dominating role of Brönsted acid sites in the benzylation of anisole by sulphated zirconia systems [42]. Systems with little or no Brönsted acidity were catalytically inactive. Arata *et al.* reported the acylation of toluene catalysed by the Lewis acid sites [37]. They explained the inactivity of the aluminosilicates for acylation based on their catalytic action by Brönsted acid sites. In the case of acylation of toluene with benzoic acid and acetic acid, the adsorption site can be a strong Lewis acid site  $Zr^{4+}$  created by the inductive effect of S=O or Brönsted acid site formed by adsorption of water on  $Zr^{4+}$  [40].

According to Bhattacharya *et al.*, the presence of strong Brönsted sites appears to be very important in the polarisation of benzyl chloride [24]. A possibility of a redox mechanism was also suggested in catalysts containing reducible cations like  $Fe^{3+}$ ,  $Sn^{4+}$  and  $Cu^{2+}$ . This explained their high activity in spite of low Lewis acidity [28,31]. Radicals being powerful reductants, can be readily oxidised to cations in presence of reducible



metallic ions. The initiation in this case proceeds by the homolytic rupture of C-Cl bond followed by the oxidation of radical.

## 4.2 BENZOYLATION OF ARENES

The general scheme of benzoylation reaction, toluene being taken as the substrate, may be represented as in Fig. 1. Similar schematic representations hold good for other substrates as well. Electrophilic substitution occurs at the *ortho* and *para* positions of the aromatic ring.

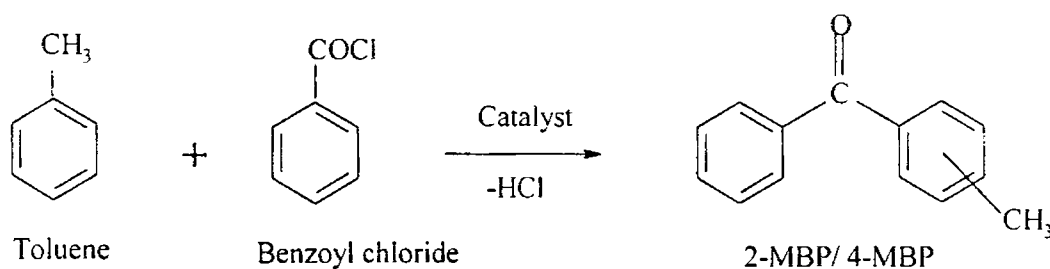


Fig. 4.1 General scheme for the benzoylation of toluene

The catalytic activity for a given catalytic system for any reaction depends strongly on various experimental conditions. Any study of catalytic activity remains incomplete without optimisation of the reaction conditions. Thus it becomes our major objective to examine the influence of the various reaction parameters on the catalytic activity. The catalytic activity of the different catalytic systems for the benzoylation of toluene was tested under optimised reaction conditions. The influence of different reaction parameters on the catalytic activity and selectivity is discussed in detail in the following sections.

### 4.2.1 INFLUENCE OF CATALYST COMPOSITION

The catalytic activity being a function of the catalyst properties, it is very much relevant to examine the influence of catalytic activity on catalyst composition.

#### *i) Influence of sulphate content*

The sulphate content remarkably affects the physico-chemical properties like surface area, crystallinity and even the acidic properties. Thus, the sulphate content should have a deciding hand on the catalytic performance. The influence of sulphate

content on the catalytic activity towards benzoylation of toluene was examined taking sulphated zirconia and iron incorporated sulphated zirconia systems as representatives and the results are presented in Table 4.1.

Table 4.1 Influence of sulphate loading on catalytic activity

Catalyst systems	Conversion (%)	Selectivity (%)	
		Ortho	Para
SZ-2.5	19.69	15.79	84.21
SZ-5.0	22.54	16.85	83.15
SZ-7.5	28.47	17.03	82.97
SZ-10	34.35	16.12	83.88
FeSZ-2.5	56.38	18.54	81.46
FeSZ-5.0	64.82	17.97	82.03
FeSZ-7.5	71.60	16.58	83.42
FeSZ-10	86.61	15.16	84.84

Reaction temperature-110°C, catalyst-0.1 g, molar ratio (toluene/benzoyl chloride)-5:1  
Duration-1 hour

The percentage conversion increased with increasing sulphate content in the samples. The same trend was observed in the case of iron promoted systems also. Benzoylation of toluene resulted in the formation of *ortho* and *para* methylbenzophenones, with a selectivity of around 80-85% to the *para* isomer. The selectivity remained almost impassive to the sulphate content.

The acid-base properties of metal oxide carriers can significantly affect the final selectivity of heterogeneous catalysts [47]. An attempt was made to correlate the catalytic activity with the acidic characteristics determined by the TPD and adsorption studies. The increase in the percentage conversion correlated with the increase in the Lewis acidity of the samples obtained by perylene adsorption studies (Fig. 4.2). Considering the acid site distribution from the TPD measurements, the increase in the strong acid sites with increasing sulphate content is in agreement with the enhanced activity at high sulphate loadings (Fig. 4.3). Thus, strong acid sites may be considered to be involved in the Friedel-Crafts benzoylation of toluene.

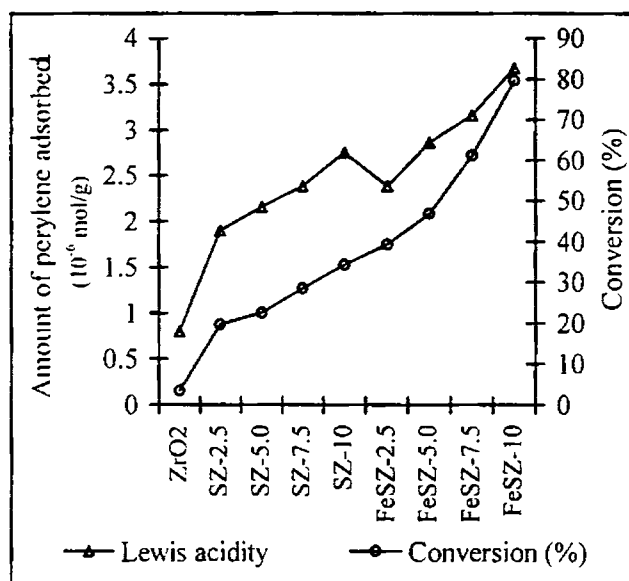


Fig. 4.2 Correlation of benzoylation activity with Lewis acidity

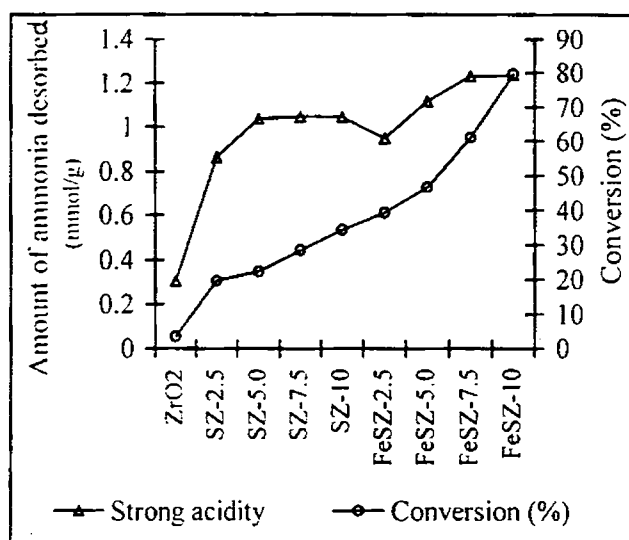


Fig. 4.3 Correlation of benzoylation activity with the strong acid sites

### ii) Influence of metal incorporation

Pure ZrO<sub>2</sub> exhibited poor reactivity (around 3%) towards benzoylation of toluene at the refluxing temperature. Benzoylation of toluene proceeded very efficiently over different sulphated zirconia systems. In comparison with the simple sulphated system, metal incorporated samples were more efficient for the benzoylation of toluene with benzoyl chloride (Table 4.2).

Fe incorporated samples showed the highest activity when compared with the other systems. The low activity of the vanadium-incorporated system may be attributed to the predominant monoclinic phase as evident from the XRD patterns. In the case of V, Cr, Mn, Fe and Mo promoted systems, only *ortho* and *para* isomers were detected whereas for the other ones, formation of around 2-3% of *meta* isomer was also observed. In most cases *ortho* and *para* isomers were obtained with a selectivity of around 80% for the *para* isomer. Vanadia, iron and manganese supported system showed maximum selectivity of around 84-86% to the *para* isomer. Lowest *para* selectivity (73%) was obtained in the case of copper system.

Table 4.2 Benzoylation of toluene over transition metal promoted sulphated zirconia

Catalyst	Conversion (%)	Selectivity (%)		
		Ortho	Meta	Para
ZrO <sub>2</sub>	3.45	-	-	100
SZ	34.35	16.12	-	83.88
VSZ	36.95	13.06	-	86.94
CrSZ	50.90	18.96	-	81.04
MnSZ	67.54	16.70	-	83.30
FeSZ	79.61	15.16	-	84.84
CoSZ	63.65	16.50	2.68	80.80
NiSZ	69.75	17.48	2.82	79.69
CuSZ	49.77	24.50	2.28	73.21
ZnSZ	64.40	17.91	2.64	79.45
WSZ	68.89	17.73	2.40	79.87
MoSZ	71.13	17.39	-	82.61

Reaction temperature-110°C, catalyst-0.1 g, molar ratio (toluene/benzoyl chloride)-5:1, Duration-1 hour,

Attempts were made to find a correlation between the catalytic activity and the acidic properties. The incorporation of transition metals did not have a pronounced influence on the acidity values. However, the catalytic activity differed much between the various systems. Keeping this in view, the catalytic activity may be considered to be a combined effect of the acidic properties as well as the structural influence of the transition

metal species. A crude correlation could be sketched between the percentage conversions for the different systems and the Lewis acidity values determined from the perylene adsorption data (Fig. 4.4). The percentage conversions for different metal promoted systems were also in line with the amount of strong acid sites as revealed by the ammonia TPD data (Fig. 4.5).

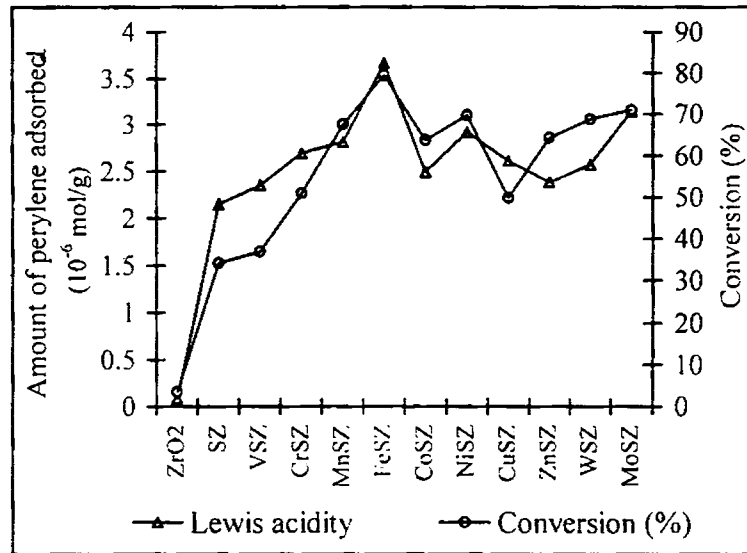


Fig. 4.4 Correlation of catalytic activity with Lewis acidity

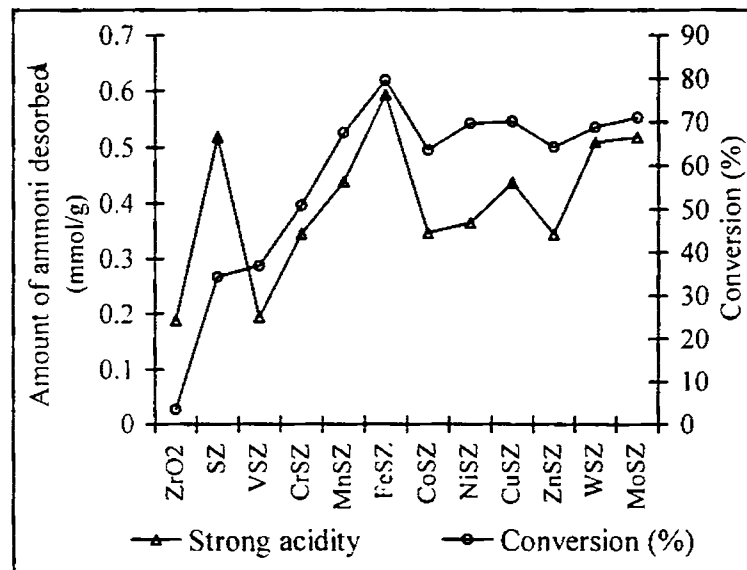


Fig. 4.5 Correlation of catalytic activity with the strong acid sites

However, it was observed that the conversion was very low in the case of unpromoted sulphated zirconia system in spite of its high concentration of strong acid sites. This may be ascribed to the structural and chemical effect of the promoters. All the sites of the simple sulphated system may not be accessible to the reactants due to its higher crystalline size and low pore volume. The lower activity of vanadia-incorporated system is also explainable based on its lower amount of strong acid sites even though the system possesses sufficiently high amounts of Lewis acidity.

### iii) Influence of iron content

Among the different metal promoted systems, iron doped system was the most active for the benzoylation of toluene. So an attempt to investigate the influence of the iron loading on catalytic activity is quite reasonable. As expected, variation in iron loading had a significant impact on the catalytic activity. An increase in iron content resulted in enhanced catalytic activity without altering the selectivity (Table 4.3). The variation in the iron content had negligible influence on the product selectivity. An increase in the iron loading resulted in a slight enhancement in the para selectivity. *Ortho*- and *para*-methylbenzophenones were obtained with around 83-85% selectivity to the *para* isomer. The higher selectivity to the *para* isomer may be related to the steric hindrance of the methyl group towards the incoming bulky acyl group.

Table 4.3 Benzoylation of toluene over iron promoted sulphated zirconia systems

Catalyst	Time (min)	Conversion (%)	Selectivity (%)	
			<i>Ortho</i>	<i>Para</i>
ZrO <sub>2</sub>	60	3.45	-	100
SZ	60	34.35	16.12	83.88
Fe(2)SZ	60	79.61	15.16	84.84
Fe(4)SZ	60	88.56	15.85	84.15
Fe(6)SZ	60	96.49	15.38	84.62
Fe(8)SZ	45	100	14.95	85.05
Fe(10)SZ	30	100	14.43	85.57

Reaction temperature-110°C, 0.1 g catalyst, molar ratio (toluene/benzoyl chloride) - 5:1

The high activity of the iron promoted systems, on a face level, may be attributed to the redox properties of iron as well as its strong acidity as evident from TPD studies. Thermodesorption of 2,6-DMP predicts a trivial enhancement in the Brønsted acidity with increasing iron content whereas perylene adsorption studies provide a clear evidence for a distinct enhancement of Lewis acidity upon increasing the iron loading. The marginal enhancement in Brønsted acidity value seems quite inadequate in explaining the increase in the catalytic activity. However, the Lewis acidity enhancement predicted by perylene adsorption studies parallels the steady increase in reactivity observed with the increase in the percentage iron composition (Table 4.4).

Table 4.4 Correlation between catalytic activities of iron promoted systems with Lewis and strong acidity values

Catalyst	Time (min)	Conversion (%)	Lewis acidity Perylene adsorbed ( $10^{-6}$ mol/g)	Strong acidity Ammonia desorbed (mmol/g)
ZrO <sub>2</sub>	60	3.45	0.085	0.189
SZ	60	34.35	2.153	0.5185
Fe(2)SZ	60	79.61	3.673	0.5952
Fe(4)SZ	60	88.56	4.183	0.6569
Fe(6)SZ	60	96.49	7.373	0.6959
Fe(8)SZ	45	100	8.845	0.7573
Fe(10)SZ	30	100	10.688	0.8183

#### 4.2.2 INFLUENCE OF SUBSTRATE

Benzoylation of benzene, toluene and xylene were carried out at the corresponding refluxing temperatures for one hour over Fe(2)SZ system. The reactivities were in the order benzene < toluene < xylene (Table 4.5). This can be well explained on the basis of the *ortho-para* directing effect of the alkyl substituent on the aromatic ring. The electron releasing nature of the alkyl groups favours the electrophilic substitution at the aromatic nucleus. The predominant *para* substitution may be accounted for as due to the bulky nature of the acyl group. Only mono-substitution was observed in all the cases. The

absence of dibenzoylated products can be attributed to the deactivating nature of the RCO group, after the introduction of which, the reaction comes to a stop.

Benzoylation of benzene results in the formation of benzophenone. *Ortho*- and *para*-methylbenzophenones (2-MBP and 4-MBP) were obtained by the benzoylation of toluene with around 84% selectivity to the *para* isomer. 3,4-dimethylbenzophenone (3,4-DMBP) and 2,3-dimethylbenzophenone (2,3-DMBP) results from the aromatic substitution of *o*-xylene, the 3,4-isomer being formed with a selectivity of about 89%. The slightly higher selectivity towards the *para* isomer in the case of xylene when compared with toluene, may be attributed to the steric hindrance by two methyl groups of xylene to the incoming bulky acyl group.

Table 4.5 Influence of substrate on catalytic activity and selectivity

Substrate	Conversion (%)	Selectivity (%)	
		<i>ortho</i> substitution	<i>para</i> substitution
Benzene	15.37%	15.37	
Toluene	79.61%	15.16	84.84
Xylene	96.23%	11.3	88.7

Molar ratio (Substrate: benzoyl chloride) – 5:1, Refluxing temperature, 0.1 g Fe(2)SZ

### 4.2.3 INFLUENCE OF REACTION TEMPERATURE

Selection of an appropriate reaction temperature is critical for a chemical reaction. At very low temperatures, the conversions may be very low or even the reaction may not take place whereas too high a temperature may cause unwanted side reactions. The influence of reaction temperature on the percentage conversion and selectivity was followed for toluene and xylene and the results are illustrated in Figs. 4.6 and 4.7. In the case of toluene, 100% selectivity to the *para* isomer was obtained at 60°C. Formation of *ortho* isomer was also observed above 70°C. An increase in the reaction temperature resulted in an increase in the conversion at the expense of selectivity. At the refluxing temperature, *para* isomer was obtained with a selectivity of about 85%.



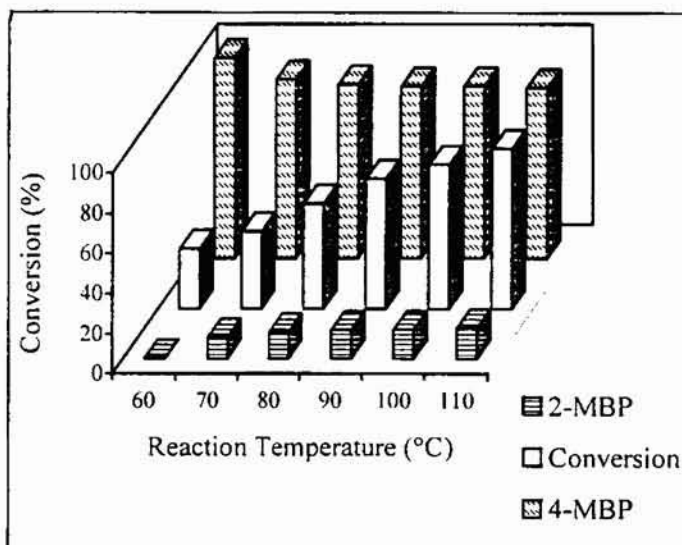


Fig. 4.6 Benzoylation of toluene with benzoyl chloride –Influence of reaction temperature.

Molar ratio (toluene:benzoyl chloride)-5:1; Duration-1 hour,  
Fe(2)SZ Catalyst – 0.1 g

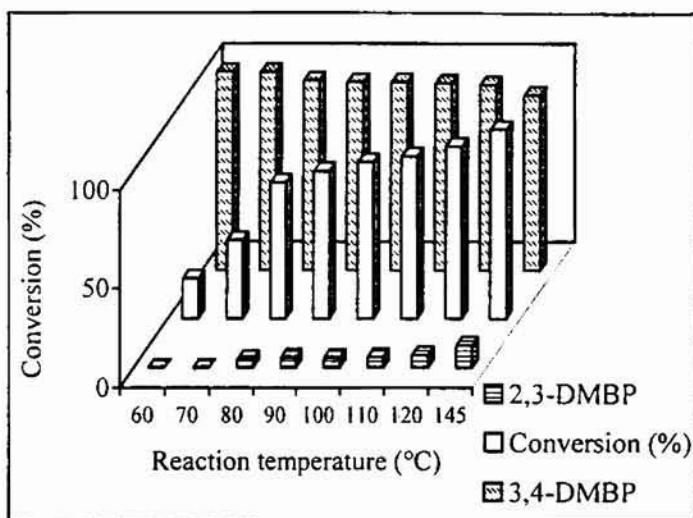


Fig. 4.7 Benzoylation of xylene –Influence of reaction temperature.

Molar ratio (xylene:benzoyl chloride) – 5:1; Duration – 1 hour,  
Fe(2)SZ Catalyst – 0.1 g

In the case of xylene, 3,4-dimethylbenzophenone was the only product when reaction was carried out at 60°C and 70°C. As the reaction temperature was raised the selectivity was lowered and at refluxing temperature, around 89% of 3,4-

dimethylbenzophenone was formed. Selectivity remained almost constant till 120°C and thereafter it increased to around 11% at the refluxing temperature

#### 4.2.4 INFLUENCE OF REACTION TIME

The reaction time also can have a deciding effect on the catalytic activity and product selectivity. Prolonged reaction time may result in the generation of undesirable products. The influence of reaction time on the reactivity and selectivity for the benzylation of xylene is illustrated in Fig 4.8. The continuous increase in percentage conversion was registered with increase in reaction time while the selectivity remained constant.

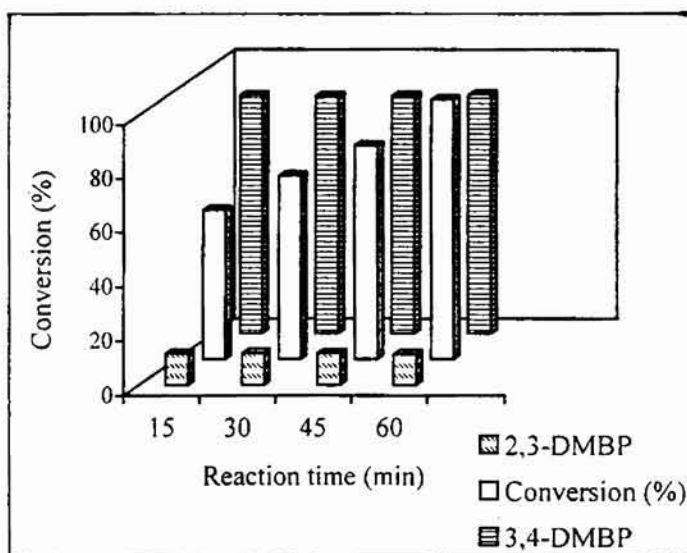


Fig. 4.8 Variation in conversion and selectivity with reaction time - benzylation of xylene with benzoyl chloride.

Reaction temperature-110°C, 0.1 g Fe(2)SZ catalyst, Duration- 1 hour,  
Molar ratio (Xylene: Benzoyl chloride) -5:1

#### 4.2.5 INFLUENCE OF MOLAR RATIO

The catalytic activity for Fe(2)SZ system was scanned for different molar ratios and the results are shown in Fig. 4.9. Molar ratio had a marked influence on the reaction rate. An increase in the toluene to benzoyl chloride ratio resulted in a lowering of percentage conversion. A drastic decrease in the percentage conversion was observed when the molar ratio was changed from 15:1 to 20:1. Traces of secondary reaction products could be detected at a toluene to benzoyl chloride ratio of 3:1.

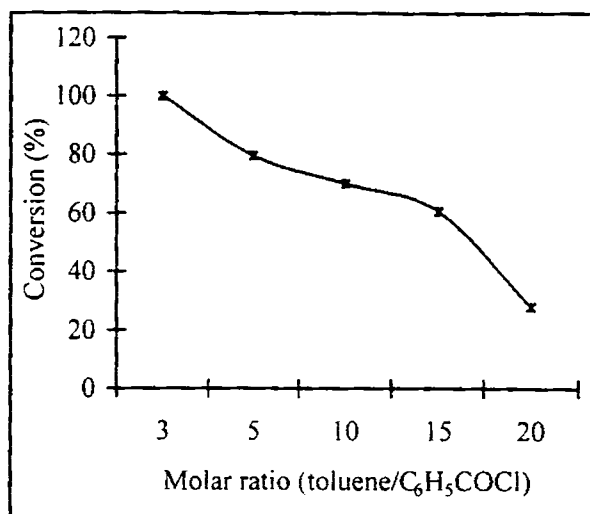


Fig. 4.9 Influence of molar ratio on catalytic activity

0.1 g Fe(2)SZ catalyst, Duration- 1 hour.  
Reaction temperature – 110°C

Considering the effect of molar ratio on reactivity, two explanations can be put forth - the competitive adsorption of reactants and the dilution effect of the solvent. Toluene being taken in excess amounts, serves the purpose of a solvent. The competitive adsorption principle can be ruled out bearing in mind the non polar nature of the toluene molecules. Thus, the decrease in the percentage conversion with increasing toluene to benzoyl chloride ratio may be explained on the basis of the relative concentration of benzoyl chloride in the reaction mixture. According to Ostwald's isolation principle, the reaction rate will be decided by the effective concentration of benzoyl chloride. The lowering of catalytic activity at high toluene to benzoyl chloride ratios arises from the dilution effect.

#### 4.2.6 INFLUENCE OF CALCINATION TEMPERATURE

Table 4.6 illustrates the dependence of the catalytic activity on the calcination temperature of the catalyst, taking the specific case of Fe(2)SZ. An increase in calcination temperature was found to facilitate the reaction. At low calcination temperatures (500°C) only *para* isomer was obtained which may be due to the extremely low conversion. The increase in conversion was followed by a concomitant decrease in the selectivity.

Table 4.6 Influence of calcination temperature on catalytic activity and selectivity

Calcination Temperature (°C)	Conversion (%)	Selectivity (%)	
		Ortho	Para
500	8.56	-	100
550	15.12	3.49	96.51
600	23.72	12.68	87.32
650	49.83	14.74	85.26
700	79.61	15.16	84.84

Reaction temperature - 110°C, catalyst - 0.1 g, molar ratio (toluene/benzoyl chloride) - 5:1

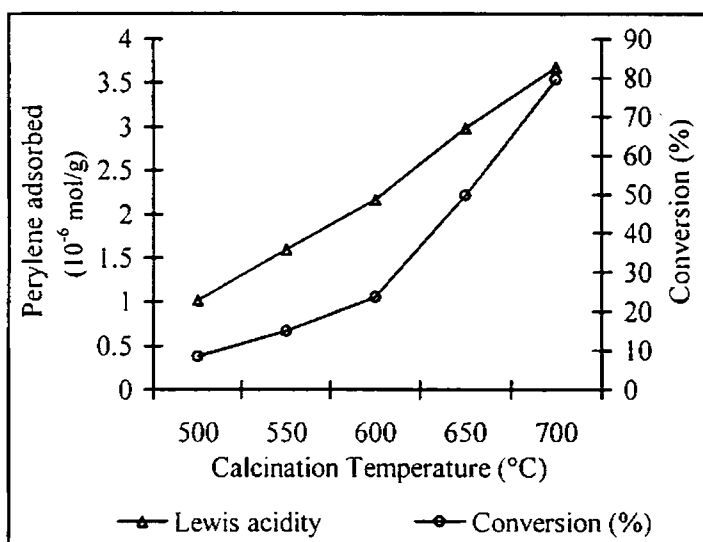


Fig. 4.10 Correlation between catalytic activity and Lewis acidity at different calcination temperatures

Reaction Temperature-110°C, Duration-1 hour, Catalyst Fe(2)SZ-0.1g, Toluene:Benzoyl chloride molar ratio- 5:1.

Keeping in mind the correlation observed between the catalytic activity and Lewis acidity, we attempted to find a correlation between the two in this case also. IR studies on adsorbed pyridine by Morterra *et al.* [48] support the gradual elimination of all but a small fraction of the Brönsted acid sites after high temperature calcination and the reversible transformation of Lewis to Brönsted acidity upon exposure of the sample to moisture. The increase in the catalytic activity observed with increasing calcination temperature

parallels the enhancement of Lewis acidity of the samples obtained by perylene adsorption studies (Fig. 4.10). A rather sharp rise in the conversion was obtained when the calcination temperature was increased from 600°C while the Lewis acidity showed a gradual increase in this range. This may be partially attributed to the development of the catalytically active tetragonal phase in the sample during this temperature range.

#### 4.2.7 REUSABILITY OF THE CATALYST SYSTEMS

One of the major objectives guiding the development of solid acid catalysts includes the easy separation of final products from the reaction mixture and efficient catalyst recovery. The reusability of our catalyst systems was subjected to investigation, taking Fe(2)SZ and Fe(10)SZ as representative systems. The catalyst was removed by filtration from the reaction solution, washed thoroughly with acetone and then dried and calcined at 700°C for three hours. No pronounced change could be observed in the XRD pattern, except a light lowering of intensity, symptomatic of the retention of the crystalline nature (Fig. 4.11). No remarkable fall in the activity could be monitored till three successive regenerations (Table 4.7). This suggests the resistance to rapid deactivation acquired by the incorporation of iron. However, the decrease becomes more pronounced as the cycles are repeated.

Table 4.7 Regeneration of catalyst

No: of cycles		1	2	3	4	5
Conversion	Fe(2)SZ	79.61	77.46	74.12	65.51	53.92
(%)	Fe(10)SZ	100	95.12	91.29	80.86	72.54

0.1 g catalyst, Duration- 1hr for Fe(2)SZ and 30 min for Fe(10)SZ, Molar ratio (Toluene:Benzoyl chloride) – 5:1, Reaction Temperature – 110°C.

#### 4.2.8 METAL LEACHING

An important requisite for a good catalyst is its stability under the reaction conditions. Major causes that can lead to the deactivation of a catalyst include the disruption of the crystalline structure and chemical composition. Previous section establishes that the crystalline nature of the catalyst remains almost unaltered during the recycling operations. Now this turns our attention to any changes in the heterogeneity that

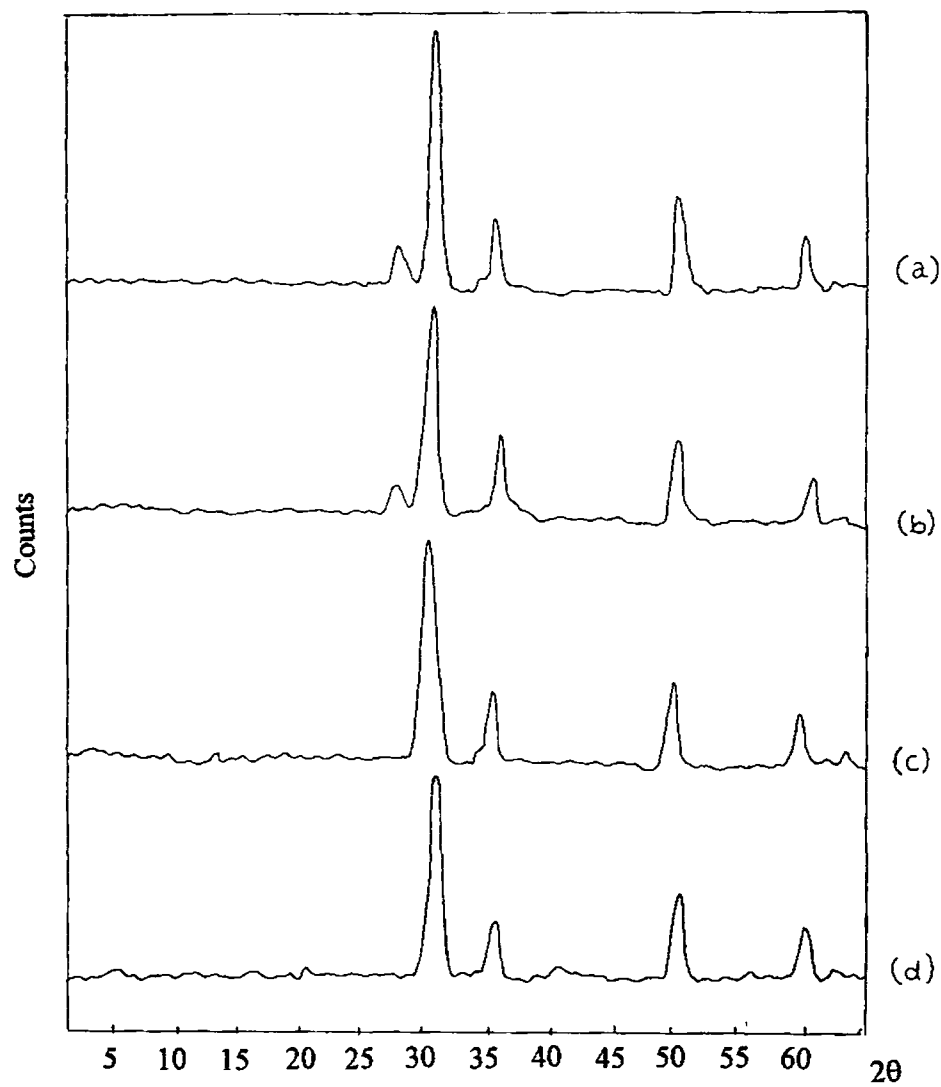


Fig. 4.11 XRD Patterns of fresh and recycled systems

a) Fe(2)SZ - Fresh

b) Fe(2)SZ -Used

c) Fe(10)SZ - Fresh

d) Fe(10)SZ- Used

may occur during the reaction. The absence of dark brown colour of the solution after the reaction points to the absence of  $\text{Fe}^{3+}$  in solution. To confirm this, the catalyst (Fe(2)SZ) was filtered out and the reaction was continued for 15 to 30 minutes. No noticeable change in conversion could be detected indicating the absence of metal leaching. The retention of the iron content was also confirmed by the EDX analysis of the sample after the reaction. The recovered catalyst showed an iron content of 1.95%, which implies the retention of the chemical identity of the catalyst. However, with repeated recycling a slight loss in the iron content was observed. The EDX analysis after five successive regenerations showed an iron content of 1.56%. The reduction in the iron content explains the loss in the activity during recycling.

At high iron loadings (Fe(10)SZ), a slight leaching out of the iron was observed from the EDX analysis results (Fe content-8.14%). However, the continued stirring after filtering of the catalyst failed to give any further progress in the reaction suggesting that the leached out iron was inactive in catalysing the reaction. From the afore-mentioned observations, we conclude that iron chloride if at all formed by the probable reaction of benzoyl chloride or HCl evolved in the reaction with the iron component of the catalyst, exists on the catalyst surface, which may be later washed off. This suggests the reaction to be mainly heterogeneous in nature.

#### 4.2.9 INFLUENCE OF MOISTURE

The activity of a catalyst depends mainly on its acidic characteristics especially on the nature of acidic sites, whether they are Brønsted or Lewis. The calcination temperature and the atmospheric exposure strongly influence the relative concentrations of Lewis and Brønsted acid sites. Thus, it becomes important to test the influence of moisture adsorption on the catalytic activity. For this the activated catalyst was kept in a desiccator containing water for 48 hours before testing for the catalytic activity. Parallel runs were conducted using fresh catalyst. The adsorption of moisture resulted in a loss of catalytic activity. This may be correlated with the reversible transformation of the Lewis acid sites into Brønsted acid sites upon exposure to moisture. A lowering of the percentage conversion goes together with a decrease in the Lewis acidity.

Table 4.8 Influence of moisture on catalytic activity

Conversion (%)	Presence of moisture	67.19
	Calcined sample (700°C)	79.61

Reaction Temperature-110°C, Duration- 1 hour, Catalyst Fe<sub>2</sub>O<sub>3</sub>/SZ-0.1 g,  
Toluene:Benzoyl chloride molar ratio- 5:1

#### 4.2.10 MECHANISM OF THE REACTION

The general function of a catalyst is to provide assistance for a particular chemical reaction by providing an alternate path of lower activation energy. The mechanism of a particular reaction varies depending on the catalyst chosen. Based on the catalyst nature the reaction can be driven by Brønsted or Lewis acid sites. Prediction of a reaction mechanism demands the compilation of the catalytic activity results under different experimental conditions.

The results obtained in the case of different transition metal incorporated systems as well as the systems with different sulphate content suggest the dominating role of the Lewis acid sites in deciding the catalytic activity (Fig. 4.2, 4.4). In the case of iron promoted systems also, good correlations could be obtained between the catalytic activity and Lewis acidity (Table 4.4). The active participation of the Lewis acid sites in the benzoylation reaction is also supported by the catalytic activity studies at different calcination temperatures of the catalyst (Fig. 4.10). A considerable loss in activity (Table 4.8) observed when the catalyst was exposed to moisture also lends support to the proposed involvement of the Lewis acid sites in catalysing the reaction.

From the above discussions, it seems reasonable to suggest that the benzoylation of arenes over the sulphated zirconia systems proceeds *via* an electrophilic attack. Benzoyl chloride gets polarised on the catalyst surface to generate  $C_6H_5CO^+$  species, which then attack the aromatic ring to form the substituted benzophenones. The influence of substrate to benzoyl chloride molar ratio on the catalytic activity also supports the view that, for the reaction to occur the benzoyl chloride molecule should get adsorbed on the catalyst surface. This is also reasonable when the nonpolar nature of toluene is considered. The strong acid sites, especially the Lewis acidic centers, may be considered to facilitate the formation of electrophilic species. The adsorption of benzoyl chloride can



occur *via* the chlorine atom or the oxygen atom. Adsorption *via* oxygen atom is more relevant when Brönsted sites are involved, while the chlorine atom gets more readily adsorbed at the Lewis acid sites [42]. The essentiality of the strong acid sites for the reaction stems from the highly electronegative character of the chlorine atom, on account of which the adsorption *via* the lone pair of electrons becomes rather difficult. A plausible mechanism for the reaction is represented in Fig 4.12.

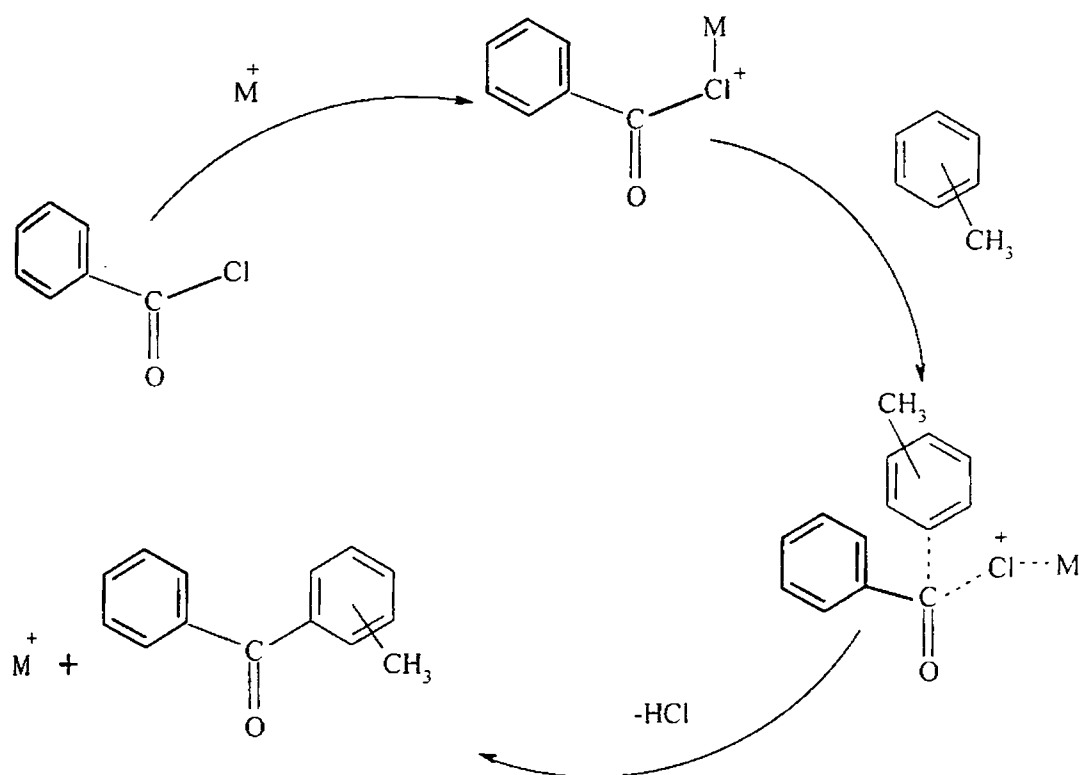


Fig. 4.12 Plausible mechanism for the benzoylation of toluene

### 4.3 BENZYLATION OF AROMATICS

Benzylation was carried out using benzyl chloride and benzyl alcohol as benzylating agents. The influence of various reaction parameters on the catalytic activity is discussed in the following sections.

#### 4.3.1 BENZYLATION WITH BENZYL CHLORIDE

The alkylation of aromatic compounds containing electron-donating groups (like -OH, alkyl or alkoxy) can be easily accomplished while it becomes difficult in absence of

an activating group. Thus, benzene was chosen as the substrate for comparing the activities of the different catalyst systems. The general scheme of the reaction can be represented as in Fig. 4.13.

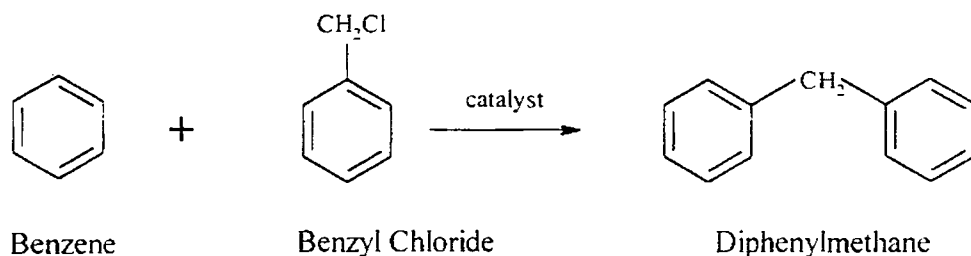


Fig. 4.13 General scheme of benzylation of benzene with benzyl chloride

#### 4.3.1.1 Influence of catalyst composition

In general, sulphated zirconia systems proved to be efficient catalysts for Friedel-Crafts benzylation of aromatics using benzyl chloride as the benzylating agent. The specific influence of the catalyst composition is presented below.

##### i) Influence of metal incorporation

Table 4.9 presents the results of benzylation of benzene using benzyl chloride over different metal promoted sulphated zirconia systems. Pure  $\text{ZrO}_2$  gave very low conversions under the specified reaction conditions. However, satisfactory yields of diphenylmethane were obtained for most of the sulphated zirconia systems. An interesting observation was that only monoalkylated product was obtained in all the cases except for iron promoted system. In the case of iron-incorporated sample, a very low percentage (2.48%) of secondary alkylated products could also be detected.

As in the case of benzoylation reaction, a good correlation could be observed between the catalytic activity and the Lewis acidity in most of the cases (Fig. 4.14). The exceptionally low activity of the vanadia promoted system, in spite of its Lewis acidity comparable with other systems, may be correlated to the predominant monoclinic phase. The monoclinic phase is generally considered to be the catalytically inactive phase of zirconia. A notable deviation was observed in the case of Fe and Cu incorporated systems. Abnormally high conversions, which do not commensurate with the Lewis acidity values, may be attributed to the reducible character of these ions. Attempts were also made to

correlate the activity with the acidity values obtained by the TPD measurements. A crude correlation could be obtained between the amount of strong acidity and the catalytic activity for majority of the samples (Fig. 4.15).

Table 4.9 Benzylation of benzene with benzyl chloride

Catalyst	Conversion (%)
ZrO <sub>2</sub>	8.89
SZ	19.52
V(2)SZ	20.38
Cr(2)SZ	44.36
Mn(2)SZ	54.50
Fe(2)SZ	91.68
Co(2)SZ	39.34
Ni(2)SZ	58.48
Cu(2)SZ	80.34
Zn(2)SZ	35.79
W(2)SZ	41.58
Mo(2)SZ	62.16

Reaction temperature  $-80^{\circ}\text{C}$ , Duration-1 hour, catalyst - 0.1 g, benzene to benzyl chloride molar ratio-5:1.

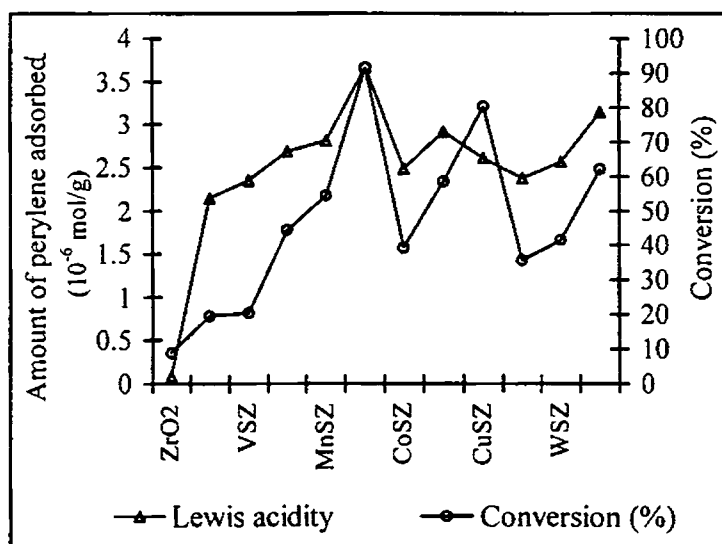


Fig. 4.14 Catalytic activity correlated with the Lewis acidity

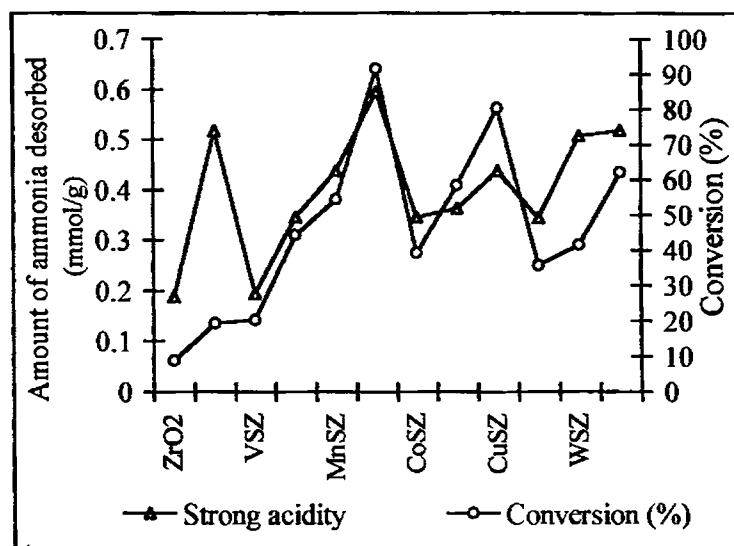


Fig. 4.15 Catalytic activity correlated with the amount of strong acid sites

Major exceptions were observed in the case of simple sulphated system as well as Cu promoted system. Simple sulphated zirconia gave poor yields even though the amount of strong acid sites for the sample was sufficiently high. This may be accounted for on the basis of its low Lewis acidity. The low activity of the vanadia-incorporated system seems justifiable when its strong acidity value is considered. Thus, the amount of strong acid sites and the Lewis acidity of the systems seem to have a combined role in deciding the catalytic activity. The percentage conversions obtained with Fe and Cu incorporated samples were higher than those expected based on their Lewis acidity and strong acidity values. This may be explained based on the reducible character of the  $\text{Fe}^{3+}$  and  $\text{Cu}^{2+}$  ions.

## ii) Influence of iron content

Iron incorporated systems exhibited high reactivity for the benzylation of benzene with benzyl chloride. Influence of iron content on the catalytic activity and selectivity is presented in Table 4.10. An increase in iron content seemed beneficial for the reaction. The percentage conversion increased gradually with an increase in the iron loading and levelled off after an iron content of 8%. However, with increased iron loading, secondary alkylated products increased considerably. The increase in percentage conversion was rather marginal when compared to the decrease in the selectivity. The selectivity to diphenylmethane was reduced from 97.52 to 71.13% when the iron content was increased from 2 to 10%.

Table 4.10 Benzylation of benzene over iron promoted sulphated zirconia

Catalyst	Conversion (%)	Selectivity (%)	
		DPM	Others
Fe(2)SZ	68.49	97.52	2.48
Fe(4)SZ	74.29	91.41	8.59
Fe(6)SZ	86.57	82.36	17.64
Fe(8)SZ	96.38	75.70	24.30
Fe(10)SZ	98.51	71.13	28.87

Molar ratio (benzene: benzyl chloride) -5:1, Time - 30 min, catalyst - 0.1 g  
Reaction temperature - 80°C.

As for the different transition metal promoted systems, catalytic activity of the iron promoted systems could also be correlated with the Lewis acidity. The dependence of catalytic activity on the Lewis acidity for the different iron loaded systems is sketched in Fig. 4.16. The increase in Lewis acidity was rather sharp when the iron loading was varied. However, such a sharp rise could not be observed in the percentage conversions obtained. This may be an indication of the fact that the iron content or the Lewis acidity is not the only factor favouring the reaction.

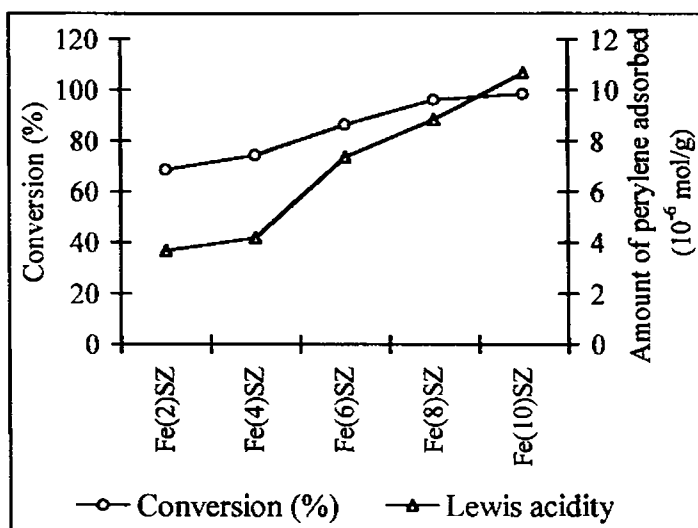


Fig. 4.16 Dependence of catalytic activity on Lewis acidity

The catalytic activity was also in line with the amount of strong acid sites in the samples (Fig. 4.17). The leveling off the conversions at higher iron loadings indicates that

there exists a critical value for the acidity beyond which the reaction seems to be independent of acidity.

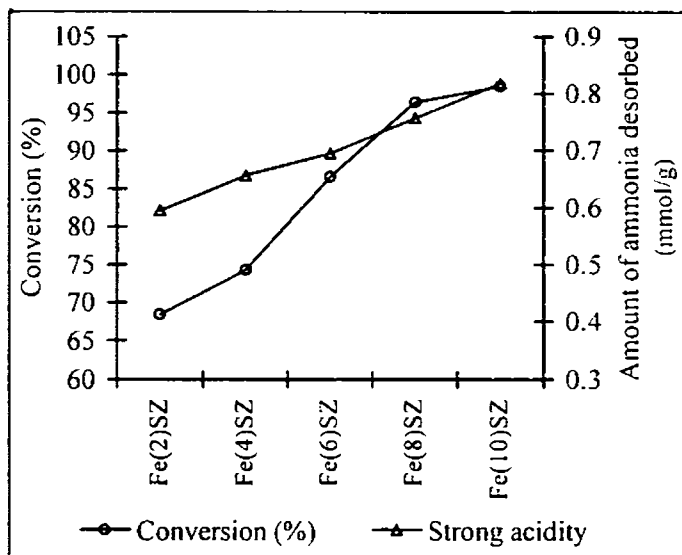


Fig. 4.17 Dependence of catalytic activity on the amount of strong acid sites

#### 4.3.1.2 Influence of substrate

The influence of substrate on the catalytic activity was examined taking Fe(2)SZ as representative system. As observed in the case of benzoylation reaction, the reactivity was in the order xylene > toluene > benzene, which is in perfect agreement with the electron releasing nature of the alkyl groups. The inductive effect of methyl groups makes the reaction more facile in the case of toluene and still higher is the conversion in the case of xylene due to the cumulative effect of the two methyl groups. The reactions were conducted at the corresponding refluxing temperatures and the results are tabulated (Table 4.11).

The nature of substrate also had a deciding effect on the selectivity towards monoalkylation. High selectivity to monoalkylated product was obtained in the case of benzene and the selectivity decreased in the case of toluene and xylene. The selectivity for monoalkylation was higher for toluene when compared with that for xylene. Steric hindrance by two methyl groups reduces the accessibility of the alkylating moiety for a second attack. A comparison of the activities at 80°C is presented in Table 4.12. The

increase in activity follows the same order benzene < toluene < xylene. The selectivity pattern also remains the same as for the refluxing temperature.

Table 4.11 Influence of substrate on catalytic activity and selectivity

Substrate	Time (min)	Conversion (%)	Selectivity (%)	
			MAP	DAP
Benzene	60	91.68	97.52	2.48
Toluene	10	100	91.46	8.54
Xylene	5	100	95.49	4.51

Molar ratio (Substrate: benzyl chloride) – 5:1, Refluxing temperature, catalyst - 0.1 g Fe(2)SZ  
MAP-Monoalkylated Products, DAP- Dialkylated Product

Table 4.12 Benzylation of different substrates with benzyl chloride at 80°C

Substrate	Time (min)	Conversion (%)	MAP	DAP
Benzene	60	91.68	97.52	2.48
Toluene	30	97.56	98.08	1.92
Xylene	30	89.05	99.42	0.58

Molar ratio (Substrate:benzyl chloride) – 5:1, 0.1 g Fe(2)SZ, MAP-Monoalkylated Products  
DAP- Dialkylated Product

#### 4.3.1.3 Influence of reaction temperature

The reaction temperature seems to play a major role in deciding the catalytic activity and selectivity. The results of benzylation of toluene and xylene at different reaction temperatures are presented in Tables 4.13 and 4.14. At low temperatures the percentage conversion was very low. An increase in the temperature results in enhanced activity. An interesting observation was the sharp rise in the conversion obtained when the temperature was varied in a narrow range of 10°C from 60°C to 70°C. A further increase in temperature only had a minor influence on the percentage conversion. Temperature also had marked influence on the selectivity. At low temperatures 100% selectivity to the monoalkylated products was obtained. An increase in reaction temperature results in a lowering of selectivity. Even at the refluxing temperatures high selectivity to monoalkylation was observed. The higher selectivity

towards monoalkylated product in the case of xylene may be attributed to the steric hindrance of the methyl groups.

Table 4.13 Benzylation of toluene – influence of reaction temperature

Temperature (°C)	Time (min)	Conversion (%)	Selectivity (%)	
			MDPM	Others
50	60	8.54	100	-
60	60	30.52	100	-
70	60	93.37	100	1.08
80	30	97.56	98.08	1.92
90	20	97.40	96.52	3.48
100	20	100	95.14	4.86
110	10	100	91.46	8.54

Molar ratio (toluene:benzyl chloride) - 5:1, 0.1 g Fe(2)SZ catalyst

Table 4.14 Benzylation of xylene at different reaction temperatures

Temperature (°C)	Time (min)	Conversion (%)	Selectivity (%)	
			DMDPM	Others
50	60	8.62	100	-
60	60	18.76	100	-
70	60	97.57	100	-
80	30	89.05	99.42	0.58
90	30	94.37	98.71	1.29
100	15	98.56	97.58	2.42
110	15	99.61	96.61	3.39
120	15	100	95.99	4.01
145	5	100	95.49	4.51

Molar ratio (xylene:benzyl chloride) - 5:1, 0.1 g Fe(2)SZ

The sharp shooting of the catalytic activity for a temperature change of 10°C in the interval 60°C to 70°C cannot be discarded as a mere temperature effect. Another interesting aspect noted was that such a leap was not perceptible in the case of other



systems except for the copper incorporated sample. This suggests the involvement of a different reaction mechanism in the case of iron and copper promoted systems as proposed in succeeding sections. This also explains the anomalously high conversions obtained in these cases.

### 3.1.4 Influence of reaction time

The progress of reaction monitored with time in the case of benzylation of toluene at 70°C with benzyl chloride is portrayed in Fig. 4.18. An induction period was noticed at the beginning in the case of iron-doped systems. After the first 30 minutes the reaction was almost rapidly driven to completion, when Fe(2)SZ system was employed. In the case of Fe(10)SZ, the reaction was almost completed within 15 minutes even at 70°C. The induction period was considerably shortened at high iron loadings. The existence of an induction period was also observed with the CuSZ systems. However, such a rapid progress of reaction could not be observed with other systems as tested using Cr, Mn and W doped systems.

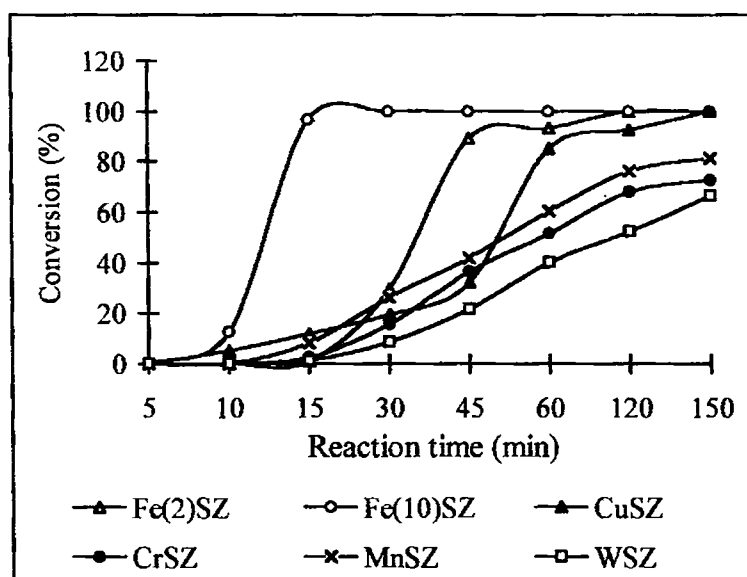


Fig. 4.18 Catalytic activity as a function of reaction time

The variation in the product selectivity with time was also subjected to screening. In the case of iron doped systems, at the beginning of reaction when the percentage conversions were low, only monoalkylated products were detected. At higher conversions secondary alkylation was also observed. The amount of dialkylated products increased

with increase in the reaction time. The degree of secondary alkylation was almost negligible for other systems under the reaction conditions specified.

#### 4.3.1.5 Influence of molar ratio

The variation in the catalytic activity with toluene to benzyl chloride molar ratio was also examined for Fe(2)SZ and Fe(10)SZ systems (Fig 4.19). The product selectivities at different molar ratios are also illustrated (Figs. 4.20, 4.21). The increase in toluene to benzyl chloride molar ratio resulted in lowering of the percentage conversion in the case of Fe(2)SZ system. However, the molar ratio had little effect on the catalytic activity at higher iron loadings. In the case of Fe(10)SZ, complete conversion was obtained irrespective of the molar ratio selected. The negative influence of higher toluene to benzyl chloride molar ratios may be explained on the basis of the dilution effect at high solvent levels.

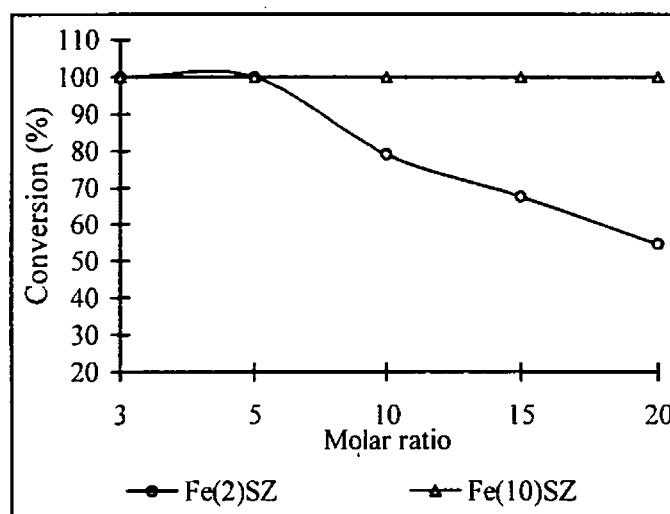


Fig. 4.19 Influence of molar ratio on catalytic activity

Refluxing temperature, catalyst- 0.1 g, Duration-15 min

Irrespective of the catalyst composition, the product selectivity depended on the molar ratio. At higher toluene to benzyl chloride ratios, the amount of dialkylation was negligible while it considerably increased at low molar ratios. This may be rationalised on the basis of the relative concentration of benzyl chloride molecules. At low toluene to benzyl chloride ratios, high concentrations of benzyl chloride species in the reaction mixture favour successive alkylation.

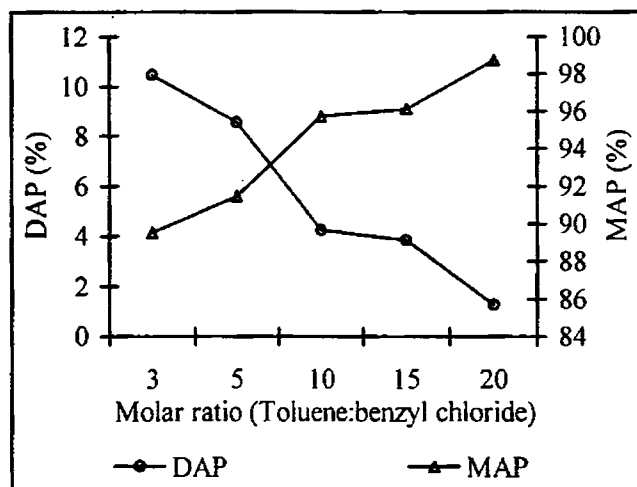


Fig. 4.20 Effect of molar ratio on product selectivity for the benzylation of toluene with Fe(2)SZ

Refluxing temperature, 0.1 g catalyst, Duration-15 min

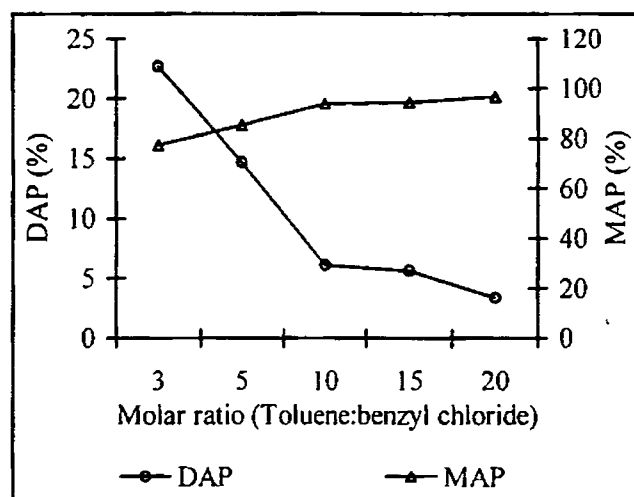


Fig. 4.21 Effect of molar ratio on product selectivity for the benzylation of toluene with Fe(10)SZ

Refluxing temperature, 0.1 g catalyst, 15 min duration

#### 4.3.1.6 Influence of calcination temperature

The influence of calcination temperature on the catalytic activity for the benzylation of benzene was also tested. An increase in the calcination temperature resulted in a progressive increase in the catalytic activity (Fig. 4.22). As in the case of

benzoylation reaction, maximum activity was obtained after calcination at 700°C. At low calcination temperatures, 100% selectivity to the monoalkylated products was obtained. For higher calcination temperatures, percentage conversion increased at the expense of selectivity. The progressive increase in the percentage conversion correlates with the increase in Lewis acidity obtained by perylene adsorption studies (Fig. 4.22). After 600°C, the increase was rather sharp, which suggests that the crystalline nature of the catalyst may also be contributing to the activity. Tetragonal phase formation starts at a calcination temperature of about 600°C.

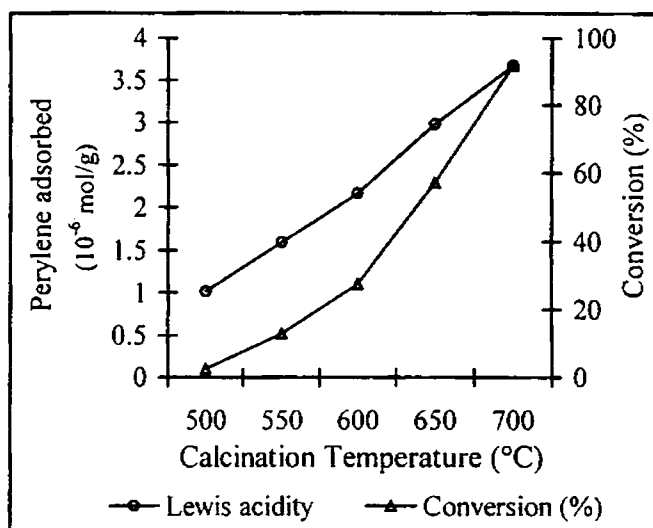


Fig. 4.22 Correlation between catalytic activity with Lewis acidity at different calcination temperatures

Duration 1 hour, catalyst - 0.1 g Fe(2)SZ, refluxing temperature,  
Benzene: Benzyl chloride molar ratio- 5:1

#### 4.3.1.7 Reusability of the catalyst systems

The reusability of the systems for the benzoylation reaction was also investigated. Gradual drop off was observed in the percentage conversion as the catalyst was subjected to regeneration (Table 4.15). Even after five successive recycling operations, satisfactory yields were obtained suggesting the recycling capacity of the catalyst systems. XRD patterns of the catalyst systems were recorded after the reaction to test for any alteration in the crystalline structure during repeated recycling (Fig. 4.23). The XRD pattern of the used catalyst confirms the retention of crystalline nature in Fe(2)SZ system, except for a slight lowering of intensity. However, an alteration of crystalline structure was detected in

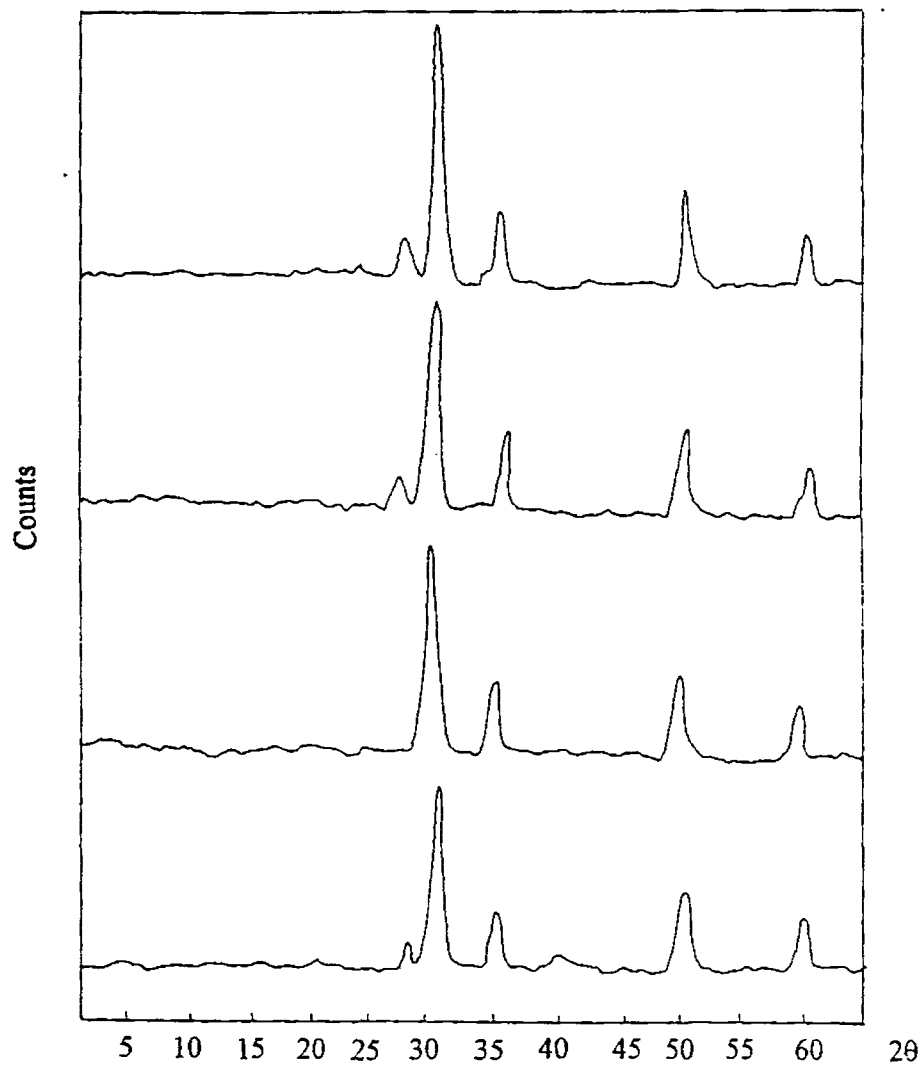


Fig. 4.23 XRD Patterns of fresh and recycled systems

a) Fe(2)SZ - Fresh

b) Fe(2)SZ -Used

c) Fe(10)SZ - Fresh

d) Fe(10)SZ- Used

the case of Fe(10)SZ. Recycling operations resulted in the appearance of monoclinic phase, which was absent in the fresh sample.

Table 4.15 Regeneration of catalyst

No: of cycles		1	2	3	4	5
Conversion	Fe(2)SZ	91.68	87.42	79.14	72.81	65.20
(%)	Fe(10)SZ	98.51	92.32	88.17	86.34	79.58

Catalyst-0.1 g, Duration-1hr for Fe(2)SZ and 30 min for Fe(10)SZ, Molar ratio (Benzene:Benzyl chloride) – 5:1, Reaction Temperature – 80°C.

#### 4.3.1.8 Metal leaching

The alteration in the crystalline structure observed in the XRD pattern encourages some investigations on the chemical changes invoked in the catalyst during recycling. In order to test for the metal leaching, the reaction was continued after filtering off the catalyst and the results are tabulated (Table 4.16). A slight enhancement in the percentage conversion was monitored suggesting the partially homogeneous nature of the reaction. The increase in the case of Fe(10)SZ was more predominant when compared with Fe(2)SZ. The increase in the conversion after filtering off the catalyst is more prominent for high loaded iron system, indicating that the homogeneous character increases with increasing iron content.

Table 4.16 Metal leaching for different systems

Time (min)		0	5	10	15	20	25	30
Conversion	Fe(2)SZ	68.49	69.12	70.54	71.98	72.12	73.37	73.50
(%)	Fe(10)SZ	71.12	74.86	76.80	78.35	80.74	81.06	81.32

0.1 g catalyst, Molar ratio (Benzene:Benzyl chloride) - 5:1, Reaction Temperature - 80°C. The notation "0" indicates the time when the catalyst was filtered off which is 30 min for Fe(2)SZ and 15 min for Fe(10)SZ.

The retention of chemical composition was also tested by the EDX analysis, which reveals a slight reduction in the iron content (Fe content - 1.86% for Fe(2)SZ and 9.58% for Fe(10)SZ). Recycling resulted in a gradual lowering of the iron content and after five successive regenerations, the iron content obtained was 1.58% for Fe(2)SZ and

5.32% for Fe(10)SZ. This suggests that the catalyst is chemically stable at low iron loadings perhaps due to the fine dispersion of the iron particles on the catalyst. The appearance of monoclinic phase in Fe(10)SZ during recycling may be a consequence of the reduction in the iron content. The XRD patterns of the fresh samples reveal traces of monoclinic phase at iron loadings beyond 6%.

#### 4.3.1.9 Influence of moisture

The influence of moisture adsorption on the catalytic activity was also examined. The catalyst after activation followed by exposure to moisture was used for the catalytic run. The results show a negative effect of moisture adsorption on the catalytic activity (Table 4.17). This lends support to our assumption that the Lewis acid sites are involved in the reaction. However, the decrease was rather small when compared with the drop observed in the case of benzylation reaction.

Table 4.17 Influence of moisture on catalytic activity

Conversion (%)	Presence of moisture	
	Calcined sample (700°C)	84.62
		93.37

Reaction Temperature-70°C, Duration- 1 hour, 0.1 g Fe(2)SZ catalyst, Toluene:Benzyl chloride molar ratio- 5:1

#### 4.3.1.10 Mechanism of the reaction

The catalytic activity studies on different transition metal promoted systems suggest the involvement of Lewis acid sites in the reaction (Fig. 4.14). Such a correlation was obtained for iron promoted systems also even though a leveling off the activity was observed at higher loadings (Fig. 4.16). The progressive increase in the catalytic activity with the increase in calcination temperature (Fig. 4.22) also supports the suggestion. To substantiate this, the influence of moisture on the catalytic activity was determined taking Fe(2)SZ as the representative system (Table 4.17). The detrimental influence of moisture confirms the dominating role of Lewis acidity in deciding the catalytic activity.

The benzyl chloride molecule may be polarised at the Lewis acidic centres on the catalyst surface. The attack of the alkylating moiety on the aromatic ring results in the formation of the diphenylmethane derivatives. The negative influence of increasing

aromatic substrate to benzyl chloride molar ratio on the catalytic activity (Fig. 4.19) also supports the polarisation of the benzoyl chloride molecule as an initial step in the reaction. The nonpolar nature of the substrate molecules also supports the formation of the electrophilic species by adsorption of benzyl chloride molecule on the catalyst surface. A plausible mechanism for the reaction can be represented schematically as shown in Fig. 4.24.

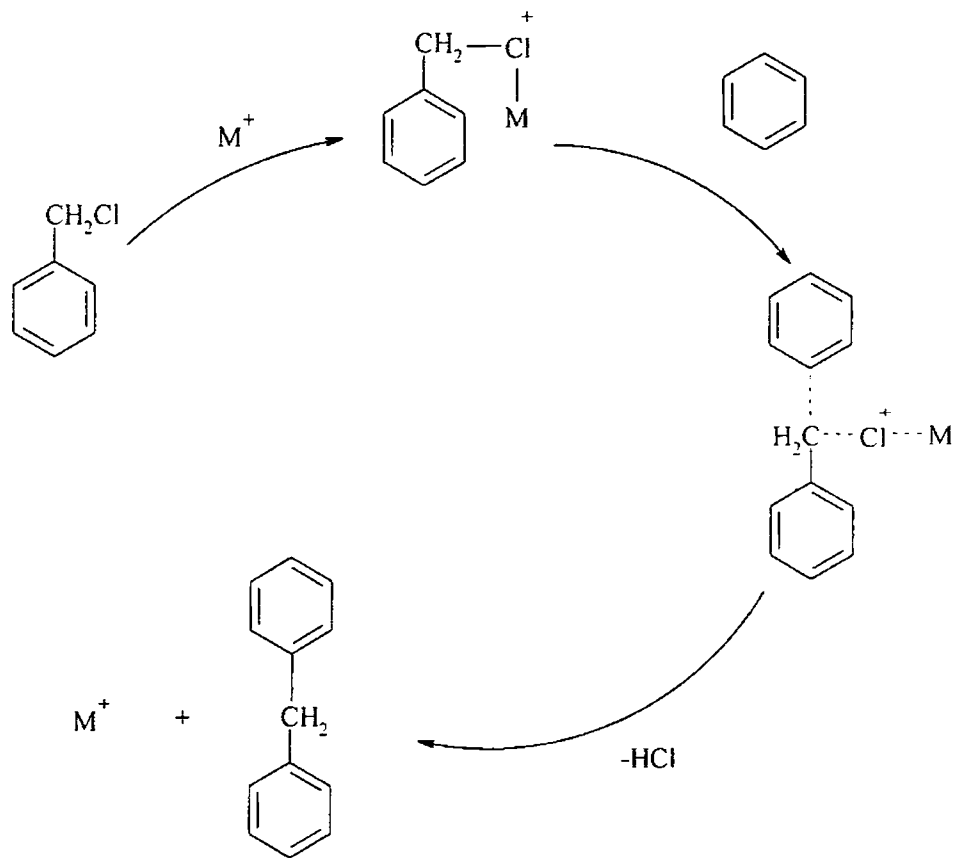


Fig. 4.24 Mechanism of Friedel-Crafts Benzylation using benzyl chloride with active involvement of Lewis acid sites

However, the use of reducible cations like  $\text{Fe}^{3+}$ ,  $\text{Cu}^{2+}$ , etc. induces very high activity, which do not commensurate with the acidity values. The percentage conversions obtained in these cases were much higher than that expected from its Lewis acidity or the amount of strong acid sites. Also the influence of reaction temperature was different for these systems when compared with others. At  $50^\circ\text{C}$  and  $60^\circ\text{C}$ , the conversions obtained were very low. At  $70^\circ\text{C}$ , a drastic rise in the percentage conversion was obtained which



cannot be explained as a mere temperature effect (Tables 4.13, 4.14). Such a sudden increase was absent for other systems. The plot of the catalytic activity as a function of reaction time (Fig. 4.18) also presents an interesting observation. An induction period was quite perceptible in the case of Fe and Cu promoted systems while a gradual increase was obtained with others. The induction period was considerably shortened in samples with high iron loading.

Considering all the aspects, we propose the existence of a redox or a free radical mechanism in the case of Fe and Cu promoted samples side by side with the involvement of Lewis acid sites. Radicals are powerful reductants, which can readily be oxidised to cations in presence of reducible metal cations. Thus the high activity associated with these reducible cations involves the initiation of the reaction by the homolytic cleavage of the C-Cl bond followed by the oxidation of the radical to the corresponding ions. A convenient pathway is shown in Fig. 4.25.

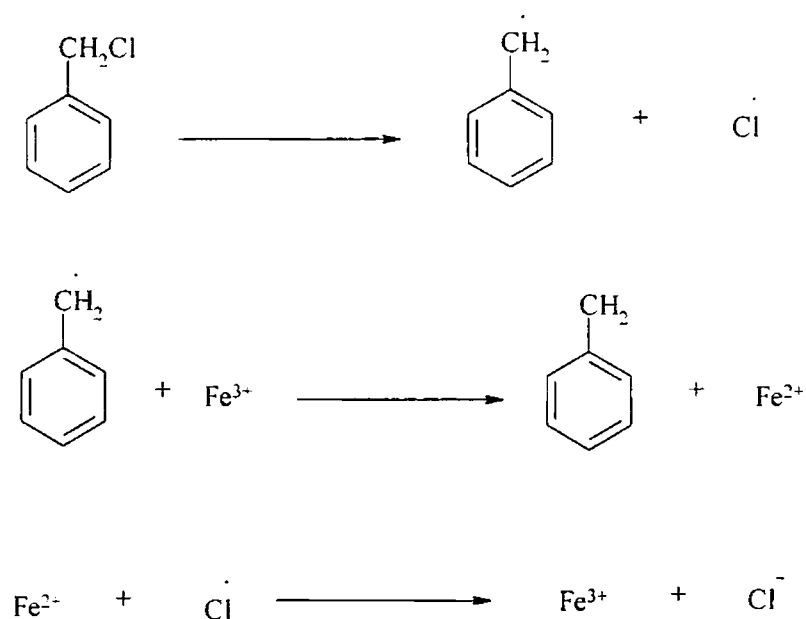


Fig. 4.25 Free radical mechanism for Benzylation of toluene

The possibility of a redox mechanism has been previously reported to explain the high activity obtained in catalysts containing reducible cations like  $\text{Sn}^{4+}$ ,  $\text{Fe}^{3+}$  and  $\text{Cu}^{2+}$  [16,28]. At high iron loadings, the free radical mechanism may be considered to predominate as evident from the leveling off the activities and the shortening of the



Table 4.18 Benzylation of toluene with benzyl alcohol over different sulphated zirconia systems

Catalyst	Conversion (%)	Selectivity (%)		
		2-MDPM	4-MDPM	Dibenzyl ether
ZrO <sub>2</sub>	8.96	-	5.95	94.05
SZ	27.61	14.58	26.95	58.47
VSZ	17.75	15.46	34.51	50.03
CrSZ	27.71	11.69	56.80	31.51
MnSZ	19.08	18.46	29.15	52.39
FeSZ	29.10	40.59	29.52	29.89
CoSZ	31.42	12.47	31.90	55.63
NiSZ	36.25	7.65	39.75	52.61
CuSZ	15.05	8.94	21.58	69.48
ZnSZ	27.67	-	-	100
MoSZ	21.36	9.36	25.41	65.23
WSZ	29.56	13.28	26.47	60.25

Refluxing temperature, Toluene:benzyl alcohol molar ratio-5:1, Duration – 2 hours, catalyst-0.1 g

As stated above along with the diphenylmethane derivatives, benzyl ether was obtained as a major side product. In the case of Zn incorporated system benzyl ether was the only product obtained. Maximum selectivity towards the alkylated product was obtained for the iron and chromium incorporated systems. For all other cases, the selectivity towards benzyl ether was in the range 50-70%. The conversion percentage of different metal incorporated systems could be correlated with the Brönsted acidity of the systems (Fig. 4.27). The comparatively lower product yield can be explained on the basis of the low Brönsted acidity of the catalyst systems, which may be a consequence of the high calcination temperature employed. However, the product selectivity to benzylated products and benzyl ether did not follow any common pattern.

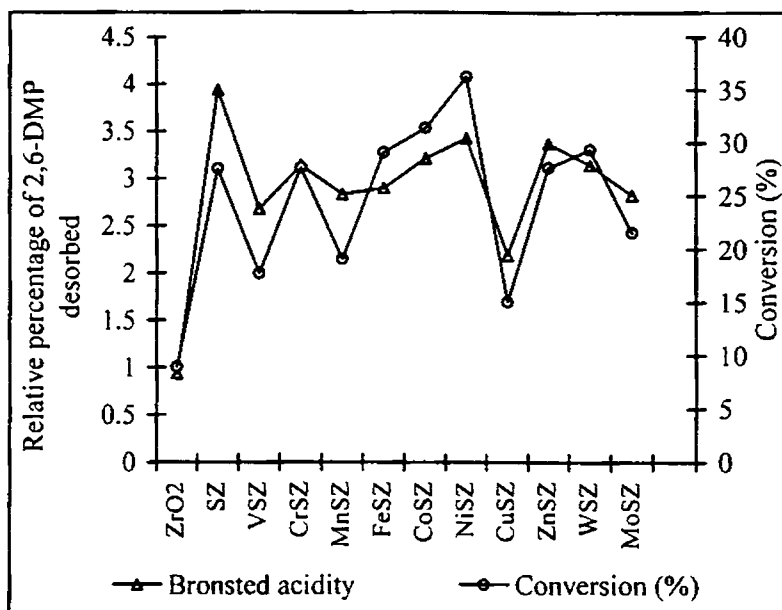


Fig. 4.27 Correlation between catalytic activity and Brönsted acidity

### ii) Influence of iron content

Benylation of toluene over iron promoted sulphated zirconia systems also gave satisfactory results (Table 4.19).

Table 4.19 Benzylation of toluene with benzyl alcohol over iron incorporated sulphated zirconia systems

Catalyst	Conversion (%)	Selectivity (%)		
		2-MDPM	4-MDPM	Dibenzyl ether
Fe(2)SZ	29.10	40.59	29.52	29.89
Fe(4)SZ	33.57	38.42	33.15	28.43
Fe(6)SZ	37.51	35.37	38.56	26.07
Fe(8)SZ	42.13	32.31	43.18	24.51
Fe(10)SZ	45.84	28.56	50.95	20.49

Refluxing temperature, Toluene:benzyl alcohol molar ratio-5:1, Duration-2 hours, Catalyst-0.1 g

An increase in the iron content resulted in a gradual increase in the percentage conversion. Iron content also had an impact on the selectivity pattern. High iron content resulted in an increase in the desired product selectivity at the expense of

benzyl ether. Another outcome of an increase in iron content was the change in the relative selectivity for the alkylated products. An increase in iron loading resulted in an increase in the selectivity towards 4-MDPM, whereas 2-MDPM was predominant for the low loaded iron systems. In the case of iron promoted systems also, a correlation could be observed between the catalytic conversion and the Brönsted acidity of the samples as shown in Fig. 4.28.

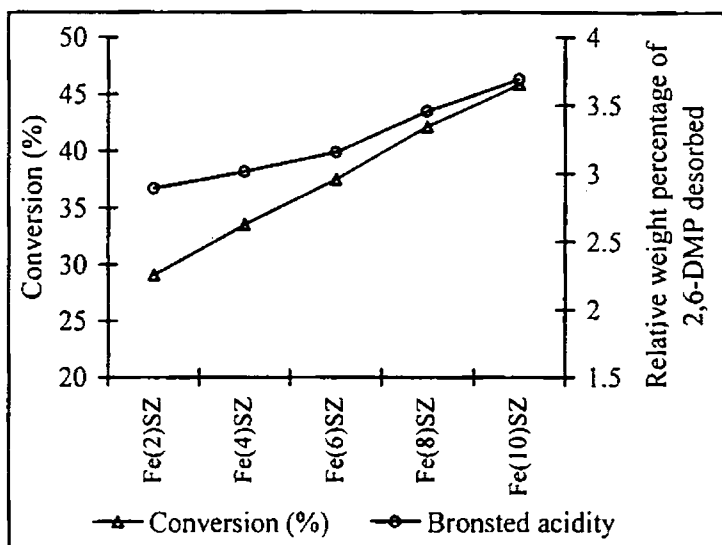


Fig. 4.28 Catalytic activity for benzylation of toluene with benzyl alcohol correlated with the Brönsted acidity of the iron promoted systems

#### 4.3.2.2 Influence of reaction temperature

The influence of reaction temperature on the catalytic activity and product selectivity is displayed in (Table 4.20).

Table 4.20 Influence of reaction temperature on catalytic activity and selectivity

Reaction Temperature (°C)	Conversion (%)	Selectivity (%)		
		2-MDPM	4-MDPM	Dibenzyl ether
110	29.10	40.59	29.52	29.89
100	15.87	26.14	18.44	55.42
90	8.54	-	-	100

Toluene:benzyl alcohol molar ratio - 5:1, 0.1 g Fe(2)SZ catalyst, Duration- 2 hours.

The percentage conversion showed a steady decline with decrease in the reaction temperature. Considerably low conversions were obtained at temperatures below the refluxing temperature. Selectivity pattern also altered in a corresponding way. Below 100°C, benzyl ether was the only product obtained, which may be partially due to the relatively low conversions obtained.

#### 4.3.2.3 Influence of reaction time

The progress of the reaction plotted as a function of time is shown in Fig. 4.29.

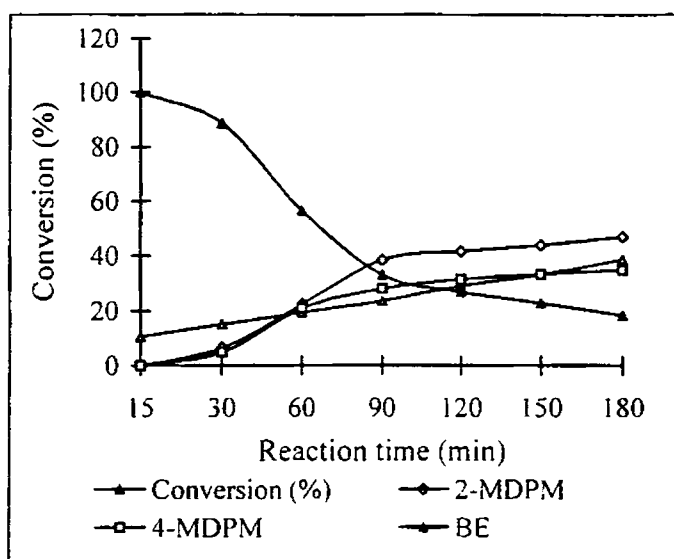


Fig. 4.29 Influence of reaction time on catalytic activity and selectivity  
 Refluxing temperature, Toluene:benzyl alcohol molar ratio - 5:1,  
 0.1 g Fe(2)SZ catalyst.

An increase in the reaction time resulted in a slight enhancement in the percentage conversion. However, the more prominent effect observed was the increase in the selectivity towards the benzylated products with a concomitant decrease in the yield of benzyl ether. This leads us to assume that during the initial stages of the reaction, benzyl ether is formed by the self-condensation of benzyl alcohol and in due course of the reaction, it gets converted into the benzylated products. The role of benzyl ether in the reaction has been reported earlier [45, 46].

#### 4.3.2.4 Influence of molar ratio

Toluene to benzyl alcohol molar ratio also affected the conversion and product selectivity as evident from Fig. 4.30.

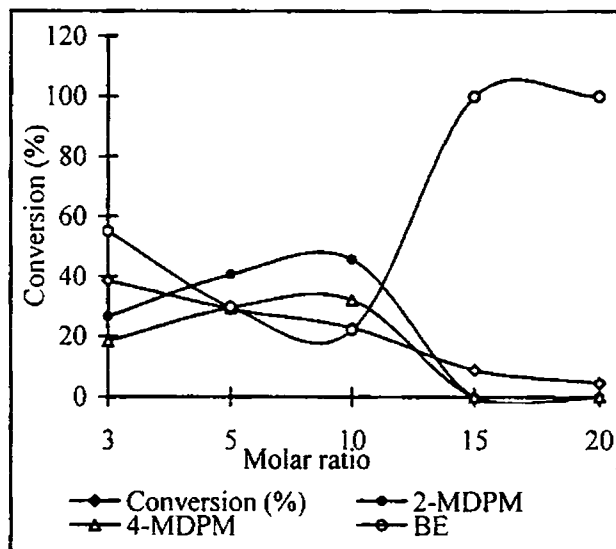


Fig. 4.30 Influence of molar ratio on the catalytic activity and selectivity

Toluene:benzyl alcohol molar ratio-5:1, catalyst - 0.1 g Fe(2)SZ,  
Duration-2 hours

An increase in the molar ratio resulted in a decrease in the percentage conversion, which is quite explainable on the basis of dilution effect of the solvent. The relatively lower concentration of benzyl alcohol diminishes the possibility of dimerisation, hindering the formation of benzyl ether. Benzyl ether being the intermediate in the formation of alkylated products; higher toluene to benzyl alcohol molar ratio has a negative effect on the catalytic activity. When the molar ratio was changed from 5:1 to 10:1, only a slight reduction was observed in the conversion rate. Above a molar ratio 10:1, no significant reaction occurred and the only product obtained was benzyl ether.

#### 4.3.2.5 Influence of calcination temperature

The influence of calcination temperature on the catalytic activity was tested in order to lend support to our theory of the involvement of Brønsted acid sites in the reaction. An increase in the calcination temperature resulted in a gradual reduction in the percentage conversion value without altering the selectivity in a serious way (Fig. 4.31).

This is in line with the conversion of Brönsted acid sites into Lewis acid sites *via* dehydroxylation at higher calcination temperatures.

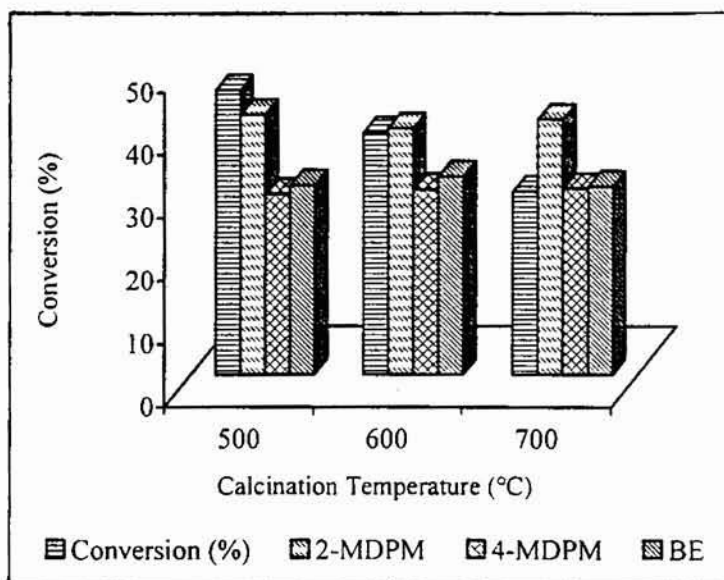


Fig. 4.31 Influence of calcination temperature on catalytic activity

#### 4.3.2.6 Metal leaching and reusability

The catalyst was tested for metal leaching and reusability and satisfactory results were obtained. There was no significant loss in activity even after five successive regenerations. The results are tabulated (Table 4.21). The metal content also remained constant after the recycling operations indicating the stability of the catalyst. The retention of the chemical identity may be a consequence of the fact that the reaction with benzyl alcohol does not evolve any acid during the reaction course.

Table 4.21 Regeneration of catalyst

No: of cycles	1	2	3	4	5
Conversion (%)	29.10	29.01	28.94	25.83	25.08

0.1 g Fe(2)SZ catalyst, Duration- 2hr, Molar ratio (Toluene: Benzyl alcohol)-5:1, Refluxing Temperature

#### 4.3.2.7 Influence of moisture

The investigation on the influence of moisture adsorption on the catalytic activity establishes the Brönsted acid catalysis of the reaction. The catalyst after activation a



700°C was placed in desiccators containing water for 48 hours to allow sufficient time for attainment of equilibrium. The moisture adsorption resulted in an enhancement in the catalytic activity towards benzylation with benzyl alcohol (Table 4.22).

Table 4.22 Influence of moisture on catalytic activity

	Conversion (%)
Presence of moisture	57.41
Calcined sample (700°C)	29.10

Refluxing Temperature, Duration-2 hour, Catalyst Fe(2)SZ- 0.1 g, Toluene:Benzyl alcohol molar ratio- 5:1

The beneficial effect of moisture on the catalytic activity may be explained as follows. The exposure to moisture results in a reversible transformation of Lewis acid sites into Brønsted acid sites as represented in Fig. 4.32. The increased availability of the Brønsted acid sites facilitates the reaction.

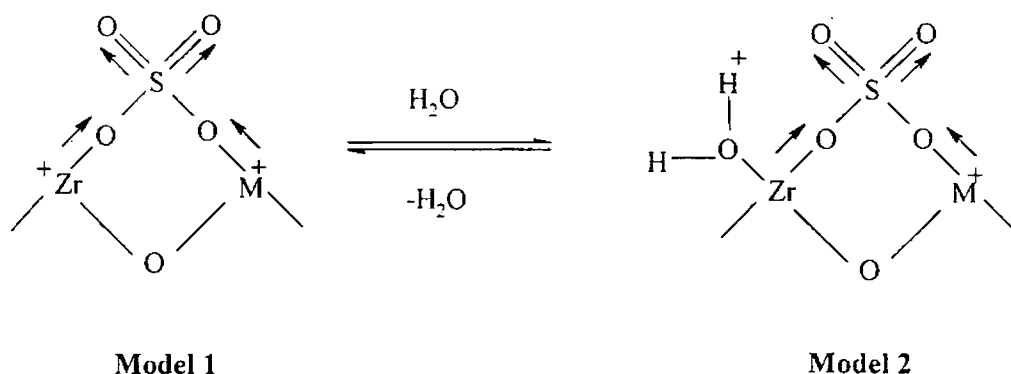


Fig. 4.32 Reversible transformation of Lewis acid sites into Brønsted acid sites

#### 4.3.2.8 Mechanism of the reaction

Good correlations could be observed between the Brønsted acidity and catalytic activity for the different systems studied as indicated by Figs. 4.27 and 4.28. The beneficial effect of moisture on the reactivity also supports the involvement of the Brønsted acid sites in catalysing the reaction. The steady decline in the activity with increasing calcination temperature also supports our postulate. The general mechanism for the reaction may be represented as in Fig. 4.33.

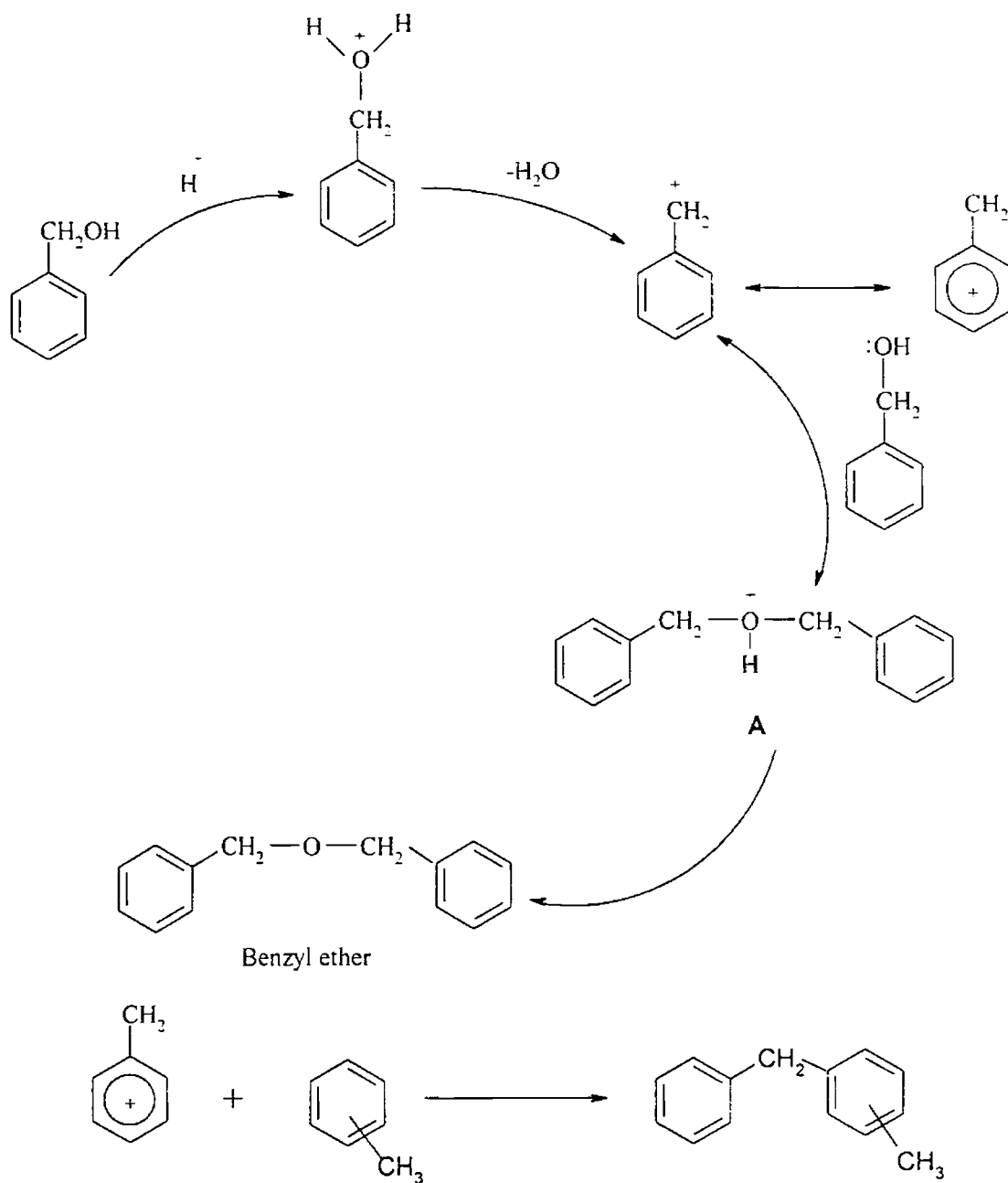


Fig. 4.33 Mechanism for the benzylation of toluene using benzyl alcohol

The experimental observations indicate the initial formation of benzyl ether, the relative percentage of which decreases with passage of time. The increase in the desired product selectivity with time was less prominent when compared with the reduction in the amount of the benzyl ether. This may be accounted for on the basis of the reversibility of the step 3 in the mechanism. The species A reverts back to the benzyl cation, which on

reaction with toluene gives the alkylated products. This explains the relatively steady state level of benzyl alcohol in the reaction mixture.

### 4.3.3 COMPARISON OF THE BENZYLATING AGENTS

Under this section we attempt to get a comparative evaluation of the two benzylating agents namely benzyl chloride and benzyl alcohol in carrying out the benzylation reaction of toluene. The major differences can be listed as follows.

1. Benzyl chloride seemed to be more efficient in carrying out the benzylation reaction. When benzyl chloride was used, at 110°C, complete conversion was observed after 10 minutes. However, for benzyl alcohol, even after 2 hours of reaction, the conversion obtained was only 29%. Further, benzylation with benzyl alcohol needed high reaction temperatures. Notable conversion could be obtained only at the refluxing temperature. In the case of benzyl chloride, even at 70°C, about 93% conversion was obtained within one hour.
2. In the case of benzyl chloride, alkylation occurred with 100% selectivity, while when benzyl alcohol was used, self-condensation of benzyl alcohol to benzyl ether was a serious side reaction. The relative selectivity towards ether and alkylated products varied from catalyst to catalyst. However, the formation of dialkylated products, which was observed with benzyl chloride as alkylating agent, was completely absent when benzyl alcohol was used. The percentage of dialkylated products formed in the case of benzyl chloride as alkylating agent was however negligible when compared with the amount of benzyl ether formed as side product during the use of benzyl alcohol.
3. Benzylation using benzyl chloride was mainly driven by the Lewis acid sites, while benzylation with benzyl alcohol was mainly Brönsted acid catalysed. Thus, increase in the calcination temperature and adsorption of moisture had an adverse effect on the catalytic activity in the case of benzyl chloride, while the effect was beneficial for benzyl alcohol.
4. In the case of iron and copper incorporated systems, abnormally high conversions obtained point out to a free radical mechanism operating side by side with benzyl

chloride was employed as the benzylating agent, while such an observation was absent when benzyl alcohol was used. The appearance of an induction period and the temperature effect support the redox mechanism.

5. The major drawback when benzyl chloride is used includes the formation of acid (hydrochloric acid) in the reaction mixture, which results in the leaching out of the metal species from the catalyst. Leaching was prominent when iron was present in the system. Such a shortcoming could be eliminated by the use of benzyl alcohol since there is not possibility of acid generation.

## SECTION 2 - ANILINE ALKYLATION

### 4.4 VAPOUR PHASE METHYLATION OF ANILINE

#### 4.4.1 INTRODUCTION

The manifold utilities of substituted anilines render the methylation of aniline an industrially important reaction. N-methyl aniline (NMA), N,N-dimethylaniline (NNMA) and toluidines serves as essential intermediates for the manufacture of a wide class of agrochemicals, dyes, plastics, pharmaceuticals and explosives. Due to the growing environmental considerations, worldwide attempts are going on to replace the conventional Friedel-Crafts type of reagents by eco-friendly solid acid catalysts. A broad class of solid acid catalysts has been tested for its utility towards this commercially important reaction. The major steps in the aniline methylation reaction may be represented by the general scheme shown in Fig. 4.34. N-methyl aniline arises from the side chain alkylation of aniline while toluidines are the products of ring alkylation. Consecutive reaction can result in N,N-dimethylaniline or N-methyltoluidines. Transalkylation can also occur as a side reaction.

Different systems employed for the aniline methylation include zeolites [49-55], clays and metal oxides [56-60]. The investigations on gas phase aniline methylation over various zeolites suggest that the various factors influencing the activity and selectivity of the reaction are the acid-base properties and shape selectivity of the solid acid catalyst [61-63]. Chen *et al.* [61] found HZSM-5 zeolite modified by alkali metal species to boost the selectivity towards N,N-dimethyl aniline. They suggested that N-alkylation could be

promoted by the additional basicity introduced by metal oxide modifiers. Barthomeuf *et al.* [62,63] studying the reaction over zeolites concluded that it involves acidic (cations) and basic (oxygen) sites. The more basic zeolites (X and Y exchanged with K, Rb or Cs) favour production of N-alkylates while zeolites with more acidic cations Li and Na lead to C-alkylation. Large pore zeolites favour both ring and side chain alkylation. Metal oxides show better selectivity for N-alkylation but majority of them favour both the mono and di-substitution on nitrogen.

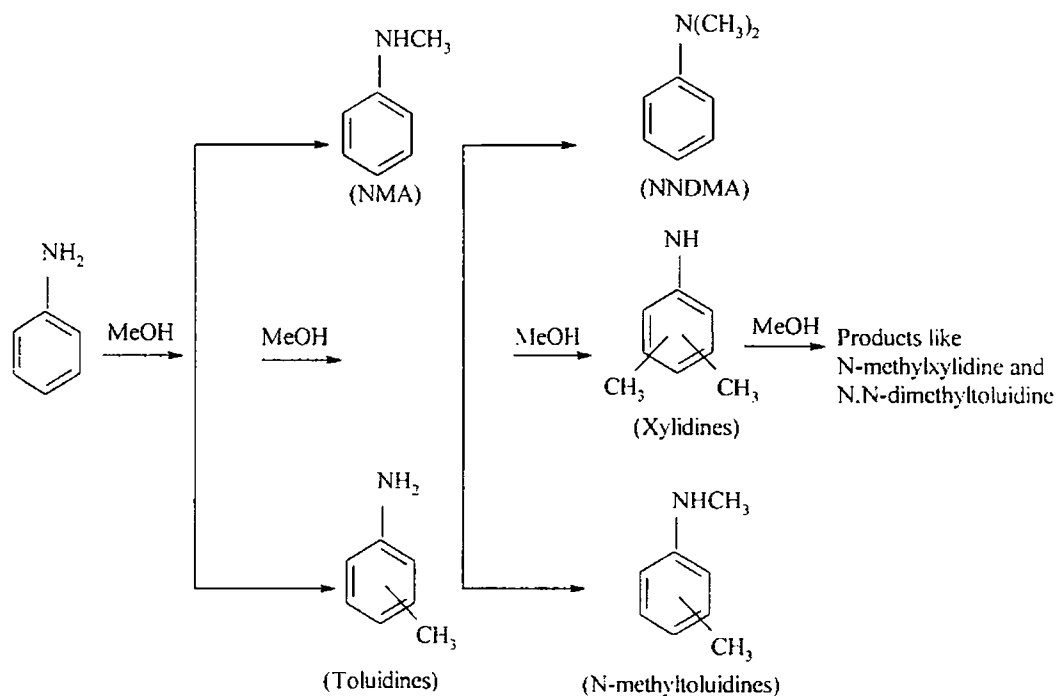


Fig. 4.34 General scheme of aniline alkylation

Woo *et al.* investigated the selective alkylation of aniline over several metallosilicates [64,65]. They suggested that strong, medium and weak acid sites are responsible for the formation of C-alkylate and coke, NNMA and N-methyltoluidines and NMA respectively. M.A.Aramendia *et al.* [66,67] reported the activity and selectivity of various magnesium orthophosphates for the gas phase methylation of aniline. No C-alkylates was detected, which is consistent with the weak acidity observed with magnesium orthophosphates. Elangovan *et al.* conducted methylation of aniline over AFI and AEL types of molecular sieves and obtained a direct relationship between conversion

and total acidity [68]. The product distribution was influenced by reaction conditions like temperature, methanol to aniline molar ratio etc.

Ferrosipinel systems were found to be highly active and selective for the N-monomethylation of aniline using methyl alcohol as the alkylating agent [69, 70]. High yields of NMA could be obtained even at sufficiently high methanol to aniline ratios. The spinel structure, the cation distribution between the tetragonal and octahedral sites etc. plays an important role in deciding the activity of the systems.

The mechanism of aniline alkylation reaction was well established by Ko *et al.* [57]. For the adsorption of methanol, the methoxy species is co-ordinatively bonded to the Lewis acid sites and the hydrogen atoms of the undissociated hydroxyl groups interact with the Lewis basic sites. Adsorption of aniline also follows a similar pattern. Electrophilic attack of the methyl group of the methanol on the nitrogen atom of adsorbed aniline leads to NMA, which on subsequent methylation leads to NNMA. The mechanism accounts for the need of moderate amounts of both acidic and basic Lewis sites for the system. A different mechanism was proposed by Rao and coworkers [51] for ALPO and SAPO, for which the adsorption and subsequent polarisation of the substrates is mainly caused by the Brønsted acidity on the surface. Any factor that alters the acidity or basicity will significantly affect the activity and selectivity of the system. The rate of the reaction mainly depends on the probability that aniline and methanol molecules are adsorbed on adjacent sites.

#### **4.4.2 METHYLATION OF ANILINE OVER SULPHATED ZIRCONIA SYSTEMS**

This section discusses the catalytic activity of the different sulphated zirconia systems towards the methylation of aniline. The influence of external parameters on the activity and product selectivity is also investigated.

##### **4.4.2.1 Influence of catalyst composition**

Methylation of aniline over different sulphated zirconia systems resulted in the formation of N-methylaniline (NMA), N,N-dimethylaniline (NNMA) and toluidines (T). The percentage conversion obtained and the relative product selectivity depended strongly on the nature of the catalyst and its acidic characteristics.

### i) Influence of metal incorporation

Table 4.23 presents the results of the vapour phase methylation of aniline over different transition metal incorporated sulphated zirconia systems. N-alkylation occurred predominantly resulting in the formation of NMA and NNMA. Toluidines were obtained in minor quantities. V, Fe and Mo incorporated systems were the least active. In all other cases, a percentage conversion remained in the range 30-45%.

Table 4.23 Methylation of aniline over metal promoted sulphated zirconia systems

Catalyst	Conversion (%)	Selectivity (%)		
		NMA	NNDMA	Toluidines
ZrO <sub>2</sub>				
SZ	31.26	47.95	45.82	6.23
VSZ	15.91	47.64	39.58	12.46
CrSZ	38.03	53.58	41.05	5.19
MnSZ	42.49	38.87	51.32	9.56
FeSZ	17.59	73.17	20.19	6.64
CoSZ	29.42	53.54	36.94	8.95
NiSZ	32.80	56.27	35.97	2.58
CuSZ	45.41	57.60	37.43	5.97
ZnSZ	36.78	79.02	18.46	2.52
MoSZ	16.59	70.46	20.47	8.49
WSZ	37.75	7.92	36.99	13.99

0.25 g catalyst, Flow rate-6 ml/hr. methanol:aniline molar ratio-5:1, Temperature-350°C.  
Time on stream-2 hours

An attempt was made to correlate the catalytic activity of the systems with the acidic properties of the systems. No apparent dependence could be obtained between the catalytic activity and the relative amounts of strong, medium or weak acid sites. The relative amounts of Lewis or Brønsted acid centers also seemed immaterial. The alkylation activity shows a trend not commensurating with the acidity. So unlike the reactions reported before, we conclude that acidity cannot be sole deciding factor for the catalytic activity. Another possibility is that the catalytic activity may be a result of the

collective contribution of the different acidic sites. Catalytic activity depends strongly on catalyst composition and reaction conditions. Since aniline is a strong base, even weak Lewis acid sites can co-ordinate to it and therefore the liability of the systems towards alcohol adsorption becomes more important. The difference in the nature of the metal incorporated may have a deciding hand on the catalytic activity.

It was postulated that weak and moderate acid sites are sufficient for N-alkylation, whereas strong acid sites initiate C-alkylation [71-73]. However, in our studies we couldn't get such a correlation, which indicates the cumulative effect of the acidic characteristics along with the specific character of the individual metal species incorporated. Toluidines were formed with selectivity in the range from 2.52% to 13.99%. The selectivity to NMA and NNMA varied from system to system. Maximum selectivity to NMA was obtained in the case of Zn promoted system and least for Mn incorporated system. In general, decreasing the acid strength and increasing the basic strength could promote N-monoalkylated product promoted while strong acid sites enhance successive alkylation of monoalkylated product [60]. However, due to the lack of the data regarding the basicity of the systems, a generalisation could not be obtained regarding the relative product selectivity. The higher amount of dialkylation observed may be due to the relatively strong acidity of the sulphated zirconia systems.

## ii) Influence of iron content

The percentage conversions and the relative selectivities obtained for different iron promoted systems are listed in Table 4.24. Contrary to our previous observations, iron promoted systems, which were highly active for benzoylation and benzylation reactions, gave very low conversions for aniline methylation. The influence of iron content was also subtle. An increase in iron content from 2 to 10% resulted in a slight drop off in the activity from 17.59% to 13.67%. This can be viewed in the light of the strong acidity of the iron promoted systems. It has been proposed that in the case of strong acid catalysts, the activity may be suppressed by the adsorption of aniline, which is a strong base. Therefore strong acids cannot be employed as catalysts for the reaction [60]. Within the iron series a correlation could be obtained between the selectivity and acidity of the samples. An increase in the strong acidity of the systems with increasing



iron content goes well with the increase in the amount of toluidines formed. Such a correlation, however, was difficult for the selectivity for NMA and NNMA. With increasing iron loading an increase in the selectivity to NMA was observed in spite of the decrease in the amount of weak and moderate acid sites and the increase in strong acidity. In general, the amount of secondary alkylation has to be enhanced by increasing strong acidity, which was contrary to our results. Thus we have to assume that the relative selectivity for NMA and NNMA has to be guided by some other factors apart from acidity.

Table 4.24 Methylation of aniline over iron promoted sulphated zirconia systems

Catalyst	Conversion (%)	Selectivity (%)		
		NMA	NNDMA	Toluidines
Fe(2)SZ	17.59	73.17	20.19	6.64
Fe(4)SZ	17.17	75.57	15.54	8.59
Fe(6)SZ	16.98	79.12	11.82	9.06
Fe(8)SZ	16.64	81.72	7.08	11.12
Fe(10)SZ	13.67	81.48	5.12	13.40

0.25 g catalyst, flow rate- 6ml/hr, Temperature- 350°C, methanol:aniline molar ratio-5:1, Time on stream – 2 hrs

#### 4.4.2.2 Influence of reaction temperature

CuSZ was selected as a representative system for the optimisation of the reaction temperature. The reaction temperature had a profound influence on the catalytic activity as well as the product selectivity as obvious from the Fig. 4.35. An increase in the reaction temperature resulted in a gradual increase in the aniline conversion up to 350°C. A further increase in the temperature had an adverse effect on the conversion. Thus, 350°C was chosen as an optimised reaction temperature for the further studies. The lowering of aniline conversions at higher temperatures may be due to the side reactions of methanol forming polymeric aromatics or gaseous products or even coke [74]. Coke deposition results in a decrease in the number of available active sites thereby inducing a reduction in the catalytic activity [75]. The decomposition of methanol was also

confirmed by testing for mass balance when considerable amounts of C-oxides were detected.

The reaction temperature also affected the product selectivity. An increase in the NMA selectivity was observed with the increase in the reaction temperature. At the same time the amounts of NNMA and toluidines showed a decline. In spite of the low aniline conversions, the NMA selectivity remained high at elevated temperatures.

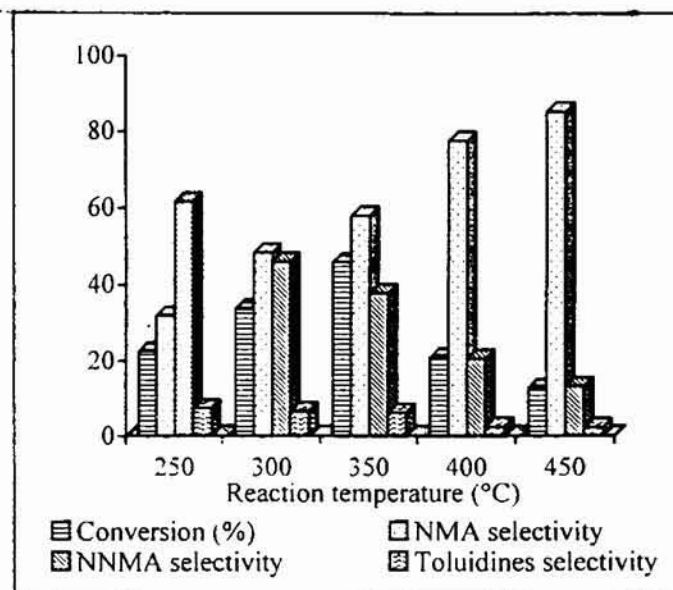


Fig. 4.35 Influence of reaction temperature on aniline methylation reaction

0.25 g CuSZ catalyst, feed rate- 6 ml/hr, Time on stream-2 hrs,  
Methanol:aniline molar ratio-5:1

#### 4.4.2.3 Influence of molar ratio

In an attempt to scan the effect of molar ratio on the aniline conversion and selectivity, a series of runs were conducted over copper promoted sulphated zirconia system at 350°C and at a feed rate of 6ml/hr for a time on stream value fixed at 2 hours. The results are compiled in Fig. 4.36. Increasing methanol to aniline molar ratio enhances the alkylation rate up to a certain optimum level after which the aniline conversion dropped. The decrease in aniline conversion at high molar ratios may be attributed to the competitive adsorption of methanol at high methanol concentrations. This invariably hinders the adsorption of aniline, which ultimately results in a lowering of the aniline conversion. A direct consequence of the increasing molar ratio on product selectivity was

a decrease in the amount of NMA with a concomitant increase in the amount of NNMA. Considering the formation of toluidines, the amount of C-alkylation showed an initial increase when the molar ratio was increased from 1:1 to 3:1. Thereafter a continuous decrease was observed till a molar ratio of 9:1 and thereafter at a ratio of 11:1 a sharp rise was registered.

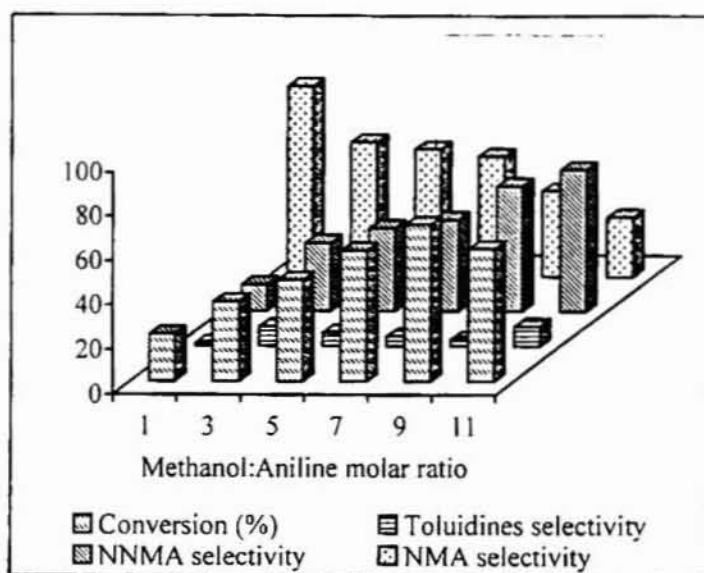


Fig. 4.36 Variation in aniline conversion and product selectivity with molar ratio  
0.25 g CuSZ catalyst, feed rate-6 ml/hr, Time on stream-2 hrs,  
Temperature-350°C

#### 4.4.2.4 Influence of feed rate

The contact time between the catalysts and the reactants greatly influence the reaction rate. Very low contact time (high feed rate) may evoke poor reaction on account of the fact that little time is available for the adsorption of the reactants on the catalyst surface. At the same time, very high contact time (low feed rate) mostly results in undesirable side reactions. Thus each reaction requires an optimum contact time with which maximum conversion and desired product yield is achieved. For the optimization of the feed rate, experimental runs were performed over CuSZ system at different flow rates selecting a constant reaction temperature of 350°C and a methanol to aniline molar ratio of 5:1. The results are pictured in Fig. 4.37. The flow rates selected for the study were 4, 5 and 6 ml/hr. At a flow rate of 4 ml/hr, about 69% aniline conversion was obtained. However, the relative selectivity towards NMA was comparatively low. As the

flow rate was increased, conversion followed a decreasing trend, while the selectivity for NMA increased progressively. The relative selectivity to toluidines also decreased at high flow rates. Thus 6 ml/hr was taken as a convenient feed rate for the reaction.

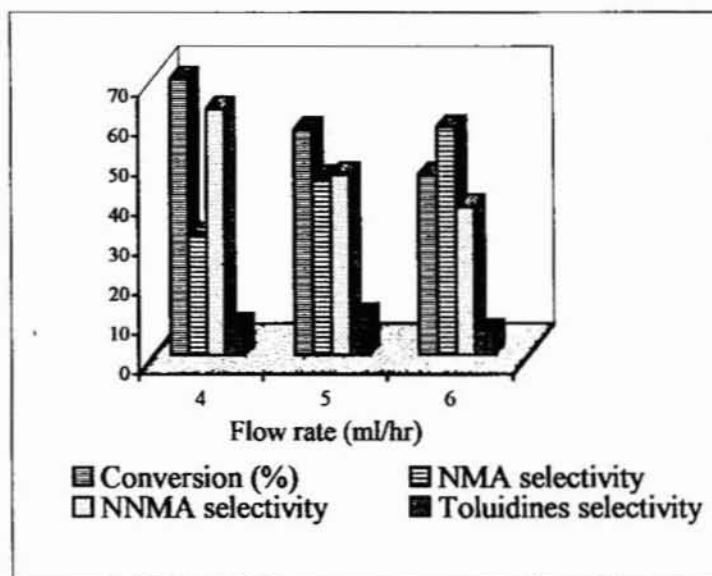


Fig. 4.37 Influence of flow rate on aniline conversion and product selectivity

0.25 g CuSZ catalyst, Time on stream – 2 hrs, Temperature- 350°C  
Methanol:aniline molar ratio – 5:1

#### 4.4.2.5 Influence of time on stream - Deactivation studies

One of the major criterion required for a good catalyst is its stability over the course of the reaction. Retention of the catalytic activity and desired product selectivity is the most sought after property of a catalyst. Thus, a time on stream study becomes highly important in the field of catalysis. A time on stream study was performed with different systems under optimised conditions (Reaction temperature-350°C, flow rate-6ml/hr, methanol:aniline molar ratio-5:1). The time on stream effect varied from system to system as revealed by the Fig 4.38 - 4.40. According to the behaviour, the systems can be grouped into three categories. (1) Zn and Cu incorporated systems in which a slight enhancement in the activity was observed with passage of time and thereafter the conversion leveled off, (2) Ni, Co and W incorporated systems which were sufficiently stable against deactivation with a slight lowering of the conversions and (3) simple sulphated zirconia as well as Fe, Mn, V, Cr and Mo incorporated systems, where

deactivation was more pronounced. The deactivation may be attributed to the blockage of the active sites by coke deposition.

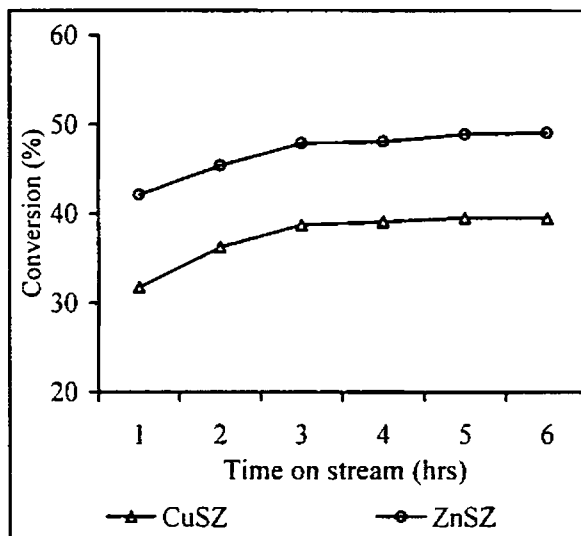


Fig. 4.38 Deactivation studies on CuSZ and ZnSZ systems

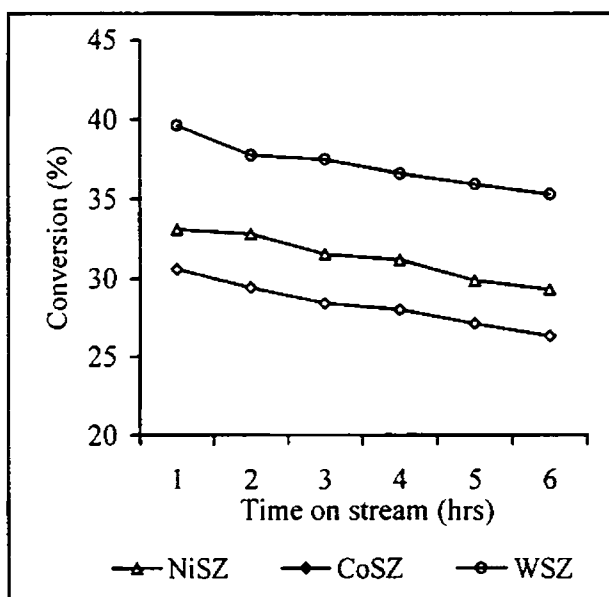


Fig. 4.39 Deactivation studies on Ni, Co and W systems

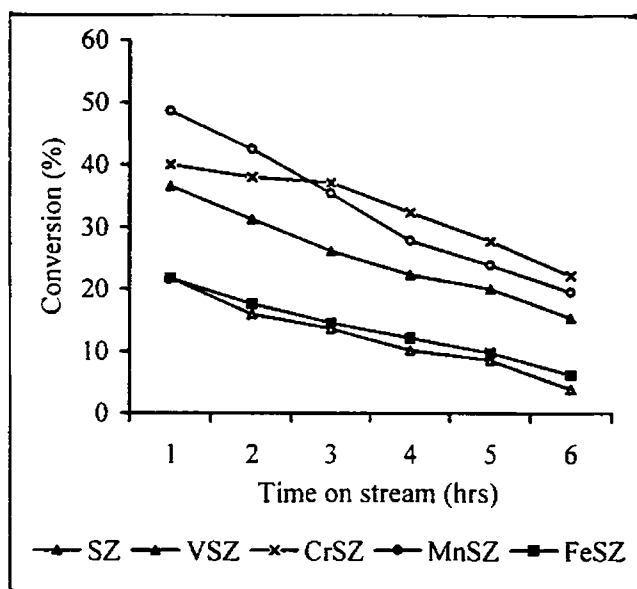


Fig. 4.40 Deactivation studies on SZ, VSZ, CrSZ, MnSZ and FeSZ systems

Time on stream also had its influence on the product selectivity. However, the varying trend observed in the aniline conversion pattern did not appear in the product selectivity. In all the cases, the NMA selectivity increased with the time on stream value. A constant decrease was also noted in the toluidine and NNMA yield and selectivity. The decrease in overall conversion due to coke formation has a stronger effect on the NNMA yield rather than NMA yield. This suggests that the deactivation might be due to the poisoning of the sites responsible for the formation of NNMA and toluidines.

#### 4.4.2.6 Mechanism of the reaction

The experimental observations failed to give any proper correlation between the surface acidic properties. In general, the strong acidity of the systems may be considered to play an important role in the relatively poor selectivity towards NMA. In general, it is agreed that strong acidic sites favour C-alkylation in preference to N-alkylation and even when taking the case of N-alkylation, successive alkylation is greatly facilitated by the strong acid sites [60,64,65,71-73]. Similarly no correlation could be observed between the Brönsted and Lewis acidity of the samples and the respective conversions and product selectivities. Thus, we assume that a combined effect of the different acidic sites along

with the basic nature may be deciding the catalytic activity of the systems for methylation of aniline. The individual characteristics of the metal ion incorporated may be important in deciding the final effect. Based on these considerations, a general mechanism involving Brønsted and Lewis acidic sites may be proposed for the reaction (Fig. 4.41).

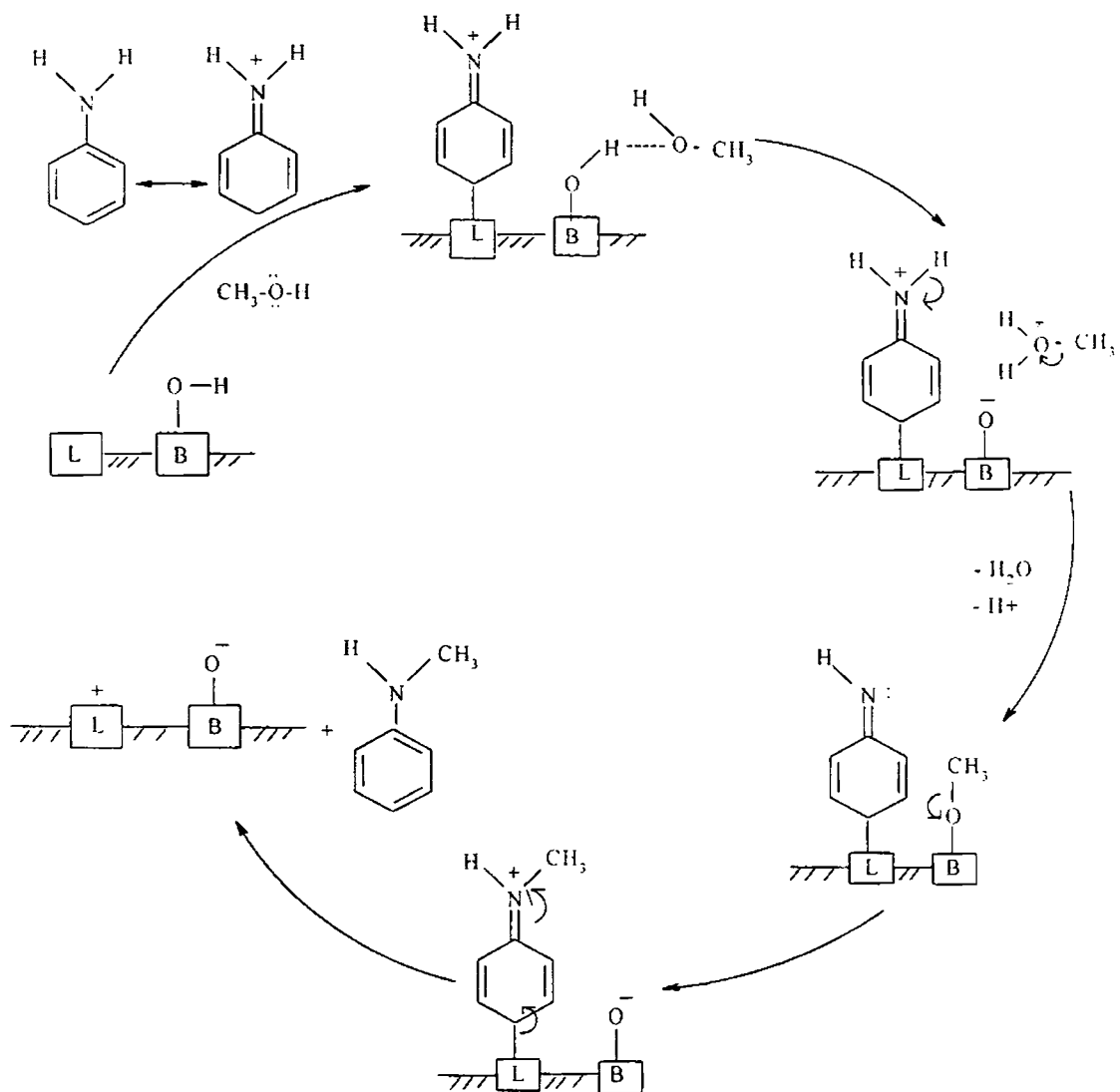


Fig. 4.41 Mechanism of aniline alkylation

## CONCLUSIONS

Metal promoted sulphated zirconia systems were found to be excellent catalysts for different Friedel-Crafts reactions. The parameters like catalyst composition, reaction temperature, substrate to alkylating or acylating agent molar ratio, calcination temperature and moisture content of the catalyst, reaction time, etc. were found to influence the catalytic activity and selectivity. The catalyst reusability was also satisfactory. In the case of benzylation using benzyl chloride, secondary alkylation was a side reaction, depending on the reaction conditions and the catalyst. The nature of the acid sites was critical in deciding the catalytic activity. In the case of benzylation and benzoylation using benzyl chloride and benzoyl chloride as reagents, Lewis acid sites were responsible for the catalytic activity while in benzylation with benzyl alcohol, the reaction was driven by the Brønsted acid sites. A side-by-side operation of a free-radical mechanism explains the exceptionally high activity of iron and copper-doped systems for the benzylation with benzyl chloride. In the case of aniline alkylation, no distinct correlation could be obtained between the catalytic activity and the nature of acid sites. N-alkylation predominated over C-alkylation. Secondary N-alkylation was a serious side reaction, which may be a consequence of the relatively strong acidity of the sulphated zirconia systems. On the basis of the experimental observations, a reaction mechanism involving the combined action of Brønsted and Lewis acid sites has been proposed for the alkylation of aniline over sulphated zirconia systems.



## REFERENCES

1. Olah G.A. *Friedel-Crafts and Related Reactions*. Vols.1-4, Wiley-Interscience, New York, London (1963-1964).
2. Olah G.A. *Friedel-Crafts Chemistry*, Wiley-Interscience, New York, London, Sydney, Toronto (1973).
3. A. Cornelis, C.Dony, P.Laszlo, K.M.Nsunda. *Tetrahedron Lett.*, 34 (1993) 529.
4. R.Stroh, J.Ebersberger, H.Haberland, W.Hahn, *Ger. Patent* (1959) 1 051 271.
5. R.VanHelden, C.F.Koht, H.D.Scharf, *Brit. Patent* (1968) 1 110 029.
6. V.R.Choudhary, S.K.Jana, B.P.Kiran, *Catal. Lett.*, 59 (1999) 217.
7. A.P.Singh, D.Bhattacharya, *Catal. Lett.*, 32 (1995) 327.
8. A.P.Singh, D.Bhattacharya, S.Sarma, *J. Mol. Catal. A: Chem.*, 102 (1995) 139.
9. B.Jacob, S.Sugunan, A.P.Singh, *J. Mol. Catal. A: Chem.*, 139 (1999) 43.
10. A.P.Singh, B.Jacob, S.Sugunan, *Appl. Catal. A: Gen.*, 174 (1998) 51.
11. Y.Izumi, K.Urabe, *Stud. Surf. Sci. Catal.*, 90 (1994) 1.
12. I.Yusuke, O.Mayumi, U.Kazuo, *Appl. Catal. A: Gen.*, 132 (1995) 127.
13. Y.Isumi, N.Natsuma, H.Takamine, J.Tamaoki, K.Urabe, *Bull. Chem. Soc. Jpn.*, 62 (1989) 2159.
14. V.R.Choudhary, S.K.Jana, B.P.Kiran, *J. Catal.*, 192 (2000) 257.
15. S.Jun, R.Ryoo, *J. Catal.*, 195 (2000) 237.
16. N.He, S.Bao, Q.Xu, *Appl. Catal. A: Gen.*, 169 (1998) 29.
17. D.B-Barbier, A.Dormond, F.D-Montagne, *J. Mol. Catal. A: Chem.*, 149 (1999) 215.
18. D.Baudry, A.Dormond, F.D-Montagne, *New J. Chem.*, 18 (1994) 871.
19. A.Pandey, A.P.Singh, *Catal. Lett.*, 44 (1997) 129.
20. R.Sreekumar, R.Padmakumar, *Synth. Commun.*, 27 (5) (1997) 777.
21. B.Chiche, A.Finiels, C.Gauthier, P.Geneste, J.Graille, D.Ploch, *J. Org. Chem.*, 51 (1986) 2128.
22. U.Freese, F.Heinrich, F.Roessner, *Catal. Today*, 49 (1999) 237.
23. P.Botella, A.Corma, J.M.Lopez Nieto, S.Valencia, R.Jacquot, *J. Catal.*, 195 (2000) 161.
24. D.Bhattacharya, A.K.Pandey, A.P.Singh, *Recent Advances in Basic and Applied Aspects of Industrial Catalysts*, T.S.R.Prasada Rao and G. Murali Dhar (Eds.) *Stud. Surf. Sci. Catal.*, Vol. 113 (1998) p. 737.
25. C.N.Rhodes, D.R.Brown, *J. Chem. Soc. Faraday Trans.*, 88 (15) (1992) 2269.
26. J.R.Butruille, T.J.Pinnavaia, *Catal. Today*, 14 (1992) 141.
27. A.Geatti, M.Lenarda, L.Storaro, R.Ganzerla, M.Perissinotto, *J. Mol. Catal. A: Chem.*, 121 (1997) 119.
28. B.M.Choudary, M.L.Kantam, M.Sateesh, K.K.Rao, P.L.Santhi, *Appl. Catal. A: Gen.*, 149 (1997) 257.

29. J.H.Clark, A.P.Kybett, D.J.Macquarrie, S.J.Bariow, P.Landon, *J. Chem. Soc. Chem. Commun.* (1989) 1353.
30. K.R.Sabu, R.Sukumar, M.Lalithambika, *Bull. Chem. Soc. Jpn.*, 66 (1993) 3535.
31. T.Cseri, S.Bekassy, F.Figueras, S.Rizner, *J. Mol. Catal. A: Chem.*, 98 (1995) 101.
32. K.R.Sabu, R.Sukumar, R.Rekha, M.Lalithambika, *Catal. Today*, 49 (1999) 321.
33. R.Sukumar, R.Sabu, L.V.Bindu, M.Lalithambika in "Recent Advances in Basic and Applied Aspects of Industrial Catalysts", T.S.R.Prasada Rao and G.Murali Dhar (Eds.) *Stud. Surf. Sci. Catal.*, Vol. 113 (1998) p. 557.
34. M.Lenarda, L.Storaro, G.Pellegrini, L.Piovesan, R.Ganzerla, *J. Mol. Catal. A: Chem.*, 145 (1999) 237.
35. P.M.Price, J.H.Clark, K.Martin, D.J.Macquarrie, T.W.Bastock, *Org. Process. Res. Dev.*, 2 (1998) 221.
36. G.D.Yadav, A.A.Pujari, *Green Chem.*, 1 (1999) 69.
37. K.Arata, H.Nakamura, M.Shouji, *Appl. Catal. A: Gen.*, 197 (2000) 213.
38. K.Arata, M.Hino, *Appl. Catal.*, 59 (1990) 197.
39. C.G.Jia, M.Y.Huang, Y.Y.Jiang, *Chin. J. Chem.*, 11 (1993) 452.
40. M.Hino, K.Arata, *J. Chem. Soc. Chem. Commun.*, (1985) 112.
41. J.H.Clark, G.L.Monks, D.J.Nightingale, P.M.Price, J.F.White, *J. Catal.*, 193 (2000) 348.
42. V. Quaschnig, J.Deutsch, P.Druska, H.-J. Niclas, E.Kemnitz, *J. Catal.*, 177 (1998) 164.
43. S.K.Samantaray, T.Mishra, K.M.Parida, *J. Mol. Catal. A: Chem.*, 156 (2000) 267.
44. W.Hua, Y.Xia, Y.Yue, Z.Gao, *J. Catal.*, 196 (2000) 104.
45. G.D.Yadav, T.S.Thorat, P.S.Kumbhar, *Tetrahedron Letters*, 34 (3) (1993) 529.
46. G.D.Yadav, T.S.Thorat, *Tetrahedron Letters*, 37 (30) (1996) 5405.
47. K.Tanabe, "Solid acids and bases and their catalytic properties", Academic Press, New York (1970) 103.
48. C.Morterra, G.Cerrato, F.Pinna, M.Signoretto, *J. Phys. Chem.*, 98 (1994) 12373.
49. W.W.Kaeding, R.E.Holland, *J. Catal.*, 109 (1988) 212.
50. S.Prasad, B.S.Rao, *J. Mol. Catal.*, 62 (1990) L 17.
51. P.S.Singh, R.Bandyopadhyay, B.S.Rao, *Appl. Catal. A: Gen.*, 136 (1996) 177.
52. O.Onaka, K.Ishikawa, Y.Isumi, *Chem. Lett.* (1992) 1783.
53. S.Narayanan, A.Sulthan, K.Krishna, *React. Kinet. Catal. Lett.*, 52 (1994) 1783.
54. S.Yuvaraj, V.V.Balasubramanian, M.Palanichamy, *Appl. Catal. A: Gen.*, 176 (1999) 111.
55. S.Yuvaraj, M.Palanichamy, in "Catalysis: Modern trends", N.M.Gupta, D.K.Chakrabarty (Eds.), Narosha Publishing House, New Delhi (1995) 131.
56. H.Matsushashi, K.Arata, *Bull. Chem. Soc. Jpn.*, 64 (1991) 2605.
57. A.N.Ko, C.L.Yang, W.Zhu, H.Lin, *Appl. Catal. A: Gen.*, 134 (1996) 53.

58. C.M.Naccache, Y.B.Tarit, *J. Catal.*, 22 (1971) 171.
59. F.M.Bautista, J.M.Campelo, A.Garcla, D.Luna, J.M.Marrinas, A.A.Romero, M.R.Urbano, *J. Catal.*, 172 (1997) 103.
60. F.M.Bautista, J.M.Campelo, A.Garcla, D.Luna, J.M.Marrinas, A.A.Romero, *Appl. Catal. A: Gen.*, 166 (1998) 39.
61. P.Y.Chen, S.J.Chu, N.S.Chang, T.K.Chuang, *Stud. Surf. Sci. Catal.*, 49 B (1989) 1105.
62. B.L.Su, D.Barthomeuf, *Appl. Catal. A: Gen.*, 124 (1995) 73.
63. B.L.Su, D.Barthomeuf, *Appl. Catal. A: Gen.*, 124 (1995) 81.
64. S.I.Woo, J.K.Lee, S.B.Hong, Y.K.Park, Y.S.Uh, *Stud. Surf. Sci. Catal.*, 49 (1989) 1905.
65. Y.K.Park, K.Y.Park, S.I.Woo, *Catal. Lett.*, 26 (1994) 169.
66. M.A.Aramendia, V.Borau, C.Jimenez, J.M.Marrinas, F.J.Romero, *Appl. Catal. A: Gen.*, 183 (1999) 73.
67. M.A.Aramendia, V.Borau, C.Jimenez, J.M.Marrinas, F.J.Romero, *Colloids and Surfaces A: Physico-chemical and Engineering Aspects*, 170 (2000) 51.
68. S.P.Elangovan, C.Kannan, B.Arabindoo, V.Murugesan, *Appl. Catal. A: Gen.*, 174 (1998) 213.
69. K.Sreekumar, T.Raja, B.P.Kiran, S.Sugunan, B.S.Rao, *Appl. Catal. A: Gen.*, 182 (1999) 327.
70. K.Sreekumar, T.M.Jyothi, M.B.Talawar, B.P.Kiran, B.S.Rao, S.Sugunan, *J. Mol. Catal. A: Chem.*, 152 (2000) 225.
71. P.Y.Chen, M.C.Chen, H.Y.Chu, N.S.Chang, T.K.Chuang, *Stud. Surf. Sci. Catal.*, 28 (1986) 739.
72. S. Narayanan and K. Deshpande, *Appl. Catal. A: Gen.*, 199 (2000) 1.
73. S. Narayanan and K. Deshpande, *Stud. Surf. Sci. Catal.*, 113 (1998) 773.
74. V.R.Choudhary, V.S.Nayak, *Zeolites*, 5 (1985) 328.
75. B.Gielen, M.G.Palekar, *Zeolites*, 9 (1989) 208.

## PHENOL HYDROXYLATION

---

**5.1 INTRODUCTION**

The developments in catalysis during the last few decades have been mandated mainly by the considerations related to the abatement and prevention of pollution, conservation of raw materials and efficient production of fine chemicals. With growing ecological concern, chemical producers have been subjected to increasing pressure to minimise the dispersion of waste chemicals. The organic effluents containing phenolic compounds from pharmaceutical, fine chemical and petrochemical industries, on account of their poor biodegradability, form a major threat to the ecological balance. The selective oxidation of phenol to industrially useful diphenols (catechol and hydroquinone) forms a convenient route to their efficient disposal. High temperatures and pressures involved in supercritical oxidation render it totally uneconomical for phenol oxidation [1,2]. Hydrogen peroxide constitutes a very efficient agent for the selective partial oxidation of organic compounds under mild conditions.

The homogeneous liquid phase hydroxylation of phenol catalysed by mineral acids [3], simple metal ions and their complexes [4-6] has been widely investigated. In spite of the potential catalytic activity, the inherent disadvantages associated with homogeneous catalysis demand their replacement with solid acids. The various catalysts employed for the process include molecular sieves like TS-1, TS-2, Ti-MCM-41, Ti-ZSM-48, V-ZSM-11 [6-15], copper-aluminium hydrotalcite like compounds [16] and zeolite encapsulated metal salen complexes [17]. Pure and supported metal oxides such as  $\text{Co}_3\text{O}_4$  [18],  $\text{Fe}_2\text{O}_3/\text{Al}_2\text{O}_3$  [19],  $\text{CuO}/\text{SiO}_2$  [20],  $\text{V}_2\text{O}_5$  and  $\text{TiO}_2$  colloidal particles [21] suffer from either low catalytic activity or undesirable product selectivity.

Yu *et al.* [22,23] investigated the catalytic performance of vanadium (V-Zr-O) complex for the hydroxylation of phenol with hydrogen peroxide. Pure  $\text{ZrO}_2$  was completely inactive for the reaction while pure  $\text{V}_2\text{O}_5$  gave very low phenol conversion and undesirable product distribution. The complex  $\text{H}_x\text{V}_2\text{Zr}_2\text{O}_9 \cdot \text{H}_2\text{O}$  showed high catalytic

activity and selectivity to catechol and hydroquinone comparable with that obtained for TS-1. The influence of surface area and particle size of the catalyst, solvents, reaction time, reaction temperature, molar ratio of phenol and hydrogen peroxide and the catalyst amount on the catalytic activity was systematically investigated.  $V^{+5}$  was established to be the catalytically active species responsible for the reaction. The catalytic properties of the heteropoly compound,  $K_{0.5}(NH_4)_{5.5}[MnMo_9O_{32}].6H_2O$  for phenol hydroxylation with  $H_2O_2$  as oxidant was investigated by Lin *et al.* [6]. The experimental results indicate that the heteropoly complex in presence of  $V_2O_5$  was an effective catalyst for phenol oxidation with hydrogen peroxide.

Complex oxides ( $La_{1.9}Sr_{0.1}CuO_4$ ) containing transition metals were also tested for their activity towards phenol hydroxylation [24]. Iron oxide nanoparticles, prepared inside the pores of macroporous resins by *in situ* forced hydrolysis of  $Fe^{3+}$  ions chemisorbed at the pore walls, show hydroxylation activity; but the active component is lost easily and the phenol conversion is not high enough [25]. Xiong *et al.* synthesised iron based complex oxides like Fe-Si-O, Fe-Mg-O and Fe-Mg-Si-O for the hydroxylation of phenol, which exhibited high activities after a short induction period [26]. The high activity has been attributed to the free radical mechanism, which involves initiation on the catalyst surface and homogeneous or heterogeneous propagation in the liquid phase. The induction period is shortened with an increase in the surface area of the catalysts.

Thangaraj *et al.* [27] observed an increase in the phenol conversion with increasing Ti content up to a certain stoichiometric value and thereafter it remained constant. Pure silicate-I, amorphous and crystalline silicates as well as physical mixtures of silicate-I and  $TiO_2$  were inactive in the reaction suggesting that titanium ions associated with the MFI framework structure are responsible for the catalytic activity. Martens *et al.* [9] investigated the catalytic performance of a standard titanium molecular sieve catalyst, EUROTS-1 for phenol hydroxylation reaction. The calcination conditions of the catalyst, use of internal standards and the nature and amount of solvent added to the reaction mixture were found to be the major factors determining the phenol conversion and product selectivity. Phenol hydroxylation on TS-1 seems to be a combination of the intracrystalline catalysis and catalysis at the external crystal surfaces. The shape

selectivity of the intracrystalline space favours the hydroquinone formation while catechol and tar are formed mainly at the external surface [7,9]. 1,4-benzoquinone formation predominate at low phenol conversions as well as in cases of quick addition of hydrogen peroxide instead of gradual addition.

Van der Pol *et al.* [8], while investigating on the problem why some titanium silicate samples are inactive for phenol hydroxylation, reached at a conclusion that the particle size determined the catalytic activity of the system. The higher activity of the smaller crystallites is not caused by a larger contribution of the outer surface of the catalyst particles but by higher catalyst efficiency as a result of less pore diffusion limitation. Both internal and external catalytic sites of TS-1 play an important role in the oxidation of phenol with  $H_2O_2$  [7]. A series of MCM-48 catalysts were prepared and investigated for the hydroxylation of phenol. MCM-48 systems were found to be active for the selective hydroxylation of phenol to diphenols. Ti system showed higher conversion when compared to V, Cr and Mn incorporated systems [28]. Zeolite encapsulated Mn-SALEN, Fe-SALEN and VO-SALEN complexes were found to be active redox catalysts capable of effecting phenol hydroxylation [17] with more than 99% selectivity to dihydroxybenzenes.

Santos *et al.* reported the aqueous phase oxidation of phenol using a series of commercial copper containing catalysts at elevated temperatures and oxygen pressures [29,30]. Catalytic wet peroxide oxidation of phenol over unpromoted  $MnO_2/CeO_2$  revealed that even after complete removal of organic carbon from the solution was achieved, an important fraction of the initial carbon was transformed into a polymeric material strongly adsorbed on the catalyst surface [31-33]. This deposit was shown to be responsible for the catalyst deactivation *via*. physical blockage of the active sites [32]. The use of noble metal containing catalyst like platinum over alumina generates lesser build up. However, due to its weaker reactivity, longer reaction times and higher oxidation temperatures are required [31]. Hamoudi *et al.* also investigated the catalytic oxidation of phenol in aqueous solution in presence of Pt and Ag promoted  $MnO_2/CeO_2$  [34]. Hocevar *et al.* [35], investigating on the catalytic wet peroxide oxidation of copper containing systems observed that  $Ce_{1-x}Cu_xO_{2.8}$  system was insoluble in hot acidic

solutions. The same system when prepared in the form of highly dispersed copper oxide phases on  $\text{CeO}_2$  support by sol-gel method was catalytically active under mild conditions. Catalysts based on  $\text{CuO}/\gamma$ -alumina,  $\text{CuAl}_2\text{O}_4/\gamma$ -alumina,  $\text{NiO}/\gamma$ -alumina,  $\text{NiAl}_2\text{O}_4/\gamma$ -alumina and bulk  $\text{CuAl}_2\text{O}_4$  have been tested for their activity towards phenol oxidation [36].

Zirconia has gained wide attention as a catalyst and as a catalyst support. The superacidic properties associated with sulphated zirconia have been exploited in several industrially important reactions including paraffin isomerisation, paraffin cracking, isoparaffin alkylation and acylation of aromatics, esterification, etherification, nitration, etc. [37,38]. Redox properties of the afore mentioned catalytic systems have been rarely exploited. Thus, it becomes our major concern to test the applicability of the systems for phenol oxidation reaction. The primary advantage with these systems lies in the fact that the reaction proceeds under atmospheric pressures and at relatively lower temperatures.

## 5.2 PHENOL OXIDATION OVER SULPHATED ZIRCONIA SYSTEMS

Phenol Hydroxylation reaction seems to proceed along a complex pathway involving a series of consecutive reactions (Fig. 5.1)

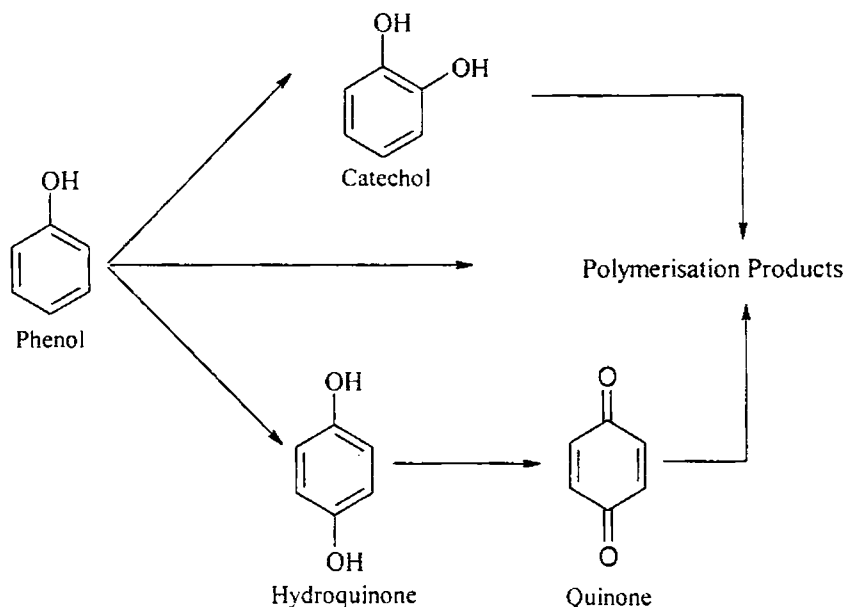


Fig. 5.1 General scheme of phenol hydroxylation

### 5.2.1 INFLUENCE OF CATALYST COMPOSITION

Literature survey indicates that a wide range of catalysts have been employed for the phenol oxidation process, the activity and selectivity depending on the nature of the catalyst employed. Metal promoted sulphated zirconia systems catalysed the formation of catechol and hydroquinone with high selectivity when compared to the unidentified tarry products. Traces of quinone were also observed in some cases. A quantitative estimation of the tarry products was not attempted in the present survey.

#### *i) Influence of metal incorporation*

Catalytic activity of the zirconia systems for the oxidation of phenol under atmospheric pressure and at 70°C is tabulated (Table 5.1).

Table 5.1 Phenol hydroxylation over different zirconia systems

Catalyst	Time (hrs)	Conversion (%)	Selectivity (%)		
			Catechol	Hydroquinone	Quinone
ZrO <sub>2</sub>	3	-	-	-	-
SZ	3	-	-	-	-
VSZ	1	55.37	60.86	31.78	7.36
CrSZ	3	37.27	31.18	68.81	-
MnSZ	3	25.61	75.20	24.80	-
FeSZ	1	36.03	70.10	29.90	-
CoSZ	3	21.34	48.94	48.98	2.08
NiSZ	3	33.43	68.17	31.83	-
CuSZ	1	86.71	56.53	33.27	10.20
ZnSZ	3	11.97	98.51	1.49	-
WSZ	3	8.52	100	-	-
MoSZ	3	9.18	100	-	-

Reaction conditions- 0.1 g catalyst, Reaction temperature-70°C, H<sub>2</sub>O<sub>2</sub> / Phenol ratio- 5:1

Pure and sulphated systems were completely inactive for the reaction. Since no activity could be observed for the pure and simple sulphated zirconia systems, we need to conclude that the metal incorporation is crucial in imparting the catalytic activity. The



nature of interaction of the metal species with the zirconia surface may be responsible for the catalytic activity. The reaction time required to obtain a satisfactory yield of products was different for different systems. Low reaction time seemed insufficient for the initiation of the reaction while prolonged reaction time resulted in the formation of undesirable tarry products. In the case of V, Fe and Cu systems, duration of one hour was sufficient for a satisfactory yield. However, for other systems no significant conversion could be noticed at this time interval and the reaction was continued for two more hours. An attempt to carry out the reaction at room temperature did not work with all the systems since only V, Fe and Cu promoted systems responded to the reaction under these conditions. For sake of comparison, the reaction was carried out at 70°C. The high activity of Fe and Cu incorporated systems can be rationalised on the basis of the well-known redox properties of the Fe<sup>3+</sup> and Cu<sup>2+</sup> ions. Vanadia species with V<sup>+5</sup>, on the other hand, is a recognised oxidation catalyst.

Several reports are available regarding the factors determining the catalytic activity towards phenol oxidation. These factors include the surface area and crystallite size, pore volume and the redox properties [7,8,23,26,34]. Attempt was made to draw out a correlation between any such catalyst characteristics and the catalytic activity. Nevertheless, no clear-cut dependence could be observed between different types of acidity and the catalytic activity. Phenol hydroxylation being a redox reaction, we were interested in examining the influence of the redox properties of the systems on the catalytic properties. A direct correlation could not be achieved in this case also. The surface area and the crystallite as determined by the Scherrers equation did not vary much among the different systems. Thus we have to conclude that the catalytic activity of the metal incorporated sulphated zirconia systems may be a collective outcome of afore mentioned properties rather than of a single effect. The relative product selectivity also seemed to be an inherent property of the system decided by some structural factors. No general trend could be drawn out from the relative product distributions obtained for the different systems. It is believed that catechol and tarry products are formed on the external surface of the catalyst while hydroquinone formation takes place in the intracrystalline space [7,9]. Quinone may be formed by the further oxidation of hydroquinone.

### ii) Influence of iron content

Fig. 5.2 portrays the variation in the phenol conversion and product selectivity with the iron content. The reaction was performed at room temperature and atmospheric pressure. Pure and simple sulphated systems were completely inactive towards phenol conversion under the specified conditions whereas iron incorporated systems showed high activity. An increase in iron loading improved the phenol conversion. A profound influence on the product selectivity was observed with variation in iron loading. High selectivity to catechol formation was observed at low iron loading. An increase in the iron content resulted in a gradual decline in the selectivity for catechol. At an iron loading of 10% the product selectivities were 65% for catechol and 35% for hydroquinone. Formation of benzoquinones was not observed in any case.

Obtaining a correlation between the catalyst properties and activity should be rather easy for the iron promoted systems. This assumption is drawn on the basis of the fact that the incorporated metal species remains the same for the different systems, the variable being its amount. So the only effect to be expected is the cumulative effect of any factor contributing to the catalytic activity.

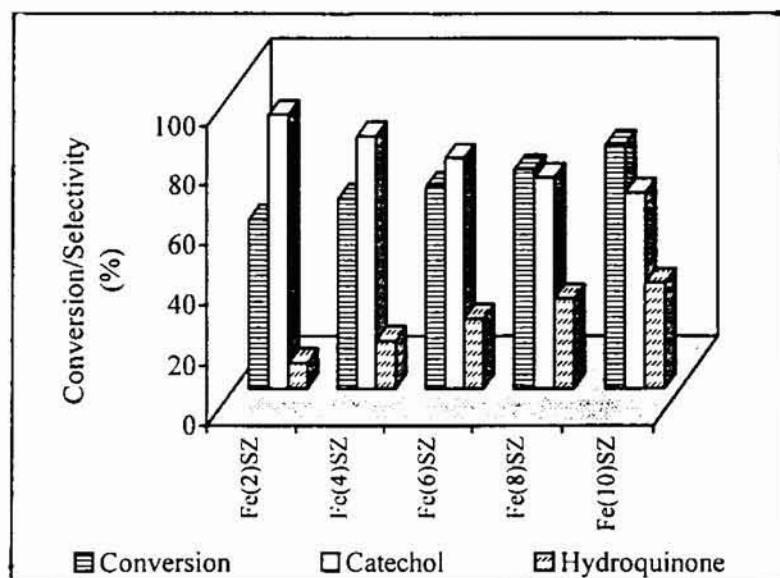


Fig. 5.2 Phenol conversions and product selectivities for iron promoted systems

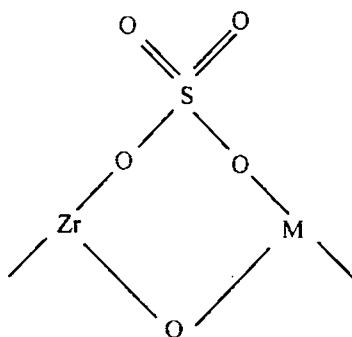
0.1 g Fe(2)SZ catalyst, Duration-1 hr, Room temperature, H<sub>2</sub>O<sub>2</sub>/Phenol ratio-5:1

The redox property of the iron can be considered to play a crucial role in the initiation of the reaction. The high reduction potential of  $\text{Fe}^{3+}/\text{Fe}^{2+}$  system (+0.78 V) favours the abstraction of the hydrogen atom from phenol,  $\text{Fe}^{3+}$  getting reduced to  $\text{Fe}^{2+}$ . Another contributing factor may be the Lewis acidity (one electron accepting capacity) of the systems. The special one electron oxidising ability of the catalyst system as a whole arises from the interaction of the sulphate groups with the metal ions. The fact that simple sulphated system could not initiate the reaction leads us to propose that the  $\text{Fe}^{3+}$  ion may be the active site for phenol hydroxylation reaction. Incorporation of iron may also enhance the acid strength *via* electronic interactions. Introduction of  $\text{Fe}^{3+}$  into the crystal lattice may result in the formation of some complex structures (**Scheme 1**) in some local areas on the surface. According to the principle of electronegativity equalisation proposed by Sanderson, [39] the electronegativity  $S_{\text{int}}$  of the complex structure and the partial charge  $\delta_{\text{Zr}}$  on  $\text{Zr}^{4+}$  can be written as

$$S_{\text{int}} = [S_{\text{M}}^x S_{\text{Zr}} S_{\text{S}} S_{\text{O}}^z]^{1/2+x+z}$$

$$\delta_{\text{Zr}} = (S_{\text{int}} - S_{\text{Zr}}) / 2.08 S_{\text{Zr}}^{1/2}$$

where  $S_{\text{M}}$ ,  $S_{\text{Zr}}$ ,  $S_{\text{S}}$  and  $S_{\text{O}}$  are the electronegativities of M, Zr, S and O and x, z are the numbers of M and O in the neighbourhood of  $\text{Zr}^{4+}$ . The electronegativity of  $\text{Fe}^{3+}$  being larger than that of  $\text{Zr}^{4+}$ , the electronegativity of the surface complex,  $S_{\text{int}}$  is increased and  $\delta_{\text{Zr}}$  becomes more positive when Fe is introduced, thereby resulting in enhanced electron accepting capacity. An increased iron loading, thus, proves beneficial for the reaction.



**Scheme 1**

### 5.2.2 INFLUENCE OF REACTION TEMPERATURE

The reaction temperature plays a significant role in deciding the percentage conversion and selectivity (Table 5.2).

Table 5.2 Influence of catalyst composition in deciding the temperature effect on phenol hydroxylation

Reaction Temperature (°C)	Catalyst	Conversion (%)	Product Selectivity (%)	
			Catechol	Hydroquinone
RT	Fe(2)SZ	56.21	91.58	8.42
	Fe(10)SZ	81.54	65.10	34.93
50	Fe(2)SZ	50.35	84.38	15.62
	Fe(10)SZ	77.12	64.43	35.57
60	Fe(2)SZ	42.52	76.37	23.63
	Fe(10)SZ	73.59	65.31	33.69
70	Fe(2)SZ	36.03	70.10	29.90
	Fe(10)SZ	70.19	66.05	33.95
80	Fe(2)SZ	28.45	65.38	34.62
	Fe(10)SZ	48.53	65.01	33.99

Reaction conditions- 0.1 g catalyst, Duration-1 hr, H<sub>2</sub>O<sub>2</sub>/Phenol ratio-5:1

Parallel runs were conducted at temperatures ranging from room temperature to 90°C using Fe(2)SZ and Fe(10)SZ as representative systems. Maximum conversion to diphenols and selectivity to catechol were obtained at room temperature. The decrease in phenol conversion with increase in reaction temperature is consistent with the exothermic nature of the reaction. The accelerated decomposition of H<sub>2</sub>O<sub>2</sub> at elevated temperatures may also contribute to the drop off in the conversion. It has been reported that the activation energy for the decomposition of H<sub>2</sub>O<sub>2</sub> is lower than that for the hydroxylation of phenol [22,23]. Above 90°C, the amount of residual phenol in the reaction mixture was rather negligible. However, no peaks could be detected in the GC analysis corresponding to the products. This may be due to the overoxidation resulting in tarry products. The catalyst composition seems to counterbalance the influence of the reaction temperature. A

decrease in the activity in the case of Fe(10)SZ system was rather trivial till 70°C, above which a perceptible decline in conversion was obtained. Another interesting observation in this context was that the reaction temperature had little effect on the product selectivity at high iron loadings.

### 5.2.3 INFLUENCE OF REACTION TIME

The progress of the reaction monitored at regular intervals of time (Fig. 5.3) showed a progressive increase in the percentage conversion with time at the expense of selectivity. During the first 30 minutes an induction period was observed when the percentage conversion was very low. After half an hour a sharp rise was observed in the yield of diphenols, which leveled off after one hour. Thereafter the continued stirring resulted in a sharp decline in the diphenol yield. It was quite interesting to note that there was no formation of benzoquinones, the further oxidation products of diphenols. A direct overoxidation to tarry products was observed in all the cases after an optimum reaction time. Thus, prolonged reaction time even though beneficial for the phenol conversion reduces the selectivity to diphenols. Darkening of the solution with time may be due to the formation of the tarry materials by the overoxidation of diphenols or the polymerisation of the phenoxy radicals.

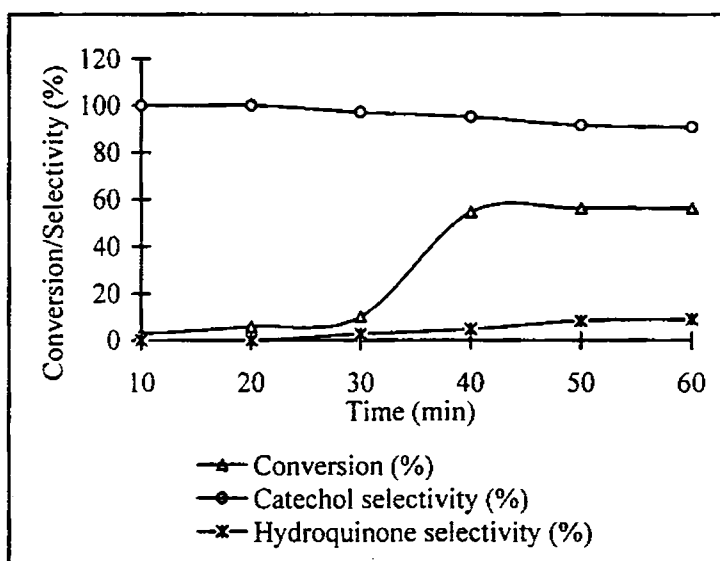


Fig. 5.3 Variation in conversion and percentage selectivity with time

Fe(2)SZ catalyst - 0.1 g, Room temperature, H<sub>2</sub>O<sub>2</sub> / Phenol ratio-5:1

### 5.2.4 INFLUENCE OF H<sub>2</sub>O<sub>2</sub> TO PHENOL RATIO

The dependence of the percentage conversion and product selectivity on the H<sub>2</sub>O<sub>2</sub>/phenol volume ratio is illustrated in Fig. 5.4. The phenol conversion first increases with the increase in the ratio to a certain extent and thereafter an increase in the H<sub>2</sub>O<sub>2</sub> to phenol ratio causes a drastic reduction in the percentage conversion. The drastic reduction may be related to the overoxidation of phenol to tarry products at high peroxide concentration. The selectivity to catechol is also influenced by the H<sub>2</sub>O<sub>2</sub>/phenol volume ratio.

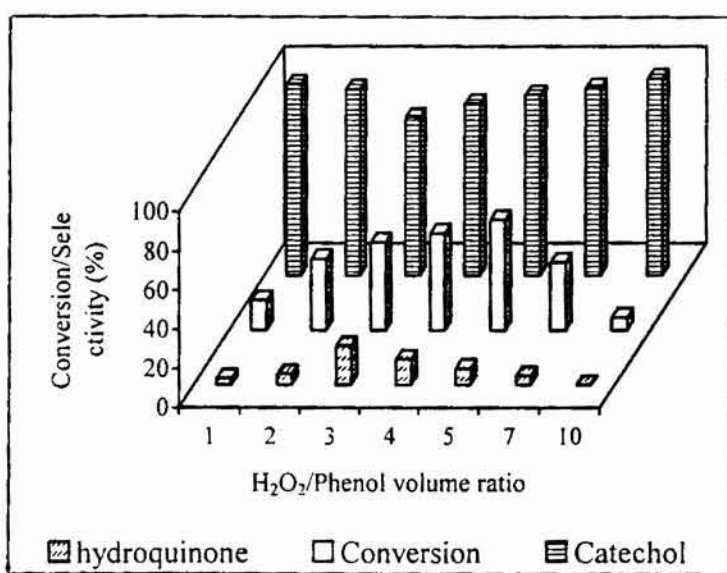


Fig. 5.4 Dependence of phenol conversion and product selectivity on H<sub>2</sub>O<sub>2</sub>/phenol ratio  
Fe(2)SZ catalyst - 0.1 g. Duration 1 hour, room temperature

### 5.2.5 INFLUENCE OF SOLVENT

Previous reports indicate that solvent effect to be a critical deciding factor in phenol hydroxylation process [6,22,23,28]. Water, methanol, acetonitrile and acetone were selected as solvents in the present venture and the results are presented in Table 5.3. Fe(2)SZ was selected as the representative system. The selection of the solvent had a vital influence on the phenol conversion and product selectivity. Water was found to be the best solvent for phenol hydroxylation at the temperatures studied. At room temperature only water and acetonitrile were effective as solvents. Acetonitrile showed low percentage

conversion (20.7% in 2.5 hours), whereas methanol failed to give any reaction. High selectivity to catechol (91.8%) was observed when water was the solvent. At 70°C, the reactivity was in the order water > methanol > acetonitrile. Methanol gave high selectivity to catechol (98.5%) even at elevated temperatures whereas selectivity was lowered in the case of water (70.10%). With acetone as solvent there was no reaction at all. The influence of solvent can be interpreted on the basis of polarity. Phenol conversion increases with solvent polarity. However this explanation seems inadequate to explain the activity at room temperature since acetonitrile proved to be a better solvent than methanol. The product distribution also seems to have a complex dependence on the solvent, which needs further investigation.

Table 5.3 Solvent effects on phenol conversion and selectivity

Solvent	Reaction Temperature (°C)	Time (Hours)	Conversion (%)	Selectivity (%)	
				Catechol	Hydroquinone
Water	RT	1	56.21	91.58	8.42
	70	1	36.03	70.10	29.90
Methanol	RT	2.5	-	-	-
	70	1	28.54	98.50	1.50
Acetonitrile	RT	2.5	20.70	69.10	30.90
	70	1	12.41	65.18	34.82
Acetone	RT	2.5	-	-	-
	70	1	5.67	100	-

Reaction Conditions: Fe(2)SZ catalyst - 0.1 g. H<sub>2</sub>O<sub>2</sub> / Phenol ratio- 5:1, RT-28°C

### 5.2.6 MECHANISM OF THE REACTION

Even though a strict correlation could not be obtained between any of the catalyst properties and the catalytic activity among the different metal promoted systems, a general trend of increasing catalytic activity was evident in the iron promoted systems with increasing iron content. Among the systems incorporated with different transition metals, the individual effects created by the addition of the metal species may be playing a dominating role in deciding the catalytic activity. This supports the active involvement of the incorporated metal species in deciding the catalytic activity. A cooperative

involvement of various factors like surface area, crystallite size, redox properties and the electron accepting properties may be the driving force for the reaction.

A heterogeneous-homogeneous reaction mechanism has been proposed for the liquid phase oxidation over solid catalysts [40,41]. The appearance of an induction period and the exponential increase in the percentage conversion with time in the present study support the involvement of a free radical mechanism. An induction period was quite noticeable with all the systems, the time being dependent on the system chosen. This again suggests a free radical mechanism to be operating irrespective of the catalytic system selected. The high susceptibility of the aromatic ring of phenols towards oxidation can be attributed to the possible generation of the delocalised aryloxy radical *via* the removal of a hydrogen atom. The generation of phenoxy radicals may occur on the catalyst surface. At the same instant, catalyst surface can also trigger the homolytic cleavage of the hydrogen peroxide. A general mechanism of the reaction taking iron system as the representative is sketched in Fig. 5.5. The formation of catechol and hydroquinone is believed to occur *via* the attack of OH $\cdot$  on the benzene ring. The formation of phenoxy radicals occurs at the catalyst surface after which the propagation of the reaction can occur either in the liquid phase or on the catalyst surface. A further investigation into the course of the reaction is essential for a clear-cut prediction of the actual mechanism.

Another important observation was the preferential formation of the *ortho* isomer (catechol) in comparison with the *para* product, hydroquinone. This may be a consequence of some sort of association between the phenoxy radicals and the catalyst surface. This leaves the *ortho* position more prone to attack by the hydroxy radicals generated on the catalyst surface. Another possibility is that the diffusion of the radicals from the catalyst surface may be a slow process when compared with the attack of the hydroxy radicals. Thus, before the radical gets sufficient time to drift apart the attack by the OH $\cdot$  occurs preferentially at the *ortho* position.



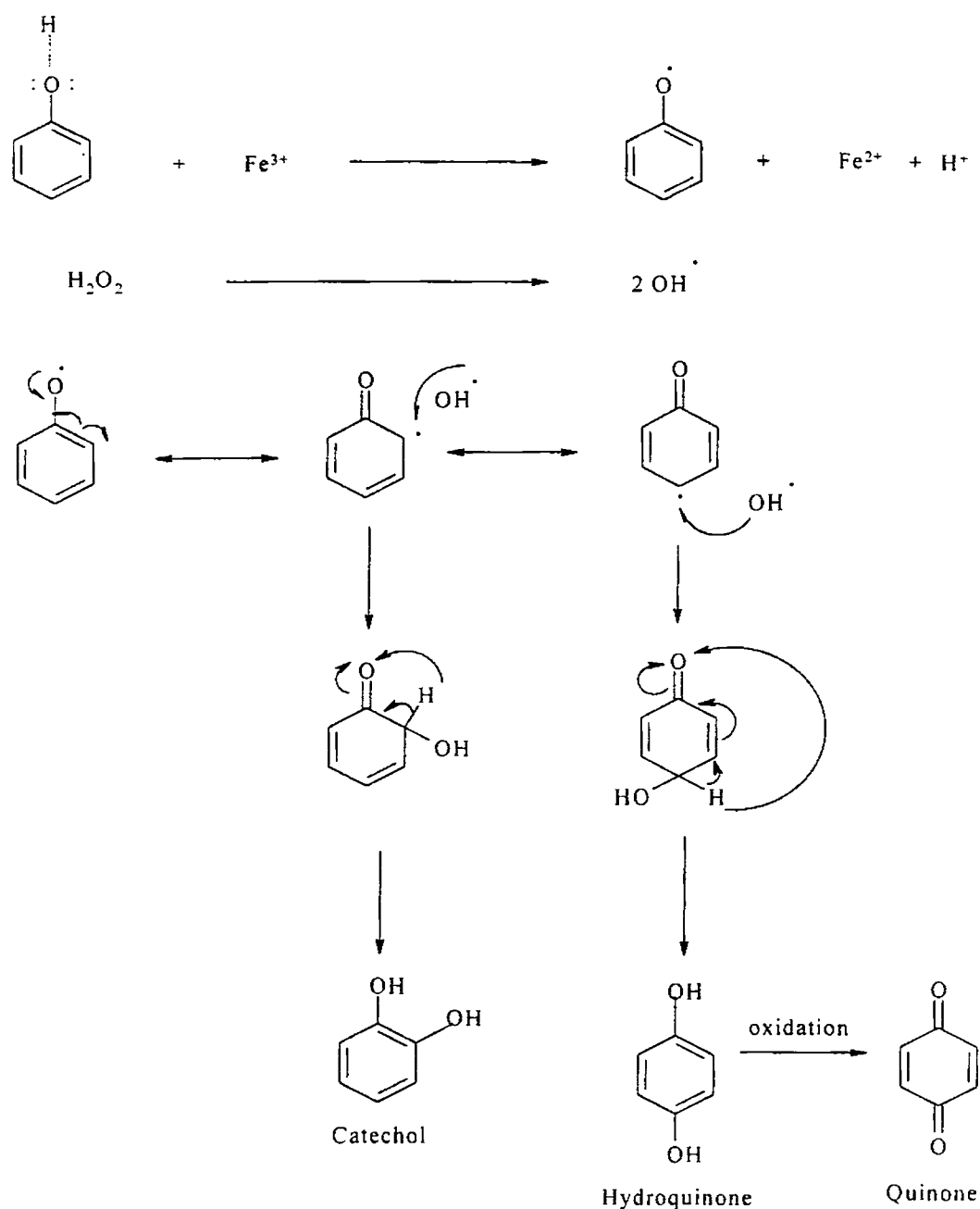


Fig. 5.5 Mechanism of phenol hydroxylation over iron promoted sulphated zirconia

## CONCLUSIONS

The catalytic wet peroxide oxidation of phenol over metal promoted sulphated zirconia seems to have a complex dependence on the nature of the metal incorporated. In the case of iron promoted systems, an increase in the iron content seemed to have a beneficial effect on the catalytic activity. The  $\text{H}_2\text{O}_2$  to phenol ratio and the reaction

temperature was also crucial in deciding the activity. The temperature influence seemed to be a function of the catalyst composition. Selection of an optimum reaction time also demands prime importance, if one has to achieve maximum desired product selectivity. The solvent employed had a deciding effect on the phenol conversion and product distribution. Under all the conditions water seemed to be the best solvent for the reaction. The experimental results suggest the involvement of a free radical mechanism with the active involvement of the incorporated metal species. However, a meticulous investigation of the reaction course is essential before a clear-cut prediction of the mechanism can be made. In any case, the metal incorporated sulphated zirconia systems seem to be promising catalysts for the disposal of phenolic wastes.

## REFERENCES

1. M.Krajnec, J.Leeve, *Appl. Catal. B: Environmental*, 3 (2-3) (1994) 101.
2. H.Takaya, Y.Suzuki, J.Kadokawa, M.Karasu, *Chem. Lett.*, N1 (1997) 47.
3. M.Uohama, *Japan Patent*, 0 334 948 [91 34948] (1991).
4. L.Y.Litvintsv, *Kinet. Catal.*, 34 (1993) 71.
5. D.R.C.Hytbrechts, *Catal. Lett.*, 8 (1991) 273.
6. S.Lin, Y.Zhen, S-M.Wang, Y-M.Dai, *J. Mol. Catal. A: Chem.*, 156 (2000) 113.
7. A.Tuel, S.M-Khouzami, Y.B.Taarit, C.Naccache, *J. Mol. Catal.*, 68 (1991) 45.
8. A.J.H.P.van der Pol, A.J.Verduyn, J.H.C.van Hooff, *Appl. Catal. A:Gen.*, 92 (1992) 113.
9. J.A.Martens, Ph.Buskens, P.A.Jacobs, A.vander Pol, J.H.C.van Hooff, C.Ferrini, H.W.Kouwenhoven, P.J.Kooyman, H.van Bekkum, *Appl. Catal. A: Gen.*, 99 (1993) 71.
10. J.S.Reddy, S.Sivasanker, P.Ratnasamy, *J. Mol. Catal.*, 71 (1992) 373.
11. J.S.Reddy, S.Sivasankar, *Catal. Lett.*, 11 (1994) 241.
12. N.Ulagappan, V.Krishnasamy, *J. Chem. Soc. Chem. Commun.* (1995) 374.
13. A.Thangaraj, R.Kumar, P.Ratnasamy, *Appl. Catal.*, 57 (1990) L1.
14. K.R.Jiri, Z.Amost, H.Jiri, *Collect Czech. Chem. Commun.* 60 (1995) 451.
15. D.P.Serrano, H.-X.Li, M.E.Davis, *J. Chem. Soc. Chem. Commun.* (1992) 745.
16. K.Z.Zhu, C.B.Liu, X.K.Ye, *Acta. Chim. Sin.*, 56 (1998) 32.
17. N.Ulagappan, V.Krishnasamy, *Ind. J. Chem.*, 35A (1996) 787.
18. M.Ai, *J. Catal.*, 54 (1978) 223.
19. N.Al-Hayck, *Water. Res.*, 19 (1985) 657.
20. A.Njnibeako, *Prepr. Can. Symp. Catal.*, 5 (1977) 170.
21. S.Goldstein, G.Czapski, J.Robani, *J. Phys. Chem.*, 98 (1994) 6586.
22. R.Yu, F-S. Xiao, D.Wang, J.Sun, Y.Liu, G.Pang, S.Feng, S.Qiu, R.Xu, C.Fang, *Catal. Today*, 51 (1999) 39.
23. R.Yu, F-S. Xiao, D.Wang, Y.Liu, G.Pang, S.Feng, S.Qiu, R.Xu, *Catal. Lett.*, 49 (1997) 49.
24. C.B.Lui, Z.Zhang, X.G.Yang, Y.Wu, *J. Chem. Soc. Chem. Commun.*, (1996) 1019.
25. D.Y.Wang, Z.Q.Liu, F.Q.Liu, *Appl. Catal. A: Gen.*, 174 (1998) 25.
26. C.Xiong, Q.Chen, W.Lu, H.Gao, W.Lu, Z.Gao, *Catal. Lett.*, 69 (2000) 231.
27. A.Thangaraj, R.Kumar, S.P.Mirajkar, P.Ratnasamy, *J. Catal.*, 130 (1991) 1.
28. Ch.Subrahmanyam, B.Louis, B.Viswanathan, A.Renken, T.K.Varadarajan, *Eurasian Chem. Tech. Journal*, 3 (2001) 59.
29. A.Santos, E.Barroso, F.G-Ochoa, *Catal. Today*, 48 (1999) 109.
30. A.Santos, P.Yustos, B.Durban, F.G-Ochoa, *Catal. Today*, 66 (2001) 511.
31. S.Hamoudi, F.Larachi, A.Sayari, *J. Catal.*, 177 (1998) 247.

32. S.Hamoudi, K.Belkacemi, F.Larachi, *Chem. Eng. Sci.*, 54 (1999) 3569.
33. S.Hamoudi, F.Larachi, A.Adnot, A.Sayari, *J. Catal.*, 185 (1999) 333.
34. S.Hamoudi, A.Sayari, K.Belkacemi, L.Bonneviot, L.Larachi, *Catal. Today*, 62 (2000) 379.
35. S.Hocevar, U.O.Krasovec, B.Orel, A.S.Arigo, H.Kim, *Appl. Catal. B: Environ.*, 28 (2000) 113.
36. A.Alejandro, F.Medina, P.Salagre, A.Fabregat, J.E.Sueiras, *Appl. Catal. B: Environ.*, 18 (1998) 307.
37. X.Song, A. Sayari, *Catal. Rev. Sci. Eng.*, 38 (3) (1996) 329.
38. G.D.Yadav, J.J.Nair, *Microporous and Mesoporous Materials*, 33 (1999) 1.
39. R.T.Sanderson, "*Chemical Bonds and Bond Energy*", Academic Press, NewYork (1976) p.75.
40. C.Meyer, G.Clement, J.C.Balaceanu, "*Proc. 3<sup>rd</sup> Int. Congr. On Catalysis*", Vol. 1 (1965) p. 184.
41. A.Sadana, J.R.Katzer, *J. Catal.*, 35 (1974) 140.

## 6.1 INTRODUCTION

Nitrotoluenes and dinitrotoluenes find application as intermediate products in the synthesis of dyes, pharmaceuticals, explosives and so on. Industrial aromatic nitrations are achieved by employing a mixture of nitric and sulphuric acids [1]. Sulphuric acid aids the formation of nitronium ions, the actual nitrating species, by the protonation of nitric acid [2]. Sulphuric acid also serves as a water binder and heat sink for the highly exothermic reaction. The general scheme of the reaction can be written as in Fig. 6.1. The mixed acid process poses a major problem of spent acid disposal. All these considerations urge the development of solid acid catalysts for the process. Solid acids effectively play the role of sulphuric acid in the reaction, assisting the formation of nitronium species. Formation of water during the reaction causes the dilution of the reaction mixture, thereby reducing the rate of nitration as the reaction proceeds. Thus, one of the key issues in the successful application of solid acids in the nitration of toluene and nitrotoluene to dinitrotoluene is the handling of water in the reaction mixture.

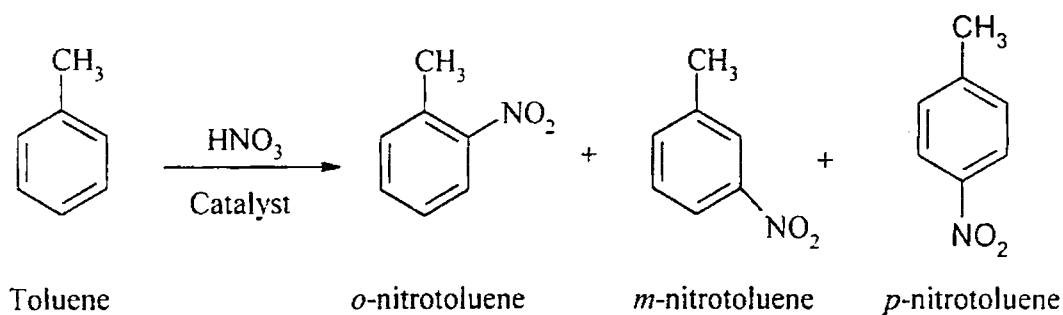


Fig. 6.1 General scheme for nitration of toluene

A variety of combinations of solid acids have been investigated for their suitability as nitration systems for aromatics [2]. Different solid acids tested so far includes zeolites [3] partially dealuminated [4] or cation exchanged zeolites [5], sulphonated ion exchange

resins (polystyrenesulphonic acid) [6], clay supported metal nitrates [7],  $\text{Fe}^{3+}$  on K-10 montmorillonite [8], modified silica [5], silica-alumina and supported acids [9,10]. Various nitration procedures have been described in the last few years making use of different nitrating agents like  $\text{NO}_2$  ( $\text{N}_2\text{O}_4$ ),  $\text{N}_2\text{O}_5$ , molten nitrate salts, alkyl and acyl nitrates, etc. [2,11].

Vassena *et al.* demonstrated the nitration of toluene to nitrotoluene and dinitrotoluene in liquid phase at ambient temperature using silica supported sulphuric acid and 65% nitric acid [12]. Nonpolar solvents were required to prevent the dissolution of the impregnated acid. Solvent free nitration was limited by the necessity to maintain a mixture that can be stirred. They also extended the work to the vapour phase nitration of toluene with different solid acids, as well as nitration combined with distillation (reactive distillation) of nitrotoluene. In vapour phase set up, the dinitro yield was rather very small and maximum conversion could be obtained with preshaped silica impregnated with sulphuric acid, but with a continuous loss of sulphuric acid with time on stream [13]. H- $\beta$ , H-ZSM-5, etc. was also tested for their nitration activity [13]. Enhanced selectivity to 4-nitrotoluene was obtained in case of H- $\beta$  which was linked to the steric hindrance induced by the adsorption rather than to the shape selectivity [14] because both 2- and 4-nitrotoluene can easily diffuse in the pore system of H- $\beta$ . Active and stable mordenite catalysts have been developed by the dealumination of synthetic mordenite by heat and acid treatment for selective nitrobenzene production by the vapour phase nitration of benzene [4].

Akolekar *et al.* [15] reported the high-pressure nitration of toluene using  $\text{NO}_2$  and zeolite catalysts. Only limited dinitrotoluene (DNT) yields were obtained at relatively drastic conditions and the product selectivity was characteristic of radical nitration with a high 3-nitrotoluene fraction. Olin Corporation developed a new industrial single acid DNT process [16]. The process avoids sulphuric acid by using concentrated nitric acid for nitration and nitrate salts during the nitric acid reconcentration step to break up the azeotrope of nitric acid-water binary system. It was also demonstrated that toluene could be nitrated adiabatically in a single step to DNT using classical mixed acid [17]. An

adiabatic liquid phase nitration process is already in use on an industrial scale for the mononitration of benzene [18,19].

McKee and Wilhelm [20] studied the vapour phase nitration of benzene and toluene using nitrogen dioxide as nitrating agent and silica gel as catalyst. Smith *et al.* [21] described a procedure for removing water by chemical trapping with acetic anhydride. The route suffers from the limitations such as the cost involved for the reactant (acetic anhydride), safety aspects (acetyl nitrate, the active species in the reaction, needs special care in handling) and the need to dispose the acetic acid formed during the reaction. Othmer *et al.* first proposed to continuously nitrate benzene [22] and toluene [23] in a distillation column with nitric acid only as the nitrating agent and removing water by azeotropic water-benzene or water-toluene mixture. Du Pont disclosed an azeotropic process for the mononitration of benzene in mixed acid [24] and described a method for removing water by passing inert gas through the reaction mixture [25].

Waller *et al.* [26,27] reported the use of lanthanide (III) triflates, water tolerant Lewis acids, as catalysts for the nitration of simple arenes with 69% nitric acid in 1,2-dichloroethane. Sato *et al.* [28] investigated nitration over different solid acid catalysts utilising nitric acid as the nitrating agent. Montmorillonite ion exchanged with multivalent cations and mixed metal oxides containing  $\text{TiO}_2$  and  $\text{ZrO}_2$  exhibited high activity. Currie *et al.* [29] attempted the regio-selective nitration of phenols and anisole in a cationic surfactant-based microemulsion system and the results were compared with those of nitration in a two-phase system. Almost selective *para* nitration was achieved in microemulsion.

Yadav *et al.* [30] proposed the selective synthesis of *para* nitro derivative from chlorobenzene by using nitric acid over an electrically engineered sulphated zirconia carbon molecular sieve catalyst. When acetic anhydride is used as solvent, nitration proceeds *via* the intermediate formation of acetylnitrate obtained by the reaction between nitric acid and acetic anhydride. Doping with dodecatungstophosphoric acid could not give an increase in the *para* selectivity, which may be accounted for on the basis of its large size, preventing deep penetration into the pores of sulphated zirconia. Parida *et al.*

[31] also established sulphated zirconia as efficient catalysts for nitration of chlorobenzene.

Mixed metal oxides treated with sulphuric acid were found to be efficient for the nitration reaction [32]. The increase in the activity was attributed to the increase in the Brönsted acidity created by the high temperature treatment with sulphuric acid. The life of the catalyst depends on the support's capability of holding sulphuric acid to prevent its diffusion. Sato *et al.* [33] succeeded in maintaining high nitration activity of the supported sulphuric acid catalyst for more than two months by co-feeding trace amounts of sulphuric acid. The catalytic activity of heteropoly acids (phosphomolybdic acid) also was enhanced by partial neutralisation with Cs or Tl ions [32].

## 6.2 NITRATION OF TOLUENE OVER SULPHATED ZIRCONIA SYSTEMS

Nitration of toluene was carried out in a double-necked round-bottomed flask fitted with a condenser. The R.B flask containing toluene and 0.1 g catalyst was allowed to attain the required reaction temperature in an oil bath. HNO<sub>3</sub> solution was added dropwise under continuous stirring. After the required reaction time, the product analysis was achieved gas-chromatographically using SE-30 column and FID detector. Prior to injection in GC, unreacted nitric acid in the reaction mixture was neutralised using Na<sub>2</sub>CO<sub>3</sub> solution to a pH 6-7. The impact of different experimental parameters was analysed by conducting parallel runs.

### 6.2.1 INFLUENCE OF CATALYST COMPOSITION

#### *i) Influence of metal incorporation*

The results of toluene nitration over different metal promoted sulphated zirconia systems at 90°C are tabulated below (Table 6.1). Pure ZrO<sub>2</sub> failed to give any reaction. In all other cases, nitrotoluenes were formed exclusively with no trace of dinitration: the selectivity being around 64-66% *ortho* and 31-33% *para* and 1-3% *meta* isomers. Nitration of toluene was found to proceed with predominant formation of *ortho* isomer [34] for which the results of Nelson and Brown [35] are representative. Pople CNDO/2 calculations by Olah *et al.* [36] demonstrated that the charge density is highest around the *ortho* and *para* positions, which when coupled with the 2:1 availability of *ortho:para*



positions, rationalises the observed preference. Purely statistical analysis without consideration of the electron donating inductive effect of the methyl group would predict 67% *ortho* and 33% *para* products. In our case also preference to the *ortho* isomer was observed in spite of the steric factor.

On a primary examination, no absolute correlation could be noticed between the surface acidity and the catalytic activity. However, a closer scrutiny established a crude association between the catalytic activity and the amount of medium+strong Brønsted acid sites (Fig. 6.2). The nature of the metal incorporated had a little effect on the product selectivity. The product selectivity remained almost constant immaterial of the nature of the metal incorporated.

Table 6.1 Nitration of toluene over metal-incorporated sulphated zirconia systems

Catalyst	Time (hrs)	Conversion (%)	Selectivity (%)		
			<i>ortho</i>	<i>meta</i>	<i>para</i>
ZrO <sub>2</sub>	6	-	-	-	-
SZ	6	33.12	66.57	1.31	32.11
VSZ	6	29.67	65.18	2.64	32.18
CrSZ	6	38.29	65.09	2.32	32.59
MnSZ	6	57.91	64.68	2.64	32.68
FeSZ	6	65.10	65.63	2.19	32.18
CoSZ	6	48.11	65.86	2.57	31.57
NiSZ	6	32.37	64.63	2.49	32.88
CuSZ	6	20.09	64.79	2.18	33.03
ZnSZ	6	24.31	65.33	2.75	31.92
WSZ	6	12.96	65.42	2.43	32.15
MoSZ	6	16.14	65.86	2.81	31.33

Temperature-90°C, Toluene:HNO<sub>3</sub> ratio-1:1, HNO<sub>3</sub> percentage-60%, catalyst-0.1 g.

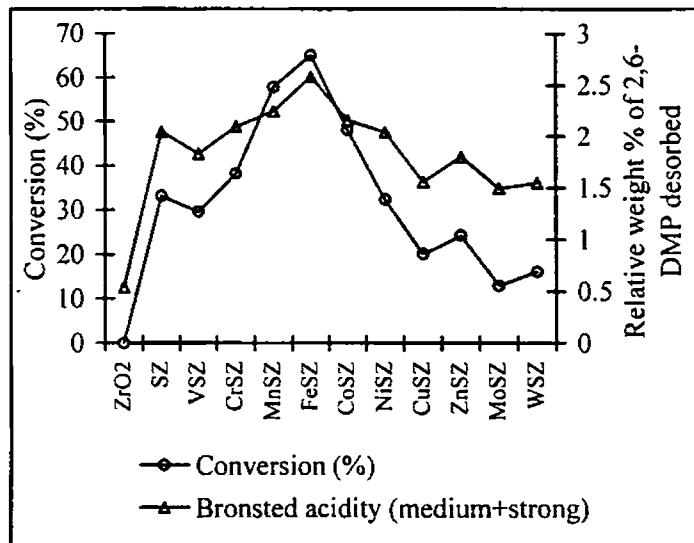


Fig. 6.2 Catalytic activity for nitration correlated with the Brönsted acidity

### ii) Influence of iron content

Iron promoted systems was found to be the most active one for nitration of toluene under the experimental conditions selected. An increase in iron content proved beneficial for the reaction as evident from Table 6.2. The percentage conversion increased with iron loading without altering the product selectivity. The increase in catalytic activity parallels the increase in the medium + strong Brönsted acidity of the samples (Fig. 6.3).

Table 6.2 Nitration of toluene over iron-incorporated sulphated zirconia systems

Catalyst	Time (hrs)	Conversion (%)	Selectivity (%)		
			<i>ortho</i>	<i>meta</i>	<i>para</i>
ZrO <sub>2</sub>	6	-	-	-	-
SZ	6	33.12	66.57	1.31	32.11
Fe(2)SZ	6	65.10	65.63	2.19	32.18
Fe(4)SZ	6	72.54	65.12	2.82	32.06
Fe(6)SZ	6	77.98	64.86	2.75	32.39
Fe(8)SZ	6	83.61	66.29	2.29	31.42
Fe(10)SZ	6	89.17	65.68	1.95	32.37

Reaction temperature-90°C, Toluene:HNO<sub>3</sub> ratio-1:1, HNO<sub>3</sub> percentage-60%, catalyst-0.1 g.

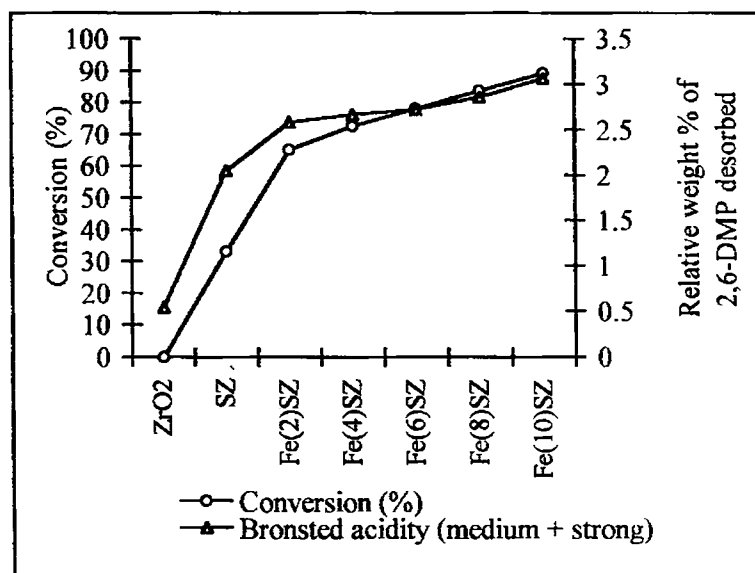


Fig. 6.3 Correlation between catalytic activity and Brønsted acidity

As in the case of different transition metal promoted systems, a preferential formation of *ortho* isomer was observed in the case of iron-doped systems also. An increase in the iron loading had little impact on relative product selectivity.

### 6.2.2 INFLUENCE OF REACTION TEMPERATURE

The influence of reaction temperature on the catalytic activity and product selectivity was examined taking Fe(2)SZ as representative system. The results are furnished in Table 6.3.

Table 6.3 Influence of reaction temperature on catalytic activity and product selectivity

Temperature (°C)	Time (hrs)	Conversion (%)	Selectivity (%)		
			<i>ortho</i>	<i>meta</i>	<i>para</i>
70	6	5.67	64.25	3.77	31.93
80	6	37.25	63.81	3.43	32.76
90	6	65.10	65.63	2.19	32.18

Fe(2)/SO<sub>4</sub><sup>2-</sup>/ZrO<sub>2</sub> 0.1 g, Toluene:HNO<sub>3</sub> - 1:1, 60% HNO<sub>3</sub>

At low temperatures the conversion was negligible. Even after 6 hours only 5% of conversion was observed at the reaction temperature of 70°C. An increase in the temperature resulted in a gradual rise in the percentage conversion. 90°C was found to be

the optimum temperature for the reaction. Above that temperature evolution of brown fumes of nitric oxide indicated the decomposition of nitric acid. The influence of reaction temperature on product selectivity was rather subtle. Only 2 to 3% variation could be noticed in the relative product selectivity.

### 6.2.3 INFLUENCE OF HNO<sub>3</sub> CONCENTRATION

The catalytic activity of Fe(2)SZ system was tested by varying the percentage of nitric acid. Nitric acid percentage was varied from 20 to 80%. An increase in the percentage of nitric acid used as nitrating agent resulted in an enhancement in the catalytic activity as expected. However, high nitric acid concentration created lot of problems during the work-up. The whole mass formed a slurry when the nitric acid percentage was increased beyond 80%, so that the recovery of organic layer was quite difficult. The results are presented in Table 6.4.

Previous reports suggest the absence of any significant alteration of the product selectivity with change in the concentration of nitrating agent [35]. However, a slight alteration of product selectivities was observed in our case when the nitric acid concentration was varied. The selectivity for *o*-nitrotoluene decreased from 68 to 59% when the HNO<sub>3</sub> weight percentage was increased from 20 to 80%. The approximate charge distribution of phenonium ion arising from the protonation of benzene as calculated by Olah and co-workers [36] is shown in Fig. 6.4.

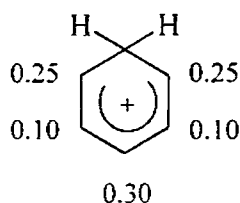


Fig. 6.4 Approximate charge distribution in the phenonium ion

If used as a model for the arenium ion in the electrophilic aromatic substitution, the *para* substituent has a greater effect on the adjacent carbon than an *ortho* substituent. In the absence of other effects, this would predict a product ratio higher than 33% for the *para* isomer and less than 67% for the *ortho* isomer.

Table 6.4 Influence of HNO<sub>3</sub> percentage on catalytic activity

HNO <sub>3</sub> (%)	Time (hrs)	Conversion (%)	Selectivity (%)		
			<i>o</i> -nitrotoluene	<i>m</i> -nitrotoluene	<i>p</i> -nitrotoluene
20	8	20.54	68.54	0.79	30.67
30	6	17.97	65.13	1.29	33.58
40	6	29.63	64.81	1.21	33.97
50	6	47.49	64.98	1.09	33.93
60	6	65.10	65.63	2.19	32.18
70	4	57.11	60.10	3.51	36.40
80	4	64.56	59.10	4.51	36.40

Fe(2)/SO<sub>4</sub><sup>2-</sup>/ZrO<sub>2</sub>- 0.1 g, Toluene:HNO<sub>3</sub> - 1:1, Reaction temperature - 90°C

#### 6.2.4 INFLUENCE OF VOLUME RATIO

Toluene to HNO<sub>3</sub> ratio also influenced the percentage conversion even though the impact on product selectivity was rather delicate. The results are furnished in Table 6.5. An increase in the toluene to HNO<sub>3</sub> volume ratio has a positive effect on the catalytic activity. However, the selectivity towards *ortho* isomer showed a constant decline.

Table 6.5 Influence of volume ratio on catalytic activity and product selectivity

Tol:HNO <sub>3</sub>	Time (hrs)	Conversion (%)	Selectivity (%)		
			<i>o</i> -nitrotoluene	<i>m</i> -nitrotoluene	<i>p</i> -nitrotoluene
5:1	4	5.74	54.49	4.70	40.81
2:1	4	36.85	58.57	4.73	36.70
1:1	4	57.11	60.10	3.51	36.40
1:2	4	75.16	63.93	1.23	34.74

70 % HNO<sub>3</sub>, Catalyst Fe(2)/SO<sub>4</sub><sup>2-</sup>/ZrO<sub>2</sub> - 0.1 g, Reaction temperature - 90°C,

#### 6.2.5 INFLUENCE OF CALCINATION TEMPERATURE

Our experimental studies with different catalyst systems showed a crude correlation between the catalytic activity and the Brønsted acidity of the samples. The involvement of the Brønsted acid sites in catalysing the reaction was further confirmed by

testing the influence of calcination temperature of the catalyst on the percentage conversion. An increase in the calcination temperature caused a decrease in the percentage conversion obtained. Maximum conversion was obtained at 500°C, when the catalyst (even though amorphous in nature) possessed the maximum amount of Brönsted acidity as revealed from the 2,6-DMP thermodesorption studies. The relation between the Brönsted acidity of the system and the catalytic activity is evident from Fig. 6.5. This is quite explainable on the basis of the reversible transformation of Brönsted acidic sites to Lewis acidic sites at elevated temperatures [37]. The calcination temperature did not affect the product selectivity in any considerable way and the relative selectivity remained the same.

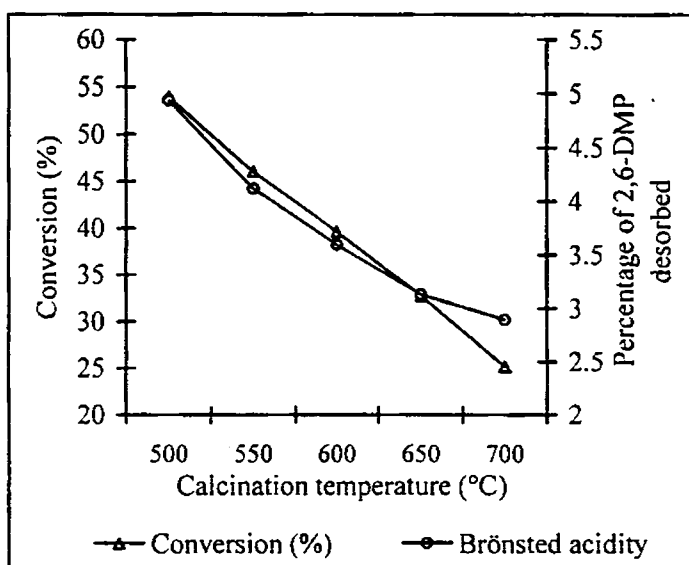


Fig. 6.5 Catalytic activity as a function of calcination temperature

Fe(2)/SO<sub>4</sub><sup>2-</sup>/ZrO<sub>2</sub>- 0.1 g, Toluene:HNO<sub>3</sub> - 1:1,  
Reaction temperature - 90°C, 60% HNO<sub>3</sub>, Time-6 hrs.

### 6.2.6 METAL LEACHING AND REUSABILITY

The catalyst was also tested for metal leaching and reusability. A continuous decline in the conversion was observed after each regeneration indicating the deactivation of the catalyst (Fig. 6.6). The XRD analysis after the reaction indicates a phase change, which becomes predominant after third recycling as revealed from Fig. 6.7. The EDX analysis of the catalyst sample after recycling indicates a loss in the iron content after each cycle (Fig. 6.6). Thus, the leaching out of the iron content may be identified as the

possible cause of deactivation and phase changes. It has been stated earlier that the iron moieties serve to stabilise the tetragonal phase and also enhance the sulphate retaining capacity. The leaching out of the iron may be considered to be a consequence of the contact with nitric acid. Thus, it was interesting to determine the metal leaching under different nitric acid concentrations. It was found that an increasing nitric acid concentration enhances the metal loss during the reaction. Below 40% HNO<sub>3</sub>, no considerable leaching could be detected (Table 6.6). Similarly the extent of deactivation was lowered when the nitrating agent concentration was reduced. Deactivation studies conducted at low nitrating agent concentrations indicate the retention of catalytic activity for five successive regenerations. This indicates that the amount of nitric acid employed for the reaction plays an important role in maintaining the catalytic activity.

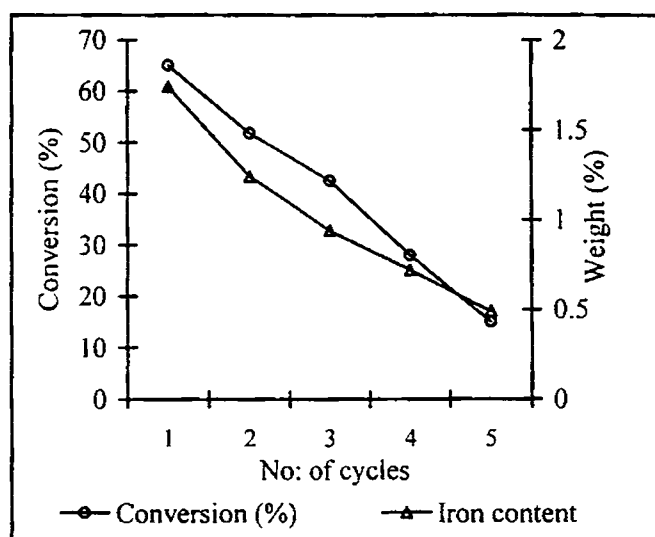


Fig. 6.6 Catalyst deactivation correlated with metal leaching

Fe(2)/SO<sub>4</sub><sup>2-</sup>/ZrO<sub>2</sub>- 0.1 g, Toluene:HNO<sub>3</sub> - 1:1,  
Reaction temperature - 90°C, 60% HNO<sub>3</sub>, Time-4 hrs.

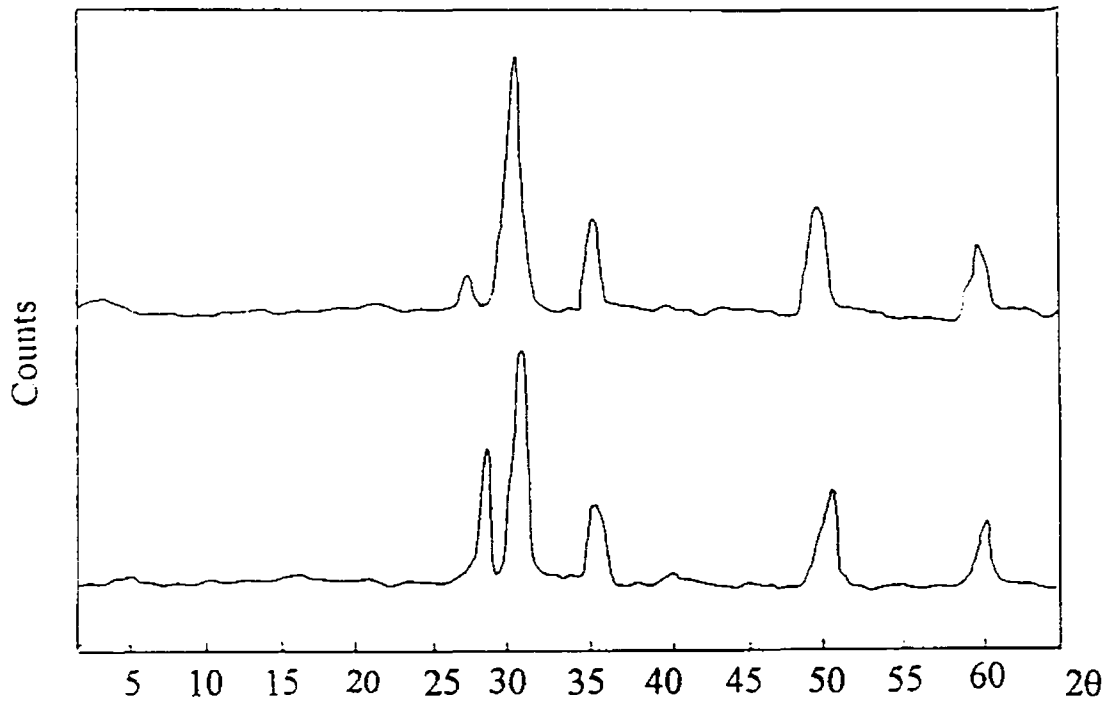


Fig. 6.7 XRD Patterns of fresh and recycled systems

a) Fe(2)SZ - Fresh

b) Fe(2)SZ -Used



Table 6.6 Deactivation studies at different nitrating agent concentrations

HNO <sub>3</sub> (%)		No: of cycles				
		1	2	3	4	5
20 (8)	Iron content	1.91	1.86	1.84	1.79	1.74
	Conversion (%)	20.54	20.11	19.63	19.25	18.91
30 (8)	Iron content	1.89	1.80	1.75	1.71	1.63
	Conversion (%)	27.97	16.85	16.04	15.56	15.11
40 (6)	Iron content	1.86	1.72	1.69	1.54	1.39
	Conversion (%)	29.63	26.32	22.09	18.33	16.67
50 (6)	Iron content	1.81	1.67	1.36	1.22	1.06
	Conversion (%)	47.49	35.06	29.58	23.73	20.97
60 (6)	Iron content	1.74	1.24	0.94	0.72	0.49
	Conversion (%)	65.1	51.83	42.54	28.06	15.12
70 (4)	Iron content	1.36	1.02	0.79	0.61	0.33
	Conversion (%)	57.11	48.64	31.17	20.83	9.54

Fe(2)/SO<sub>4</sub><sup>2-</sup>/ZrO<sub>2</sub>- 0.1 g, Toluene:HNO<sub>3</sub> - 1:1, Reaction temperature - 90°C.  
The figure in parentheses denotes the respective reaction time in each case.

### 6.2.7 MECHANISM OF THE REACTION

A close examination of the experimental results suggests a crude correlation between the Brönsted acidity of the systems and the catalytic activity for nitration (Figs. 6.2 and 6.3). The activity studies by varying the calcination temperature of the catalyst also suggest the involvement of the Brönsted acid sites in the reaction (Fig. 6.5). The medium and strong Brönsted acid sites were found to have an influential hand on the reaction. The reaction may be considered to proceed *via* a carbocation mechanism in which the nitronium ion is generated by the interaction of nitric acid with the Brönsted acid sites, especially the strong and medium ones. The *ortho* and *para* attack of the nitronium ion is favoured due to the stabilisation of the specific *ortho* and *para* resonance structures *via* an electron-donating inductive effect of the methyl groups. The regioselectivity of the final product may be due to a combined effect of the relative stabilities of the corresponding arenium ions in accordance with the Hammond postulate along with

the statistical factors. A plausible mechanism for the reaction is suggested below (Fig. 6.8).

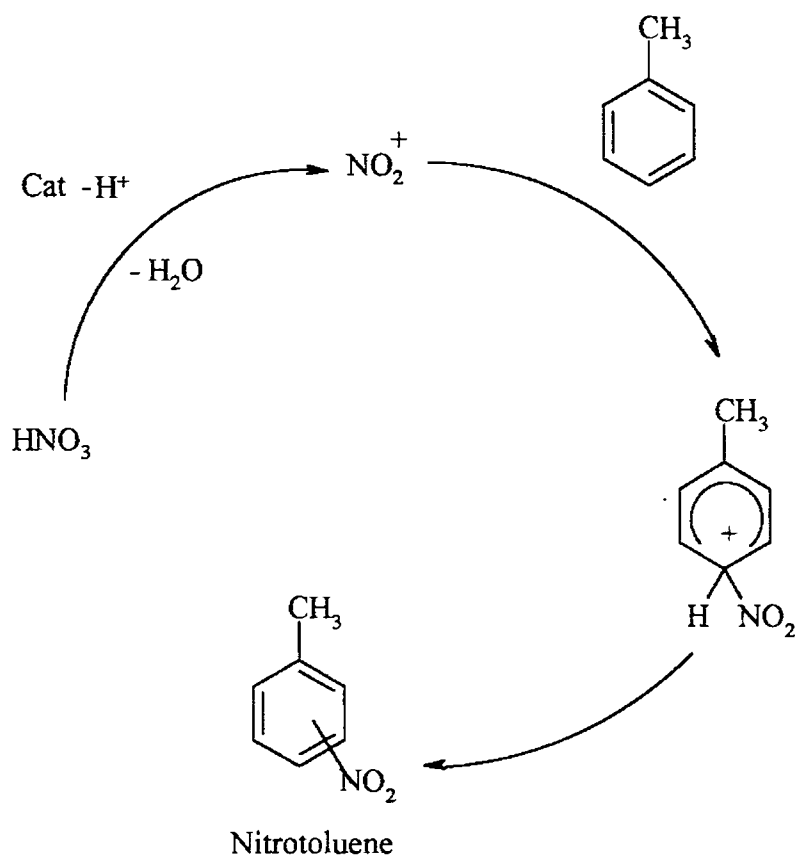


Fig. 6.8 Plausible mechanism for the nitration of toluene using nitric acid

## CONCLUSIONS

Sulphated zirconia systems proved to be efficient substitutes for the mixed acid process. Mononitrotoluenes were formed with 100% selectivity without any contamination of secondary nitration. The nature of catalyst and the reaction conditions had little influence on relative product selectivity. A predominant formation of the *ortho* isomer was observed in all the cases suggesting involvement of the statistical factors in determining the relative product selectivity. The concentration of nitric acid employed as nitrating agent played an important role in determining the maintenance of the catalytic activity. A simple carbocationic mechanism with the formation of nitronium ion intermediate has been postulated for the reaction based on experimental observations.

## REFERENCES

1. *Ulmann's Encyclopedia of Industrial Chemistry*, Vol. A17, 5<sup>th</sup> edn, VCH, Weinheim (1991) p. 411.
2. G.A.Olah, R.Malhotra, S.C.Narang, "Nitration, Methods and Mechanism", VCH, NewYork (1974).
3. L.V.Malysheva, E.A.Paukshtis, K.G.Ione, *Catal. Rev.- Sci. Eng.*, 37 (1995) 179.
4. L.Berteau, H.W.Kouwenhoven, R.Prins, *Appl. Catal. A: Gen.*, 129 (1995) 229.
5. K.Smith, *Bull. Soc. Chim. Fr.*, (1989) 272.
6. O.L.Wright, J.Teipel, D.Thoennes, *J. Org. Chem.*, 30 (1965) 1301.
7. P.Laszlo, J.Vandormaal, *Chem. Lett.*, (1988) 1843.
8. B.M.Choudary, M.Ravichandra Sarma, K.Vijayakumar, *J. Mol. Catal.*, 87 (1994) 33.
9. J.M.Riego, Z.Sedin, J.M.Zaldivar, N.C.Marziano, C.Torato, *Tetrahedron Lett.*, 37 (1996) 513.
10. E.Suzuki, K.Tohmori, Y.Ono, *Chem. Lett.*, (1987) 2273.
11. H.Sato, K.Hirose, *Appl. Catal. A: Gen.*, 174 (1998) 77.
12. A.Kogelbauer, D.Vassena, R.Prins, J.N.Armor, *Catal. Today*, 55 (2000) 151.
13. A.Kogelbauer, D.Vassena, R.Prins, *Catal. Today*, 60 (2000) 275.
14. D.Vassena, A.Kogelbauer, R.Prins, *Stud. Surf. Sci. Catal.*, 125 (1999) 501.
15. D.B.Akolekar, G.Lemey, A.Sayari, S.Kaliagnine, *Res. Chem. Intermed.*, 21 (1995) 7.
16. A.B.Quakenbush, B.T.Pennington, in L.F.Albright, R.V.C.Carr, R.J.Schmitt (Eds.)  
"Nitration: Recent Laboratory and Industrial Developments", ACS Symposium Series,  
Vol. 623 (1996) p. 214.
17. T.Schieb, G.Wiechers, R.Sunderman, U.Zarnack, *Canada Patent*, 2 102 587 (1994).
18. V.Alexanderson, J.B.Trecek, C.N.Vanderwaart, *US Patent*, 4 021 498 (1977).
19. V.Alexanderson, J.B.Trecek, C.N.Vanderwaart, *US Patent*, 4 091 042 (1978).
20. R.H.McKee, R.H.Wilhelm, *Ind. Eng. Chem.*, 28 (1936) 662.
21. K.Smith, A.Musson, G.A.DeBoos, *J. Org. Chem.*, 63 (1998) 8448.
22. D.F.Othmer, J.J.Jacobs, J.F.Levy, *Ind. Eng. Chem.*, 34 (1942) 286.
23. D.F.Othmer, H.L.Kleinhans, *Ind. Eng. Chem.*, 36 (1944) 447.
24. M.W.Dassel, *US Patent*, 3 928 475 (1975).
25. R.McCall, *US Patent*, 4 331 819 (1982).
26. J.F.Waller, A.G.M.Barrett, D.C.Braddock, D.Ramprasad, *J. Chem. Soc. Chem. Commun.*  
(1997) 613.
27. J.F.Waller, A.G.M.Barrett, D.C.Braddock, D.Ramprasad, *Tetrahedron Lett.*, 39 (1998) 1641.
28. H.Sato, K.Hirose, K.Nagai, H.Yoshioka, Y.Nagaoka, *Appl. Catal. A: Gen.*, 175 (1998) 201.
29. F.Currie, K.Holmberg, G.Westman, *Colloids and Surfaces A: Physico-chemical and  
Engineering Aspects*, 182 (2001) 321.
30. G.D.Yadav, J.J.Nair, *Catal. Lett.*, 62 (1999) 49.

31. K.M.Parida, P.K.Pattnayak, T.S.R.Prasada Rao and G.Murali Dhar (Eds.) "*Recent Advances in Basic and Applied Aspects of Industrial Catalysis*", *Stud. Surf. Sci. Catal.*, Vol. 113 (1998) 247.
32. H.Sato, K.Nagai, H.Yoshioka, Y.Nagaoka, *Appl. Catal. A:Gen.*, 175 (1998) 209.
33. H.Sato, K.Nagai, H.Yoshioka, Y.Nagaoka, *Appl. Catal. A:Gen.*, 180 (1999) 359.
34. L.M.Stock, "*A Classical Mechanism for Aromatic Nitration*" in *Progr. Phys. Org. Chem.*, 12 (1976) 21.
35. K.L.Nelson, H.C.Brown, *J. Am. Chem. Soc.*, 73 (1951) 5605.
36. G.A.Olah, *Acc. Chem. Res.*, 4 (1970) 240 and the references cited therein.
37. C.Morterra, G.Cerrato, C.Emanuel, V.Bolis, *J. Catal.*, 142 (1993) 349.

SUMMARY AND CONCLUSION

---

**7.1 SUMMARY**

The prime intention of the present project was a systematic investigation of the physico-chemical properties and catalytic activity of some transition metal promoted sulphated zirconia systems. The characterisation and catalytic activity results were compared with that of pure  $ZrO_2$  and simple sulphated zirconia systems. Sulphated zirconia samples were prepared by a controlled impregnation technique. In the case of metal incorporated systems, a single step impregnation was carried out using required amounts of sulphuric acid and metal salt solutions. As a preliminary step, optimisation of calcination temperature and sulphate content was achieved. For further studies, the optimised sulphate loading of 10 ml per gram of hydrous zirconium oxide and a calcination temperature of  $700^\circ C$  was employed. Metal incorporation had a positive influence on the physico-chemical properties. Vapour phase cumene conversion served as a test reaction for acidity. Some industrially important reactions like Friedel-Crafts reaction, phenol hydroxylation, nitration, etc. were selected to test the catalytic activity of the prepared systems.

The chapter-wise organisation of the thesis is as follows.

*Chapter 1* covers a brief literature review on different sulphated zirconia systems. The effect of sulphate doping on the physico-chemical characteristics and catalytic properties is included in this chapter. The mechanism of acidity generation and nature of acidity in sulphated zirconia systems is discussed in detail. The effect of incorporation of a second metallic species is also reviewed.

*Chapter 2* is devoted to a complete description of the materials used in the present work and the experimental techniques employed for the catalyst characterisation. The

preparation methods adopted are described in detail. The experimental details for the evaluation of catalytic activity are also incorporated in this chapter.

*Chapter 3* discusses the physico-chemical characteristics of the catalyst systems. The catalyst systems were characterised by surface area and pore volume measurements, XRD analysis, thermal studies and IR spectroscopy. The elemental composition was revealed by EDX analysis. Selected samples were also analysed by Laser Raman Spectroscopy and Scanning Electron Microscopy. Surface acidic properties were examined by three independent techniques namely ammonia TPD, perylene adsorption and thermodesorption studies using pyridine and 2,6-dimethylpyridine as probe molecules. Cumene conversion reaction served as a test reaction for acidity.

*Chapter 4* focuses on the application of the catalytic systems for Friedel-Crafts reactions. Benzoylation of aromatics was achieved using benzoyl chloride. Benzyl chloride and benzyl alcohol were employed as reagents for Friedel-Crafts benzylation. Methylation of aniline was accomplished in vapour phase using methanol as alkylating agent. The influence of different reaction parameters on the catalytic activity and selectivity was subjected to investigation. The reusability of the catalytic systems was also checked. Attempt has been made to correlate the catalytic activity with the surface acidic properties of the catalyst systems and plausible mechanisms have been drawn out in each case based on the experimental observations.

*Chapter 5* illuminates the application of sulphated zirconia systems as efficient catalysts for the hydroxylation of phenol. Here also, the variation in the catalytic activity and product selectivity with experimental parameters has been taken care of. A possible mechanism has been suggested after a critical analysis of the catalytic performance.

*Chapter 6* discusses the nitration reaction of toluene over sulphated zirconia systems under different reaction conditions.

*Chapter 7* presents the summary and important conclusions of the present work.

## 7.2 CONCLUSIONS

The following are the conclusions elucidated from the present study.

- ❖ Sulphate loading modifies the physico-chemical properties of pure zirconia. The major outcome includes enhancement of surface area and stabilisation of the catalytically active tetragonal phase. Traces of monoclinic phase appear at high sulphate loading indicating the diminution of the special stabilisation of the tetragonal phase.
- ❖ Sulphate doping considerably improves the surface acidic properties, the nature of the surface acidity being a function of the calcination temperature, sulphate loading, etc.
- ❖ Incorporation of transition metal promoters enhances the sulphate retention capacity, thermal stability and the surface acidic properties. Among the different metal promoted systems, total acidity remains comparable whereas the acid strength distribution varies considerably.
- ❖ An increase in iron loading for a given sulphate loading results in a reduction in surface area, gradual disappearance of the monoclinic phase, enhancement of Lewis acidity and generation of strong acid sites at the expense of weak acid sites.
- ❖ Vapour phase cumene conversion reaction works out as a test reaction for acidity. Good correlation was obtained between cumene conversion and the amount of strong acidic sites. Cracking and dehydrogenation product selectivity could be correlated with the Brønsted acidity and Lewis acidity of the systems respectively.
- ❖ Transition metal incorporated sulphated zirconia systems exhibited improved catalytic activity for the benzylation of aromatics when compared with pure  $ZrO_2$  and simple sulphated zirconia systems. Iron incorporation was found to be most effective for the reaction. An increase in iron loading enhanced the catalytic activity. In all the cases, *para* isomer was formed preferentially with around 80-84% selectivity. The reaction seemed to be driven by the Lewis acidic sites,

which was further confirmed by the positive influence of the calcination temperature of the catalyst and the negative influence of moisture on the reaction. The catalyst systems were found to be sufficiently stable for repeated operations.

- ❖ Pure and metal promoted sulphated zirconia systems were found to be efficient for the benzylation of benzene, the most efficient being the iron promoted systems. An increased iron loading seems beneficial for the reaction at the expense of selectivity towards monoalkylated product. Investigations on temperature influence showed that high reaction temperature favours dialkylation. Negative influence of moisture and the positive influence of calcination temperature of the catalyst suggest the involvement of the Lewis acid sites in the reaction. Exceptionally high activity in the case of iron and copper promoted samples leads us to propose the operation of a free radical mechanism side-by-side with the involvement of Lewis acid sites.
- ❖ Benzyl alcohol seemed a less efficient reagent for benzylation when compared with benzyl chloride. Benzyl ether was a major side product in this case. The catalytic activity seems to be a function of the Brønsted acidity of the systems. The low conversions observed may be a result of the low Brønsted acidity of the sulphated zirconia systems.
- ❖ Vapour phase methylation of aniline over sulphated zirconia systems gave predominantly N-alkylated products. Parameters like reaction temperature, molar ratio, feed rate, etc. profoundly influenced the catalytic activity and product selectivity. The strong acidity of the sulphated zirconia systems promotes secondary alkylation resulting in the formation of N,N-dimethyl aniline in high proportions. A balanced action of Brønsted as well as Lewis acid sites seems to be essential for the efficient advancement of the reaction.
- ❖ Transition metal promoted sulphated zirconia systems proved to be efficient catalysts for the disposal of phenolic wastes. The reaction was found to be sensitive towards the reaction conditions like reaction temperature, duration of



*Chapter 7- Summary and Conclusion*

run, H<sub>2</sub>O<sub>2</sub> to phenol ratio and catalyst composition. The experimental observations prompt us to suggest a free-radical mechanism for the reaction.

- ❖ Nitration of toluene proceeded efficiently over metal incorporated sulphated zirconia systems. Brønsted acid sites, especially the medium and strong ones, decided the catalytic activity. The product selectivity seemed to be governed mainly by the statistical factors. The product selectivity remained the same for different catalytic systems while a slight alteration was observed with variation in the reaction conditions.